AD_____

Award Number: DAMD17-00-1-0542

TITLE: Genetic Factors that Affect Tumorigensis in NF1

PRINCIPAL INVESTIGATOR: Karen Stephens, Ph.D.

CONTRACTING ORGANIZATION: University of Washington
Seattle, WA 98105-6613

REPORT DATE: November 2003

TYPE OF REPORT: **Annual**

PREPARED FOR: U.S. Army Medical Research and Materiel Command
Fort Detrick, Maryland 21702-5012

DISTRIBUTION STATEMENT: Approved for Public Release;
Distribution Unlimited

The views, opinions and/or findings contained in this report are those of the author(s) and should not be construed as an official Department of the Army position, policy or decision unless so designated by other documentation.

REPORT DOCUMENTATION PAGE

Form Approved
OMB No. 074-0188

1. AGENCY USE ONLY (Leave blank)	2. REPORT DATE	3. REPORT TYPE AND DATES COVERED
	November 2003	Annual (29 Oct 2002 - 28 Oct 2003)

4. TITLE AND SUBTITLE

Genetic Factors that Affect Tumorigensis in NF1

5. FUNDING NUMBERS

DAMD17-00-1-0542

6. AUTHOR(S)

Karen Stephens, Ph.D.

7. PERFORMING ORGANIZATION NAME(S) AND ADDRESS(ES)

University of Washington
Seattle, WA 98105-6613

E-Mail: millie@u.washington.edu

8. PERFORMING ORGANIZATION REPORT NUMBER

9. SPONSORING / MONITORING AGENCY NAME(S) AND ADDRESS(ES)

U.S. Army Medical Research and Materiel Command
Fort Detrick, Maryland 21702-5012

10. SPONSORING / MONITORING AGENCY REPORT NUMBER

11. SUPPLEMENTARY NOTES

Original contain color plates: ALL DTIC reproductions will be in black and white

12a. DISTRIBUTION / AVAILABILITY STATEMENT

Approved for Public Release; Distribution Unlimited

12b. DISTRIBUTION CODE

13. ABSTRACT (Maximum 200 Words)

Neurofibromatosis type 1 affects 1/4000 individuals worldwide and predisposes to the growth of both benign and malignant tumors. Our research is focused on NF1 microdeletions that are associated with an early onset, and subsequent heavy burden, of cutaneous neurofibromas. We reported that the deletions arise by homologous recombination between 51 kb repeat elements (NR1REP) that flank the NF1 gene. We identified recombination hotspots where 69% of NF1 microdeletions occur and developed robust and sensitive assays to detect microdeletions in a patient blood sample. We analyzed the structure and sequence of four NF1REP paralogs in the genome and described sequence features that may mediate recombination at these sites. We developed new quantitative PCR assays that will detect nonrecurrent *NF1* microdeletions that occur either in the germline or in somatic tissues including tumors. Our data make substantial contributions to understanding how *NF1* microdeletions occur, create resources to inquire whether some individuals are more susceptible, and which deleted sequences may cause the severe tumor phenotype of these patients.

14. SUBJECT TERMS

Neurofibroma, NF1 deletion, modifier genes, tumorigenesis

15. NUMBER OF PAGES

156

16. PRICE CODE

17. SECURITY CLASSIFICATION OF REPORT	18. SECURITY CLASSIFICATION OF THIS PAGE	19. SECURITY CLASSIFICATION OF ABSTRACT	20. LIMITATION OF ABSTRACT
Unclassified	Unclassified	Unclassified	Unlimited

Table of Contents

Introduction

Neurofibromatosis type 1 affects 1/4000 individuals worldwide and predisposes to the growth of both benign and malignant tumors. We hypothesized that the early age at onset of cutaneous neurofibromas observed in patients with *NF1* microdeletions is caused by the co-deletion of *NF1* and a second gene *NPL* (neurofibroma-potentiating locus)(1-3). This hypothesis was supported by our findings that the majority of *NF1* microdeletion breakpoints are clustered at large repetitive elements (NF1REPs) that flank the *NF1* locus (4). In this application, we proposed to test the following hypotheses: [1] *NF1* microdeletion breakpoints occur at a small segment that defines a meiotic recombination hotspot(s) within the 15-100 kb NF1REP elements and that homologous recombination at the hotspot is facilitated by a nearby recombinogenic element. [2] Polymorphism in NF1REP number, orientation, and/or complexity predisposes certain individuals to *NF1* microdeletion and the consequent high neurofibroma burden. [3] *NF1* microdeletion increases the risk of developing a solid tumor malignancy. [4] NF1REP-mediated *NF1* microdeletion in somatic cells is an underlying mechanism of loss of heterozygosity at the *NF1* locus in malignant tumors of NF1 patients. This research will identify specific genetic loci and mechanisms that play a role in tumor development in NF1 patients.

Body

Progress described for items/timeline described in the original "Statement of Work" in the grant proposal.

Year 1:

- **Development of a probe to detect NF1REP-mediated *NF1* deletion junction fragments**

We have mapped and sequenced the breakpoints of deletion patients and identified two recombination hotspots for recurrent NF1 microdeletion, along with mapping and sequencing three novel breakpoints. We have developed rapid and accurate polymerase chain reaction (PCR) assays that can detect the recurrent NF1 microdeletions in a blood sample from a patient. These results far exceed our original statement of work, when we envisioned development of a probe for use on Southern blots to detect *NF1* microdeletion junction fragment. Together, these data have confirmed and proven our first hypothesis that *NF1* microdeletion breakpoints occur at a small segment that defines a meiotic recombination hotspot(s) within the 15-100 kb NF1REP elements and that homologous recombination at the hotspot is facilitated by a nearby recombinogenic element. These results are published in the attached manuscripts (5-7).

Stephens K. Genetics of neurofibromatosis 1-associated peripheral nerve sheath tumors. Cancer Invest, in press.

Dorschner MO, Brems H, Le R, et al. Two paralogous recombination hotspots mediate 69% of NF1 microdeletions. submitted.

In summary, we have shown that the majority (14/17) *NF1* microdeletions were 1.5 Mb in length and arose by a mechanism of recombination between misaligned directly-oriented repeat elements that flank the *NF1* gene [termed NF1REP-P1 (proximal) and –M (medial)] of about 15-100 kb in length (4)(Figure 1 below). These repeats are paralogs, which are sequences of high identity that arise by duplication within a species. This year we introduced the term paralogous recombination to describe the process of homologous recombination between paralogs (6). When we mapped *NF1* deletion breakpoints to the sequence level, we unexpectedly discovered that 46% of patients with entire *NF1* gene deletions (N=54) have breakpoints that map to a 2 kb recombination hotspot within the NF1REPs (5). A PCR assay to detect deletion junction fragments was developed by locating the upstream primer in NF1REP-P1 and the downstream primer in NF1REP-M taking advantage of paralogous sequence variants (PSV, which are NF1REP-specific nucleotide differences) between the two paralogs. A 3.4 kb amplicon is produced from deleted chromosomes with breakpoints at this hotspot; however, amplification of the 1.5 Mb segment from normal chromosomes cannot occur.

By mapping and sequencing *NF1* microdeletion breakpoints of additional patients, we have extended the location of this original NF1 microdeletion hotspot and have identified a second hotspot, developed assays to detect deletions at both hotspots, and determined the frequency of *NF1* microdeletion that occurs at these hotspots. These data are described in detail in the attached manuscript Dorschner et al, which is submitted for publication (7)(see attached). In summary, the first hotspot was extended to 4.1 kb in length and designated as paralogous recombination site 1 (PRS1). The second cluster was 6.3 kb in length and extended the cluster harboring the previously defined 2 kb recombination hotspot. This cluster, designated as paralogous recombination site 2 (PRS2), was about 15 kb telomeric to PRS1.

Figure 1. Schematic of the paralogous recombination sites within the NF1REP paralogs. Paralogous recombination between the NF1REP elements results in a recurrent 1.5 Mb deletion of the entire *NF1* locus. The location of the paralogous recombination sites, PRS1 and PRS2, are shown. The stippled portion of PRS2 designates the previously reported 2 kb recombination hotspot, while the hatchmarks designate the extended portion of the site reported here. The basepair coordinates are relative to BAC 271K11, which contains NF1REP-P1.

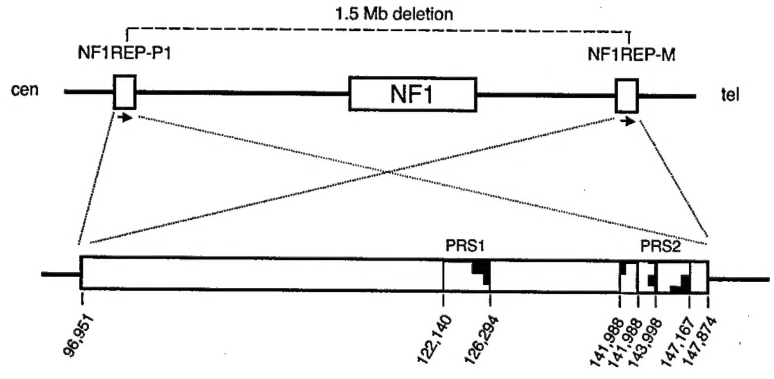

We developed new, rapid, efficient PCR assays that detect *NF1* microdeletions at either PRS1 or PRS2. We applied these assays to screening a larger cohort of *NF1*deletion patients (N=78) and determined that 18% of deletions occurred at PRS1, while (51%) occurred at PRS2. As expected, neither the 7 kb PRS1 nor the 7 kb PRS2 deletion-junction assays generated products upon amplification of 150 normal chromosomes. These assays can be used in clinical laboratories for the diagnosis of NF1 patients that carry the recurrent 1.5 Mb *NF1* microdeletion and in research laboratories to identify patients for phenotype/genotype studies.

In addition to these studies of germline *NF1* microdeletions, we have determined breakpoints in patients who have somatic mosaicism for an *NF1* microdeletion no not occur at the PRS1 or PRS2 hotspots. This implies that these microdeletions may occur by a different mechanism(s). This is important to determine since the somatic *NF1* loss that occurs during tumorigenesis may occur by a similar mechanism. We have mapped two mitotic *NF1* microdeletion breakpoint to the sequence level (Figure 1; UWA186-1 and UWA208-1), developed a deletion junction fragment specific assay, and are using that to determine if other patients mosaic for *NF1* microdeletions have breakpoints clustered at this location. Manuscripts describing these patients and their breakpoints are currently in preparation, (Stephens et al. and Forbes et al.).

NF1REPs are comprised of a complex modular arrangement of paralogs of different sequence families.

Mapping *NF1* breakpoints necessitated a detailed understanding of the structure and sequence of the NF1REP paralogs in order to design appropriate primers and avoid co-amplification of other paralogs. We have determined the structure of four NF1REP paralogs by STS mapping, sequencing, BLAST and BLAT analyses, and sequence alignments. These data do not identify a sequence-specific motif responsible for the recombination hotspots, but rather indicate that multiple factors contribute to the location of the recombination events. These data are detailed in the attached manuscript Forbes et al, which has been submitted for publication (8).

In summary, the relative locations of NF1REP-P1, -P2, and -M are shown in Figure 1, while the paralog designated as E19 is located on chromosome 19p. We are highly confident of the structure of NF1REP-P1, NF1REP-P2, and E19, which are each carried primarily by a single BAC that has been completely sequenced by the public Human Genome Project. Selected PCRs and sequencing in our laboratory of BACs 640N20 and 951F11 (Human Genome Project sequence is incomplete) are consistent with the structure of NF1REP-M. Accuracy of the sequence and structure of the NF1REPs is further supported by numerous long range PCRs, which were consistent with the structures depicted in Figure 2 below.

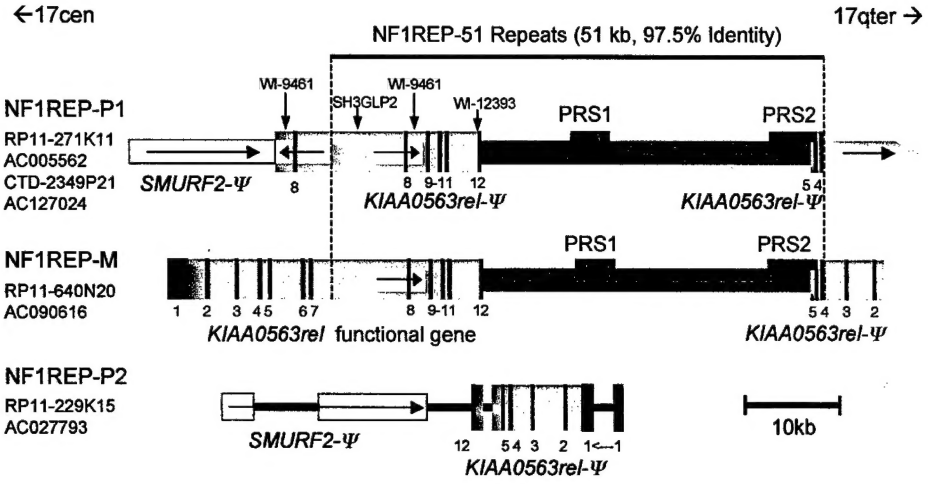
←17cen
17qter →
NF1REP-51 Repeats (51 kb, 97.5% Identity)
NF1REP-P1
RP11-271K11
AC005562
CTD-2349P21
AC127024
WI-9461
SH3GLP2
WI-9461
WI-12393
PRS1
PRS2
SMURF2-Ψ
8
8 9-11 12
KIAA0563rel-Ψ
5 4
KIAA0563rel-Ψ
NF1REP-M
RP11-640N20
AC090616
PRS1
PRS2
1 2 3 4 5 6 7
8 9-11 12
5 4 3 2
KIAA0563rel functional gene
KIAA0563rel-Ψ
NF1REP-P2
RP11-229K15
AC027793
SMURF2-Ψ
12 5 4 3 2 1←1
KIAA0563rel-Ψ
10kb

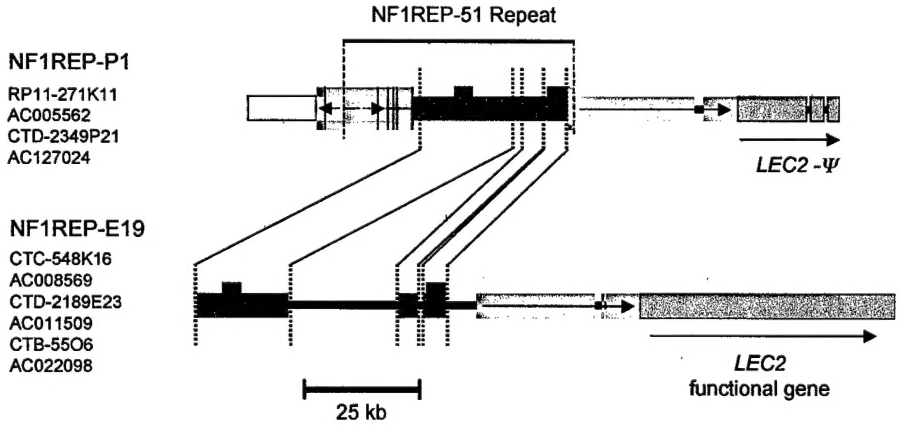
NF1REP-51 Repeat
NF1REP-P1
RP11-271K11
AC005562
CTD-2349P21
AC127024
LEC2 -Ψ
NF1REP-E19
CTC-548K16
AC008569
CTD-2189E23
AC011509
CTB-55O6
AC022098
LEC2
functional gene
25 kb

Figure 2. *Top panel*: The three paralogs in the NF1 region are shown oriented from centromere to telomere. BAC identities and accession numbers are shown. Green color indicates sequences of the KIAA0563rel functional gene and related pseudogene fragments (Ψ), with numbered black vertical bars designating exons or related, exon-derived sequences. Light green boxes within KIAA0563rel copies indicate the orientation of a 5.8 kb inverted repeat with two copies on NF1REP-P1, and a third copy in NF1REP-M. Landmark STSs in the KIAA0563rel gene and pseudogenes cited previously (4) are indicated above NF1REP-P1. Yellow boxes depict SMURF2-derived pseudogene fragments, and red boxes denote the PRS. *Lower panel*: Comparison of NF1REP-P1 to NF1REP-E19 located at chromosome 19p13.13. Colored boxes match those described for panel B. PRS1 and PRS2 sites in NF1REP-E19 are not known to serve as recombination substrates. NF1REP-E19 contains the LEC2 functional gene and NF1REP-P1 contains pseudogene fragments of LEC2 (purple).

As detailed in Forbes et al. (8), we found that theThe NF1REPs are complex with a modular paralog structure that is essentially comprised of mix-and-match components. The principal sequences responsible for the two 51-kb blocks with 97.5% sequence identity (NF1REP-P1-51 and NF1REP-M-51). Here we show that these paralogs belong to a complex group of paralogs from different sequence families with three components on 17q and another at 19p13. Multiple breakpoint sequencing reveals two paralogous recombination hotspots within the 51-kb blocks. We seek to explain the location of the hotspots based on sequence motifs, quality of alignment match, and nucleotide sequence identity. Hotspot locations with respect to relatively large paralogous alignment gaps suggest that the gaps may a primary factor localizing pairing and exchange. Gene conversion tests reveal a 700 bp gene conversion tract at the predominant paralogous recombination hotspot. Thus, high sequence identity at a hotspot may be a result, as well as a potential cause, of propensity to pair at a particular site. Whether alignment gaps are a key breakpoint localization factor may be eventually assessed by discovery and comparison of more systems that—like the NF1REPs—show relatively high levels of alignment mismatch between paralogs.

Constructing a fine, sequence-based map of each NF1REP as described in Forbes et al., was necessary to facilitate experiments to test our second hypothesis that polymorphism in NF1REP number, orientation, and/or complexity predisposes certain individuals to *NF1* microdeletion and the consequent high neurofibroma burden. We are currently examining the NF1REP-P1 and NF1REP-M structure and sequence of the parental chromosomes that underwent recombination to create the de novo *NF1* microdeletion in the affected child. We have constructed human-rodent somatic cell hybrids to separate the two chromosomes 17 of each of the parents. Analysis of the such hybrid lines has identified the two chromosomes that were substrates for the recombination. Analysis of the NF1REP-P1 and NF1REP-M of these chromosomes is currently underway. Originally, we simply amplified NF1REP regions from the genomic DNA of each parent, cloned the amplimers and sequenced the region. However, we found unusual and inconsistent sequences that could not be easily explained. To determine if they were from polymorphism or unusual NF1REP structure, we embarked on the somewhat arduous task of constructing the hybrid lines. Direct sequencing of NF1REP from these lines will avoid cloning artifacts and is expected to determine the precise structure of the parental NF1REP recombination substrates. In addition, we are beginning to screen hybrid lines of normal individuals and genomic DNA of normal

individuals for polymorphism in the NF1REP regions by Southern blot analysis and selected PCR assays.

Gene and transcript map of the *NF1* microdeletion region.

In important resource for understanding the genetic basis of the more severe phenotype observed in *NF1* microdeletion patients is a complete physical map of the *NF1* deletion region at chromosome 17q112. In collaboration with Dr. Dieter E. Jenne (Max-Planck-Institute of Neurobiology), we have combined our map and sequence data and constructed a physical and transcript map of the >2 Mb *NF1* microdeletion region. These data are detailed in the attached manuscript (9).

Years 2 and 3:

- **Ascertainment and sample collection of NF1 patients with tumors**
- **Employ the PRS1 and PRS2 *NF1* gene dosage assays to determine if the frequency of NF1 microdeletions is greater in patients that develop malignancies**

On May 12, 2003, the USAMRMC Human Subjects committee finally approved our protocol. The difficulty of getting this relatively simple protocol approved by this committee has been a major, and unexpected, disappointment of this study. To facilitate completion of this portion of the study, we have a one year no-cost extension for this grant award.

We have identified 430 adults with malignant peripheral nerve sheath tumors (MPNST) that were referred to the University of Washington Medical Center (UWMC). Careful examination of the medical records revealed that 41 had neurofibromatosis 1. We have sent letters to their UWMC care providers and/or their primary referring providers to determine if the patients are alive and to forward a letter to them to determine if they are interested in participating in our study. In addition, we have ascertained 17 children affected with NF1 who had solid tumor malignancies, primarily optic glioma and MPNST. We are currently preparing materials to be sent to their care providers to determine interest in our study.

In addition, we are screening the tumor database at UWMC to identify NF1 patients who had solid malignancies other than MPNST. If sufficient patients are identified, we will also screen them for *NF1* microdeletions.

Year 3:

Genotype grandparents to determine meiotic mechanism of microdeletion

For the following reasons, we have decided not focus on this one small aspect of our study. We will proceed to collect grandparental samples, but this aim may not be accomplished during the grant period. The reasons are:

1. We have little time remaining to obtain grandparental samples because of the extended length of time it took to obtain approval from the USAMRMC Human Subjects committee,
2. With the limited time we have left to accomplish the work, we have decided to focus our efforts the phase of the study regarding risk of malignancy

3. This aim is of less importance because another research group has investigated and published work related to this question (10).

Employ *NF1* microdeletion assays to detect NF1REP-mediated deletion junction fragment in tumor tissue of *NF1* patients

Hypothesis number 4 that NF1REP-mediated *NF1* microdeletion in somatic cells is an underlying mechanism of loss of heterozygosity at the *NF1* locus in malignant tumors of NF1 patients awaits our obtaining such tissues for analysis now that our Human Subject protocol has been approved by the Army.

However, this hypothesis has been disproven for benign neurofibromas. Using the PRS1 and PRS2 deletion junction-specific amplification assays, we have screened DNA from 171 cutaneous and plexiform neurofibromas and have not detected *NF1* microdeletions at these recombination hotspots. If somatic paralogous recombination is a mechanism of loss of heterozygosity at *NF1* during neurofibromagenesis, it occurs at novel sites.

Development of new quantitative PCR assays to detect novel *NF1* microdeletions that occur in germline or somatic tissues.

Since approval of our Human Subjects protocol was delayed much longer than we anticipated, we made valuable use of our time by developing new, highly sensitive, quantitative PCR assays to detect *NF1* microdeletions of any length in either germline or somatic tissues.

These assays required the capability and sensitivity to determine if a locus or gene has no deletion (2 copies), one gene deletion (1 copy), two gene deletion (0 copies), or amplification (likely >10 copies). Two gene deletion and gene amplification are simple to detect using various methods of quantitative PCR. The difficulty is in reliably differentiating one versus two copies of a gene. Therefore, we have been focusing on developing the best assay to detect a one gene deletion. To determine which quantitative PCR methods were sensitive, we choose to develop an assay at intron 31 of the NF1 gene. To validate the assays we used DNA from normal individuals (2 NF1 genes) and DNA from NF1 patients with deletions involving the NF1 gene (1 NF1 gene). Initially, we tried using SYBR green (binds double stranded DNA) fluorescence as a method of detection during real-time PCR in the LightCycler instrument (Roche). There was considerable overlap between the crossing point values (Ct) for samples with one and two NF1 genes indicating that the assay was not as sensitive or specific as required (data not show). Secondly, we sought to increase specificity and sensitivity by using a NF1- specific fluorescently-labeled primer. We constructed a LUX primer (Invitrogen), which is a hybrid primer comprised of NF1 specific sequences and anonymous sequences that are capable of fold-back annealing. LUX primers are touted as having high specificity because they only fluoresce at high temperatures when the fold backs are melted. We had multiple problems with LUX primers and decided to abandon that approach (data not shown). The third method we developed was precise, sensitive, and specific and involves SYBR green for detection, competitive quantitative PCR, and melting curve analysis as detailed below.

We chose to employ SYBR green for detection in combination with competitive PCR, which is the most suitable method of quantification when highly accurate determinations are required. We adapted and modified a method published by Ruiz-Ponte et al. (11). In this method, a known copy number of a competitor is introduced directly in the PCR mixture along with the target DNA of the patient/tumor. The competitor, which is almost identical to the target DNA but distinguishable by product length, is amplified with the same set of primers so that efficiency of amplification for the two amplicons is the same. Calibration curves of different competitor concentrations determines the optimal concentration that equals that of the target DNA. Figure 3 below shows the melting curves of a normal control DNA samples (2 copies of NF1), where competitor and intron 31 are co-amplified with equal efficiency and the area under the curves are equal (roughly equivalent to peak height in this example). We constructed the competitor such that it would be amplified with the intron 31 primers, but have a different melting curve by replacing an internal TTT sequence with a CCC sequence. As expected, negative samples lacking human DNA did not amplify.

Figure 4 below shows the melting curve of a patient with an NF1 deletion (1 copy of NF1) versus that of the normal control individual. Note that the amplitude of the melting curve of the NF1 amplicon for the deletion patient is less that of the competitor amplicon because there are fewer targets in the deleted patient's DNA. For precision, we use the peak areas of each melting curves for quantitation rather than peak height. A ratio of peak area of normal control (2 copies) over the peak are of the patient target DNA is calculated, see below.

Figure 3. Melting curve analysis after competitive, quantitative PCR at NF1 intron 31 in genomic DNA of a normal control individual. The peaks representing the melting curve of the amplicon of the competitor and the amplicon of the patient's target DNA are indicated. The negative control without DNA shows evidence of amplificiation.

Figure 4. Melting curve analysis after competitive, quantitative PCR at NF1 intron 31 can differentiate one gene copy versus two gene copies. The results of two reactions are shown, closed circles represent target DNA from a normal control individual and closed squares represent target DNA from an NF1 patient with a deletion of one gene. The peaks representing the melting curve of the amplicon of the competitor and the amplicon of the patient's target DNA are indicated. The negative control without DNA shows evidence of amplification.

Once the concentration of competitor is determined for a certain concentration of the normal control DNA, it is essential that all subsequent reactions with unknown patient DNA samples contain exactly the same concentration of target DNA. Prior to the competitive quantitative PCR assay, we determine the exact concentration of each patient sample using real-time quantitative PCR at a different locus. We amplify the TPA (tissue plasminogen activator) gene on chromosome 12 in each patient and compare that to a standard curve using the normal control DNA. From this reaction, we can calculate exactly what volume of patient DNA must be added to the competitive quantitative PCR assay. An example of the TPA real-time PCR and standard curve is shown in Figure 5.

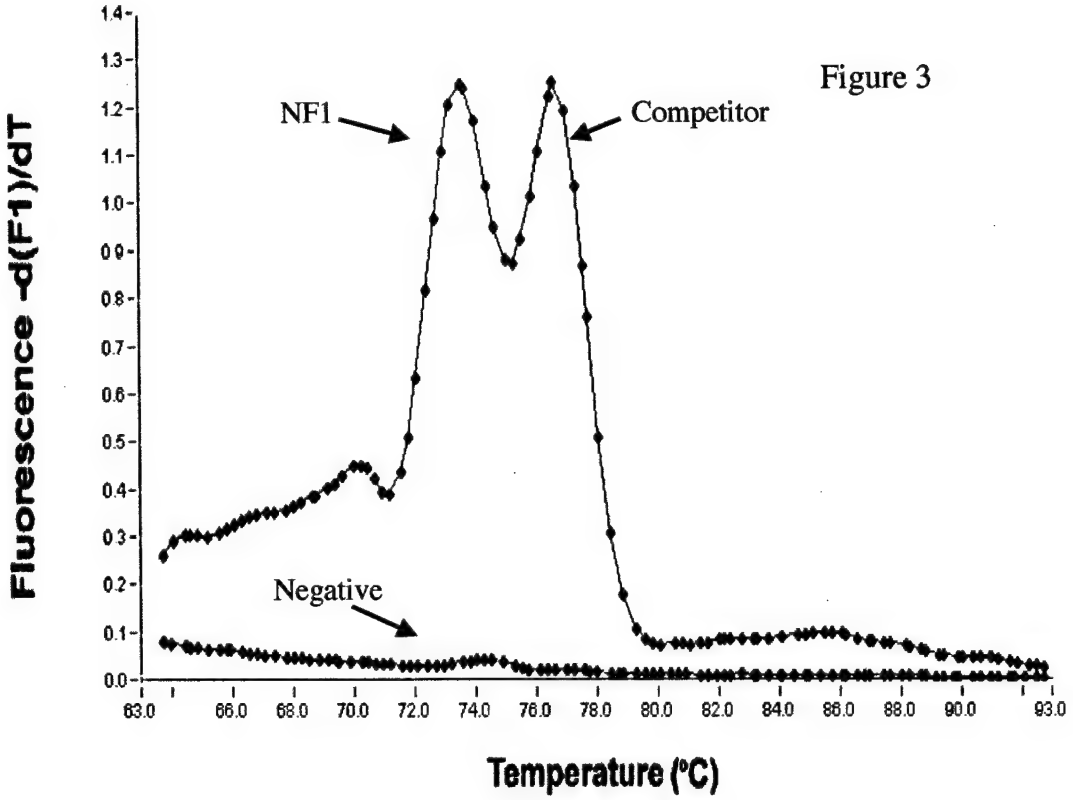

Figure 3

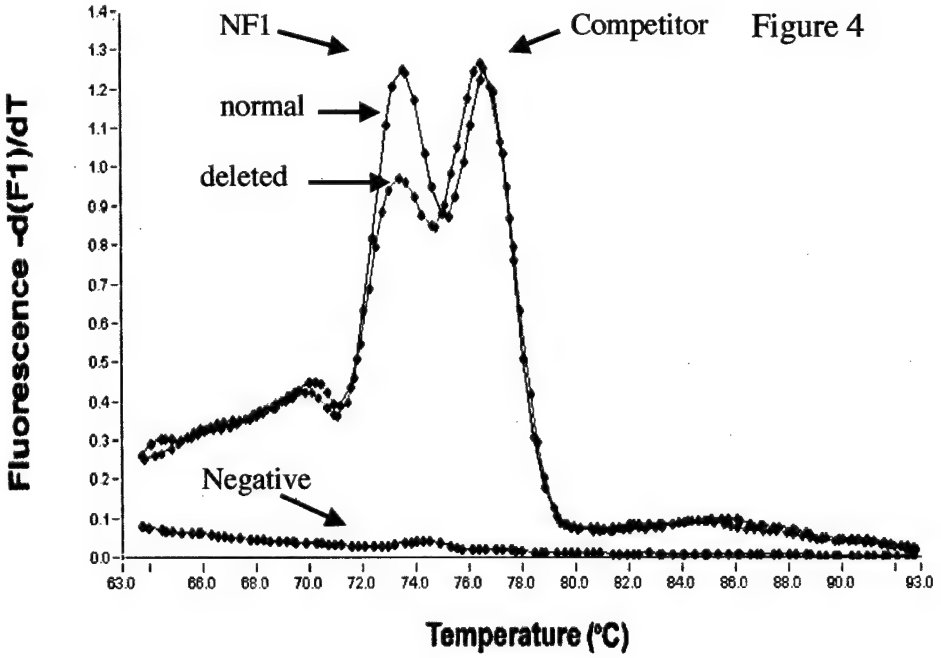

Figure 4

Figure 5. LightCycler real-time PCR at TPA locus showing standard curve. The upper panel shows the results of real-time PCR of the TPA locus of a dilution series of a normal control individual. The reaction consists of unlabeled primers and uses an internal labeled (fluorescence resonance energy transfer (FRET) probe for detection of product. The crossing point (Ct) is defined as the fractional cycle at which fluorescence begins to increase exponentially and is calculated by the LightCycler. Ct becomes larger as the number of TPA targets decreases. The lower panel shows the standard curve calculated from the above data. Note the low error and high correlation coefficient.

The competitive quantitative gene dosage assay we have developed for intron 31 of the NF1 gene is very precise and shows minimal variability. Figures 6 and 7 below shows melting curves for 6 replicates of an NF1 deletion patient and a normal control individual, respectively.

Figure 6. Melting curves of competitive quantitative PCR at NF1 intron 31 of 6 replicates of an NF1 deletion patient. Six curves (color replaced by grey tones for this report) are overlaid to demonstrate the precision and lack of variability in replicate samples.

Figure 7. Melting curves of competitive quantitative PCR at NF1 intron 31 of 6 replicates of a normal control individual. Six curves (color replaced by grey tones for this report) are overlaid to demonstrate the precision and lack of variability in replicate samples.

Figure 5

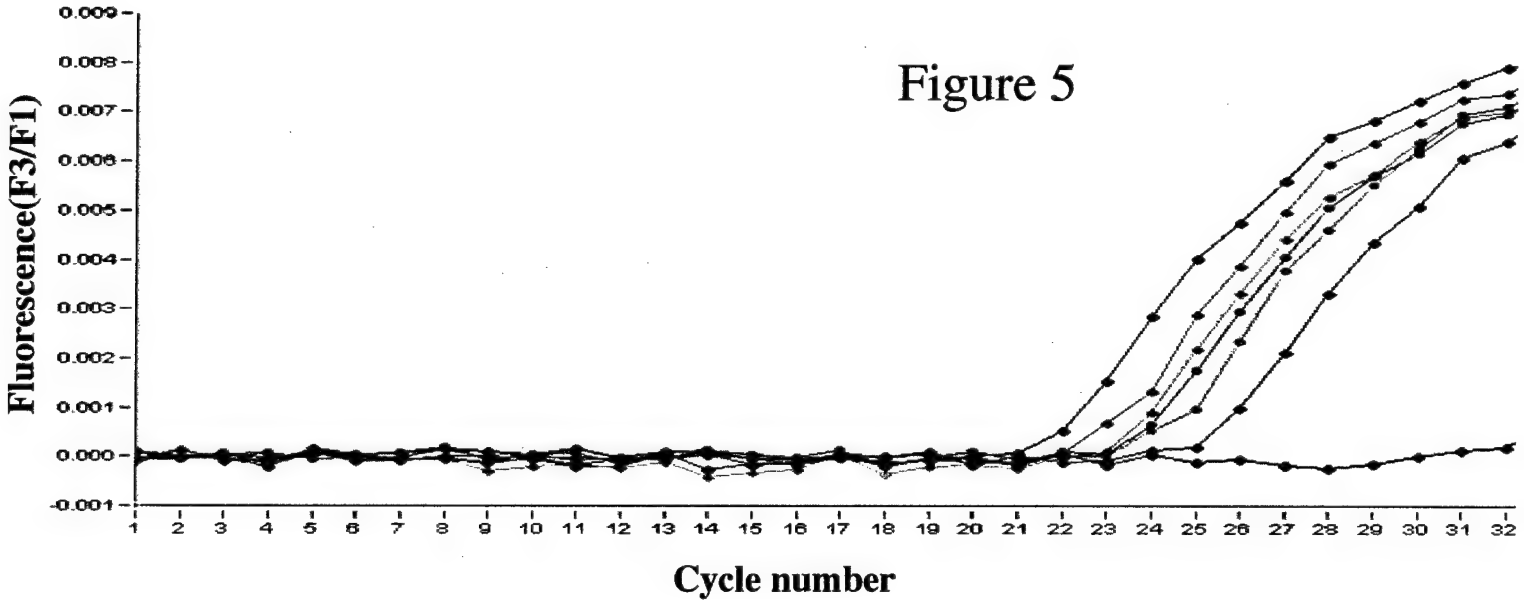
Fluorescence(F3/F1)
0.009
0.008
0.007
0.006
0.005
0.004
0.003
0.002
0.001
0.000
-0.001
1 2 3 4 5 6 7 8 9 10 11 12 13 14 15 16 17 18 19 20 21 22 23 24 25 26 27 28 29 30 31 32
Cycle number

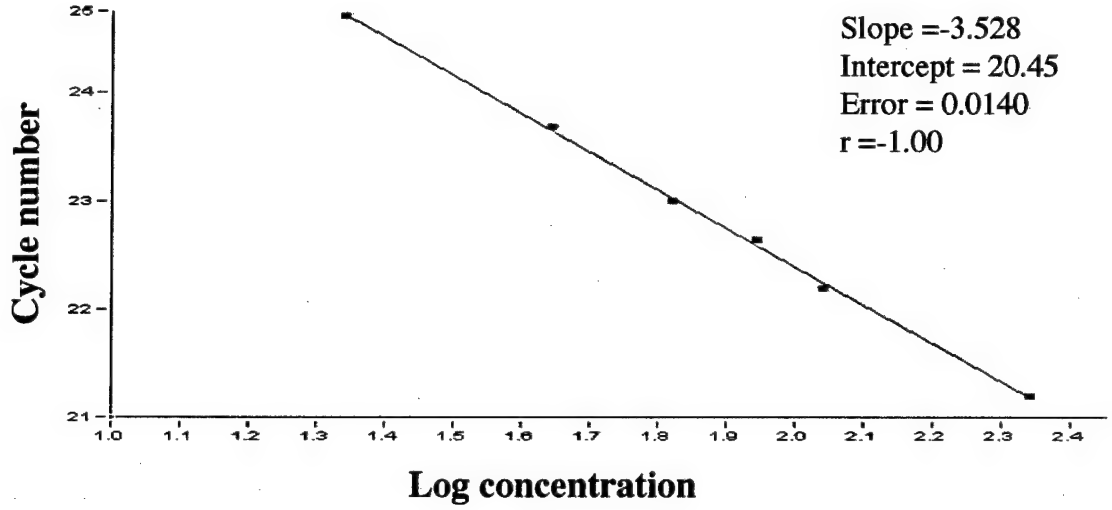
Cycle number
25
24
23
22
21
1.0 1.1 1.2 1.3 1.4 1.5 1.6 1.7 1.8 1.9 2.0 2.1 2.2 2.3 2.4
Log concentration
Slope =-3.528
Intercept = 20.45
Error = 0.0140
r =-1.00

Figure 6

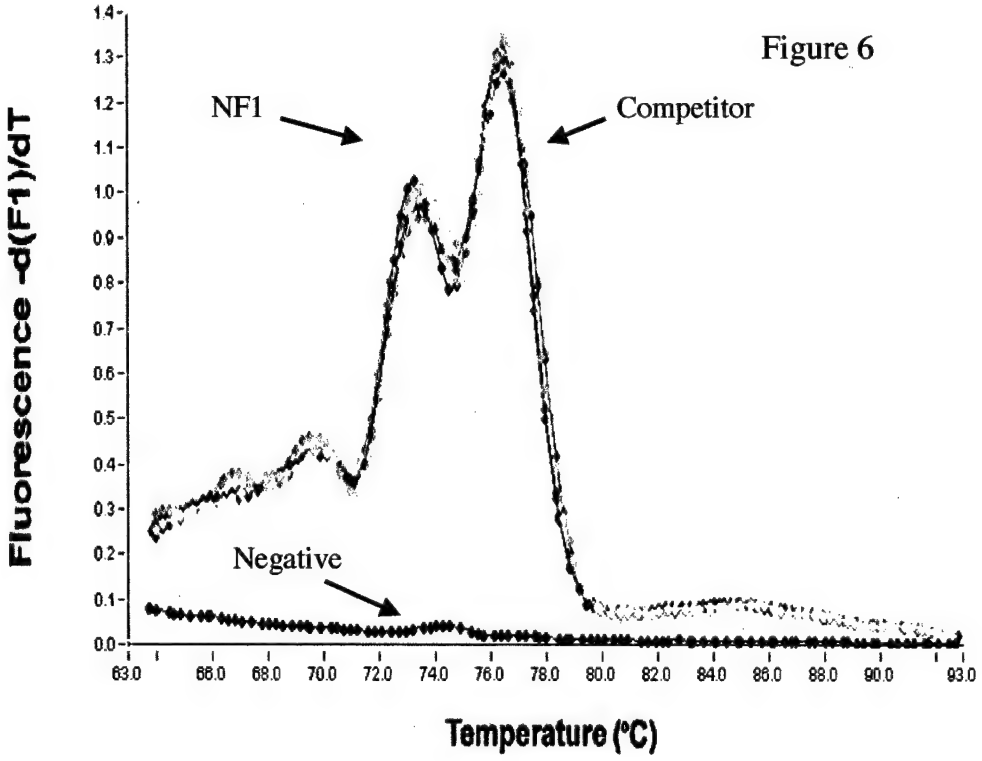

Figure 7

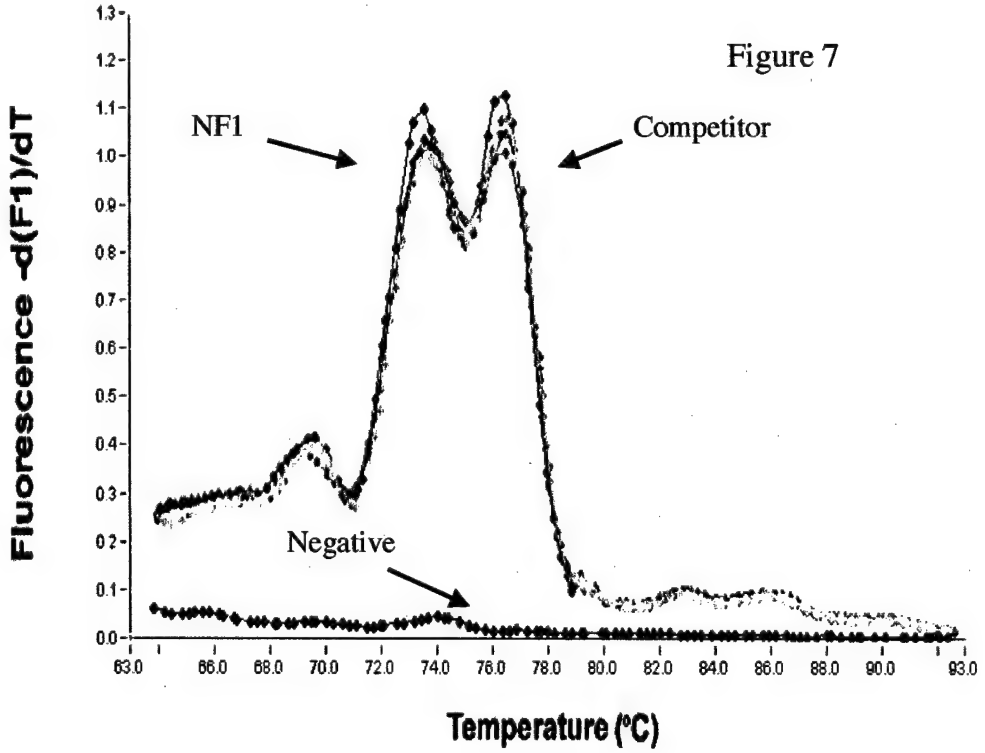

These data will be analyzed as shown in the tables below. First, note the precision of the assay; the standard deviations are only 2% and 3% of the means of the assay for normal control individuals and deletion patients, respectively. As expected the ratio of NF1:competitor peak areas is essential 1.0 for samples with two copies of the NF1 gene and is 0.5 for samples with one copy of the NF1 gene. We have screened a large collection of NF1 deletion patients and normal individuals and found that there is no overlap of ratio values between these two populations.

Therefore, we have developed a sensitive and specific assay that differentiates reliably between one versus two copies of a gene. We are now applying this same assay to determine its ability to quantitate amplified loci.

Replicates of competitive quantitative PCR for intron 33 of NF1 or normal control individual

No.	Area of *NF1* peak	Area of Competitor Peak	Ratio	Mean Ratio	S.D.
1	3.219	2.957	1.088		
2	3.262	3.296	0.989		
3	3.097	3.255	0.951		
4	3.464	3.26	1.062		
5	3.433	3.278	1.047		
6	3.091	2.918	1.059		
				1.033	0.0211

Replicates of competitive quantitative PCR for intron 33 of NF1 for deleted patient

No.	Area of *NF1* peak	Area of Competitor Peak	Ratio	Mean Ratio	S.D.
1	1.937	3.85	0.503		
2	2.103	3.68	0.571		
3	1.952	3.755	0.519		
4	2.052	3.356	0.611		
5	1.851	3.665	0.505		
6	1.934	3.33	0.580		
				0.548	0.0185

We are currently developing similar quantitative PCR assays for *NF1* exon 5 and two loci that flank the gene (AN and AH). These assays can be used together to identify and crudely map the extent of new *NF1* microdeletions.

New grant awarded based on this research:

4/7/03-4/6/07 US Army Medical Research & Materiel Command DAMD 17-03-1-0203
Clinical and Molecular Consequences of NF1 Microdeletion
Principal Investigator: Karen Stephens, PhD

Key Research Accomplishments

- Identification of two recombination hotspots where 69% of germline *NF1* microdeletions occur. This is important because 1) these hotspots can be analyzed in detail to investigate why recombination is favored at these sites and 2) the majority of microdeletion patients will have virtually the same genotype and will therefore constitute an important patient cohort for genotype/phenotype analyses.
- Development of simple and reliable PCR assays that detect the presence of the recurrent 1.5 Mb germline *NF1* microdeletion in a patient blood sample.
- Showed that loss of heterozygosity in benign neurofibromas does not commonly occur at the *NF1* microdeletion hotspots found in germline *NF1* microdeletions
- Somatic mosaic microdeletions occur at different sites than germline microdeletions. This implies that they occur by a novel mechanism, which may also apply during tumorigenesis.
- A detailed structural and sequence analysis of the *NF1* paralogs, NF1REP-P1, P2, and M, which identified factors that may contribute to the recombination at hotspots PRS1 and PRS2.
- Developed a specific and sensitive competitive, quantitative PCR methodology that can differentiate one copy from two copies in a genome. Employed real-time PCR of the TPA locus as a means of precise DNA quantification. Validated the competitive, quantitative PCR methodology by assay of the NF1 locus in normal control individuals and NF1 deletion patients.

- Documented the reproducibility of the competitive, quantitative PCR method.

Reportable Outcomes

Manuscripts, Peer-reviewed, primary research:

Messiaen L, Riccardi V, Peltonen J, Maertens O, Callens T, Karvonen SL, Leisti E-L, Koivunen J, Vandenbroucke I, Stephens K, Pöyhönen M. Type of NF1 mutations in two large families with spinal neurofibromatosis cannot account for the clinical homogeneity in severity of the disease. J Med Genet 40:122-126, 2003.

Jenne DE, Tinschert S, Dorschner MO, Hameister H, Stephens K, Kehrer-Sawatzki H. Complete physical map and gene content of the human NF1 tumor suppressor region in human and mouse. Genes Chromosomes Cancer 37:111-20, 2003

Fishbein L, Sanek N, Stephens K, Wallace MR. An association between the ERBB2 codon 655 polymorphism and NF1. Am J Med Genet, submitted.

Dorschner MO, Brems H, Le R, et al. Two paralogous recombination hotspots mediate 69% of NF1 microdeletions. submitted.

Forbes, S.H., Dorschner, M.O., Le, R. and Stephens, K. Genomic context of paralogous recombination substrates mediating the recurrent NF1 region microdeletion. Genome Res, submitted.

Invited Reviews:

Stephens K. Genetics of neurofibromatosis 1-associated peripheral nerve sheath tumors. Cancer Invest, in press (Dec, 2003).

Book Chapters:

Stephens K. Neurofibromatosis. In *Molecular Pathology in Clinical Practice*, Eds. D.G.B. Leonard, A. Bagg, A. Caliendo, K. Kaul, K. Snow-Bailey, V. Van Deerlin, Springer-Verlag, in press.

Abstracts

Stephens, K. About 70% of NF1 microdeletions are recurrent and occur at discrete recombination sites within the flanking NF1REP paralogs, which are complex modular assemblies of low-copy repeats of different sequence families. National Neurofibromatosis Foundation International Consortium on Gene Cloning and Gene Function of NF1 and NF2. Aspen, CO, June, 2003.

Conference speaker, invited:

National Neurofibromatosis Foundation International Consortium on Gene Cloning and Gene Function of NF1 and NF2. "Megabase Deletions", Aspen, CO, June, 2003.

Invited speaker to lay organizations, Community Service

NF1 Roundtable Discussion and Symposium, Washington Chapter of the National Neurofibromatosis Foundation, Seattle, WA, May 10, 2003, Panelist

NF1 Research. Illinois Neurofibromatosis, Inc., Chicago, IL, October 19, 2003.

Development of clinical diagnostic assays to detect *NF1* microdeletion.
Simple and reliable assays were developed to detect the presence of an NF1 microdeletion in a patient blood sample. Using two different polymerase chain reaction assays, we can detect 69% of NF1 microdeletions. We have transferred the technology and resources for these assays to the UWMC Genetics Laboratory and an *NF1* microdeletion clinical test is now available to physicians worldwide.

Development of research assays to detect *NF1* microdeletion

Development of competitive, quantitative PCR assays for differentiating one versus two copies of NF1 gene intron 31.

Training

Stephen H. Forbes, PhD, is being trained in the molecular genetics of neurofibromatosis 1.
Bingbing Wang, PhD, MD, Postdoctoral Fellow, is being trained in the molecular genetics of neurofibromatosis 1.

Funding Awarded based on work supported by this award

4/7/03-4/6/07 US Army Medical Research & Materiel Command DAMD 17-03-1-0203
Clinical and Molecular Consequences of NF1 Microdeletion
Principal Investigator: Karen Stephens, PhD

Conclusions

Neurofibromatosis type 1 affects 1/4000 individuals worldwide and predisposes to the growth of both benign and malignant tumors. Genetic factors, in addition to defects in the NF1 gene itself, clearly play a role in tumor development. Our research is focused on identifying specific DNA sequences and genetic mechanisms important in the development of cutaneous neurofibromas, which occur in virtually all NF1 patients, and in the development of solid malignancies. We have analyzed NF1 microdeletions that are associated with an early onset, and subsequent heavy burden, of cutaneous neurofibromas. We determined the mechanism by which these deletions arise and identified recombination hotspots where 69% of NF1 microdeletions. We developed developed robust and sensitive assays to detect microdeletions in a patient blood sample; these assays can be directly applied in clinical diagnostic laboratories. We identified four NF1REP paralogs, analyzed their structure and sequence, and identified unique features that may mediate recombination at these sites and make some chromosome susceptible to NF1 microdeletion. In addition, we found that the NF1 microdeletions in some patients occurred early during embryonic development resulting in somatic mosaicism. We developed quantitative PCR assays to detect novel *NF1* microdeletions that occur either in the germline or in somatic tissues. An understanding of how *NF1* microdeletions occur, whether some individuals are more susceptible, and why they potentiate the development of neurofibromas is important for patient care, genetic counseling, and the design of effective pharmacological intervention strategies.

References

1. Kayes, L.M., Burke, W., Riccardi, V.M., Bennett, R., Ehrlich, P., Rubenstein, A. and Stephens, K. (1994) Deletions spanning the neurofibromatosis 1 gene: identification and phenotype of five patients. *American Journal Of Human Genetics,* **54,** 424-36.
2. Leppig, K.A., Viskochil, D., Neil, S., Rubenstein, A., Johnson, V.P., Zhu, X.L., Brothman, A.R. and Stephens, K. (1996) The detection of contiguous gene deletions at the neurofibromatosis 1 locus with fluorescence in situ hybridization. *Cytogenetics and Cell Genetics.,* **72,** 95-8.
3. Leppig, K., Kaplan, P., Viskochil, D., Weaver, M., Orterberg, J. and Stephens, K. (1997) Familial neurofibromatosis 1 gene deletions: cosegregation with distinctive facial features and early onset of cutaneous neurofibromas. *American Journal of Medical Genetics,* **73,** 197-204.
4. Dorschner, M.O., Sybert, V.P., Weaver, M., Pletcher, B.A. and Stephens, K. (2000) NF1 microdeletion breakpoints are clustered at flanking repetitive sequences. *Hum Mol Genet,* **9,** 35-46.
5. Lopez-Correa, C., Dorschner, M., Brems, H., Lazaro, C., Clementi, M., Upadhyaya, M., Dooijes, D., Moog, U., Kehrer-Sawatzki, H., Rutkowski, J.L. *et al.* (2001) Recombination hotspot in NF1 microdeletion patients. *Hum Mol Genet,* **10,** 1387-1392.
6. Stephens, K. (in press) Genetics of neurofibromatosis 1-associated peripheral nerve sheath tumors. *Cancer Invest,* in press.
7. Dorschner, M.O., Brems, H., Le, R., De Raedt, T., Wallace, M.R., Curry, C.J., Aylsworth, A.S., Haan, E.A., Zackai, E.H., Lazaro, C. *et al.* (submitted) Two paralogous recombination hotspots mediate 69% of *NF1* microdeletions.
8. Forbes, S.H., Dorschner, M.O., Le, R. and Stephens, K. (submitted) Genomic context of paralogous recombination substrates mediating the recurrent NF1 region microdeletion. *Genome Res.*
9. Jenne, D.E., Tinschert, S., Dorschner, M.O., Hameister, H., Stephens, K. and Kehrer-Sawatzki, H. (2003) Complete physical map and gene content of the human NF1 tumor suppressor region in human and mouse. *Genes, Chromosomes and Cancer.,* **37,** 111-20.
10. Lopez-Correa, C., Brems, H., Lazaro, C., Marynen, P. and Legius, E. (2000) Unequal Meiotic Crossover: A Frequent Cause of NF1 Microdeletions. *American Journal Of Human Genetics,* **66,** 1969-1974.
11. Ruiz-Ponte, C., Loidi, L., Vega, A., Carracedo, A. and Barros, F. (2000) Rapid real-time fluorescent PCR gene dosage test for the diagnosis of DNA duplications and deletions. *Clinical Chemistry.,* **46,** 1574-82.

Appendices

1. Messiaen L, Riccardi V, Peltonen J, Maertens O, Callens T, Karvonen SL, Leisti E-L, Koivunen J, Vandenbroucke I, Stephens K, Pöyhönen M. Type of NF1 mutations in two large families with spinal neurofibromatosis cannot account for the clinical homogeneity in severity of the disease. J Med Genet 40:122-126, 2003.
2. Jenne DE, Tinschert S, Dorschner MO, Hameister H, Stephens K, Kehrer-Sawatzki H. Complete physical map and gene content of the human NF1 tumor suppressor region in human and mouse. Genes Chromosomes Cancer 37:111-20, 2003
3. Stephens K. Genetics of neurofibromatosis 1-associated peripheral nerve sheath tumors. Cancer Invest, in press.
4. Stephens K. Neurofibromatosis. In *Molecular Pathology in Clinical Practice*, Eds. D.G.B. Leonard, A. Bagg, A. Caliendo, K. Kaul, K. Snow-Bailey, V. Van Deerlin, Springer-Verlag, in press.
5. Fishbein L, Sanek N, Stephens K, Wallace MR. An association between the ERBB2 codon 655 polymorphism and NF1. Am J Med Genet, submitted.
6. Dorschner MO, Brems H, Le R, et al. Two paralogous recombination hotspots mediate 69% of NF1 microdeletions. submitted.
7. Forbes, S.H., Dorschner, M.O., Le, R. and Stephens, K. Genomic context of paralogous recombination substrates mediating the recurrent NF1 region microdeletion. Genome Res, submitted.
8. Abstract: Stephens K. About 70% of *NF1* microdeletions are recurrent and occur at discrete recombination sites within the flanking NF1REP patalogs, which are complex modular assemblies of low-copy repeats of different sequence families.

LETTER TO JMG

Independent *NF1* mutations in two large families with spinal neurofibromatosis

L Messiaen, V Riccardi, J Peltonen, O Maertens, T Callens, S L Karvonen, E-L Leisti, J Koivunen, I Vandenbroucke, K Stephens, M Pöyhönen

J Med Genet 2003;**40**:122–126

The neurofibromatoses are a group of neurocutaneous disorders that show extreme clinical heterogeneity and are characterised by growth abnormalities in tissues derived from the embryonic neural crest.[1 2] Two main clinical forms exist, type 1 (NF1) and type 2 (NF2), as well as several alternate and related forms.[2 3] NF1 and NF2 are the only clinically well defined disorders and both genes have been identified.[4–8] The NIH diagnostic criteria for NF1, as defined by the conference statement,[9] are met if two or more of the following are found: six or more CAL spots; two or more neurofibromas of any type or one plexiform neurofibroma; axillary or inguinal freckling; optic glioma; two or more Lisch nodules; a distinct osseous lesion; a first degree relative (parent, sib, or offspring) with NF1 according to the above criteria.

Spinal nerve sheath tumours are described as symptomatic findings in only 5% of NF1 patients,[10] although they can be observed by MRI in up to 36% of patients.[11–13] The presence of a wide, symmetrical distribution of spinal neurofibromas, occurring in all adult affected members of the same family and segregating in an autosomal dominant fashion, is however extremely rare. This form, familial spinal NF (FSNF), has been considered an alternate form of NF since patients generally lack dermal neurofibromas and Lisch nodules, both typical hallmarks of NF1, and since symptomatic and generalised spinal neurofibromas are uncommon in classical NF1. FSNF has been reported in only four families.[12 14 15] Three multigenerational families with spinal neurofibromas and CAL spots were shown to be linked to markers surrounding the *NF1* locus.[12 14 15] In the fourth family, presenting with spinal neurofibromas without CAL spots, linkage to the *NF1* locus was excluded.[14] Only in one FSNF family has the underlying molecular defect been documented so far,[15] which was a unique frameshift mutation 8042insA in *NF1* exon 46. Here we describe the identification of the *NF1* mutation in both remaining FSNF families originally described by Pulst *et al*[14] and Pöyhönen *et al*.[12] Our current findings emphasise that FSNF (with CAL macules) is caused by mutations in the *NF1* gene, but does not support the hypothesis that it is caused by a unique type of *NF1* mutation.

Key points

- Familial spinal neurofibromatosis (FSNF) is considered to be an alternate form of neurofibromatosis, with a limited phenotype of multiple spinal nerve root neurofibromas and café au lait (CAL) macules in all affected adults. Only three multigeneration families with FSNF have been reported and in one of them the genetic defect was identified previously: 8042insA in exon 46 of the *NF1* gene.
- As NF1 is notorious for its extreme phenotypic variability even within the same family, the striking homogeneity of the phenotype in these families suggests that a particular type of mutation might underlie this condition.
- We identified the *NF1* mutation in the remaining two FSNF families whose phenotype was known to be linked to chromosome 17q11.2 markers. In the first family, a novel substitution at the splice donor site of exon 39 (7126+3A>C), leading to skipping of exon 39, was found. In the second family, a missense mutation L357P in exon 8 was identified as the sole alteration. The mutation segregates with the disease in both families.
- The current findings emphasise that FSNF (with CAL macules) is caused by mutations in the *NF1* gene, but does not support the hypothesis that it is caused by a specific type of *NF1* mutation. It is anticipated that expression studies and mutation analysis, in the first instance of the genes tightly linked to the *NF1* locus, in both families may lead to the detection of (a) modifier(s) for this specific phenotype.

MATERIALS AND METHODS

Subjects

The pedigrees of the families studied are shown in figs 1A and 2.

Skin samples of controls were obtained from operations carried out for cosmetic reasons from four healthy persons at the Department of Dermatology, University of Oulu, Finland, with the consent of the Ethical Committee of Oulu University Hospital.

NF1 mutation analysis

Epstein-Barr virus (EBV) lymphoblastoid cell cultures from two affected members of family 1 and fibroblast cell cultures from two affected members of family 2 were treated with and without puromycin before total RNA extraction as described previously.[16] DNA was extracted from EBV cell cultures or fibroblasts from all family members.

The optimised PTT for the entire coding region was applied essentially as described previously with abnormal fragments further analysed by cDNA and genomic sequencing.[16] Then, for both families, the entire *NF1* cDNA was sequenced using dye-primer chemistry on an automatic genetic analyser (ALFexpress). Information on the sequencing primers used is available upon request.

Western blot analysis

Western blot analysis, using an anti-NF1 antibody (NF1GRD(D)) (Santa Cruz Biotechnology Inc, Santa Cruz, CA) and peroxidase linked donkey anti-rabbit (NA 934) (Amersham International plc, Little Chalfont, Buckinghamshire, England) as a secondary antibody, was carried out essentially as previously described.[17]

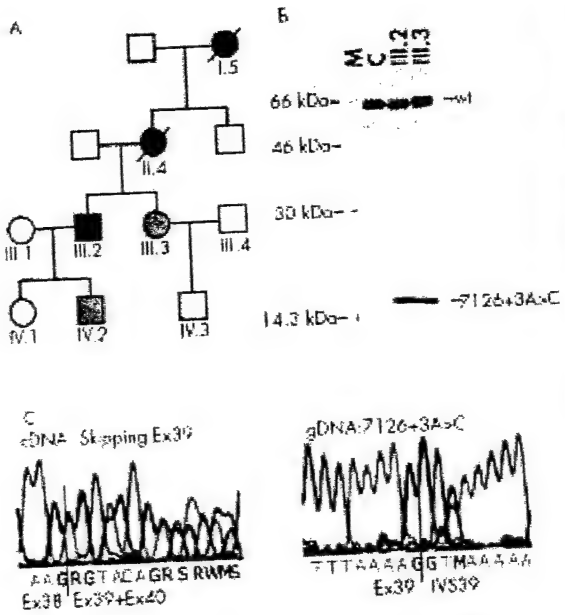

Figure 1 Pedigree and PTT results of family 1 with mutation 7126+3A>C. (A) In the pedigree, blackened symbols denote affected subjects with spinal neurofibromas and CAL spots, grey symbols denote affected subjects with CAL spots only, and white symbols denote healthy subjects. (B) PTT results using primers encompassing exons 34 to 49 of a control (C) and of patients III.2 and III.3. The wild type (wt) and aberrant band caused by skipping of exon 39 are shown. M denotes a protein marker with sizes in kDa. (C) Direct cycle sequencing of mutant cDNA transcripts and genomic DNA. By direct cDNA sequencing of the patient, heterozygosity for transcripts containing exon 39 and transcripts in which exon 39 is skipped are seen. In the genomic DNA, heterozygosity for A and C at position +3 of the splice donor site of exon 39 is seen in the patient.

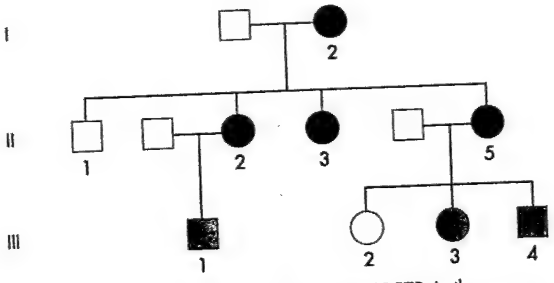

Figure 2 Pedigree of family 2 with mutation L357P. In the pedigree, blackened symbols denote affected subjects with spinal neurofibromas and CAL spots, grey symbols denote affected subjects with CAL spots only, and white symbols denote healthy subjects.

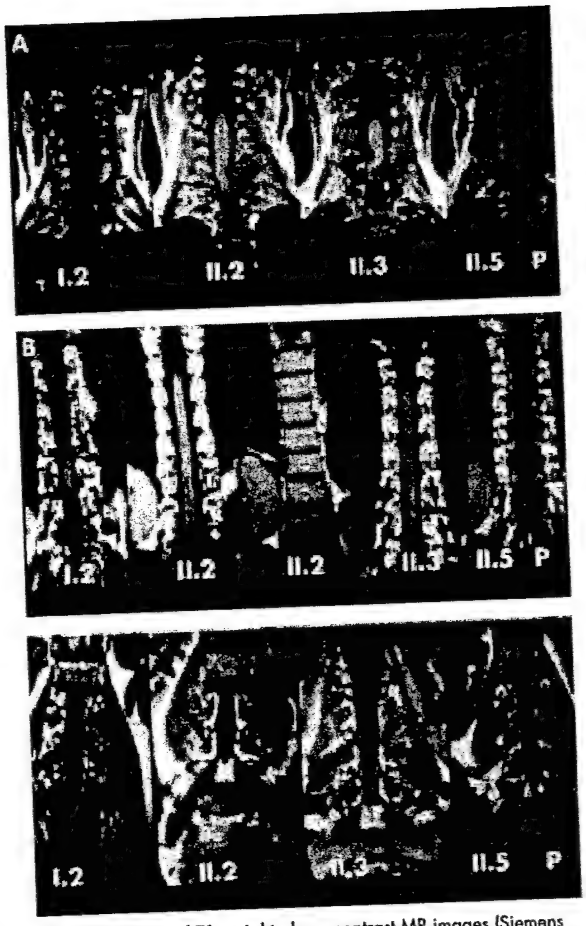

Figure 3 Coronal T1 weighted non-contrast MR images (Siemens Magnetom 1.0T, SE, TR 500, TE 15, slice thickness 3 mm) of patients I.2, II.2, II.3, and II.5 (P=proband) from family 2, carrying the mutation L357P. (A) Cervical spine. (B) Thoracic spine. (C) Lumbar spine. Several extradural, intraspinal neurofibromas compressing the spinal cord (black curved arrows) and extraspinal neurofibromas (black straight arrows) are seen in all patients. Not all tumours are marked. II.2 also has a right sided paraspinal thoracic mass (white arrow). The intra- and extraspinal components of a dumb-bell tumour in the lumbar spine (thick black arrow) in patient II.3 are shown.

RESULTS

Clinical evaluation

In both families all affected adults, except for one 45 year old female in family 1 (III.3) showed multiple symmetrically distributed spinal neurofibromas in the cervical, thoracic, and/or lumbar region (fig 3). All 12 affected members in both families also had more than six (size over 15 mm) cutaneous CAL spots, but no iris Lisch nodules were present. Clinical data, originally described by Pulst *et al*[14] and Pöyhönen *et al*,[12] have been updated and are summarised in table 1.

Molecular analysis

In family 1, PTT analysis of the *NF1* cDNA of patients III.2 and III.3, encompassing exons 35 to 49, showed in addition to the wild type 68.5 kDa product a truncated polypeptide of approximately 19 kDa, suggesting a truncating mutation between nucleotides 6900 and 7200 (fig 1B). Sequencing of the RT-PCR product showed absence of the whole of exon 39 (fig 1C). By genomic DNA sequencing, a novel substitution, 7126+3A>C (fig 1C), was found at the splice donor site of exon 39. This is a novel mutation not identified previously in classical NF1 patients. We calculated the splice site donor strength from the wild type sequence (7126+3A) and the mutant sequence (7126+3C) using the algorithms developed by Shapiro and Senepathy[18] (S&S) and using the Splice Site Prediction by Neural Network (SSPNN, http://www.fruitfly.org/seq_tools/splice.html) program. The scores for the mutant sequence (69.9 (S&S) and 0.09 (SSPNN)) were significantly lower than the wild type sequence scores (79.9 (S&S) and 0.82 (SSPNN)). Hence, less efficient binding of splice factors at the mutant splice donor site will modulate the splicing efficiency leading to skipping of exon 39. In order to exclude the presence of a putative second alteration in the *NF1* gene, the complete *NF1* cDNA was sequenced using direct cycle sequencing, but no other pathogenic alteration was

Table 1 Clinical features of affected patients in FSNF families 1 and 2

	Family 1					Family 2							
	I.5	II.4	III.2	III.3	IV.2	I.2	II.2	II.3	II.5	III.1	III.3	III.4	Totals
Age (now)	Died at 70	Died at 56	46	45	15	68	45	43	39	9	8	7	
>6 CAL (>15 mm)	+	+	+	+	+	+	+	+	+	+	+	+	12/12
Spinal neurofibromas	+	+ T	+ L, T	–	?	+ C, T, L	+ C, T, L	+ C, T, L	+ C, T, L	ND	–	–	7/10
Cutaneous/plexiform neurofibromas	ND	–	–	–	?	–	–	4*	1†	–	–	–	2/10
Lisch nodules	ND	–	–	–	?	–	–	–	–	–	–	–	0/10
Freckling	ND	–	–	–	?	+	–	–	–	–	–	–	1/10
Paraparesis	+	–	+	–	–	+	Weakness	Weakness	Weakness	–	–	–	6/12
Other findings								MRI‡					

C=cervical; T=thoracal; L=lumbar; ND=no data.
III.3 did not have any spinal neurofibromas 10 years ago, current status unknown.
*One histology proven neurofibroma. †Not biopsied. ‡5 mm tumour right frontal lobe. Unidentified bright object? Cerebral peduncle?

found. 7126+3A>C was present in all affected subjects (II.4, III.2, III.3, and IV.2) and was absent in the healthy family members (III.1, III.4, IV.1, IV.3).

In family 2, only normal sized fragments were discerned by PTT analysis of the total coding region, indicating the absence of a truncating mutation. Later, direct cycle sequencing of the total *NF1* cDNA was performed and a missense mutation was identified in exon 8 as the sole alteration, changing leucine at amino acid 357 to proline (L357P). Patients I.2, II.2, II.3, II.5, III.1, III.3, and III.4 were shown to bear the mutation L357P, whereas the healthy family members II.1 and III.2 did not carry this mutation. This indicates that the mutation segregates with the disease. Furthermore, this alteration was not found by analysing 200 normal chromosomes. L357 is also conserved in *Fugu rubripes* (AF064564), *Drosophila* (L26501), mouse (L10370), and rat (D45201). Proline is a very rigid amino acid and its presence creates a fixed kink in a polypeptide chain, which might have dramatic consequences for the protein structure. Altogether, these data indicate that L357P is the pathogenic *NF1* mutation in this family.

Western blot analysis

Four fibroblast cell cultures from normal subjects and three fibroblast cell cultures initiated independently from the normal skin of patient II.5 carrying the missense mutation L357P (family 2) were analysed by Western transfer analysis. This showed that the levels of NF1 protein were slightly higher in three out of four fibroblast cell lines from normal subjects compared to fibroblasts cultured from patient II.5 (data not shown).

DISCUSSION

Familial spinal NF has been considered an alternate form of NF1 because of the exceptional occurrence of multiple spinal neurofibromas affecting spinal roots symmetrically in all affected adult members of the same family accompanied by very mild cutaneous signs of NF1 and absence of Lisch nodules.[3] Only three such well documented families have been described and CAL spots were considered the sole cutaneous sign present in all affected members.[12 14 15] Although the clinical manifestations in the family members fulfil the NIH criteria for NF1 (presence of more than six CAL spots, two neurofibromas of any type, in this case multiple spinal neurofibromas, and also a first degree relative (parent, sib, or offspring) with NF1), they are very atypical of NF1. First, freckles, dermal neurofibromas, and Lisch nodules are found in more than 80%, 90%, and 90% respectively of classical NF1 patients but these signs were generally absent in all affected members of the FSNF families studied. One affected member had freckles in the axillary area and two had dermal neurofibromas, but no Lisch nodules were seen. Secondly, symptomatic spinal neurofibromas are rare in NF1 patients (<5%). Furthermore, the presence of multiple spinal neurofibromas affecting all spinal roots symmetrically in affected patients leading to severe neurological impairment is generally atypical of NF1, a disease noted for its variable expressivity among family members with identical *NF1* mutations. These very specific clinical findings suggest that a genotype-phenotype correlation might be found in these families and that a specific type of gene defect with a special effect on neural crest cells and/or their precursors in the nerve roots might be present in these families.

In one of these families, the pathogenic lesion had been identified previously, a unique frameshift at the 3′ end of the *NF1* gene in exon 46, 8042insA.[15]

We have now identified a bona fide pathogenic mutation in the affected members of both the other families. In family 1, a splice donor mutation was identified (7126+3A>C) resulting in out of frame skipping of exon 39 at the mRNA level. This is a novel mutation not identified previously in classical NF1 patients. In family 2, a recurrent missense mutation in exon 8 was found (L357P). This mutation was reported previously[19] in an NF1 patient, but no clinical findings are available so we are unable to correlate this genotype with the specific phenotype.

The current findings underline that FSNF with CAL spots is not only linked to the region flanked by the markers HHH202 and pEW206, encompassing the *NF1* locus, but is clearly allelic with NF1. Furthermore, taking the data from Ars *et al*[15] and ours together, it is clear that all three well defined FSNF families carry a different private *NF1* mutation, as also is the case for classical NF1. Moreover, it is unlikely that a specific type of mutation located in a specific region of the gene underlies this phenotype, as a frameshift, a splice mutation, and a missense mutation were found, all located in different parts of the gene. However, it is noteworthy that the mutations found in the three FSNF families might be mild mutations with some residual function as they are a truncating mutation at the very 3′ end of the gene 8042insA, a splicing error 7126+3A>C, and a missense mutation L357P. Recently, Kaufmann *et al*[20] described two families with multiple spinal tumours without CAL spots. Although overall the cutaneous signs were very mild in the affected patients, several of them had cutaneous neurofibromas. In these families too, the underlying *NF1* mutation was a splicing (IVS31-5A>G) and a missense mutation (L2067P). It has been proposed that the FSNF phenotype might arise through a negative residual function of the mutant neurofibromin with a special effect on the development of the neural crest cell.[15] When a total gene deletion or a nonsense mutation in the gene is encountered, these mutations will result in a null allele or in transcripts that become degraded by the nonsense mediated RNA decay, leading to haploinsufficiency. For the mutations found in the FSNF families, however, it is conceivable that a negative residual function might still exist, that is, that a mutant neurofibromin with the single amino acid change is formed by the L357P allele, a 2680 amino acid truncated protein is formed

by mutation 8042insA, and a 2353 amino acid truncated protein is formed by 7126+3A>C, albeit probably in a minimal amount. This assumption was tested by western blotting of the EBV cell lines of two patients carrying 7126+3A>C, using the antibody SC67, but no shortened neurofibromin was found (data not shown). However, we do not think that this is enough evidence to draw definitive conclusions as the molecular tools available for these studies are still limited today.

Mild mutation can however not be the sole factor predisposing to the development of multiple spinal tumours, as a number of similar frameshift mutations at the 3′ end of the *NF1* gene, splicing, and missense mutations were found in patients without spinal involvement[16 19 21] (unpublished data) and with classical cutaneous manifestations. It is generally accepted that bona fide missense mutations may point to critical functional domains in a protein[19] as they may lead to the production of a mutant protein. The RasGAP activity of the central GAP related domain as well as the structure of the GRD of neurofibromin have been well characterised[22 23] and the effects of specific missense mutations in this domain have been studied in detail.[24] No functional significance has been contributed so far to the region encompassing exon 8 in which the L357P mutation was found. Recently, the neurofibromin content of cells from three NF1 patients with spinal neurofibromas without CAL spots was found to be reduced to half of the amount of normal control cells, suggesting functional haploinsufficiency.[20] Interestingly, one of the mutations tested was a missense mutation L2067P. In order to substantiate these findings further, we have performed western blot analysis on control normal fibroblast cell cultures (n=4) and fibroblast cell cultures (n=3), independently initiated from patient II.5, carrying the mutation L357P. The levels of NF1 protein were slightly higher in three out of four control normal fibroblast cell lines compared to the L357P cell lines. No apparent differences were noted between fibroblasts from one normal control compared to patient II.5 with FSNF. This most probably is because the *NF1* gene is not a housekeeping gene and the same cell line can display marked expression changes when analysed at different times.[25] However, we do not think that this evidence is enough to form a definitive conclusion of haploinsufficiency. It was also proposed that the FSNF was the result of the presence of a second *NF1* mutation, either on the normal allele (in *trans*) or, more likely, on the same allele that also contains the already identified mutation (in *cis*).[15] As we applied the complete cascade of techniques used to find the mutation in >95% of classical NF1 patients[16] and did not find a second alteration, it is unlikely that a second change in the *NF1* gene is present concomitantly.

Finally, it is possible that an additional mutation in another gene lying within the region flanked by the markers HHH202 and EW206 and shown to be linked in both families influences the striking clinically homogeneous phenotypic outcome. Analysis of additional highly polymorphic microsatellite markers in both families will allow narrowing down of the linked region of interest for further investigation. It has been suggested that a modifier gene resides in close proximity to the *NF1* gene[26] and that its deletion together with the *NF1* gene results in the severe "*NF1* microdeletion" phenotype with early onset of growth and an excessive number of cutaneous neurofibromas. A mutation (for example, with a dominant negative effect on the development of the neural crest cells that are responsible for the NF1/FSNF phenotype) in one of the genes flanking the mutant *NF1* gene might cooperate with the *NF1* mutation to result in FSNF. Furthermore, the same type of alteration, present in *trans* with an *NF1* mutation or occurring as a somatic event may be the modifier causing spinal tumours in a proportion of NF1 patients, but not in their offspring carrying only the *NF1* mutation. Expression and mutation analysis of the genes residing in this region, in the patients from FSNF families and in isolated patients presenting with this specific phenotype, will shed more light on this hypothesis and should help in understanding the molecular alterations that cause this severe neurological phenotype.

ACKNOWLEDGEMENTS

This work was supported by a grant from Ghent University to IV (BOF 01107799 and 011D3801) and by a grant from the Interuniversity Attraction Poles P5 to LM. This work was supported by grants DAMD17-00-1-0542 and DAMD 17-01-1-0721 awarded to KS and by grants from the Finnish Cancer Societies (JP) and Oulu University Hospital (JP). We wish to thank the patients and their families for excellent cooperation.

L Messiaen, T Callens, I Vandenbroucke, Centre for Medical Genetics, Ghent University Hospital, Belgium
V Riccardi, The Neurofibromatosis Institute, La Crescenta, CA, USA
J Peltonen, S L Karvonen, J Koivunen, Department of Anatomy and Cell Biology, University of Oulu, Finland
J Peltonen, S L Karvonen, Department of Dermatology, University of Oulu, Finland
J Peltonen, Department of Medical Biochemistry, University of Turku, Finland
E-L Leisti, Department of Radiology, University Hospital of Oulu, Finland
K Stephens, Departments of Medicine & Laboratory Medicine, University of Washington, Seattle, WA, USA
M Pöyhönen, Department of Medical Genetics, Väestöliitto, Family Federation of Finland, Helsinki, Finland

Correspondence to: Dr L Messiaen, Centre for Medical Genetics, University Hospital Ghent-0K5, De Pintelaan 185, 9000 Ghent, Belgium; Ludwine.Messiaen@rug.ac.be

REFERENCES

1 **Riccardi VM.** Von Recklinghausen neurofibromatosis. *N Engl J Med* 1981;**305**:1617-27.
2 **Friedmann JM,** Riccardi VM. *Neurofibromatosis: phenotype, natural history, and pathogenesis.* Baltimore: Johns Hopkins University Press, 1999.
3 **Carey JC,** Viskochil DH. Neurofibromatosis type 1: a model condition for the study of the molecular basis of variable expressivity in human disorders. *Am J Med Genet* 1999;**89**:7-13.
4 **Cawthon RM,** O'Connell P, Buchberg AM, Viskochil D, Weiss RB, Culver M, Stevens J, Jenkins NA, Copeland NG, White R. Identification and characterization of transcripts from the neurofibromatosis 1 region: the sequence and genomic structure of EVI2 and mapping of other transcripts. *Genomics* 1990;**7**:555-65.
5 **Viskochil D,** Buchberg AM, Xu G, Cawthon RM, Stevens J, Wolff RK, Culver M, Carey JC, Copeland NG, Jenkins NA, White R, Cawthon RM. Deletions and a translocation interrupt a cloned gene at the neurofibromatosis type 1 locus. *Cell* 1990;**62**:187-92.
6 **Wallace MR,** Marchuk DA, Andersen LB, Letcher R, Odeh HM, Saulino AM, Fountain JW, Brereton A, Nicholson J, Mitchell AL, Brownstein BH, Collins FS. Type 1 neurofibromatosis gene: identification of a large transcript disrupted in three NF1 patients. *Science* 1990;**249**:181-6.
7 **Trofatter JA,** MacCollin MM, Rutter JL, Murrell JR, Duyao MP, Parry DM, Eldridge R, Kley N, Menon AG, Pulaski K, Haase VH, Ambrose CM, Munroe D, Bove C, Haines JL, Martuza RL, MacDonald ME, Seizinger BR, Short MP, Buckler AJ, Gusella JF. A novel moesin-, ezrin-, radixin-like gene is a candidate for the neurofibromatosis 2 tumor suppressor. *Cell* 1993;**72**:791-800.
8 **Rouleau GA,** Merel P, Lutchman M, Sanson M, Zucman J, Marineau C, Hoang-Xuan K, Demczuk S, Desmaze C, Plougastel B, Pulst SM, Lenoir G, Bijlsma E, Fashold R, Dumanski J, de Jong P, Parry D, Eldrige R, Aurias A, Delattre O, Thomas G. Alteration in a new gene encoding a putative membrane-organizing protein causes neuro-fibromatosis type 2. *Nature* 1993;**363**:515-21.
9 **Stumpf D,** Alksne J, Annegers J, Brown S, Conneally P, Housman D, Leppert M, Miller J, Moss M, Pilegi A, Rapin I, Strohman R, Swabson L, Zimmersman A. Neurofibromatosis conference statement. *Arch Neurol* 1991;**45**:955-61.
10 **Huson S,** Hughes RA. *The neurofibromatoses: a clinical and pathogenic overview.* London: Chapman & Hall, 1994.
11 **Thakkar SD,** Feigen U, Mautner VF. Spinal tumours in neurofibromatosis type 1: an MRI study of frequency, multiplicity and variety. *Neuroradiology* 1999;**41**:625-9.
12 **Poyhonen M,** Leisti EL, Kytola S, Leisti J. Hereditary spinal neurofibromatosis: a rare form of NF1? *J Med Genet* 1997;**34**:184-7.
13 **Egelhoff JC,** Bates DJ, Ross JS, Rothner AD, Cohen BH. Spinal MR findings in neurofibromatosis types 1 and 2. *AJNR Am J Neuroradiol* 1992;**13**:1071-7.
14 **Pulst SM,** Riccardi VM, Fain P, Korenberg JR. Familial spinal neurofibromatosis: clinical and DNA linkage analysis. *Neurology* 1991;**41**:1923-7.
15 **Ars E,** Kruyer H, Gaona A, Casquero P, Rosell J, Volpini V, Serra E, Lazaro C, Estivill X. A clinical variant of neurofibromatosis type 1: familial spinal neurofibromatosis with a frameshift mutation in the NF1 gene. *Am J Hum Genet* 1998;**62**:834-41.

16 **Messiaen LM**, Callens T, Mortier G, Beysen D, Vandenbroucke I, Van Roy N, Speleman F, De Paepe A. Exhaustive mutation analysis of the NF1 gene allows identification of 95% of mutations and reveals a high frequency of unusual splicing defects. *Hum Mutat* 2000;**15**:541-55.
17 **Koivunen J**, Kuorilehto T, Kaisto T, Peltonen S, Peltonen J. Ultrastructural localization of NF1 tumor suppressor protein in human skin. *Arch Dermatol Res* 2002;**293**:646-9.
18 **Shapiro MB**, Senapathy P. RNA splice junctions of different classes of eukaryotes: sequence statistics and functional implications in gene expression. *Nucleic Acids Res* 1987;**15**:7155-74.
19 **Fahsold R**, Hoffmeyer S, Mischung C, Gille C, Ehlers C, Kucukceylan N, Abdel-Nour M, Gewies A, Peters H, Kaufmann D, Buske A, Tinschert S, Nurnberg P. Minor lesion mutational spectrum of the entire NF1 gene does not explain its high mutability but points to a functional domain upstream of the GAP-related domain. *Am J Hum Genet* 2000;**66**: 790-818.
20 **Kaufmann D**, Muller R, Bartelt B, Wolf M, Kunzi-Rapp K, Hanemann CO, Fahsold R, Hein C, Vogel W, Assum G. Spinal neurofibromatosis without cafe-au-lait macules in two families with null mutations of the NF1 gene. *Am J Hum Genet* 2001;**69**:1395-400.
21 **Ars E**, Serra E, Garcia J, Kruyer H, Gaona A, Lazaro C, Estivill X. Mutations affecting mRNA splicing are the most common molecular defects in patients with neurofibromatosis type 1. *Hum Mol Genet* 2000;**9**:237-47.
22 **Kim M**, Tamanoi F. Neurofibromatosis 1 GTPase activating protein-related domain and its functional significance. In: Upadhyuya M, Cooper DN, eds. *Neurofibromatosis type 1: from genotype to phenotype*. Oxford: BIOS Scientific Publishers, 1998:89-112.
23 **Scheffzek K**, Ahmadian MR, Wiesmuller L, Kabsch W, Stege P, Schmitz F, Wittinghofer A. Structural analysis of the GAP-related domain from neurofibromin and its implications. *EMBO J* 1998;**17**:4313-27.
24 **Klose A**, Ahmadian MR, Schuelke M, Scheffzek K, Hoffmeyer S, Gewies A, Schmitz F, Kaufmann D, Peters H, Wittinghofer A, Nurnberg P. Selective disactivation of neurofibromin GAP activity in neurofibromatosis type 1. *Hum Mol Genet* 1998;**7**:1261-8.
25 **Pummi K**, Ylä-Outinen H, Peltonen J. Oscillation and rapid changes of NF1 mRNA steady-state levels in cultured human keratinocytes. *Arch Dermatol Res* 2000;**292**:422-4.
26 **Dorschner MO**, Sybert VP, Weaver M, Pletcher BA, Stephens K. NF1 microdeletion breakpoints are clustered at flanking repetitive sequences. *Hum Mol Genet* 2000;**9**:35-46.

GENES, CHROMOSOMES & CANCER 37:111–120 (2003)

RESEARCH ARTICLE

Complete Physical Map and Gene Content of the Human NF1 Tumor Suppressor Region in Human and Mouse

Dieter E. Jenne,[1] Sigrid Tinschert,[2] Michael O. Dorschner,[3] Horst Hameister,[4] Karen Stephens,[3] and Hildegard Kehrer-Sawatzki[4]*

[1]Department of Neuroimmunology, Max-Planck-Institute of Neurobiology, Martinsried, Germany
[2]Charité, Institute of Medical Genetics, Humboldt-University, Berlin, Germany
[3]Departments of Medicine and Laboratory Medicine, University of Washington, Seattle, Washington
[4]Department of Human Genetics, University of Ulm, Ulm, Germany

Duplicon-mediated microdeletions around the *NF1* gene are frequently associated with a severe form of neurofibromatosis type I in a subgroup of patients who show an earlier onset of cutaneous neurofibromas, dysmorphic facial features, and lower IQ values. To clarify the discrepancies between published maps of the *NF1* tumor-suppressor gene region as well as the length of gaps in these assemblies and to validate the recently described tandem duplication of the human *NF1* locus, we assembled a contiguous high-density map of BAC and PAC clones from different genomic libraries. Although two *WI-12393*–derived low-copy fragments are known to occur at the proximal and distal boundaries of the 1.5-Mb segment that is usually deleted in NF1 microdeletion patients, we identified an additional *WI-12393*–related segment between the *MGC13061* and the *NF1* gene, which appears to trigger interstitial deletions of smaller size as observed in two patients. Moreover, we completed the genomic organization and cDNA structure of all functional genes, *CYTOR4*, *FLJ12735*, *FLJ22729*, *CENTA2*, *MGC13061*, *NF1*, *OMG*, *EVI2B*, *EVI2A*, *KIAA1821*, *MGC11316*, *HCA66*, *KIAA0160*, and *WI-12393*, from this region. A comparison of the human map to the orthologous region on mouse chromosome 11 revealed significant differences in the number and arrangement of genes, indicating that many chromosomal breaks with partial duplications, inversions, and deletions occurred predominantly in the primate lineage.

INTRODUCTION

Neurofibromatosis type I (NF1) [MIM 162200] is an autosomal dominant disorder which predisposes to benign and malignant tumors. NF1 is caused by mutations of the gene encoding neurofibromin at 17q11.2. The detailed and precise structure of the *NF1* gene and its flanking regions is important in the context of mutation analysis in NF1 patients and is essential to understand the pathogenetic mechanisms underlying submicroscopic deletions at 17q11.2. In 5–20% of NF1 patients, a heterozygous deletion is found, which includes not only the *NF1* gene, but also further genes in the adjacent regions (Kayes et al., 1994; Cnossen et al., 1997; Valero et al., 1997; Rasmussen et al., 1998; Upadhyaya et al., 1998). The majority of these interstitial 17q11.2 microdeletions of about 1.5 Mb are caused by unequal recombination between two highly homologous 35-kb spanning segments (located between positions 113000 and 148000 on R-271K11, accession number AC005562) of two low-copy repeats (LCRs), which contain duplicated portions of the *KIAA0563*-related gene, also called *WI-12393*, and chromosome 19p13.1–derived sequences (López Correa et al., 1999, 2001; Dorschner et al., 2000; Jenne et al., 2000, 2001). These LCRs are localized at a distance of about 400 kb proximal and 700 kb distal to the *NF1* gene.

In addition to the bona fide *NF1* gene at 17q11.2, several *NF1* pseudogenes have been identified, which are derived from the proximal part of the *NF1* gene. These *NF1*-related sequences are located at 2q21 and in the pericentromeric region of chromosomes 12, 14, 15, 18, 21, and 22 (Legius et al., 1992; Marchuk et al., 1992; Suzuki et al., 1994; Purandare et al., 1995; Cummings et al., 1996; Hulsebos et al., 1996; Kehrer-Sawatzki et al.,

Supported by: Deutsche Forschungsgemeinschaft; Grant numbers: JE 194/1-1, KF0113/1, HA 1082/16-1, 16-2; University of Munich; Grant number: SFB469; Grant numbers: DAMD 17-00-1-0542, DAMD 17-01-1-0721 awarded by the US Army Medical Research Acquisition Activity, 820 Chandler St, Fort Detrick, MD 21702-5014.

*Correspondence to: Dr. Hildegard Kehrer-Sawatzki, Department of Human Genetics, University of Ulm, Albert-Einstein-Allee 11, D-89081 Ulm, Germany.
E-mail: hildegard.kehrer-sawatzki@medizin.uni-ulm.de

Received 9 October 2002; Accepted 8 January 2003
DOI 10.1002/gcc.10206
Published online 10 March 2003 in Wiley InterScience (www.interscience.wiley.com).

1997a; Regnier et al., 1997; Luijten et al., 2000). All these findings suggest that pericentromeric plasticity and/or local chromosomal instability have reshaped the *NF1* locus and adjacent regions quite often during evolution of primate genomes.

The spread of multiple *NF1* pseudogene fragments onto different chromosomes and the presence of several *KIAA0563*-related sequences on chromosome arm 17q have provoked further speculations about additional local duplications of the *NF1* region. Very recently, Gervasini et al. (2002) provided hybridization evidence for a tandem duplication of the *NF1* gene and its immediately flanking regions at 17q11.2, by use of high-resolution FISH on stretched chromosomes and DNA fibers. According to their observations, the *NF1* gene is not only surrounded by duplicons derived from the *WI-12393* (*KIAA0563*-related) gene at a distance of 400 and 700 kb on each side, but also might be organized as a highly homologous tandem repeat within 17q11.2. We were puzzled by these findings, given that *NF1*-related sequences adjacent to the bona fide *NF1* gene at 17q11.2 have not been detected in previous PCR and microsatellite analyses (Jorde et al., 1993; Messiaen et al., 1993; Li et al., 1995; Purandare et al., 1996; Valero et al., 1996), physical mapping studies (Fountain et al., 1989a,b; Ledbetter et al., 1989; Yagle et al., 1990), or cytogenetic studies of constitutional translocations such as the t(17;22) (q11.2q11.2), which disrupts the *NF1* gene in intron 31 (Kehrer-Sawatzki et al., 1997b, 2002).

Facing several controversial reports on the structure of the *NF1* region (López Correa et al., 1999, 2001; Dorschner et al., 2000; Jenne et al., 2000, 2001; Riva et al., 2000, 2002; Bentivegna et al., 2001; Gervasini et al., 2002) and the still existing discrepancies between the Celera, the NCBI, and the EMBL maps around the *NF1* locus, we reexamined all existing data and performed fluorescence in situ hybridization (FISH), bacterial artificial chromosome (BAC) end mapping, and marker analyses to confirm the map of the entire 1.5-Mb region in great detail. Moreover, we compared the human *NF1* gene with the orthologous region in the mouse and found clear differences in the number and order of genes in both species.

MATERIALS AND METHODS

FISH and BLAST Analysis

BACs and P1 artificial chromosome clones (PACs) were purchased from Research Genetics (Huntsville, AL) and from the BACPAC Resource Center (www.chori.org/bacpac). DNA was isolated from liquid cultures of 150 ml by use of the Midi DNA isolation kit (Qiagen, Hilden, Germany). Sequence alignments were determined by BLAST analysis against all available databases (http://www.ncbi.nlm.nih.gov/blast) and assembled by use of the GCG software package (Version 10.2; Oxford Molecular Group, Beaverton, OR) and the Sequencher software (Gene Codes, Ann Arbor, MI).

The regional probe spanning *WI-12393* exon 1 was amplified by PCR by use of the Expand Long-Template PCR system (Roche-Diagnostics, Mannheim, Germany) with primers DJ 1686 (5′-CAG GTT ATA GGG AAG GAG GAC-3′) and DJ 1863 (5′-AGC AGC GGT TAA GCA ATG ATG-3′). The 6-kb spanning PCR product was cloned with the TOPO TA cloning system (Invitrogen, Carlsbad, CA) and used as a FISH probe. Metaphase spreads were prepared either from peripheral blood lymphocytes or lymphoblastoid cell lines. Interphase nuclei for genomic distance measurements were obtained from G1 synchronized fibroblast cultures by use of standard methods. BAC DNA and the plasmid containing the *WI-12393* exon 1 were labeled by nick translation by use of biotin-16-dUTP (Roche-Diagnostics) or digoxygenin-11-dUTP (Roche-Diagnostics). Probes were either visualized with FITC-avidin and biotinylated anti-avidin (Vector Laboratories, Burlingame, CA) or detected by mouse anti-digoxygenin antibodies coupled with Texas-Red and in a second step by anti-mouse antibodies conjugated with Texas-Red (Dianova, Hamburg, Germany). Slides were counterstained with diamidinophenylindole and mounted with Vectashield antifade solution (Vector Laboratories).

Patients With 17q11.2 Microdeletions of Smaller Size

The clinical phenotype and the age of two NF1 patients (TOP, UWA113-1) with deletions smaller than 1.5 Mb (Dorschner et al., 2000; Jenne et al., 2000) are summarized in Table 1. This table also includes the clinical data of patient UW155-1, whose proximal deletion breakpoint was located within the interval of markers *SHGC35088* (*RH33498*) and *FB12A2* and the distal deletion breakpoint between markers *D17S1656* and *stSG50857* telomeric to the distal LCR (Dorschner et al., 2000).

BAC Library Screening

Filters from the RPCI-11 human BAC library and the RPCI1,3–5 human PAC libraries were ob-

TABLE 1. Clinical Features of Patients With *NF1* Deletions Smaller Than the Usual Duplicon-Mediated Deletion

Feature	TOP	UWA-113-1	UWA-155-1
Age (years)	11.5	8	27
Number of cutaneous neurofibromas	45	TNTC[a]	TNTC
Height (cm, percentile)	147.5 (97%)	unk.[b]	unk.
Head circumference	56 (50%)	59 (>97%)	59.5 (>97%)
Facies	Coarse, large nose	Coarse, hypertelorism	Coarse, ptosis
Intelligence	IQ 59	IQ 88	Moderate MR
Hands	97%	>97%	>97%
Feet	>97%		>75%
Other tumors	Optic glioma suspected No spinal MRI	—	Spinal neurofibroma Malignant peripheral nerve sheath tumor at age 28

[a]TNTC, too numerous to count.
[b]unk., unknown.

tained from the Resource Center (www.rzpd.de) and the BACPAC Resource Center (www.chori.org/bacpac). Screening of the libraries was performed by hybridization with STS markers amplified by PCR and labeled by random priming with hexamer oligonucleotides and Klenow polymerase in the presence of ^{32}P-dCTP (Amersham Pharmacia, Freiburg, Germany) in buffer containing 7% SDS, 0.5 M Na-phosphate (pH 7.2), and 1 mM EDTA at 65°C overnight. Filters were washed four times at increasing stringency, with a final wash of 0.2× SSC/0.1% SDS for 45 min. After autoradiography for 1–2 days at −70°C with intensifying screens, positive clones were identified by x/y coordinates and obtained from BACPAC resources or the Resource Center.

Characterization of Full-Length cDNAs

Full-length transcripts of the *FLJ12735*, *MGC13061*, *KIAA182*, *MGC11316*, and *FLJ11040* genes were determined by RT-PCR with human cDNAs obtained by reverse transcription by use of the Superscript II system (Life Technologies, Gaithersburg, MD) of RNA from various tissues (Total RNA panels I and II; Clontech, Palo Alto, CA). The structure of the RT-PCR products was analyzed by sequencing by use of the Big-Dye Terminator kit (Applied Biosystems, Foster City, CA). The structure of the *KIAA1821* gene was further confirmed by Northern blot hybridizations by use of the human MTN Blot (Clontech) according to the manufacturer's instructions.

RESULTS AND DISCUSSION

Notwithstanding the enormous progress in contig assembly and gene annotation, it appears that most of the mapping problems of the human *NF1* gene region originate from ambiguities and uncertainties in two genomic segments located between the BACs R-271K11 and 468F23, and on BAC R-640N20. These two regions are not fully covered by BACs and sequence assemblies in online-genome databases. More important, several of the genes from the 1.5-Mb spanning interval are only partially annotated by automatic computer algorithms and are deduced from very few experimental data.

To this end, we extended our previous assemblies and constructed a BAC/PAC contig of high clone density between the proximal *WI-12393*–related duplicon and the unique *FLJ11040* gene, which flanks the distal duplicon. We reinvestigated the structure of the genes previously mapped to the *NF1* gene region (Dorschner et al., 2000; Jenne et al., 2001) and integrated their position into our consensus contig (Fig. 1). Overall, 19 new BACs from different libraries were identified and integrated into the map by BLAST analysis of end sequences and marker analysis. BAC R-229K15 (AC027793) bridges the region between BAC 468F23 (AC004666) and R-142O6 (AC079915) and thus fills the sequence gap between 468F23 and the 5′ promoter region of the *NF1* gene. Because the entire BAC insert has now been sequenced, R-229K15 can clearly be put at this position, although it shares considerable homology with R-271K11, in particular *WI-12393* pseudogene exons as outlined below. Additionally, the meanwhile fully sequenced BACs 2349P21, 3098J15, and R-785C15 could be mapped unambiguously in the 5′ direction of BAC 468F23, thus extending the contig to the centromeric direction up to the most

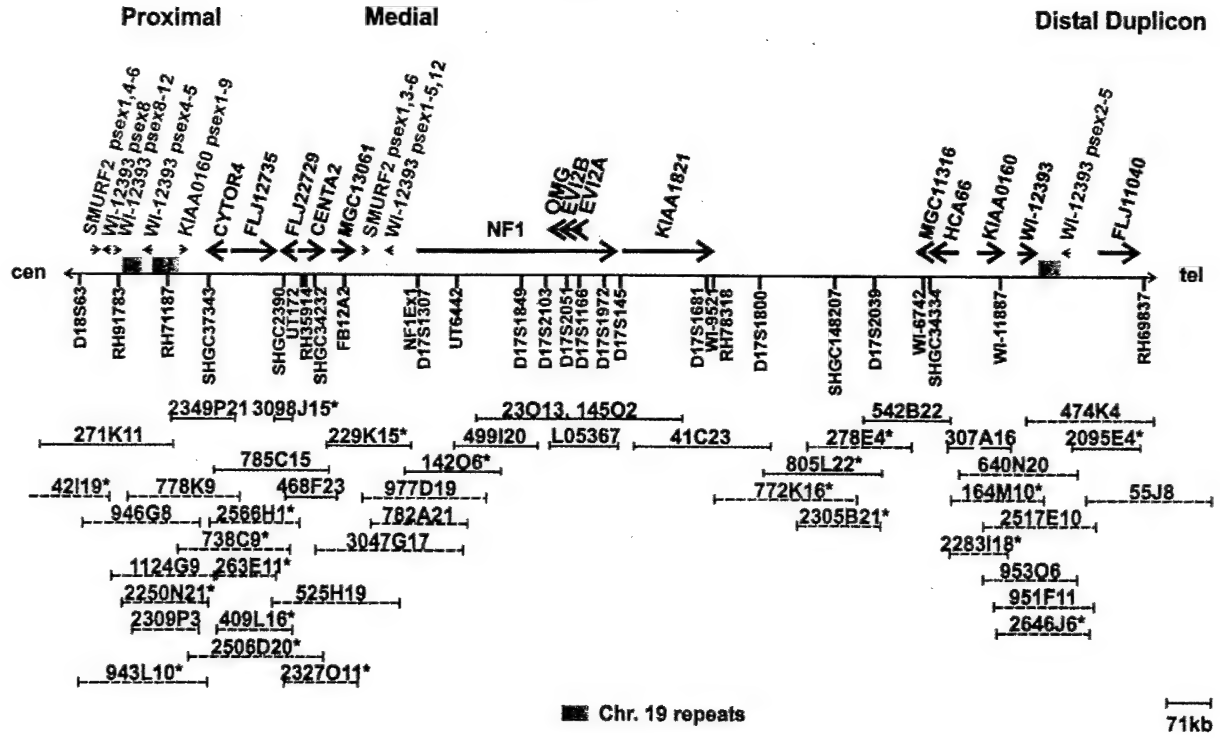

Figure 1. Complete physical and transcript map around the *NF1* locus between the proximal and distal duplicons containing various fragments of the *WI-12393* gene. Immediately 5′ to the *NF1* gene, a third, *WI-12393* pseudogene fragment (medial duplicon) was identified. Green boxes indicate the low-copy repeats with high homology to sequences on chromosome 19 (AC011509; AC008569). The arrows above the line indicate the genomic length and transcript direction of the genes mapped to this region. Functional genes are indicated in black; pseudogene (ps) exons of the *SMURF2*, the *WI-12393*, and the *KIAA0160* genes are given in red. Indicated below the line are markers that anchor the fully assembled BAC/PAC contig. Each horizontal bar represents the length of a given BAC or PAC clone. Completely sequenced clones are marked by bars in orange, whereas partially sequenced clones are indicated by dashed black lines. The contig was assembled by BLAST analysis (http://www.ncbi.nlm.nih.gov/), FISH and marker analysis by PCR. The 19 newly mapped clones are marked by asterisks. Processed pseudogenes like *EEN* and *YZA1* were omitted. The accession numbers of the fully sequenced clones are AC005562 (271K11), AC127024 (2349P21), AC109516 (785C15), AC091177 (3098J15), AC004666 (468F23), AC027793 (229K15), AC079915 (142O6), AC004222(499I29), AC004526 (23O13, 145O2), AC003101 (41C23), AC007923 (805L22), and AC004253 (542B22).

proximal *WI-12393*–related sequences. The structure of the region between BACs R-271K11 and R-785C15 was confirmed by marker analysis of the newly identified BACs 738C9, 2250N21, 943L10, and 2506D20, and their position is in full harmony with our map (Fig. 1).

In the 3′ direction to the *NF1* gene, the completely sequenced BAC R-805L22 was clearly placed between BACs 41C23 and 542B22. The accuracy of the map 3′ to the *NF1* gene was further corroborated by the identification of BAC R-772K16, which consists of fully sequenced unordered segments. The ordered overlap of BACs 41C23 and R-805L22, BACs R-805L22 and 542B22, and BACs 542B22 and 307A16 (AC003041) has been confirmed by FISH analysis in interphase nuclei with differentially labeled BAC probes (data not shown). We investigated the genomic segment between BACs 542B22 and R-474K4 in great detail because this region is still not covered by a continuous sequence. We integrated the completely sequenced BAC 2095E4, which overlaps with BAC R-474K4 and R-640N20. Because the continuous sequence of BAC R-640N20 (AC090616, version 8) was not available in public databases, we ordered the eight pieces of R-640N20 in harmony with the cDNA sequences of the *KIAA0160* and *WI-12393* transcripts and confirmed this order by PCR and RT-PCR analysis. The position of six further BAC clones integrated into the contig in this particular region (R-164M10, 2517E10, 2283I18, R-953O6, 2646J6, and R-951F11) is fully consistent with the assembly of BAC R-640N20 and the map around the distally located *WI-12393*–related sequences.

In addition, we extracted and compiled the mouse homologs for the human genes mapped to the *NF1* gene region from BAC clones that had been fully sequenced and deposited at the EMBL or GenBank database. The structure and order of the orthologous mouse loci around the *NF1* gene are illustrated in Figure 2. By comparative se-

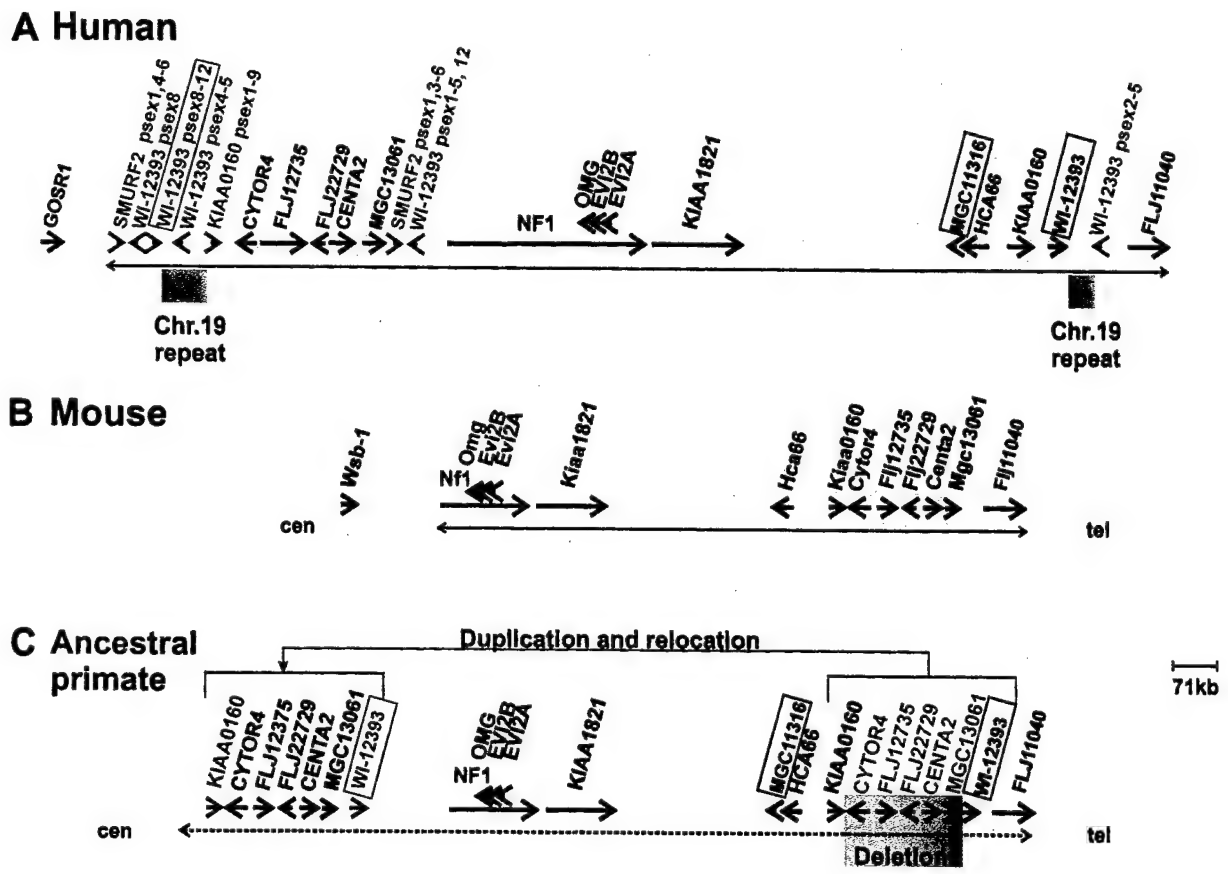

Figure 2. Physical map of the human (**A**) and murine *NF1* region (**B**) and tentative *NF1* region in ancestral primates (**C**), from centromere (left) to the telomere (right). The arrows indicate the genomic length and transcript direction of the genes mapped to the respective regions. Functional genes are indicated in black; pseudogene (ps) exons are in red. Marked by yellow boxes are the genes that have been duplicated and relocated during primate evolution as deduced from comparison of the human and mouse *NF1* gene region. The *MGC11316* and *WI-12393* genes (marked by black frames) were either inserted during primate evolution or deleted in the rodent lineage. The proposed structure of the *NF1* gene region in an ancestral primate (C) is characterized by the duplication and relocation of seven genes to the proximal side of the *NF1* gene. This duplication event was followed by a deletion of five genes (marked in blue) on the distal side. Indicated in red are the copies of the *KIAA0160* and *WI-12393* genes on the proximal side of the *NF1* gene, which have been partially lost during evolution. We assume that the primordial *WI-12393* gene was located between *MGC13061* and *FLJ11040* in the primate ancestor, showing the same transcriptional orientation as the present-day pseudogene copy on BAC R-271K11 (red labels with frame), which spans exons 8 to 12.

quence analysis of the human and mouse genome, we identified a total of 14 human genes between the proximal and the distal duplicons and updated the full-length transcript structure of five genes (*FLJ12735*, *MGC13061*, *KIAA182*, *MGC11316*, and *FLJ11040*) (Table 2). Our analysis of the fully assembled clone contig presented here disproves a local duplication of the *NF1* gene at 17q11.2 as reported by Gervasini et al. (2002). However, we identified an additional truncated copy of the *WI-12393* gene on BAC R-229K15 (AC027793) and located the latter between the proximal duplicon and the 5′UTR of the *NF1* gene (Fig. 1). Gervasini et al. (2002) used BAC R-977D19 as a FISH probe to investigate the structure of the *NF1* gene region. This BAC spans not only the 5′ region of the *NF1* gene but also contains a third non-processed pseudogene copy of the *WI-12393* gene (medial duplicon, Fig. 1). Lack of awareness of this additional LCR may have contributed to the misinterpretation of fiber FISH experiments and the supposed *NF1* gene duplication (Gervasini et al., 2002).

The medial duplicon may also be implicated in homologous recombinations with the distal *WI-12393*–containing LCR for the reasons outlined below. Two patients, TOP (Jenne et al., 2000) and UW113-1 (Dorschner et al., 2000), have been reported with deletions of shorter length. These deletions were observed in all peripheral blood cells and most likely represent constitutional germline deletions. Although their breakpoints have not been mapped at the sequence level, our analyses suggest that both the proximal and distal breakpoints in these two patients are located within

TABLE 2. Summary of the Functional Genes Around the *NF1* Locus at 17q11.2 and Mouse Orthologs on Chromosome 11 (11B5)

Gene designation (marker)	Accession number of the human cDNA (length in bp/number of exons)	Accession number of the homologous mouse cDNA (length in bp)	Features of the encoded protein
CYTOR4/CRLF3 (SHGC-37343)	NM_015986 (3320/8)	NM_018776 (2365)	Cytokine receptor-like factor 3
FLJ12735	AJ314648[a] (6245/28)	XM_126278 (1002)	Putative ATP/GTP-binding protein
FLJ22729 (SHGC-2390)	AJ314645 (1306/4)	AK003325 (1260) XM_126322 (1257) XM_109915 (1257)	
CENT2A (SHGC-34232)	NM_018404	BC027165 (1611)	Inositol(1,3,4,5)tetrakisphosphate receptor
	AJ238994 (1796/11)	XM_126230 (2289) XM_109914 (2289)	
MGC13061	AJ496729[a] (2467/5)	NM_028019 (1961)	Contains C_3HC_4 zinc finger, signal peptide
NF1	NM_000267 (89597/60)	L10370 (11690) XM_126233 (11681)	Ras GTPase stimulating protein
OMG	XM_083979 (1805/2)	NM_019409 (1794)	Oligodendrocyte myelin glycoprotein; signal peptide toll-like receptor; leucin-rich repeat protein
EVI2B	NM_006495 (1983/2)	BC017548 (1855) XM_126388 (1866)	Prolin-rich, transmembrane segment
EVI2A	NM_014210 (1563/2)	NM_010161 (1613)	Signal peptide and transmembrane segment
KIAA1821 (WI-9521)	AJ314646[a] (8311/15) Exon 1 missing	XM_137757 (3348) XM_110986 (3384)	Similar to *KIAA0665* (Rab11-family interacting protein 3), Eferin; EF hand; coiled coil
MGC11316 (WI-6742)	AJ272196[a] (918/4) XM_056730	NM_025556[b] (789) AK010573 (789)	
HCA66	NM_018428 (2032)	NM_144826 (2081)	Hepatocellular carcinoma-associated antigen 66
	XM_050084 (2021/19)	XM_110000 (3022)	HAT (half a tetratricopeptide) repeat
KIAA0160/JJAZ1	NM_015355 (4441/16)	XM_126195 (3996)	Contains C_2H_2 zinc finger domain
KIAA0563rel (*WI-12393*)	AJ314647 (3017/12)	—[c]	*KIAA0563*-related
FLJ11040	AJ496730[a] (2453/19)	AK019059 (3000)	RIF (= rho in filopodia); mitochrondrial rho-1, MIRO-1 rho-related GTP binding protein

[a]This work; updates and full-length cDNAs are reported.
[b]The mouse homolog of the *MGC11316* gene is located on mouse chromosome 8A2.
[c]A gene with similarity to human *KIAA0563rel* is located on mouse chromosome 11D5 (XM_137868).

WI-12393–related sequences of the medial and distal duplicons (Fig. 3). Marker analysis of a hybrid cell line carrying only the deleted chromosome 17 homolog of UW113-1 permits us to narrow the location of the proximal breakpoint in this patient between marker *FB12A2* and exon 1 of the *NF1* gene. The six exons (12 and 5–1) of the *WI-12393* pseudogene copy on BAC R-229K15 are dispersed between position 69416 and 86281 (numbering according to AC027793) and are arranged in the same

Figure 3. **A:** Schematic representation of the distribution of the *WI-12393* exons and pseudogene exons in the proximal, medial, and distal duplicons of 17q11.2. The hybridization sites of the PCR product amplified with primers *DJ1686* and *DJ1863* (probe *DJ1686/1863*) are shown by green rectangles. The arrows indicate the orientation of the *WI-12393* exons and pseudogene exons. The relative map positions of BACs 782A21, R-977D19, and R-640N20 are also indicated. FISH analysis of BACs 782A21 and R-640N20 to metaphase chromosomes of patient TOP resulted in reduced signals on the chromosome 17 with the microdeletion. **B:** FISH with probe *DJ1686/1863* (green signals) on metaphase chromosomes of NF1 patient TOP revealed signals on only one chromosome 17 homolog (open-headed arrow). Co-hybridization was performed with the BAC clone R-55A13 (red signals) mapping to 17q24.

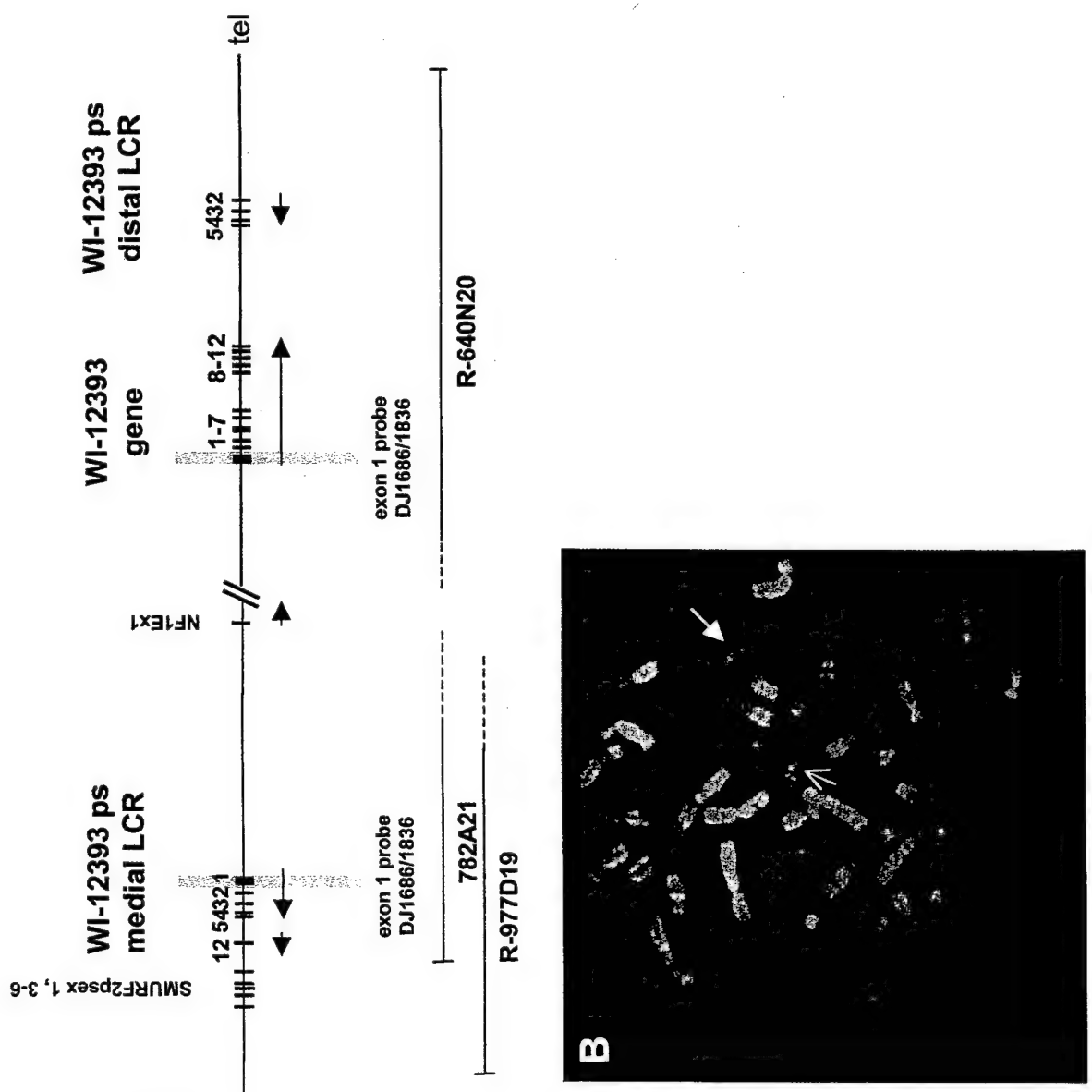
A
cen
tel
SMURF2psex 1, 4-6
WI-12393 ps proximal LCR
8
8-12
54
FB12A2
SMURF2psex 1, 3-6
WI-12393 ps medial LCR
12 5432 1
NF1Ex1
WI-12393 gene
1-7
8-12
WI-12393 ps distal LCR
5432
exon 1 probe DJ1686/1836
exon 1 probe DJ1686/1836
R-640N20
782A21
R-977D19
B

Figure 3.

orientation as the pseudogene copy on R-640N20 that recombines in the majority of NF1 microdeletion patients. Our FISH data for patient TOP indicate that the centromeric breakpoint is located on BAC R-782A21 distal to BAC 468F23. R-782A21, which overlaps with the distal portion of BAC R-229K15 up to position 65277, shows a signal of reduced intensity on one chromosome 17 homolog of patient TOP, whereas the proximally flanking BAC 468F23 yielded a signal of equal intensities over both chromosomes 17. Moreover, FISH analysis with a sub-regional probe spanning exon 1 of the *WI-12393* gene confirmed the deletion of this region in patient TOP (Fig. 3). Therefore we assume that the proximal deletion breakpoint of patient TOP most likely lies in the region of the *WI-12393* pseudogene exons 2–5 and 12. The distal breakpoint of the deletion of patients TOP and UW113-1 is located in the region of the distal duplicon, as shown previously (Dorschner et al., 2000; Jenne et al., 2000). Thus, we anticipate that the *WI-12393*–related sequences on BAC R-229K15 can also serve as a template for recombinations with the distal pseudogene copy on R-640N20.

Immediately adjacent to the *WI-12393*–derived sequences on BAC R-225K19 lies another nonprocessed pseudogene fragment, which is derived from the *SMURF2* gene. A second incomplete copy of *SMURF2* is found on BAC R-271K11 centromeric to the *WI-12393* pseudogene copy of R-271K11 (Fig. 1). The physical vicinity of *SMURF2* and *WI-12393* pseudogene fragments at these two sites suggests a discontinuous duplication of this genomic segment on the centromeric side of the *NF1* gene during primate evolution. The functional copy of the *SMURF2* gene encoding E3 ubiquitin ligase (NM_022739), however, is not clustered with the functional *WI-12393* gene, but maps to BAC R-87N3 (AC009994) on 17q22.

Our detailed analysis of the continuous map between BACs R-271K11 and R-640N20 shows that the *NF1* gene region is littered with four groups of low-copy repeat sequences derived from *WI-12393* (proximal, medial, and distal copies), *SMURF2*, *KIAA0160*, and the *LEC2* (Lecotmedin 2)/*CD97* (Leukocyte antigen CD97) intergenic region on chromosome 19, as illustrated by Figure 1. Two similar fragments of the *SMURF2* gene are found at the proximal boundary of the two *WI-12393* fragments on the centromeric side of the *NF1* gene. A large 90-kb segment originating from the intergenic region between *LEC2* and *CD97* on chromosome segment 19p13.1 (Fig. 1, green rectangles) is interspersed between the proximal *WI-12393* (exons 8–12) and the *KIAA0160* pseudogene copy. The proximal portion of this segment between 115000 and 146200 on R-271K11 (AC005562) together with exons 2 to 5 of the *WI-12393* gene reoccurs on the telomeric side of the *NF1* gene on BAC R-640N20.

To investigate the multiple rearrangements that occurred during primate evolution, we performed a comparative analysis between the human map around the *NF1* locus and the corresponding mouse syntenic region on chromosome 11 (Fig. 2). All of the duplications and pseudogene fragments described above are not present in the mouse genome, suggesting that the corresponding local rearrangements and segmental relocations occurred after the divergence of rodents and humans about 80M years ago. The long-range organization of the orthologous region in the mouse appears to reflect the primordial mammalian organization and gene order more faithfully (Fig. 2C).

Guided by parsimony considerations, we assume that the gene order (from centromere to telomere) *NF1*, *OMG*, *EVI2B*, *EVI2A*, *KIAA1821*, *MGC11316*, *HCA66*, *KIAA0160*, *CYTOR4*, *FLJ12735*, *FLJ22729*, *CENTA2*, *MGC13061*, *WI-12393*, and *FLJ11040* represents the ancestral order and covers a set of 15 functional genes. Only two events are supposed to have altered this gene ensemble in the rodent lineage during evolution, that is, the irreversible loss of *Wi-12393* and the translocation of *Mgc11316* onto mouse chromosome 8 (Fig. 2B). By contrast, the primate region has experienced a number of duplications, local rearrangements, and deletions, the largest of which appears to be the duplication and relocation of the genomic segment including the *KIAA0160–CYTOR4–FLJ12735–FLJ22729–CENTA2–MGC13061–WI-12393* genes to the centromeric side of the *NF1* gene (Fig. 2C). We assume that the primordial *WI-12393* gene was inserted between *MGC13061* and *FLJ11040* in the primate ancestor and kept the same transcriptional orientation as the present-day pseudogene copy, which spans exons 8 to 12 on BAC R-271K11 (Fig. 2A, C, red labels boxed). The order and transcriptional orientation of the *CYTOR4*, *FLJ12735*, *FLJ22729*, *CENT2A*, and *MGC13061* genes on the 5′ side of the human *NF1* locus are consistent with the present-day arrangement of the homologous mouse genes on the 3′ side of the mouse *Nf1* locus. Most probably, the duplication and relocation of the seven genes to the proximal side to the *NF1* gene in an ancestral primate predisposed these regions to further local modifications, such as the inactivation of the *KIAA0160* and *WI-12393* genes

with local inversion and duplications of the latter forming the present-day proximal and medial duplicons. The 90-kb fragment from chromosome 19, ranging from position 115000 to 203000 (numbering according to R-271K11, AC005562), is by far co-linear with the 5′ upstream region of *LEC2*, with the exception of a small *WI-12393* insertion (positions 146200 to 147900, exons 5 and 4). A subfragment of this segment (115000 to 146000, R-271K11 numbering) followed by *WI-12393* exons 2 to 5 constitutes the distal duplicon telomeric to the functional *WI-12393* gene (green boxes). Further insertions of *ALOX12B* (arachidonate 12-lipoxygenase) fragments, SMS (Smith–Magenis syndrome)-related repeats (Park et al., 2002), and *SMURF2* fragments have probably created the complex pattern of the present-day human sequence that is covered by the BAC R-271K11.

By contrast to humans, the mouse *Nf1* gene is located in the middle part of chromosome 11 (band B5) and not in a subcentromeric region. It seems plausible to assume that the multiple duplications and relocations in the *NF1* gene region during primate evolution were favored by the pericentromeric location of this region in the primate ancestor. As revealed by in silico analyses, pericentromeric and subtelomeric regions show a three- to fivefold increase in segmental duplications (Bailey et al., 2001), which foster further structural rearrangement as outlined recently (Eichler, 2001; Samonte and Eichler, 2002).

Comparative maps of the human and murine *NF1* region clearly highlight the close clustering of multiple evolutionary breakpoints and pathological breakpoints that have been identified in NF1 microdeletion patients. Coincidence of evolutionary breakpoints at the sites of low-copy repeats and repetitive pseudogene fragments has also been observed in the Williams–Beuren syndrome region at human chromosome region 7q11.23 (Valero et al., 2000).

Patients with segmental haploidy for all 14 genes (López Correa et al., 1999, 2001; Dorschner et al., 2000; Jenne et al., 2000, 2001) as well as those rare NF1 patients (patients TOP, UW113-1, and UWA155-1) (Jenne et al., 2000; Dorschner et al., 2000) (Table 1) who lack only the nine distal genes, but are diploid for the five proximal genes (*CYTOR4*, *FLJ12735*, *FLJ22729*, *CENTA2*, *MGC13061*), appear to develop a large number of benign neurofibromas at an earlier age (Table 1). This clinical observation leads us to suggest that haploidy for one of the nine distal genes may indeed predispose the patients with microdeletions to early tumor development. At present, the most intriguing candidate with regard to neurofibroma growth acceleration is the *KIAA0160* gene (*JJAZ1*, joined to *JAZF1*). *JJAZ1* has been shown to be disrupted by somatically acquired translocation t(7;17)(p15;q21) in stroma-derived endometrial sarcomas (Koontz et al., 2001). Our detailed physical description of the entire *NF1* flanking region clearly reveals the position of the functional *KIAA0160* (*JJAZ1*) gene on the distal side of the *NF1* gene as the fusion partner in t(7;17) translocations. Acquired alterations of its normal function and expression levels might contribute to enhanced cellular growth and transformation of Schwann cells in microdeletion patients.

Another frequently observed clinical feature of NF1 patients with 17q11.2 microdeletions are cognitive deficits ranging from decreased IQ value to mental retardation and developmental delay at a moderate, but significant level. Although there is a high incidence of learning disability in NF1 patients, mental retardation and cognitive impairment are observed in only 4–8% of all NF1 patients (North, 1999). In view of the high frequency of mental impairment in NF1 patients with large deletions, it is tempting to speculate that one or a combination of the adjacent genes account for subtle developmental defects of the central nervous system. All three patients (Table 1) that share hemizygosity for the nine distal genes are mentally handicapped, suggesting that one of these genes plays a critical role in normal brain function or development.

ACKNOWLEDGMENTS

We thank W. Lasinger, H. Reimann, and H. Spöri for excellent technical assistance; and Prof. H. Wekerle for his continuous interest and support of this work.

REFERENCES

Bailey JA, Yavor AM, Massa HF, Trask BJ, Eichler EE. 2001. Segmental duplications: organization and impact within the current human genome project assembly. Genome Res 11:1005–1017.

Bentivegna A, Venturin M, Gervasini C, Corrado L, Larizza L, Riva P. 2001. Identification of duplicated genes in 17q11.2 using FISH on stretched chromosomes and DNA fibers. Hum Genet 109:48–54.

Cnossen MH, van der Est MN, Breuning MH, van Asperen CJ, Breslau-Siderius EJ, van der Ploeg AT, de Goede-Bolder A, van den Ouweland AM, Halley DJ, Niermeijer MF. 1997. Deletions spanning the neurofibromatosis type 1 gene: implications for genotype-phenotype correlations in neurofibromatosis type 1? Hum Mutat 9:458–464.

Cummings LM, Trent JM, Marchuk DA. 1996. Identification and mapping of type 1 neurofibromatosis (NF1) homologous loci. Cytogenet Cell Genet 73:334–340.

Dorschner MO, Sybert VP, Weaver M, Pletcher BA, Stephens K. 2000. NF1 microdeletion breakpoints are clustered at flanking repetitive sequences. Hum Mol Genet 9:35–46.

Eichler EE. 2001. Recent duplication, domain accretion and the

dynamic mutation of the human genome. Trends Genet 17:661–669.
Fountain JW, Wallace MR, Bruce MA, Seizinger BR, Menon AG, Gusella JF, Michels VV, Schmidt MA, Dewald GW, Collins FS. 1989a. Physical mapping of a translocation breakpoint in neurofibromatosis. Science 244:1085–1087.
Fountain JW, Wallace MR, Brereton AM, O'Connell P, White RL, Rich DC, Ledbetter DH, Leach RJ, Fournier RE, Menon AG, Gusella JF, Barker D, Stephens K, Collins FS. 1989b. Physical mapping of the von Recklinghausen neurofibromatosis region on chromosome 17. Am J Hum Genet 44:58–67.
Gervasini C, Bentivegna A, Venturin M, Corrado L, Larizza L, Riva P. 2002. Tandem duplication of the NF1 gene detected by high-resolution FISH in the 17q11.2 region. Hum Genet 110:314–321.
Hulsebos TJ, Bijleveld EH, Riegman PH, Smink LJ, Dunham I. 1996. Identification and characterization of NF1-related loci on human chromosomes 22, 14, and 2. Hum Genet 98:7–11.
Jenne DE, Tinschert S, Stegmann E, Reimann H, Nürnberg P, Horn D, Naumann I, Buske A, Thiel G. 2000. A common set of at least 11 functional genes is lost in the majority of NF1 patients with gross deletions. Genomics 66:93–97.
Jenne DE, Tinschert S, Reimann H, Lasinger W, Thiel G, Hameister H, Kehrer-Sawatzki H. 2001. Molecular characterization and gene content of breakpoint boundaries in patients with neurofibromatosis type 1 with 17q11.2 microdeletions. Am J Hum Genet 69:516–527.
Jorde LB, Watkins WS, Viskochil D, O'Connell P, Ward K. 1993. Linkage disequilibrium in the neurofibromatosis 1 (NF1) region: implications for gene mapping. Am J Hum Genet 53:1038–1050.
Kayes LM, Burke W, Riccardi VM, Bennett R, Ehrlich P, Rubenstein A, Stephens K. 1994. Deletions spanning the neurofibromatosis 1 gene: identification and phenotype of five patients. Am J Hum Genet 54:424–436.
Kehrer-Sawatzki H, Schwickardt T, Assum G., Rocchi M, Krone W. 1997a. A third neurofibromatosis type 1 (NF1) pseudogene at chromosome 15q11.2. Hum Genet 100:595–600.
Kehrer-Sawatzki H, Haeussler J, Krone W, Bode H, Jenne DE, Mehnert KU, Tuemmers U, Assum G. 1997b. The second case of a t(17;22) in a family with neurofibromatosis type 1: sequence analysis of the breakpoint regions. Hum Genet 99:237–247.
Kehrer-Sawatzki H, Assum G, Hameister H. 2002. Molecular characterisation of t(17;22) (q11.2;q11.2) is not consistent with *NF1* gene duplication. Hum Genet 111:465–467.
Koontz JI, Soreng AL, Nucci M, Kuo FC, Pauwels P, van Den Berghe H, Dal Cin P, Fletcher JA, Sklar J. 2001. Frequent fusion of the JAZF1 and JJAZ1 genes in endometrial stromal tumors. Proc Natl Acad Sci USA 98:6348–6353.
Ledbetter DH, Rich DC, O'Connell P, Leppert M, Carey JC. 1989. Precise localization of NF1 to 17q11.2 by balanced translocation. Am J Hum Genet 44:20–24.
Legius E, Marchuk DA, Hall BK, Andersen LB, Wallace MR, Collins FS, Glover TW. 1992. NF1-related locus on chromosome 15. Genomics 13:1316–1318.
Li Y, O'Connell P, Breidenbach HH, Cawthon R, Stevens J, Xu G, Neil S, Robertson M, White R, Viskochil D. 1995. Genomic organization of the neurofibromatosis 1 gene (NF1). Genomics 25:9–18.
López Correa C, Brems H, Lazaro C, Estivill X, Clementi M, Mason S, Rutkowski JL, Marynen P, Legius E. 1999. Molecular studies in 20 submicroscopic neurofibromatosis type 1 gene deletions. Hum Mutat 14:387–393.
López Correa C, Dorschner M, Brems H, Lazaro C, Clementi M, Upadhyaya M, Dooijes D, Moog U, Kehrer-Sawatzki H, Rutkowski JL, Fryns JP, Marynen P, Stephens K, Legius E. 2001. Recombination hotspot in NF1 microdeletion patients. Hum Mol Genet 10:1387–1392.
Luijten M, Wang Y, Smith BT, Westerveld A, Smink LJ, Dunham I, Roe BA, Hulsebos TJ. 2000. Mechanism of spreading of the highly related neurofibromatosis type 1 (NF1) pseudogenes on chromosomes 2, 14 and 22. Eur J Hum Genet 8:209–214.
Marchuk DA, Tavakkol R, Wallace MR, Brownstein BH, Taillon-Miller P, Fong CT, Legius E, Andersen LB, Glover TW, Collins FS. 1992. A yeast artificial chromosome contig encompassing the type 1 neurofibromatosis gene. Genomics 13:672–680.
Messiaen L, De Bie S, Moens T, Van den Enden A, Leroy J. 1993. Lack of independence between five DNA polymorphisms in the NF1 gene. Hum Mol Genet 2:485.
North K. 1999. Cognitive function and academic performance. In: Friedman JM, Gutmann DH, MacCollin M, Riccardi VM, editors. Neurofibromatosis: phenotype, natural history, and pathogenesis, Third Ed. Baltimore/London: The John Hopkins University Press.
Park SS, Stankiewicz P, Bi W, Shaw C, Lehoczky J, Dewar K, Birren B, Lupski JR. 2002. Structure and evolution of the Smith-Magenis syndrome repeat gene clusters, SMS-REPs. Genome Res 12:729–738.
Purandare SM, Huntsman Breidenbach H, Li Y, Zhu XL, Sawada S, Neil SM, Brothman A, White R, Cawthon R, Viskochil D. 1995. Identification of neurofibromatosis 1 (NF1) homologous loci by direct sequencing, fluorescence in situ hybridization, and PCR amplification of somatic cell hybrids. Genomics 30:476–485.
Purandare SM, Cawthon R, Nelson LM, Sawada S, Watkins WS, Ward K, Jorde LB, Viskochil DH. 1996. Genotyping of PCR-based polymorphisms and linkage-disequilibrium analysis at the NF1 locus. Am J Hum Genet 59:159–166.
Rasmussen SA, Colman SD, Ho VT, Abernathy CR, Arn PH, Weiss L, Schwartz C, Saul RA, Wallace MR. 1998. Constitutional and mosaic large NF1 gene deletions in neurofibromatosis type 1. J Med Genet 35:468–471.
Regnier V, Meddeb M, Lecointre G, Richard F, Duverger A, Nguyen VC, Dutrillaux B, Bernheim A, Danglot G. 1997. Emergence and scattering of multiple neurofibromatosis (NF1)-related sequences during hominoid evolution suggest a process of pericentromeric interchromosomal transposition. Hum Mol Genet 6:9–16.
Riva P, Corrado L, Natacci F, Castorina P, Wu BL, Schneider GH, Clementi M, Tenconi R, Korf BR, Larizza L. 2000. NF1 microdeletion syndrome: refined FISH characterization of sporadic and familial deletions with locus-specific probes. Am J Hum Genet 66:100–109.
Riva P, Gervasini C, Larizza L. 2002. Genomic evidence versus characterisation of a single (17;22) translocation on *NF1* gene duplication: lessons from deletions in "balanced" chromosomal rearrangements. Hum Genet 111:468–469.
Samonte RV, Eichler EE. 2002. Segmental duplications and the evolution of the primate genome. Nat Rev Genet 3:65–72.
Suzuki H, Ozawa N, Taga C, Kano T, Hattori M, Sakaki Y. 1994. Genomic analysis of a NF1 related pseudogene on human chromosome 21. Gene 147:277–280.
Upadhyaya M, Ruggieri M, Maynard J, Osborn M, Hartog C, Mudd S, Penttinen M, Cordeiro I, Ponder M, Ponder BA, Krawczak M, Cooper DN. 1998. Gross deletions of the neurofibromatosis type 1 (NF1) gene are predominantly of maternal origin and commonly associated with a learning disability, dysmorphic features and developmental delay. Hum Genet 102:591–597.
Valero MC, Velasco E, Valero A, Moreno F, Hernandez-Chico C. 1996. Linkage disequilibrium between four intragenic polymorphic microsatellites of the NF1 gene and its implications for genetic counselling. J Med Genet 33:590–593.
Valero MC, Pascual-Castroviejo I, Velasco E, Moreno F, Hernandez-Chico C. 1997. Identification of de novo deletions at the NF1 gene: no preferential paternal origin and phenotypic analysis of patients. Hum Genet 99:720–726.
Valero MC, de Luis O, Cruces J, Perez Jurado LA. 2000. Fine-scale comparative mapping of the human 7q11.23 region and the orthologous region on mouse chromosome 5G: the low-copy repeats that flank the Williams-Beuren syndrome deletion arose at breakpoint sites of an evolutionary inversion(s). Genomics 69:1–13.
Yagle MK, Parruti G, Xu W, Ponder BA, Solomon E. 1990. Genetic and physical map of the von Recklinghausen neurofibromatosis (NF1) region on chromosome 17. Proc Natl Acad Sci USA 87: 7255–7259.

Appendix 3

CANCER INVESTIGATION
Vol. 21, No. 6, pp. 901–918, 2003

MOLECULAR BIOLOGY AND GENETICS OF CANCER

Genetics of Neurofibromatosis 1-Associated Peripheral Nerve Sheath Tumors

Karen Stephens*

Departments of Medicine and Laboratory Medicine, University of Washington, Seattle, Washington, USA

AQ1

INTRODUCTION

Much of our current understanding of tumorigenesis is founded on genetic studies of relatively rare individuals with inherited disorders that predispose to certain cancers, e.g., retinoblastoma[1] and colorectal tumors.[2,3] Such genetic studies are consistent with a model whereby normal tissues become highly malignant due to successive mutation of multiple genes that dysregulate cellular proliferation and homeostasis. Important classes of mutated genes include oncogenes (positive growth regulators), tumor suppressors (negative growth regulators), and those encoding cell cycle regulators, antiapototic signals, and components of the DNA replication and repair machinery. Mutation during tumorigenesis can occur at the nucleotide level as inactivation of a single gene or at the chromosomal level as losses of large segments or entire chromosomes, as a fusion of two different chromosomal segments, or as a high level amplification of a segment.[4] Screening normal and tumor tissues of patients for common genetic alterations has been a productive strategy for identifying genes that contribute to tumor formation. This article focuses on genetic changes commonly associated with peripheral nerve sheath tumors in individuals with the autosomal dominant tumor-prone disorder neurofibromatosis 1 (NF1).

Virtually all individuals affected with NF1 develop multiple peripheral nerve sheath tumors. The most common are neurofibromas, which are benign tumors that can occur anywhere along the length of epidermal, dermal, deep peripheral (including dorsal nerve roots in the paraspinal area), or cranial nerves. They do not occur in the brain or the spinal cord proper.[5] Although benign, neurofibromas can cause considerable morbidity by, e.g., infiltrating and functionally impairing normal tissues, causing limb hypertrophy, or masking an emerging malignancy. Some types of neurofibromas can transform into malignant peripheral nerve sheath tumors (MPNST), previously termed neurofibrosarcoma or malignant schwannoma. An estimated 20%–50% of MPNSTs are associated with NF1 disease,[6] and they are a significant cause of the decreased life expectancy in the NF1 patient population.[7,8] Recent population-based longitudinal studies detected an annual incidence of 1.6/1000 and a lifetime risk of 8%–13% for NF1-associated MPNST,[9] which is much higher than detected in previous cross-sectional studies[10] and over three orders of magnitude greater than that of the general population (~0.001%).[11] Furthermore, NF1-associated MPNST were diagnosed at an earlier age than sporadic tumors (26 vs. 62 years, $p < 0.001$) and associated with a poorer prognosis than sporadic MPNST (5-year survival of 21 vs. 42%, $p = 0.09$).[9]

*Correspondence: Karen Stephens, Ph.D., University of Washington, 1959 NE Pacific St., Rm I-204, Seattle, WA 98195-7720, USA; Fax: 206-685-4829; E-mail: millie@u.washington.edu.

DOI: 10.1081/CNV-120025093

0735-7907 (Print); 1532-4192 (Online)
www.dekker.com

This article reviews the genetic abnormalities that have been identified at the level of the gene, chromosome, and genome in NF1-associated neurofibromas and MPNST. Identifying commonly associated genetic alterations and the mechanisms by which they arise may potentially lead to markers for tumor staging, to new research approaches to pathogenesis, and to the identification of gene targets, which in conjunction with NF1, will be useful for mouse models.

THE MOLECULAR BASIS OF NF1

The NF1 is a common autosomal dominant disorder that affects about 1 in 3500 individuals worldwide. About 30%–50% of cases are sporadic, caused by de novo mutation in the *NF1* gene of an individual without a family history of the disorder. In addition to predisposing to tumorigenesis, NF1 is associated with characteristic changes in pigmentation and can be associated with a wide range of other manifestations such as learning disabilities and bony abnormalities (reviewed by Refs. [12–16]). All cases are caused by mutation of the *NF1* gene at chromosome 17 band q11.2, which contains 60 exons that encode the 2818 amino acid protein called neurofibromin.[17–21] Neurofibromin is widely expressed, predominantly in the central nervous system and sensory neurons and Schwann cells of the peripheral nervous system.[22,23] One functional domain of neurofibromin has been defined, the GAP-related domain (GRD), so called because of its structural and functional homology to mammalian p120-GAP (*G*TPase *a*ctivating *p*rotein) and yeast genes known to regulate the Ras pathway.[24,25] The Ras-GAP proteins function as negative regulators of Ras by catalyzing the conversion of active GTP-bound Ras to the inactive GDP-bound Ras form.[26] In NF1-associated peripheral nerve sheath tumors, it is hypothesized that neurofibromin deficiency leads to increased activated Ras, resulting in aberrant mitogenic signaling and the consequent growth of a tumor. The identification of an NF1 patient with a missense mutation in the GRD that specifically abolished the Ras-GAP activity of neurofibromin demonstrated the importance of neurofibromin GAP function in NF1 pathogenesis.[27] In at least some tissues, there is evidence that it is the Ras-GAP activity that accounts for the tumor suppressor function of neurofibromin. The most complete evidence comes from genetic and biochemical analyses of NF1-associated malignant myeloid disorders.[28,29] The tumor suppressor function of *NF1* has been reviewed recently[30–32] along with its potential as a therapeutic target.[33]

The NF1 disease is caused by haploinsufficiency for neurofibromin. The vast majority of *NF1* mutations are not in the GRD but are distributed throughout the gene. Over 80% of mutations inactivate or predict inactivation of neurofibromin; splicing defects and sequence alterations that create a premature translation termination codon are the most common.[34,35] About 10% of *NF1* mutations are missense,[35,36] which are typically clustered in the GRD or an upstream cysteine/serine-rich domain that may play a role in ATP binding.[36] Definitive evidence that neurofibromin haploinsufficiency underlies NF1 came with the identification of *NF1* whole gene deletions in an estimated 5%–10% of affected individuals.[37,38] Mutational analyses of patients with specific features, such as plexiform neurofibroma,[39] spinal neurofibroma,[40] or malignant myeloid disorders,[41] failed to detect any correlation between genotype and phenotype. A notable exception is the subset of patients heterozygous for a microdeletion spanning the entire *NF1* gene, who consistently show an early age at onset of cutaneous neurofibromas (see below).

Virtually all NF1 patients develop neurofibromas. Neurofibromas are comprised of an admixture of largely Schwann cells and fibroblasts, along with mast cells, endothelial cells, and pericytes.[42,43] Although classification schemes vary, Friedman and Riccardi[13] define four types of neurofibromas. Discrete cutaneous neurofibromas of the epidermis or dermis are the most common, typically appearing near or at puberty and increasing in number to over 100 by the fourth decade of life.[44] They are a localized tumor of small nerves in the skin that feels fleshy and soft; they are more prevalent on the trunk but also occur frequently on the face and extremities. Discrete subcutaneous neurofibromas have a spherical or ovoid shape, feel firm or rubbery, and may be painful or tender. Deep nodular neurofibromas, also called nodular plexiform neurofibromas, involve major or minor nerves in tissues beneath the dermis. On gross pathology, they appear to grow inside the peripheral nerve, causing a fusiform enlargement, and may extend the entire length of a nerve.[43] Diffuse plexiform neurofibromas have a cellular composition similar to that of cutaneous neurofibromas, but in contrast, they have a tendency to become locally invasive.[5,43] Histologically, this tumor is a tangled network involving multiple nerve fascicles or branches of major nerves with poorly defined margins that makes complete surgical resection virtually impossible. Plexiform neurofibromas can be superficial with extensive involvement of underlying tissues, or they may involve deep tissues, particularly in the craniofacial region, paraspinal structures, retroperitoneum, and gastrointestinal tract.[13] They can infiltrate soft

tissues resulting in localized hypertrophy and significant functional impairment. In contrast to other types of neurofibromas, diffuse plexiform tumors are considered congenital because they typically become evident in infancy or childhood and rarely, if ever, in late adulthood.[45,46] In a population-based study, 32% of individuals with NF1 had a plexiform neurofibroma(s) on physical examination.[47] Korf[5] recently reviewed plexiform neurofibromas.

Plexiform neurofibromas, both diffuse and nodular, are at a greater risk of transforming to an MPNST than other types of neurofibromas (reviewed in Refs. [5,43,48]). Pathological examination of MPNST from individuals, both with and without NF1, most often shows an association with a neurofibroma.[11,49–51] These data suggest that an early step in MPNST development may be preneoplastic process in the nerve sheath. Multiple pathological and molecular criteria are used to evaluate a neurofibroma for malignant transformation.[48] Several lines of evidence are consistent with cutaneous and plexiform neurofibromas and MPNSTs being clonal tumors that arise from an ancestral Schwann cell (see below).

GENETICS OF NEUROFIBROMAGENESIS

Homozygous Inactivation of *NF1*

Homozygous inactivation of a tumor suppressor gene(s) is a fundamental mechanism of tumorigenesis. It occurs by either sequential somatic inactivation of both alleles or by a somatic mutation in the single normal homolog in individuals who inherit a germline mutation in one allele. Somatic inactivation is frequently associated with loss of heterozygosity (LOH) at the tumor suppressor locus and at multiple flanking loci (reviewed in Refs. [52,53]). Evidence for such ''2nd hit'' somatic *NF1* mutations in neurofibromas has been sought in support of the hypothesis that neurofibromin functions as a tumor suppressor in Schwann cells. Initial reports of LOH at *NF1*[54] have been confirmed and extended by analyses of both primary tumor tissue and neurofibroma-derived Schwann cells. At least 25% of neurofibromas undergo LOH at *NF1*.[55,56] The cellular admixture in neurofibromas can mask allelic loss,[55,56] which is the likely explanation for reports that detected few, if any, tumors with LOH.[57–62] Compelling evidence that the somatic inactivation of the *NF1* gene itself is important was provided by the identification of a 4 bp deletion in exon 4b in a cutaneous neurofibroma of a patient with a germline *NF1* microdeletion.[63] Subsequent analyses of cDNA from neurofibromin-derived Schwann cells showed that 19% of neurofibromas carried somatic intragenic mutations, which were typically mRNA splicing defects.[34] Mutation frequency may be underrepresented due to the difficulty of recovering high-quality tumor RNA and the underrepresentation of mutant transcripts observed in some tumors. The latter could be attributed to mutations that induce nonsense-mediated decay or other mechanisms that affect mRNA content (reviewed in Ref. [64]) or to reduced expression for other reasons,[34] and/or a low proportion of mutant to normal Schwann cells in some tumors.[65,66] Homozygous inactivation of *NF1* also occurs in plexiform neurofibromas, where an estimated 40% (n = 10) showed LOH,[67] a result confirmed by subsequent reports.[57,58,68,69]

A predominant mechanism of somatic *NF1* inactivation in neurofibromas that underwent LOH was mitotic recombination.[56] A 17q proximal single mitotic recombination event near the centromere of the q arm between the normal chromosome 17 and the homolog carrying the germline *NF1* mutation can generate a cell in which both *NF1* genes carry the germline mutation and all loci distal to the recombination site are identical. Less common were double recombination events that result in chromosome 17 interstitial loci showing LOH. The *NF1* mRNA in some neurofibromas is edited such that an arginine codon is changed to a nonsense codon.[70] Although only one-third of neurofibromas examined showed a low level (<2.5%) of edited *NF1* transcripts,[71] such modulation of neurofibromin expression may be important if, e.g., editing occurred at high frequency in transcripts from a specific minor cellular component of the tumor. In other neurofibromas, somatic mutations appear to destabilize *NF1* mRNA.[66] Transcriptional silencing via hypermethylation of promoter regions, a prominent mechanism of inactivating other tumor suppressor genes,[72] has not been detected in neurofibroma tissue.[73,74] As expected from the mutational and LOH analyses, some neurofibromas had no detectable *NF1* transcripts or neurofibromin.[75,76] A quantitative Ras activity assay demonstrated that activated Ras-GTP levels were about fourfold higher in neurofibromas than levels in non-NF1-associated schwannomas.[75,77]

Neurofibromas are most likely clonal tumors derived from a Schwann cell progenitor. The detection of LOH in a tumor operationally defines it as being clonal in origin, and these data are consistent with direct marker analyses in neurofibromas.[57,61] The LOH or other somatic mechanisms that inactivate *NF1* in a Schwann cell progenitor may be an early or initiating genetic event in neurofibromagenesis. Klewe and colleagues showed

LOH in primary neurofibroma tissue and in tumor-derived Schwann cells but not fibroblasts.[78] Other investigators confirmed this observation.[66,68] Two genetically distinct Schwann cell populations, $NF1^{+/-}$ and $NF1^{-/-}$, were successfully cultured from 10 mutation-characterized neurofibromas, whereas tumor-derived fibroblasts carried only the germline $NF1^{+/-}$ genotype.[65] Sherman et al.[79] used an elegant single cell Ras-GTP assay to show elevated levels in neurofibroma-derived Schwann cells but not fibroblasts. Consistent with two Schwann cell populations, only a fraction (12%–62%) of neurofibroma-derived Schwann cells had elevated Ras-GTP levels. The basis of the Schwann cell heterogeneity is not known, but the authors speculate that the cells with high Ras-GTP (presumably neurofibromin-deficient) may recruit Schwann cells with lower Ras-GTP levels (presumably the constitutional neurofibromin-haploinsufficient cells) via the synthesis of growth factors. Whether this admixture of Schwann cells is important in tumorigenesis remains to be determined; however, its observation in primary neurofibroma tissues makes it more likely. Fluorescence in situ hybridization and immunohistochemistry demonstrated that S-100 protein (Schwann cell marker) immunopositive cells in sections of four of seven primary plexiform neurofibromas were monosomic for *NF1*.[80] Because other cells types were disomic at *NF1*, these results strongly implicate the Schwann cell as the target of the *NF1* 2nd hit mutation and verify that the results from neurofibroma-derived Schwann cells were not biased by cell culture. These data also support Schwann cell genetic heterogeneity, because the fraction of S-100 protein positive cells showing *NF1* deletion ranged from 50%–93%. Further evidence for the importance of Schwann cells in neurofibromagenesis comes from the tumorigenic properties exhibited by neurofibroma-derived cells.[81–84] In the most comprehensive studies, Muir and colleagues[83,84] showed that neurofibromin-deficient Schwann cells, derived from either dermal or plexiform neurofibromas, had high invasive potential and produce neurofibroma-like tumors when engrafted into peripheral nerves of *scid* mice.

Germline Alterations That May Modify Neurofibromagenesis

The considerable variable expressivity of NF1 disease among family members with presumably the same *NF1* mutation and results of a statistical trait analysis led to the contention that variation in an individual's genetic background modified the NF1 phenotype.[46,85] To date, no such germline modifying genes have been identified. However, the study of patients carrying *NF1* microdeletions has provided compelling evidence for a gene that modifies neurofibromagenesis. We first recognized that *NF1* microdeletion patients typically showed an early age at onset of localized cutaneous neurofibromas or, in cases in which age at onset could not be documented, they had significantly greater numbers of cutaneous neurofibromas relative to their age.[38,86] It is common to observe multiple cutaneous neurofibromas during physical examination of children under age 10 that are heterozygous for an *NF1* microdeletion,[38,87,88] whereas only about 10% in the general NF1 population have a tumor(s) by that age.[47] In our most severe case, a 5 year old with an *NF1* microdeletion had 51–100 tumors.[38] The *NF1* microdeletions can be inherited from an affected parent, and in these cases, the microdeletion cosegregated with the early age at onset of neurofibromas.[88,89] Other investigators have confirmed the early onset and heavy burden of cutaneous neurofibromas in *NF1* microdeletion patients, and over 50 such patients have been identified.[90–98]

Most *NF1* microdeletions span 1.5 MB of DNA,[87] which harbors the entire 350 kb *NF1* gene and at least 11 additional genes, most of unknown function.[87,99] The microdeletions are preferentially maternal in origin[87,91,93,100,101] and arise by homologous recombination between 60 kb misaligned paralogs (termed NF1REP) that flank the *NF1* gene.[87] Paralogs are nonallelic DNA sequences with a high degree of identity that arose via duplication, e.g., the two functional α globin genes. Over 25 human disorders are known to be caused by gene or chromosomal rearrangements mediated by homologous recombination between paralogs, a process correctly referred to as nonallelic homologous recombination in the review by Stankiewicz and Lupski.[102] Here, I propose that this process be called by the less awkward term of paralogous recombination and that disorders arising by this mechanism be called paralogous recombination disorders, rather than the currently used genomic disorders. Although the NF1REPs share >95% sequence identity over 60 kb of sequence, about 80% of the *NF1* deletion alleles are virtually identical because their breakpoints map to one of either two recombination hotspots of several kb in size located within the NF1REP[103] (M. Dorschner et al., in preparation). Although the molecular basis for these hotspots is not yet known, their existence means that the majority of microdeletion patients will be deleted for the same set of genes. The early age at onset of cutaneous neurofibromas observed in several patients with larger deletions and/or different breakpoints

indicates that generation of a deletion-specific fusion gene product is unlikely.[87]

We hypothesized that the codeletion of *NF1* and an unknown linked gene potentiates cutaneous neurofibromagenesis.[38,87] What might be the function of the putative neurofibromagenesis-potentiating locus (*NPL*)? Here I propose two models for the early age at onset of cutaneous neurofibromas in microdeletion patients. Haploinsufficiency for *NPL* could increase the frequency of somatic 2nd hit mutations in the *NF1* gene. This could result from a genomic instability in microdeletion patients, which is intriguing in view of reports detecting cytogenetic abnormalities and microsatellite instability in some neurofibromas (see below). It would be interesting to determine if somatic *NF1* mutations in cutaneous neurofibromas of microdeletion patients occur by a predominant mechanism. Only a single tumor from each of two deletion patients have been analyzed; one had a 4 bp intragenic deletion[63] and the other a splice site.[65] A second model for early onset of cutaneous neurofibromas proposes that *NPL* haploinsufficiency increases the probability that a neurofibromin-deficient progenitor cell proliferates and manifests as a neurofibroma. Multiple mechanisms could be proposed. For example, *NPL* could encode (or regulate) a cytokine, cell cycle regulator, tumor suppressor, or oncogene, which exerts a positive proliferative advantage on the progenitor cell. Because of the cellular heterogeneity of neurofibromas, this model does not necessarily require that the abnormal expression of *NPL* or its putative downstream targets occur in the neurofibromin-deficient Schwann clone.

Preliminary, but intriguing evidence suggests that genetic background, other than *NF1* microdeletion, may influence the somatic inactivation of *NF1*. In patients with multiple neurofibromas, it was determined that each of the tumors showed the same type of somatic mutation event (e.g., LOH of the entire q arm or interstitial LOH).[56] Depending on the extent of LOH and the particular genes involved, this could explain differences in the age at onset and/or numbers of neurofibromas that develop in an individual.

Somatic Alterations That May Modify Neurofibromagesis

The NF1-associated neurofibromas have been analyzed for genetic abnormalities at the chromosomal level by comparative genome hybridization (CGH) and cytogenetic analyses. Comparative genome hybridization is a powerful technique to detect and map chromosomal regions with copy number imbalances in tumor specimens (reviewed in Ref. [104]). Only two of eight neurofibromas (type not specified) examined showed chromosomal imbalances; one tumor showed three gains; the other only a single gain.[105,106] This observation is consistent with cytogenetic studies. Although Schwann cell cultures from dermal neurofibromas had normal karyotypes, cells derived from plexiform neurofibromas had abnormalities, which in some tumors consisted of unrelated non-clonal abnormalities.[107] One plexiform had structural abnormalities predominantly involving telomeres, which are typically associated with genomic instability in other syndromes/tumors.[107] Wallace et al. proposed that chromosomal abnormalities might be important in the development of plexiform neurofibromas. Chromosomal abnormalities in plexiform neurofibromas may account, at least in part, for their increased risk of malignant transformation. Whether other cellular components of neurofibromas show cytogenetic abnormalities is unclear. Some neurofibroma fibroblast-like derived cultures were reported to show an increased frequency of chromosomal aberrations,[108] whereas others were typically negative.[109]

Conflicting data have been reported regarding the presence of microsatellite instability in NF1-associated neurofibromas. Some human tumors, most notably those of patients with hereditary nonpolyposis colon cancer HNPCC, show microsatellite instability, which is detected by random changes in the length of microsatellite (simple nucleotide repeats) loci. Length mutations at multiple microsatellite loci in a tumor reflect a genome-wide instability, which in the case of HNPCC is due to a defect in any of several mismatch repair genes (reviewed in Ref. [2]). Ottini et al.[110] reported that 50% (n = 16) of neurofibromas showed altered allele lengths compared with matched normal tissue, and instability at chromosome 9 loci has also been reported.[111] Birindelli et al.[112] observed instability in a primary MPNST and a metastasis in one of 25 cases. However, no evidence of instability was detected in two subsequent studies of 80 neurofibromas, of which 5% appear to be of the plexiform type.[55,73] This disparity may be due to technical differences, the number and type of microsatellite loci examined, and/or the stage of the neurofibromas. The LOH at *NF1* was not a factor, because all three studies analyzed neurofibromas that were both positive and negative. Of the eight neurofibromas with microsatellite instability, seven were unstable at only one of the five loci tested.[110] Due to the important implications that microsatellite instability would have for neurofibromagenesis, additional loci should be examined in

these tumors, including those analyzed by the other investigators. In addition, it would be interesting to know if the neurofibromas that showed microsatellite instability were of the larger, central plexiform type, in which case they may have been transforming to malignancy. The proportion of loci that display instability is known to increase with tumor progression in HNPCC.[113]

GENETICS OF MPNST DEVELOPMENT

Homozygous Inactivation at *NF1*

The homozygous inactivation of *NF1* in NF1-associated MPNST, first reported by Skuse et al.,[60] has been confirmed in about 50% of tumors (n = 22) by LOH.[67,109,112,114,115] Mutations in both *NF1* alleles have been identified in a single MPNST.[114] Although the mechanism of LOH is not known, it does not generally involve cytogenetically detectable losses at 17q1.[116] Furthermore, NF1-associated MPNST-derived cell lines showed decreased or absent neurofibromin and high levels of active Ras-GTP,[117,118] and a quantitative Ras activity assay demonstrated that activated Ras-GTP levels in tumors were about 15-fold higher than levels in non-NF1-associated schwannomas.[77] Because homozygous inactivation of *NF1* occurs in benign neurofibromas, it is considered an early or initiating event that is necessary and sufficient for neurofibromagenesis but not MPNST development. Malignant transformation is presumably driven by predisposing genetic factors in the germline and/or by additional somatic mutations and positive growth selection in a malignant precursor cell. The role of *NF1* in the development of sporadic MPNST is not clear; only about 10% of these tumors show LOH at *NF1*.[112]

Germline Alterations That May Modify MPNST Development

Little is known about germline genetic modifiers that predispose to MPNST. Early speculation that patients with *NF1* microdeletion may be at increased risk for malignancy[38] is now supported by indirect evidence. Mutational analysis of germline DNA from seven patients who developed MPNST determined that three (42%) were heterozygous for an *NF1* microdeletion.[119] In another study, 2 of 17 (11%) unrelated *NF1* microdeletion patients developed MPNST, and affected first-degree relatives of two microdeletion patients had other malignancies.[87] Although additional cases are needed, these data suggest that the lifetime risk of MPNST in microdeletion patients may exceed the already high 10% in the general NF1 population.[9] If so, the underlying mechanism may be essentially the same as that proposed above for early onset neurofibromagenesis. Deletion of the putative *NPL* gene could result in genomic instability or exert positive growth selection for the malignant clone. If microdeletions do predispose to both cutaneous neurofibromas and MPNST, it seems reasonable to speculate that in at least this subset of patients, either the discrete cutaneous type of neurofibroma is at increased risk of malignant transformation or the frequency of nodular or diffuse plexiform neurofibromas is high.

Evidence from two families suggests the intriguing possibility that MLH1 deficiency predisposes to NF1 and early onset extracolonic tumors.[120,121] Germline heterozygous inactivating mutations in *MLH1* cause inefficient DNA mismatch repair, with the consequent increase in mutation frequency and susceptibility to hereditary nonpolyposis colorectal cancer (reviewed in Ref. [122]). Two rare and independent cases of consanguineous marriages between *MLH1* heterozygous first cousins each produced two children with NF1 disease and hematological malignancies.[120,121] The parents had no signs of NF1 and there was no family history of the disease. The MLH1 mutations were identified, confirming homozygosity in three of the four deceased children, who presented with mutiple café au lait spots (4/4), dermal neurofibromas (2/4), tibial pseudoarthrosis (1/4), non-Hodgkin's lymphoma (2/4), myeloid leukemia (2/4), and medulloblastoma (1/4). The authors suggest that these patients had a de novo postzygotic *NF1* mutation and that the *NF1* gene may be preferentially susceptible to mismatch repair deficiency. Unfortunately, the *NF1* gene was not analyzed for mutations, due in part to lack of patient tissue,[120] which could have confirmed mutation of *NF1* and differentiated between postzygotic mutation and germline mosaicism in a parent.

Somatic Alterations in NF1-Associated MPNST

All NF1-associated MPNST showed significant chromosomal imbalances by CGH.[105,106,123,124] Analysis of 27 total tumors from 19 NF1 patients showed an average of >7 imbalances per MPNST (Table 1). One tumor had only a single imbalance, a gain of chromosome 8.[123] The studies led by Mechtersheimer and Schmidt,[105,106] which include 74% of tumors examined, detected chromosomal gains more frequently than

T1.1 ***Table 1.*** Chromosomal gains and losses in MPNST detected by CGH.

		NF1-associated MPNST			Sporadic MPNST		
T1.3		Loethe[a]	Mechtersheimer[b]	Schmidt[c]	Loethe[a]	Mechtersheimer[b]	Schmidt[c]
T1.4	No. tumors/No. patients	7/7	6/6	14/6	3/3	13/13	22/20
T1.5	Imbalances	52	77	188	14	176	200
T1.6	Per tumor	7.4	11.7	13.4	4.6	13.5	9.1
T1.7	Range	1–17	6–30	7–29	1–7	0–34	0–25
T1.8	Chromosome gains	14	48	139	4	125	179
T1.9	Per tumor	2	8.0	10.0	1.3	9.6	8.1
T1.10	Range	0–3	4–18	5–20	0–2	0–23	0–21
T1.11	Chromosome losses	38	29	49	10	51	33
T1.12	Per tumor	5.4	4.8	3.5	3.3	3.9	1.5
T1.13	Range	0–14	1–12	0–11	1–4	0–11	0–9

a: Ref. [123].
b: Ref. [105].
c: Ref. [106].

losses (Table 1). Each of the 20 tumors in these studies had $\geq$4 chromosomal gains. Although the results of these two studies were comparable, they differed from a third study that found chromosomal losses more prevalent than gains.[123] The reason for the disparity is unclear; however it was also evident in the analyses of sporadic MPNST in each study (Table 1). T2 Table 2 summarizes the chromosomal segments that most frequently showed gains in NF1-associated MPNST. The most common segments were on 17q22-q24, 17q25, 7p14, 7p21, 8q22, 8q23-q24, and 7q31. Chromosomal loss of these segments was rarely, if ever, observed.[105,106,123] A combined analysis of sporadic and NF1-associated MPNST revealed a significantly decreased survival rate of patients with MPNST with gains at both 7p15-21 and 17q22-qter.[124]

In addition to chromosomal gains, CGH analyses also revealed large-scale chromosomal amplifications.[105,106,124] One-third of MPNST of both NF1 and non-NF1 patients had at least one amplified chromosomal segment (Table 3). Although the number of T3 tumors is small, there are differences in amplification patterns. In NF1-associated MPNST 7p and 17q22-qter, the same regions that commonly showed chromosomal

T2.1 ***Table 2.*** Frequency of chromosomal gains in NF1-associated MPNST.

		% MPNST			
T2.3		Loethe[a]	Mechtersheimer[b]	Schmidt[c]	Total
T2.4	No. MPNST/No. patients	7/7	6/6	14/6	27/19
T2.5	*Chromosome*				
T2.6	1q33	0	50	50	37
T2.7	5p15	28	50	35	37
T2.8	7p14	28	83	71	63
T2.9	7p21	28	50	64	52
T2.10	7q31	28	33	64	48
T2.11	8q22	28	33	64	48
T2.12	8q23-q24	14	33	85	55
T2.13	15q24-q25	0	17	71	41
T2.14	17q22-q24	42	83	85	74
T2.15	17q25	71	83	78	78

a: Refs. [105,123].
b: Ref. [105].
c: Ref. [106].

gains (Table 1) were amplified frequently. The frequency of 7p amplifications may be overestimated because these four MPNST (considered as different primary tumors) were from a single patient.[106,124] In contrast, amplifications of 5p, 8q, and 12q were the most prevalent in sporadic MPNST. There was a significant difference in the frequency of tumors with more than one chromosomal segment amplified. Only 10% of NF1-associated MPNST had more than one amplified segment, whereas the frequency was 72% in sporadic tumors (Table 3). Differences in the location and number of chromosomal segments amplified were unlikely to be due to tumor grade, because the majority of MPNST, 14 of 20 (70%) of NF1-associated and 22 of 34 (64%) of sporadic, were grade 3 (poorly differentiated). Although amplifications were more frequent in NF1-associated than sporadic MPNST (50% vs. 32%), the number of NF1-associated tumors may be overestimated because it includes multiple tumors from the same patient. Adjustment for one tumor/patient gives a frequency of 25% (5 of 20) for NF1-associated MPNST. Similarly, there was no correlation between chromosomal

Table 3. Large-scale chromosomal amplifications in MPNST.[a]

Chromosome segment amplified	No. NF1-associated MPNST[b] (N = 20)	No. sporadic MPNST[c] (N = 34)
4q12-q13		1
5p11-p15		1
5p14		1
5p15		2
5p13-pter		2
7p14-pter	2[d]	1
7p13-pter	1[d]	
7p12-pter	1[d]	
7p11-p12		1
8q12-qter		2
8q13		1
8q21-q22		1
8q22-q23		1
8q24		1
8q23-qter	1	
9p21-p23	1[e]	
9q31-q33		1
12p12	1[e]	
12p13		1
12q13-q14		1
12q14-q21		3
12q24		3
13q13-q33		1
13q32-q33		1
17p11-p12		1
17q24-qter	2	
17q22-q24	1	
20q12-qter		1
Xp11		1
Xp21-p22		1
Summary		
% tumors with an amplification	50 (10/20)	32 (11/34)
% tumors with >1 amplified segment	0.1 (1/10)	72 (8/11)
% patients with ≥ 1 tumor with an amplification	30 (4/12)	32 (11/34)

a: Centromeric regions, chromosomes 19 and Y, and 1p32-p36 were not scored for technical reasons. (From Ref. [105].)
b: Refs. [105,106,124].
c: Refs. [105,124].
d: Four of five primary MPNST from one patient. (From Ref. [106].)
e: Two of four primary MPNST from one patient. (From Ref. [106].)

amplification and progression to metastasis. Analysis of tissue from a primary tumor, recurrence, and metastasis from a single patient showed a single amplification (8q12-qter) in the recurrent tumor.[124]

Comparison of the chromosomal losses detected in the three CGH studies revealed the following five most frequent losses in 27 NF1-associated MPNST: 13q21-22 (12/27), 11q23-25 (10/27), 1p22-31 (9/27), 3q11-21 (8/27), and 17p12-pter (7/27).[105,106,123] It is of interest that the loss of 17p12-pter was detected in 50% (7 of 14) tumors in one study[106] and in none of the tumors of the other studies. The relatively low detection rate of chromosomal losses may be due to the decreased sensitivity of CGH in polyploid MPNST.[125]

The CGH analysis of multiple, presumably synchronous or metachronus, primary MPNST at different sites in three NF1 patients revealed a remarkable similarity in chromosomal gains and losses.[106,124] For example, five grade 3 (poorly differentiated) tumors of one patient each showed imbalances of +7p, −13q21, and +17q22-qter. These data showed that in the specific genetic background of each patient, a relatively limited, and defined, number of rearrangements were shared among the tumors. Similarly, nearly identical aberrations were found in different MPNST from the same patient.[125] Although limited, these data suggest that each individual's constitutional genotype sets a certain "baseline" on which a minimal and limited number of genetic alterations are necessary and sufficient for MPNST development.

Consistent with CGH analysis, the karyotype of NF1-associated MPNST-derived cells are complex with chromosomal numbers ranging from 34 to 270 indicative of hypodiploidy, hypotriploidy, hypotetraploidy, hypertriploidy, and hypertetraploidy (Refs. [109,116,125] and references therein). Although breakpoints were frequent, a common specific breakpoint was not detected. A comparison of CGH and karyotying in six MPNST revealed significant overlap in the most frequent gains and detected losses at 19q (3 of 6 tumors), a region not analyzed in the CGH studies.[106,125] Plaat et al.[116] performed a computer-assisted cytogenetic analysis of 46 MPNST reported in the literature and 7 new cases of both NF1-associated and sporadic tumors (Ref. [116] and references therein). These studies confirmed the CGH observation of high-frequency gains at chromosomes 7p and 7q and losses at 1p and 17p. However, their reported cytogenetic differences between NF1-associated and sporadic MPNST[116] were not confirmed in later studies.[125,126] In one study, near triploid or near tetraploid clones were associated with grade 3 tumors and a poor prognosis.[126] The detection of a t(X;18) translocation in MPNST[127] was not confirmed in either sporadic[128] or NF1-associated neurofibroma or MPNST.[129]

Inactivating mutations in several tumor suppressor genes have been identified in NF1-associated MPNST. Both LOH and intragenic missense mutations of *TP53*[50,62,112,130] have been detected. Like many sarcomas, NF1-associated MPNST often showed overexpression of p53 (the protein product of the *TP53* gene) as assayed by immunoreactive positivity in the nucleus.[50,112,131,132] In keeping with findings in other tumors, this most likely is mutant p53 protein, which accumulates due to its increased stability. Mutant protein is thought to promote cancer by either complexing with and sequestering functional p53 or by complexing with p63 and p73 and blocking their normal transcription factor activities (reviewed in Ref. [133]). Immunohistochemical detection of p53 was more common in NF1-associated vs. sporadic MPNST, and it was associated with poor prognosis in NF1 children.[132] About 50% of NF1-associated MPNST showed homozygous deletion for exon 2 of the *INK4A* gene, and over 90% were immunonegative for its protein product p16.[112,134,135] Homozygous deletion of exon 2 results in deficiency for both p16 and $p14^{ARF}$, two proteins encoded by alternative splicing of *INK4A* (also known as *CDKN2A*). Both of these proteins are tumor suppressors that modulate activities of the RB and p53 pathways, which are critical for cell cycle control and tumor surveillance (reviewed in Ref. [136]). MXI1 mutations in regions that encode known functional domains have been detected in the two NF1-associated MPNST analyzed.[137] Mxi1 is an agonist of the oncoprotein Myc and is thought to limit cell proliferation and help maintain the differentiated state (reviewed in Ref. [138]). *Mxi1*-deficient mice develop tumors, and *Mxi1* deficiency decreases the latency of tumors that arise in Ink4a-deficient mice.[139] If additional studies show that somatic inactivation of MXI1 is common, it would suggest a link between the pathways of Ink4a, Myc, and Ras in NF1-associated MPNST.[140,141]

Several differences observed in NF1-associated MPNST are likely involved in the malignant transformation of a preexisting neurofibroma. *TP53* or *INK4A* mutations/altered expression were not detected in neurofibromas.[50,51,54,62,67,69,112,132,134,135] Furthermore, p53-positive nuclei, typically associated with MPNST, were observed in a few cells at the transitional zone between an existing plexiform neurofibroma and an arising MPNST.[51] One plexiform neurofibroma proximal to an MPNST did show p16 immunonegativity.[112] Microdissection of a preexisting neurofibroma from its MPNST focal malignant process revealed 5 chromosomal imbalances in the neurofibroma, all of

which were novel compared to the 10 imbalances in the MPNST component.[106] These data are consistent with a restructuring of the genome during transformation. An additional distinguishing feature of MPNST is the high labeling index of the nuclear proliferating antigen Ki67, which was correlated with reduced survival in a study that combined NF1-associated and sporadic MPNST.[51,132,142]

OTHER NF1-ASSOCIATED NEOPLASMS AND MOUSE MODELS

In addition to peripheral nerve sheath tumors, individuals affected with NF1 are at increased risk for an array of other tumors. Epidemiologically associated neoplasms include medulloblastoma, pheochromocytoma, astrocytoma, and adenocarcinoma of the ampulla of Vater (Ref. [143] and references therein).[144] Primarily children affected with NF1 are at increased risk for optic pathway gliomas and brainstem gliomas, rhabdomyosarcomas, and malignant myeloid leukemias.[41,145–149] The NF1 patients are also at increased risk for a second malignancy, some of which may be treatment-related.[146,150,151] In different studies, 8%–21% of NF1 patients with a first malignancy developed a second cancer, compared to a frequency of 4% in the general population.[143] Malignancy in NF1 has been reviewed recently.[152]

Although heterozygous mutant mice ($Nf1^{+/-}$) develop tumors, they are not the characteristic peripheral nerve sheath tumors characteristic of the human disease.[153–155] The *Nf1*-deficient mice ($Nf1^{-/-}$) die in utero from cardiac defects. Mice chimeric for ($Nf1^{-/-}$) and ($Nf1^{+/+}$) cells were able to develop many microscopic plexiform neurofibromas, but dermal tumors did not develop.[156] In addition, mice doubly heterozygous for mutations in *Nf1* and *p53* developed MPNST that showed LOH at both tumor suppressor loci.[156,157] Recently, mice were constructed such that only their Schwann cells were *Nf1* deficient.[158] Different tumor phenotypes were observed, depending on whether the *Nf1*–deficient Schwann cells were in an animal with an $Nf1^{+/-}$ or an $Nf1^{+/+}$ constitutional genotype. In the $Nf1^{+/-}$ genetic background, plexiform neurofibromas composed of *Nf1*–deficient Schwann cells, and the fibroblasts and mast cells that normally occur in human neurofibromas, developed on peripheral nerves. In the $Nf1^{+/+}$ genetic background, *Nf1*–deficient Schwann cells did not participate in neurofibromagenesis but did form relatively small hyperplastic lesions of the cranial nerves containing minimal mast cells. This mouse model demonstrates that neurofibromin deficiency in Schwann cells is sufficient for generating nascent tumor lesions, but frank plexiform neurofibroma development requires neurofibromin haploinsufficiency in cells of the surrounding tissues.

With the development of mouse models, understanding the genetics, pathology, and natural history of human benign and malignant peripheral nerve sheath tumors takes on new importance. It is only by accurate modeling of the human disease that progress can be made toward therapies that can slow or halt neurofibromagenesis and reduce the high risk of malignancy associated with NF1 disease.

ACKNOWLEDGMENTS

This work was supported by grants DAMD17-00-1-0542 and DAMD 17-01-1-0721 awarded to K. S. The U.S. Army Medical Research Acquisition Activity, 820 Chandler Street, Fort Detrick, Md 21702-5014 is the awarding and administering acquisition office. The content of the information does not necessarily reflect the position or the policy of the government, and no official endorsement should be inferred.

REFERENCES

AQ2

1. Newsham, I.; Hadjistilianou, T.; Cavenee, W.K.. Retinoblastoma. In *The Metabolic & Molecular Bases of Inherited Disease,* 8th Ed.; Scriver, C.R., Beaudet, A.L., Sly, W.S., Valle, D., Eds.; McGraw-Hill: New York, 2001; Vol. 1, 819–848.
2. Muller, A.; Fishel, R. Mismatch repair and the hereditary non-polyposis colorectal cancer syndrome (HNPCC). Cancer Investig. **2002**, *20*, 102–109.
3. Bodmer, W. Familial adenomatous polyposis (FAP) and its gene, APC. Cytogenet. Cell Genet. **1999**, *86*, 99–104.
4. Lengauer, C.; Kinzler, K.W.; Vogelstein, B. Genetic instabilities in human cancers. Nature **1998**, *396*, 643–649.
5. Korf, B.R. Plexiform neurofibromas. Am. J. Med. Genet. **1999**, *89*, 31–37.
6. Sorensen, S.A.; Mulvihill, J.J.; Nielsen, A. Long-term follow-up of von Recklinghausen neurofibromatosis. Survival and malignant neoplasms. N. Engl. J. Med. **1986**, *314*, 1010–1015.
7. Poyhonen, M.; Niemela, S.; Herva, R. Risk of

malignancy and death in neurofibromatosis. Arch. Pathol. Lab. Med. **1997**, *121*, 139–143.

8. Rasmussen, S.A.; Yang, Q.; Friedman, J.M. Mortality in neurofibromatosis 1: an analysis using U.S. death certificates. Am. J. Hum. Genet. **2001**, *68*, 1110–1118.
9. Evans, D.G.; Baser, M.E.; McGaughran, J.; Sharif, S.; Howard, E.; Moran, A. Malignant peripheral nerve sheath tumours in neurofibromatosis 1. J. Med. Genet. **2002**, *39*, 311–314.
10. Huson, S.M.; Compston, D.A.; Clark, P.; Harper, P.S. A genetic study of von Recklinghausen neurofibromatosis in south east Wales. I. Prevalence, fitness, mutation rate, and effect of parental transmission on severity. J. Med. Genet. **1989**, *26*, 704–711.
11. Ducatman, B.S.; Scheithauer, B.W.; Piepgras, D.G.; Reiman, H.M.; Ilstrup, D.M. Malignant peripheral nerve sheath tumors. A clinicopathologic study of 120 cases. Cancer **1986**, *57*, 2006–2021.
12. Korf, B.R. Diagnosis and management of neurofibromatosis type 1. Curr. Neurol. Neurosci. Rep. **2001**, *1*, 162–167.
13. Friedman, J.M.; Riccardi, V.M.. Clinical and epidemiological features. In *Neurofibromatosis. Phenotype, Natural History, and Pathogenesis,* 3rd Ed.; Friedman, J.M., Gutmann, D.H., MacCollin, M., Riccardi, V.M., Eds.; The Johns Hopkins University Press: Baltimore, 1999; Vol. 1, 29–86.
14. North, K. Neurofibromatosis type 1. Am. J. Med. Genet. **2000**, *97*, 119–127.
15. Gutmann, D.H.; Aylsworth, A.; Carey, J.C.; Korf, B.; Marks, J.; Pyeritz, R.E.; Rubenstein, A.; Viskochil, D. The diagnostic evaluation and multidisciplinary management of neurofibromatosis 1 and neurofibromatosis 2. Jama **1997**, *278*, 51–57.
16. Lakkis, M.M.; Tennekoon, G.I. Neurofibromatosis type 1. I. General overview. J. Neurosci. Res. **2000**, *62*, 755–763.
17. Li, Y.; P, O.C.; Breidenbach, H.H.; Cawthon, R.; Stevens, J.; Xu, G.; Neil, S.; Robertson, M.; White, R.; Viskochil, D. Genomic organization of the neurofibromatosis 1 gene (NF1). Genomics **1995**, *25*, 9–18.
18. Marchuk, D.A.; Saulino, A.M.; Tavakkol, R.; Swaroop, M.; Wallace, M.R.; Andersen, L.B.; Mitchell, A.L.; Gutmann, D.H.; Boguski, M.; Collins, F.S. cDna cloning of the type 1 neurofibromatosis gene: complete sequence of the NF1 gene product. Genomics **1991**, *11*, 931–940.
19. Wallace, M.R.; Marchuk, D.A.; Andersen, L.B.; Letcher, R.; Odeh, H.M.; Saulino, A.M.; Fountain, J.W.; Brereton, A.; Nicholson, J.; Mitchell, A.L., et al. Type 1 neurofibromatosis gene: identification of a large transcript disrupted in three NF1 patients 1749]. Science **1990**, *249*, 181–186.
20. Viskochil, D.; Buchberg, A.M.; Xu, G.; Cawthon, R.M.; Stevens, J.; Wolff, R.K.; Culver, M.; Carey, J.C.; Copeland, N.G.; Jenkins, N.A., et al. Deletions and a translocation interrupt a cloned gene at the neurofibromatosis type 1 locus. Cell **1990**, *62*, 187–192.
21. Cawthon, R.M.; Weiss, R.; Xu, G.F.; Viskochil, D.; Culver, M.; Stevens, J.; Robertson, M.; Dunn, D.; Gesteland, R.; O'Connell, P., et al. A major segment of the neurofibromatosis type 1 gene: cDNA sequence, genomic structure, and point mutations. Cell **1990**, *62*, 193–201.
22. Daston, M.M.; Scrable, H.; Nordlund, M.; Sturbaum, A.K.; Nissen, L.M.; Ratner, N. The protein product of the neurofibromatosis type 1 gene is expressed at highest abundance in neurons, Schwann cells, and oligodendrocytes. Neuron **1992**, *8*, 415–428.
23. Huynh, D.P.; Lin, C.T.; Pulst, S.M. Expression of neurofibromin, the neurofibromatosis 1 gene product: studies in human neuroblastoma cells and rat brain. Neurosci. Lett. **1992**, *143*, 233–236.
24. Buchberg, A.M.; Cleveland, L.S.; Jenkins, N.A.; Copeland, N.G. Sequence homology shared by neurofibromatosis type-1 gene and IRA-1 and IRA-2 negative regulators of the RAS cyclic AMP pathway. Nature **1990**, *347*, 291–294.
25. Xu, G.F.; O'Connell, P.; Viskochil, D.; Cawthon, R.; Robertson, M.; Culver, M.; Dunn, D.; Stevens, J.; Gesteland, R.; White, R., et al. The neurofibromatosis type 1 gene encodes a protein related to GAP. Cell **1990**, *62*, 599–608.
26. McCormick, F. ras GTPase activating protein: signal transmitter and signal terminator. Cell **1989**, *56*, 5–8.
27. Klose, A.; Ahmadian, M.R.; Schuelke, M.; Scheffzek, K.; Hoffmeyer, S.; Gewies, A.; Schmitz, F.; Kaufmann, D.; Peters, H.; Wittinghofer, A.; Nurnberg, P. Selective disactivation of neurofibromin GAP activity in neurofibromatosis type 1. Hum. Mol. Genet. **1998**, *7*, 1261–1268.
28. Zhang, Y.Y.; Vik, T.A.; Ryder, J.W.; Srour, E.F.; Jacks, T.; Shannon, K.; Clapp, D.W. Nf1 regulates hematopoietic progenitor cell growth and ras signaling in response to multiple cytokines. J. Exp. Med. **1998**, *187*, 1893–1902.

29. The NF1 gene as a tumor suppressor in neurofibromatosis type 1. Side, L.D., Shannon, K.M., Eds.; Bios Scientific Publishers: Oxford, 1998.
30. Cichowski, K.; Jacks, T. NF1 tumor suppressor gene function: narrowing the GAP. Cell **2001**, *104*, 593–604.
31. Zhu, Y.; Parada, L.F. Neurofibromin, a tumor suppressor in the nervous system. Exp. Cell Res. **2001**, *264*, 19–28.
32. Gutmann, D.H. The neurofibromatoses: when less is more. Hum. Mol. Genet. **2001**, *10*, 747–755.
33. Weiss, B.; Bollag, G.; Shannon, K. Hyperactive Ras as a therapeutic target in neurofibromatosis type 1. Am. J. Med. Genet. **1999**, *89*, 14–22.
34. Serra, E.; Ars, E.; Ravella, A.; Sanchez, A.; Puig, S.; Rosenbaum, T.; Estivill, X.; Lazaro, C. Somatic NF1 mutational spectrum in benign neurofibromas: mRNA splice defects are common among point mutations. Hum. Genet. **2001**, *108*, 416–429.
35. Messiaen, L.M.; Callens, T.; Mortier, G.; Beysen, D.; Vandenbroucke, I.; Van Roy, N.; Speleman, F.; Paepe, A.D. Exhaustive mutation analysis of the NF1 gene allows identification of 95% of mutations and reveals a high frequency of unusual splicing defects. Human Mutat. **2000**, *15*, 541–555.
36. Fahsold, R.; Hoffmeyer, S.; Mischung, C.; Gille, C.; Ehlers, C.; Kucukceylan, N.; Abdel-Nour, M.; Gewies, A.; Peters, H.; Kaufmann, D.; Buske, A.; Tinschert, S.; Nurnberg, P. Minor lesion mutational spectrum of the entire NF1 gene does not explain its high mutability but points to a functional domain upstream of the GAP-related domain. Am. J. Hum. Genet. **2000**, *66*, 790–818.
37. Kayes, L.M.; Riccardi, V.M.; Burke, W.; Bennett, R.L.; Stephens, K. Large de novo DNA deletion in a patient with sporadic neurofibromatosis 1, mental retardation, and dysmorphism. J. Med. Genet. **1992**, *29*, 686–690.
38. Kayes, L.M.; Burke, W.; Riccardi, V.M.; Bennett, R.; Ehrlich, P.; Rubenstein, A.; Stephens, K. Deletions spanning the neurofibromatosis 1 gene: identification and phenotype of five patients. Am. J. Hum. Genet. **1994**, *54*, 424–436.
39. Kluwe, L.; Friedrich, R.E.; Korf, B.; Fahsold, R.; Mautner, V.F. NF1 mutations in neurofibromatosis 1 patients with plexiform neurofibromas. Human Mutat. **2002**, *19*, 309.
40. Kaufmann, D.; Muller, R.; Bartelt, B.; Wolf, M.; Kunzi-Rapp, K.; Hanemann, C.O.; Fahsold, R.; Hein, C.; Vogel, W.; Assum, G. Spinal neurofibromatosis without cafe-au-lait macules in two families with null mutations of the NF1 gene. Am. J. Hum. Genet. **2001**, *69*, 1395–1400.
41. Side, L.; Taylor, B.; Cayouette, M.; Conner, E.; Thompson, P.; Luce, M.; Shannon, K. Homozygous inactivation of the NF1 gene in bone marrow cells from children with neurofibromatosis type 1 and malignant myeloid disorders. N. Engl. J. Med. **1997**, *336*, 1713–1720.
42. Lott, I.T.; Richardson, E.P., Jr. Neuropathological findings and the biology of neurofibromatosis. Adv. Neurol. **1981**, *29*, 23–32.
43. Woodruff, J.M. Pathology of tumors of the peripheral nerve sheath in type 1 neurofibromatosis. Am. J. Med. Genet. **1999**, *89*, 23–30.
44. Huson, S.M.. Neurofibromatosis 1: a clinical and genetic overview. In *The Neurofibromatoses: A Pathogenetic and Clinical Overview,* 1st Ed.; Huson, S.M., Hughes, R.A.C., Eds.; Chapman and Hall Medical: London, 1994; 160–203.
45. Waggoner, D.J.; Towbin, J.; Gottesman, G.; Gutmann, D.H. Clinic-based study of plexiform neurofibromas in neurofibromatosis 1. Am. J. Med. Genet. **2000**, *92*, 132–135.
46. Riccardi, V.M. *Neurofibromatosis, Phenotype, Natural History, Pathogenesis;* The Johns Hopkins University Press: Batimore, 1992.
47. Huson, S.M.; Harper, P.S.; Compston, D.A. Von Recklinghausen neurofibromatosis. A clinical and population study in south-east Wales. Brain **1988**, *111* (Pt 6), 1355–1381.
48. Ferner, R.E.; Gutmann, D.H. International consensus statement on malignant peripheral nerve sheath tumors in neurofibromatosis. Cancer Res. **2002**, *62*, 1573–1577.
49. Molenaar, W.M.; Dijkhuizen, T.; van Echten, J.; Hoekstra, H.J.; van den Berg, E. Cytogenetic support for early malignant change in a diffuse neurofibroma not associated with neurofibromatosis. Cancer Genet. Cytogenet. **1997**, *97*, 70–72.
50. Leroy, K.; Dumas, V.; Martin-Garcia, N.; Falzone, M.C.; Voisin, M.C.; Wechsler, J.; Revuz, J.; Creange, A.; Levy, E.; Lantieri, L.; Zeller, J.; Wolkenstein, P. Malignant peripheral nerve sheath tumors associated with neurofibromatosis type 1: a clinicopathologic and molecular study of 17 patients. Arch. Dermatol. **2001**, *137*, 908–913.
51. Watanabe, T.; Oda, Y.; Tamiya, S.; Masuda, K.; Tsuneyoshi, M. Malignant peripheral nerve sheath tumour arising within neurofibroma. An immunohistochemical analysis in the comparison between benign and malignant components. J. Clin. Pathol. **2001**, *54*, 631–636.
52. Tischfield, J.A. Loss of heterozygosity or: how I

learned to stop worrying and love mitotic recombination. Am. J. Hum. Genet. **1997**, *61*, 995.

53. Fearon, E.R. Human cancer syndromes: clues to the origin and nature of cancer. Science **1997**, *278*, 1043–1050.
54. Colman, S.D.; Williams, C.A.; Wallace, M.R. Benign neurofibromas in type 1 neurofibromatosis (NF1) show somatic deletions of the NF1 gene. Nat. Genet. **1995**, *11*, 90–92.
55. Serra, E.; Puig, S.; Otero, D.; Gaona, A.; Kruyer, H.; Ars, E.; Estivill, X.; Lazaro, C. Confirmation of a double-hit model for the NF1 gene in benign neurofibromas. Am. J. Hum. Genet. **1997**, *61*, 512–519.
56. Serra, E.; Rosenbaum, T.; Nadal, M.; Winner, U.; Ars, E.; Estivill, X.; Lazaro, C. Mitotic recombination effects homozygosity for NF1 germline mutations in neurofibromas. Nat. Genet. **2001**, *28*, 294–296.
57. Daschner, K.; Assum, G.; Eisenbarth, I.; Krone, W.; Hoffmeyer, S.; Wortmann, S.; Heymer, B.; Kehrer-Sawatzki, H. Clonal origin of tumor cells in a plexiform neurofibroma with LOH in NF1 intron 38 and in dermal neurofibromas without LOH of the NF1 gene. Biochem. Biophys. Res. Commun. **1997**, *234*, 346–350.
58. John, A.M.; Ruggieri, M.; Ferner, R.; Upadhyaya, M. A search for evidence of somatic mutations in the NF1 gene. J. Med. Genet. **2000**, *37*, 44–49.
59. Stark, M.; Assum, G.; Krone, W. Single-cell PCR performed with neurofibroma Schwann cells reveals the presence of both alleles of the neurofibromatosis type 1 (NF1) gene. Hum. Genet. **1995**, *96*, 619–623.
60. Skuse, G.R.; Kosciolek, B.A.; Rowley, P.T. Molecular genetic analysis of tumors in von Recklinghausen neurofibromatosis: loss of heterozygosity for chromosome 17. Genes Chromosomes Cancer **1989**, *1*, 36–41.
61. Skuse, G.R.; Kosciolek, B.A.; Rowley, P.T. The neurofibroma in von Recklinghausen neurofibromatosis has a unicellular origin. Am. J. Hum. Genet. **1991**, *49*, 600–607.
62. Menon, A.G.; Anderson, K.M.; Riccardi, V.M.; Chung, R.Y.; Whaley, J.M.; Yandell, D.W.; Farmer, G.E.; Freiman, R.N.; Lee, J.K.; Li, F.P., et al. Chromosome 17p deletions and p53 gene mutations associated with the formation of malignant neurofibrosarcomas in von Recklinghausen neurofibromatosis. Proc. Natl. Acad. Sci. U. S. A. **1990**, *87*, 5435–5439.
63. Sawada, S.; Florell, S.; Purandare, S.M.; Ota, M.; Stephens, K.; Viskochil, D. Identification of NF1 mutations in both alleles of a dermal neurofibroma. Nat. Genet. **1996**, *14*, 110–112.
64. Mendell, J.T.; Dietz, H.C. When the message goes awry. Disease-producing mutations that influence mRNA content and performance. Cell **2001**, *107*, 411–414.
65. Serra, E.; Rosenbaum, T.; Winner, U.; Aledo, R.; Ars, E.; Estivill, X.; Lenard, H.G.; Lazaro, C. Schwann cells harbor the somatic NF1 mutation in neurofibromas: evidence of two different Schwann cell subpopulations. Hum. Mol. Genet. **2000**, *9*, 3055–3064.
66. Rutkowski, J.L.; Wu, K.; Gutmann, D.H.; Boyer, P.J.; Legius, E. Genetic and cellular defects contributing to benign tumor formation in neurofibromatosis type 1. Hum. Mol. Genet. **2000**, *9*, 1059–1066.
67. Rasmussen, S.A.; Overman, J.; Thomson, S.A.; Colman, S.D.; Abernathy, C.R.; Trimpert, R.E.; Moose, R.; Virdi, G.; Roux, K.; Bauer, M.; Rojiani, A.M.; Maria, B.L.; Muir, D.; Wallace, M.R. Chromosome 17 loss-of-heterozygosity studies in benign and malignant tumors in neurofibromatosis type 1. Genes Chromosomes Cancer **2000**, *28*, 425–431.
68. Eisenbarth, I.; Beyer, K.; Krone, W.; Assum, G. Toward a survey of somatic mutation of the NF1 gene in benign neurofibromas of patients with neurofibromatosis type 1. Am. J. Hum. Genet. **2000**, *66*, 393–401.
69. Kluwe, L.; Friedrich, R.E.; Mautner, V.F. Allelic loss of the NF1 gene in NF1-associated plexiform neurofibromas. Cancer Genet. Cytogenet. **1999**, *113*, 65–69.
70. Skuse, G.R.; Cappione, A.J.; Sowden, M.; Metheny, L.J.; Smith, H.C. The neurofibromatosis type I messenger RNA undergoes base-modification RNA editing. Nucleic Acids Res. **1996**, *24*, 478–485.
71. Mukhopadhyay, D.; Anant, S.; Lee, R.M.; Kennedy, S.; Viskochil, D.; Davidson, N.O. C→U editing of neurofibromatosis 1 mRNA occurs in tumors that express both the type II transcript and apobec-1, the catalytic subunit of the apolipoprotein B mRNA-editing enzyme. Am. J. Hum. Genet. **2002**, *70*, 38–50.
72. Jones, P.A. DNA methylation errors and cancer. Cancer Res. **1996**, *56*, 2463–2467.
73. Luijten, M.; Redeker, S.; van Noesel, M.M.; Troost, D.; Westerveld, A.; Hulsebos, T.J. Microsatellite instability and promoter methylation as possible causes of NF1 gene inactivation

in neurofibromas. Eur. J. Hum. Genet. **2000**, *8*, 939–945.

74. Horan, M.P.; Cooper, D.N.; Upadhyaya, M. Hypermethylation of the neurofibromatosis type 1 (NF1) gene promoter is not a common event in the inactivation of the NF1 gene in NF1-specific tumours. Hum. Genet. **2000**, *107*, 33–39.
75. Guha, A. Ras activation in astrocytomas and neurofibromas. Can. J. Neurol. Sci. **1998**, *25*, 267–281.
76. Peters, N.; Waha, A.; Wellenreuther, R.; Friedrich, R.E.; Mautner, V.F.; Hoffmeyer, S.; Lenartz, D.; Schramm, J.; Wiestler, O.D.; von Deimling, A. Quantitative analysis of NF1 and OMGP gene transcripts in sporadic gliomas, sporadic meningiomas and neurofibromatosis type 1-associated plexiform neurofibromas. Acta Neuropathol. (Berl) **1999**, *97*, 547–551.
77. Guha, A.; Lau, N.; Huvar, I.; Gutmann, D.; Provias, J.; Pawson, T.; Boss, G. Ras-GTP levels are elevated in human NF1 peripheral nerve tumors. Oncogene **1996**, *12*, 507–513.
78. Kluwe, L.; Friedrich, R.; Mautner, V.F. Loss of NF1 allele in Schwann cells but not in fibroblasts derived from an NF1-associated neurofibroma. Genes Chromosomes Cancer **1999**, *24*, 283–285.
79. Sherman, L.S.; Atit, R.; Rosenbaum, T.; Cox, A.D.; Ratner, N. Single cell Ras-GTP analysis reveals altered Ras activity in a subpopulation of neurofibroma Schwann cells but not fibroblasts. J. Biol. Chem. **2000**, *275*, 30740–30745.
80. Perry, A.; Roth, K.A.; Banerjee, R.; Fuller, C.E.; Gutmann, D.H. NF1 deletions in S-100 protein-positive and negative cells of sporadic and neurofibromatosis 1 (NF1)-associated plexiform neurofibromas and malignant peripheral nerve sheath tumors. Am. J. Pathol. **2001**, *159*, 57–61.
81. Sheela, S.; Riccardi, V.M.; Ratner, N. Angiogenic and invasive properties of neurofibroma Schwann cells. J. Cell Biol. **1990**, *111*, 645–653.
82. Rosenbaum, T.; Rosenbaum, C.; Winner, U.; Muller, H.W.; Lenard, H.G.; Hanemann, C.O. Long-term culture and characterization of human neurofibroma-derived Schwann cells. J. Neurosci. Res. **2000**, *61*, 524–532.
83. Muir, D.; Neubauer, D.; Lim, I.T.; Yachnis, A.T.; Wallace, M.R. Tumorigenic properties of neurofibromin-deficient neurofibroma Schwann cells. Am. J. Pathol. **2001**, *158*, 501–513.
84. Muir, D. Differences in proliferation and invasion by normal, transformed and NF1 Schwann cell cultures are influenced by matrix metalloproteinase expression. Clin. Exp. Metastasis **1995**, *13*, 303–314.
85. Easton, D.F.; Ponder, M.A.; Huson, S.M.; Ponder, B.A. An analysis of variation in expression of neurofibromatosis (NF) type 1 (NF1): evidence for modifying genes. Am. J. Hum. Genet. **1993**, *53*, 305–313.
86. Kayes, L.M.; Schroeder, W.T.; Marchuk, D.A.; Collins, F.S.; Riccardi, V.M.; Duvic, M.; Stephens, K. The gene for a novel epidermal antigen maps near the neurofibromatosis 1 gene. Genomics **1992**, *14*, 369–376.
87. Dorschner, M.O.; Sybert, V.P.; Weaver, M.; Pletcher, B.A.; Stephens, K. NF1 microdeletion breakpoints are clustered at flanking repetitive sequences. Hum. Mol. Genet. **2000**, *9*, 35–46.
88. Leppig, K.A.; Kaplan, P.; Viskochil, D.; Weaver, M.; Ortenberg, J.; Stephens, K. Familial neurofibromatosis 1 microdeletions: cosegregation with distinct facial phenotype and early onset of cutaneous neurofibromata. Am. J. Med. Genet. **1997**, *73*, 197–204.
89. Wu, B.L.; Schneider, G.H.; Korf, B.R. Deletion of the entire NF1 gene causing distinct manifestations in a family. Am. J. Med. Genet. **1997**, *69*, 98–101.
90. Wu, B.L.; Austin, M.A.; Schneider, G.H.; Boles, R.G.; Korf, B.R. Deletion of the entire NF1 gene detected by the FISH: four deletion patients associated with severe manifestations. Am. J. Med. Genet. **1995**, *59*, 528–535.
91. Upadhyaya, M.; Ruggieri, M.; Maynard, J.; Osborn, M.; Hartog, C.; Mudd, S.; Penttinen, M.; Cordeiro, I.; Ponder, M.; Ponder, B.A.; Krawczak, M.; Cooper, D.N. Gross deletions of the neurofibromatosis type 1 (NF1) gene are predominantly of maternal origin and commonly associated with a learning disability, dysmorphic features and developmental delay. Hum. Genet. **1998**, *102*, 591–597.
92. Tonsgard, J.H.; Yelavarthi, K.K.; Cushner, S.; Short, M.P.; Lindgren, V. Do NF1 gene deletions result in a characteristic phenotype? Am. J. Med. Genet. **1997**, *73*, 80–86.
93. Lazaro, C.; Gaona, A.; Ainsworth, P.; Tenconi, R.; Vidaud, D.; Kruyer, H.; Ars, E.; Volpini, V.; Estivill, X. Sex differences in mutational rate and mutational mechanism in the NF1 gene in neurofibromatosis type 1 patients. Hum. Genet. **1996**, *98*, 696–699.
94. Fang, L.J.; Vidaud, D.; Vidaud, M.; Thirion, J.P. Identification and characterization of four novel large deletions in the human neurofibromatosis

type 1 (NF1) gene. Human Mutat. **2001**, *18*, 549–550.

95. Lopez Correa, C.; Brems, H.; Lazaro, C.; Estivill, X.; Clementi, M.; Mason, S.; Rutkowski, J.L.; Marynen, P.; Legius, E. Molecular studies in 20 submicroscopic neurofibromatosis type 1 gene deletions. Human Mutat. **1999**, *14*, 387–393.
96. Ainsworth, P.J.; Chakraborty, P.K.; Weksberg, R. Example of somatic mosaicism in a series of de novo neurofibromatosis type 1 cases due to a maternally derived deletion. Human Mutat. **1997**, *9*, 452–457.
97. Cnossen, M.H.; van der Est, M.N.; Breuning, H.; van Asperen, C.J.; Breslau-Siderius, E.J.; van der Ploeg, A.T.; de Goede-Bolder, A.; van den Ouweland, A.M.W.; Halley, D.J.J.; Niermeijer, M.F. Deletions spanning the neurofibromatosis type 1 gene: implications for genotype-phenotype correlations in neurofibromatosis type 1? Human Mutat. **1997**, *9*, 458–464.
98. Jenne, D.E.; Tinschert, S.; Stegmann, E.; Reimann, H.; Nurnberg, P.; Horn, D.; Naumann, I.; Buske, A.; Thiel, G. A common set of at least 11 functional genes is lost in the majority of NF1 patients with gross deletions [in process citation]. Genomics **2000**, *66*, 93–97.
99. Jenne, D.E.; Tinschert, S.; Stegmann, E.; Reimann, H.; P, N.u.; Horn, D.; Naumann, I.; Buske, A.; Thiel, G. A common set of at least 11 functional genes is lost in the majority of NF1 patients with gross deletions. Genomics **2000**, *66*, 93–97.
100. Valero, M.C.; Pascual-Castroviejo, I.; Velasco, E.; Moreno, F.; Hernandez-Chico, C. Identification of de novo deletions at the NF1 gene: no preferential paternal origin and phenotypic analysis of patients. Hum. Genet. **1997**, *99*, 720–726.
101. Correa, C.L.; Brems, H.; Lazaro, C.; Marynen, P.; Legius, E. Unequal meiotic crossover: a frequent cause of NF1 microdeletions. Am. J. Hum. Genet. **2000**, *66*, 1969–1974.
102. Stankiewicz, P.; Lupski, J.R. Genome architecture, rearrangements and genomic disorders. Trends Genet. **2002**, *18*, 74–82.
103. Lopez-Correa, C.; Dorschner, M.; Brems, H.; Lazaro, C.; Clementi, M.; Upadhyaya, M.; Dooijes, D.; Moog, U.; Kehrer-Sawatzki, H.; Rutkowski, J.L.; Fryns, J.P.; Marynen, P.; Stephens, K.; Legius, E. Recombination hotspot in NF1 microdeletion patients. Hum. Mol. Genet. **2001**, *10*, 1387–1392.
104. Tachdjian, G.; Aboura, A.; Lapierre, J.M.; Viguie, F. Cytogenetic analysis from DNA by comparative genomic hybridization. Ann. Genet. **2000**, *43*, 147–154.
105. Mechtersheimer, G.; Otano-Joos, M.; Ohl, S.; Benner, A.; Lehnert, T.; Willeke, F.; Moller, P.; Otto, H.F.; Lichter, P.; Joos, S. Analysis of chromosomal imbalances in sporadic and NF1-associated peripheral nerve sheath tumors by comparative genomic hybridization. Genes Chromosomes Cancer **1999**, *25*, 362–369.
106. Schmidt, H.; Taubert, H.; Meye, A.; Wurl, P.; Bache, M.; Bartel, F.; Holzhausen, H.J.; Hinze, R. Gains in chromosomes 7, 8q, 15q and 17q are characteristic changes in malignant but not in benign peripheral nerve sheath tumors from patients with Recklinghausen's disease. Cancer Lett. **2000**, *155*, 181–190.
107. Wallace, M.R.; Rasmussen, S.A.; Lim, I.T.; Gray, B.A.; Zori, R.T.; Muir, D. Culture of cytogenetically abnormal schwann cells from benign and malignant NF1 tumors. Genes Chromosomes Cancer **2000**, *27*, 117–123.
108. Kehrer, H.; Krone, W. Spontaneous chromosomal aberrations in cell cultures from patients with neurofibromatosis 1. Mutat. Res. **1994**, *306*, 61–70.
109. Glover, T.W.; Stein, C.K.; Legius, E.; Andersen, L.B.; Brereton, A.; Johnson, S. Molecular and cytogenetic analysis of tumors in von Recklinghausen neurofibromatosis. Genes Chromosomes Cancer **1991**, *3*, 62–70.
110. Ottini, L.; Esposito, D.L.; Richetta, A.; Carlesimo, M.; Palmirotta, R.; Ver'i, M.C.; Battista, P.; Frati, L.; Caramia, F.G.; Calvieri, S., et al. Alterations of microsatellites in neurofibromas of von Recklinghausen's disease. Cancer Res. **1995**, *55*, 5677–5680.
111. Fargnoli, M.C.; Chimenti, S.; Peris, K. Multiple microsatellite alterations on chromosome 9 in neurofibromas of NF-1 patients. J. Invest. Dermatol. **1997**, *108*, 812–813.
112. Birindelli, S.; Perrone, F.; Oggionni, M.; Lavarino, C.; Pasini, B.; Vergani, B.; Ranzani, G.N.; Pierotti, M.A.; Pilotti, S. Rb and TP53 pathway alterations in sporadic and NF1-related malignant peripheral nerve sheath tumors. Lab. Invest. **2001**, *81*, 833–844.
113. Shibata, D.; Navidi, W.; Salovaara, R.; Li, Z.H.; Aaltonen, L.A. Somatic microsatellite mutations as molecular tumor clocks. Nat. Med. **1996**, *2*, 676–681.
114. Legius, E.; Marchuk, D.A.; Collins, F.S.; Glover, T.W. Somatic deletion of the neurofibromatosis type 1 gene in a neurofibrosarcoma supports a

tumour suppressor gene hypothesis. Nat. Genet. **1993**, *3*, 122–126.

115. Lothe, R.A.; Slettan, A.; Saeter, G.; Brogger, A.; Borresen, A.L.; Nesland, J.M. Alterations at chromosome 17 loci in peripheral nerve sheath tumors. J. Neuropathol. Exp. Neurol. **1995**, *54*, 65–73.

116. Plaat, B.E.; Molenaar, W.M.; Mastik, M.F.; Hoekstra, H.J.; te Meerman, G.J.; van den Berg, E. Computer-assisted cytogenetic analysis of 51 malignant peripheral-nerve-sheath tumors: sporadic vs. neurofibromatosis-type-1-associated malignant schwannomas. Int. J. Cancer **1999**, *83*, 171–178.

117. DeClue, J.E.; Papageorge, A.G.; Fletcher, J.A.; Diehl, S.R.; Ratner, N.; Vass, W.C.; Lowy, D.R. Abnormal regulation of mammalian p21ras contributes to malignant tumor growth in von Recklinghausen (type 1) neurofibromatosis. Cell **1992**, *69*, 265–273.

118. Basu, T.N.; Gutmann, D.H.; Fletcher, J.A.; Glover, T.W.; Collins, F.S.; Downward, J. Aberrant regulation of ras proteins in malignant tumour cells from type 1 neurofibromatosis patients. Nature **1992**, *356*, 713–715.

119. Wu, R.; Lopez-Correa, C.; Rutkowski, J.L.; Baumbach, L.L.; Glover, T.W.; Legius, E. Germline mutations in NF1 patients with malignancies. Genes Chromosomes Cancer **1999**, *26*, 376–380.

120. Wang, Q.; Lasset, C.; Desseigne, F.; Frappaz, D.; Bergeron, C.; Navarro, C.; Ruano, E.; Puisieux, A. Neurofibromatosis and early onset of cancers in hMLH1-deficient children. Cancer Res. **1999**, *59*, 294–297.

121. Ricciardone, M.D.; Ozcelik, T.; Cevher, B.; Ozdag, H.; Tuncer, M.; Gurgey, A.; Uzunalimoglu, O.; Cetinkaya, H.; Tanyeli, A.; Erken, E.; Ozturk, M. Human MLH1 deficiency predisposes to hematological malignancy and neurofibromatosis type 1. Cancer Res. **1999**, *59*, 290–293.

AQ4 122. Boland, C.R.

123. Lothe, R.A.; Karhu, R.; Mandahl, N.; Mertens, F.; Saeter, G.; Heim, S.; Borresen-Dale, A.L.; Kallioniemi, O.P. Gain of 17q24-qter detected by comparative genomic hybridization in malignant tumors from patients with von Recklinghausen's neurofibromatosis. Cancer Res. **1996**, *56*, 4778–4781.

124. Schmidt, H.; Wurl, P.; Taubert, H.; Meye, A.; Bache, M.; Holzhausen, H.J.; Hinze, R. Genomic imbalances of 7p and 17q in malignant peripheral nerve sheath tumors are clinically relevant. Genes Chromosomes Cancer **1999**, *25*, 205–211.

125. Schmidt, H.; Taubert, H.; Wurl, P.; Bache, M.; Bartel, F.; Holzhausen, H.J.; Hinze, R. Cytogenetic characterization of six malignant peripheral nerve sheath tumors: comparison of karyotyping and comparative genomic hybridization. Cancer Genet. Cytogenet. **2001**, *128*, 14–23.

126. Mertens, F.; Dal Cin, P.; De Wever, I.; Fletcher, C.D.; Mandahl, N.; Mitelman, F.; Rosai, J.; Rydholm, A.; Sciot, R.; Tallini, G.; van Den Berghe, H.; Vanni, R.; Willen, H. Cytogenetic characterization of peripheral nerve sheath tumours: A report of the CHAMP study group. J. Pathol. **2000**, *190*, 31–38.

127. O'Sullivan, M.J.; Kyriakos, M.; Zhu, X.; Wick, M.R.; Swanson, P.E.; Dehner, L.P.; Humphrey, P.A.; Pfeifer, J.D. Malignant peripheral nerve sheath tumors with t(X;18). A pathologic and molecular genetic study. Mod. Path. **2000**, *13*, 1336–1346.

128. Ladanyi, M.; Woodruff, J.M.; Scheithauer, B.W.; Bridge, J.A.; Barr, F.G.; Goldblum, J.R.; Fisher, C.; Perez-Atayde, A.; Dal Cin, P.; Fletcher, C.D.; Fletcher, J.A. Re: O'Sullivan MJ, Kyriakos M, Zhu X, Wick MR, Swanson PE, Dehner LP, Humphrey PA, Pfeifer JD: malignant peripheral nerve sheath tumors with t(X;18). A pathologic and molecular genetic study. Mod pathol 2000;13:1336–46. Mod. Path. **2001**, *14*, 733–737.

129. Liew, M.A.; Coffin, C.M.; Fletcher, J.A.; Hang, M.T.; Tanito, K.; Niimura, M.; Viskochil, D. Peripheral nerve sheath tumors from patients with neurofibromatosis type 1 do not have the chromosomal translocation t(X;18). Pediatr. Dev. Pathol. **2002**, *5*, 165–169.

130. Legius, E.; Dierick, H.; Wu, R.; Hall, B.K.; Marynen, P.; Cassiman, J.J.; Glover, T.W. TP53 mutations are frequent in malignant NF1 tumors. Genes Chromosomes Cancer **1994**, *10*, 250–255.

131. Halling, K.C.; Scheithauer, B.W.; Halling, A.C.; Nascimento, A.G.; Ziesmer, S.C.; Roche, P.C.; Wollan, P.C. p53 expression in neurofibroma and malignant peripheral nerve sheath tumor. An immunohistochemical study of sporadic and NF1-associated tumors. Am. J. Clin. Pathol. **1996**, *106*, 282–288.

132. Liapis, H.; Marley, E.F.; Lin, Y.; Dehner, L.P. p53 and Ki-67 proliferating cell nuclear antigen in benign and malignant peripheral nerve sheath tumors in children. Pediatr. Dev. Pathol. **1999**, *2*, 377–384.

133. Guimaraes, D.P.; Hainaut, P. TP53: a key gene in human cancer. Biochimie **2002**, *84*, 83–93.

134. Kourea, H.P.; Orlow, I.; Scheithauer, B.W.;

Cordon-Cardo, C.; Woodruff, J.M. Deletions of the INK4A gene occur in malignant peripheral nerve sheath tumors but not in neurofibromas. Am. J. Pathol. **1999**, *155*, 1855–1860.

135. Nielsen, G.P.; Stemmer-Rachamimov, A.O.; Ino, Y.; Moller, M.B.; Rosenberg, A.E.; Louis, D.N. Malignant transformation of neurofibromas in neurofibromatosis 1 is associated with CDKN2A/p16 inactivation. Am. J. Pathol. **1999**, *155*, 1879–1884.

136. Sherr, C.J. The INK4a/ARF network in tumour suppression. Nat. Rev., Mol. Cell Biol. **2001**, *2*, 731–737.

137. Li, X.J.; Wang, D.Y.; Zhu, Y.; Guo, R.J.; Wang, X.D.; Lubomir, K.; Mukai, K.; Sasaki, H.; Yoshida, H.; Oka, T.; Machinami, R.; Shinmura, K.; Tanaka, M.; Sugimura, H. Mxi1 mutations in human neurofibrosarcomas. Jpn. J. Cancer Res. **1999**, *90*, 740–746.

138. Foley, K.P.; Eisenman, R.N. Two MAD tails: what the recent knockouts of Mad1 and Mxi1 tell us about the MYC/MAX/MAD network. Biochim. Biophys. Acta **1999**, *1423*, M37–M47.

139. Schreiber-Agus, N.; Meng, Y.; Hoang, T.; Hou, H., Jr.; Chen, K.; Greenberg, R.; Cordon-Cardo, C.; Lee, H.W.; DePinho, R.A. Role of Mxi1 in ageing organ systems and the regulation of normal and neoplastic growth. Nature **1998**, *393*, 483–487.

140. Serrano, M.; Gomez-Lahoz, E.; DePinho, R.A.; Beach, D.; Bar-Sagi, D. Inhibition of ras-induced proliferation and cellular transformation by p16INK4. Science **1995**, *267*, 249–252.

141. Pomerantz, J.; Schreiber-Agus, N.; Liegeois, N.J.; Silverman, A.; Alland, L.; Chin, L.; Potes, J.; Chen, K.; Orlow, I.; Lee, H.W.; Cordon-Cardo, C.; DePinho, R.A. The Ink4a tumor suppressor gene product, p19Arf, interacts with MDM2 and neutralizes MDM2's inhibition of p53. Cell **1998**, *92*, 713–723.

142. Kindblom, L.G.; Ahlden, M.; Meis-Kindblom, J.M.; Stenman, G. Immunohistochemical and molecular analysis of p53, MDM2, proliferating cell nuclear antigen and Ki67 in benign and malignant peripheral nerve sheath tumours. Virchows Arch. **1995**, *427*, 19–26.

143. Mulvihill, J.J.. Malignancy: epidemiologically associated cancers. In *The Neurofibromatoses: A pathogenetic and Clinical Overview,* 1st Ed., Huson, S.M., Hughes, R.A.C., Eds.; Chapman & Hall Medical: London, 1994; 487.

144. Koch, C.A.; Vortmeyer, A.O.; Huang, S.C.; Alesci, S.; Zhuang, Z.; Pacak, K. Genetic aspects of pheochromocytoma. Endocr. Regul. **2001**, *35*, 43–52.

145. Listernick, R.; Charrow, J.; Gutmann, D.H. Intracranial gliomas in neurofibromatosis type 1. Am. J. Med. Genet. **1999**, *89*, 38–44.

146. Gutmann, D.H.; Gurney, J.G. Other malignancies. In *Neurofibromatosis. Phenotype, Natural History, and Pathogenesis;* Friedman, J.M., Butmann, D.H., MacCollin, M., Riccardi, V.M., Eds.; The Johns Hopkins University Press: Baltimore, 1999; 231–249.

147. Kluwe, L.; Hagel, C.; Tatagiba, M.; Thomas, S.; Stavrou, D.; Ostertag, H.; von Deimling, A.; Mautner, V.F. Loss of NF1 alleles distinguish sporadic from NF1-associated pilocytic astrocytomas. J. Neuropathol. Exp. Neurol. **2001**, *60*, 917–920.

148. Shannon, K.M.; O'Connell, P.; Martin, G.A.; Paderanga, D.; Olson, K.; Dinndorf, P.; McCormick, F. Loss of the normal NF1 allele from the bone marrow of children with type 1 neurofibromatosis and malignant myeloid disorders. N. Engl. J. Med. **1994**, *330*, 597–601.

149. Matsui, I.; Tanimura, M.; Kobayashi, N.; Sawada, T.; Nagahara, N.; Akatsuka, J. Neurofibromatosis type 1 and childhood cancer. Cancer **1993**, *72*, 2746–2754.

150. Maris, J.M.; Wiersma, S.R.; Mahgoub, N.; Thompson, P.; Geyer, R.J.; Hurwitz, C.G.H.; Lange, B.J.; Shannon, K.M. Monosomy 7 myelodysplastic syndrome and other second malignant neoplasms in children with neurofibromatosis type 1. Cancer **1997**, *79*, 1438–1446.

151. Mahgoub, N.; Taylor, B.R.; Le Beau, M.M.; Gratiot, M.; Carlson, K.M.; Atwater, S.K.; Jacks, T.; Shannon, K.M. Myeloid malignancies induced by alkylating agents in Nf1 mice. Blood **1999**, *93*, 3617–3623.

152. Korf, B.R. Malignancy in neurofibromatosis type 1. Oncologist **2000**, *5*, 477–485.

153. Jacks, T.; Shih, T.S.; Schmitt, E.M.; Bronson, R.T.; Bernards, A.; Weinberg, R.A. Tumour predisposition in mice heterozygous for a targeted mutation in Nf1. Nat. Genet. **1994**, *7*, 353–361.

154. Brannan, C.I.; Perkins, A.S.; Vogel, K.S.; Ratner, N.; Nordlund, M.L.; Reid, S.W.; Buchberg, A.M.; Jenkins, N.A.; Parada, L.F.; Copeland, N.G. Targeted disruption of the neurofibromatosis type-1 gene leads to developmental abnormalities in heart and various neural crest-derived tissues. Genes Dev. **1994**, *8*, 1019–1029.

155. Tischler, A.S.; Shih, T.S.; Williams, B.O.; Jacks, T. Characterization of pheochromocytomas in a

mouse strain with a targeted disruptive mutation of the neurofibromatosis gene Nf1. Endocr. Pathol. **1995**, *6*, 323–335.

156. Cichowski, K.; Shih, T.S.; Schmitt, E.; Santiago, S.; Reilly, K.; McLaughlin, M.E.; Bronson, R.T.; Jacks, T. Mouse models of tumor development in neurofibromatosis type 1. Science **1999**, *286*, 2172–2176.

157. Vogel, K.S.; Klesse, L.J.; Velasco-Miguel, S.; Meyers, K.; Rushing, E.J.; Parada, L.F. Mouse tumor model for neurofibromatosis type 1. Science **1999**, *286*, 2176–2179.

158. Zhu, Y.; Ghosh, P.; Charnay, P.; Burns, D.K.; Parada, L.F. Neurofibromas in NF1: Schwann cell origin and role of tumor environment. Science **2002**, *296*, 920–922.

Chapter 20.

Neurofibromatosis

Karen Stephens, PhD

Research Professor

Departments of Medicine (Medical Genetics) and of Laboratory Medicine

University of Washington

Co-Director, Genetics Laboratory, University of Washington Medical Center

Molecular Pathology in Clinical Practice, in press.

Neurofibromatosis 1 and neurofibromatosis 2 are two distinct genetic disorders that predispose to the development of tumors primarily of the nervous system. A comparision of some features of these disorders is given in Table 20-1.

NEUROFIBROMATOSIS (NF1)

MOLECULAR BASIS OF DISEASE

NF1 is an autosomal dominant progressive disorder with high penetrance but extremely variable expressivity (reviewed in Ref.[1,2] and http://www.geneclinics.org/). The cardinal features are café au lait macules, intertrigenous freckling, Lisch nodules, and multiple neurofibromas. The National Institutes of Health diagnostic criteria for a diagnosis of NF1 established in 1987 are still appropriate and are widely used by clinicians and research investigators. Neurofibromas are benign nerve sheath tumors that arise on peripheral nerves. Dermal neurofibromas develop in virtually all cases of NF1, appear in late childhood, grow slowly, increase in number with age, and are at low risk for transformation to malignant peripheral nerve sheath tumors (MPNST; previously termed neurofibrosarcoma). However, diffuse plexiform neurofibromas and deep nodular plexiform neurofibromas can give rise to MPNST. Individuals affected with NF1 have a 10% lifetime risk for MPNST. Other neoplasms epidemiologically-associated with NF1 include medulloblastoma, pheochromocytoma, astrocytoma, adenocarcinoma of the ampulla of Vater. Primarily children affected with NF1 are at increased risk for optic pathway gliomas and brainstem gliomas, rhabdomyosarcomas, and malignant myeloid leukemias. NF1 patients are also at increased risk for a second malignancy, some of which may be treatment-related.

NF1 is caused by haploinsufficiency for the tumor suppressor neurofibromin, the protein product of the *NF1* gene (Table 20-1). Most constitutional mutations are private, predict the truncation of neurofibromin, and occur throughout the gene, although some exons are more mutation-rich than others

(see below). Less frequent are missense mutations and large *NF1* deletions that involve contiguous genes. About one-half of cases are familial (inherited from an affected parent) and one-half are sporadic resulting from a *de novo NF1* mutation. Neurofibromin normally functions as a negative regulator of the ras oncogene by stimulating the conversion of active GTP-bound Ras to the inactive GDP-bound form by hydrolyzing GTP. Biochemical, cell culture, and genetic studies in both NF1 patients and mouse models are consistent with a model whereby a somatic mutation inactivates the remaining functional *NF1* gene in a progenitor Schwann cell as an early, probably initiating, event in the development of neurofibromas (reviewed in [3]). Biallelic inactivation of *NF1* also occurs in progenitor cells of NF1-associated tumors other than those of the nerve sheath. Homozygous inactivation of neurofibromin leads to increased activated ras, resulting in aberrant mitogenic signaling, and consequent loss of growth control.

CLINICAL UTILITY OF TESTING

A diagnosis to NF1 can nearly always be made based on clinical findings, particularly after 8 years of age. Clinical DNA-based testing is available (http://www.geneclinics.org/). Testing is not typically used for diagnostic purposes, but can be useful for confirming a clinical diagnosis, reproductive counseling, and prenatal diagnosis. Blanket recommendations for diagnostic testing for NF1 cannot be made because the sensitivity of making a clinical diagnosis is very high and the sensitivity of molecular testing is not 100% (see below). Furthermore, benefits of diagnostic testing are subjective and may differ from family to family. Prenatal diagnosis of amniocytes or chorionic villus tissue is available only in cases where the pathogenic germline mutation has been identified previously in an affected parent.

The primary genetic counseling issue related to molecular testing of NF1 is the inability to predict the severity or course of the disorder in a patient or fetus. Even among family members who carry the same *NF1* mutation, there can be considerable variation in clinical manifestations and complications. For the majority of cases, there is no correlation between genotype and phenotype. For the ~5-10% of cases that are hemizygous for *NF1* due to a submicroscopic deletion (most commonly 1.5 Mb) there is a predisposition to an early age of onset and excessive numbers of dermal neurofibromas (Ref.[4] and

references therein). *NF1* testing may be useful to confirm a diagnosis in a patient with equivocal findings, such as child who has a few café au lait macules and carries a presumptive diagnosis of NF1. In this instance it is important to realize that the sensitivity and specificity of testing patients that do not fulfill the NIH diagnostic criteria for a diagnosis of *NF1* is unknown. For unaffected parents of a child with sporadic NF1, recurrence risk is a concern. Because germline mosaicism has been reported in an asymptomatic parent of a child with sporadic NF1[5], there is a small but unknown increased risk of recurrence even if the child's pathogenic mutation is not detected in the genomic DNA of parental lymphoblasts. Sporadic NF1 cases with post-zygotic mutations resulting in somatic mosaicism have been reported, but the frequency is unknown. Mosaic individuals, who carry the *NF1* mutation in only a fraction of their cells, may have mutation-negative test results due low signal to noise ratio, i.e., low level of mutant allele in a background of two normal *NF1* alleles. Genetic counseling regarding the clinical and reproductive implications of NF1 mosaicism is recommended.[6]

AVAILABLE ASSAYS

NF1 gene mutation is the only known cause of the disorder. Efficient detection of *NF1* gene mutations requires a multipronged approach due to the large number of exons and size of the gene (Table 20-1), variation in type and distribution of mutations, and large fraction of private mutations. About 70-80% of mutations result in a premature translation termination codon with nonsense and splicing defects being the most common.[7] These can be detected by the protein truncation test (PTT) (see Chapter 2), which identifies truncated neurofibromin polypeptides synthesized by *in vitro* translation of multiple overlapping segments of the *NF1* cDNA isolated from primary lymphoblasts or Epstein-Barr virus (EBV)-transformed lymphoblasts. A detection rate of about 80% can be attained with an optimized PTT protocol (see below). The vast majority of these mutations are private to each individual/family, although there are recurrent mutations that may account for, at most, a few percent of cases (Figure 20-1). About 10% of *NF1* mutations are missense or in-frame insertions/deletions of a few nucleotides,[7,8] some of which show clustering (Figure 20-1). Direct sequencing of cDNA or scanning of *NF1* exons and splice

junctions in genomic DNA by denaturing high performance liquid chromatography (DHPLC), temperature gradient gel electrophoresis (TGGE), single strand conformation polymorphism (SSCP), and/or heteroduplex analysis (HA) (see Chapter 2) have been used to detect missense and other subtle mutations in primary lymphoblasts. DHPLC detected both truncating, missense, and small in-frame deletions/insertions with a detection rate of 97% in a retrospective study[9] and of 72% in a prospective study.[10] For mutation scanning testing protocols, the detection rate will be laboratory-specific due to the degree of optimization of the specific technique; a survey of testing laboratories is recommended. DHLPC has the advantages of using genomic DNA and high throughput capability compared to the cDNA/gel-based PTT. However, a recently reported high-throughput PTT may be available for clinical testing in the future.[11] Fluorescent in situ hybridization (FISH; see Chapter 2) with *NF1* probes is used to detect the estimated 5-10% of cases due to submicroscopic *NF1* microdeletion[12] (Figure 20-1), although a recently reported *NF1* deletion junction-specific PCR assay may be clinically applicable in the near future.[13] Routine cytogenetic analysis is used to detect rare cases due to translocation or chromosomal rearrangement. Linkage analysis is an indirect test that tracks the inheritance of a disease allele in members of a family. Linkage testing is clinically available for at-risk individuals with multiple family members carrying a definitive diagnosis of NF1. The availability of *NF1* intragenic markers increases the informativeness of this methodology. This may be the quickest, most economical NF1 test for individuals of families that fulfill the testing criteria.

INTERPETATION OF TEST RESULTS

The detection of a truncated neurofibromin polypeptide by PTT is the most sensitive method (~80%), but can result in false positives.[7] High specificity requires identifying the underlying mutation at the genomic DNA and cDNA levels since false positives can arise during handling of the peripheral blood sample (see below). The interpretation of missense and subtle in-frame alterations as pathogenic mutations versus neutral polymorphisms is complicated by the lack of a functional assay for neurofibromin. Apparent recurrence of a putative mutation based on prior literature reports must be

interpreted with caution, as the majority of *NF1* mutational analyses did not sequence the entire gene. No comprehensive *NF1* mutation database is available, however some mutations have been submitted to the Human Gene Mutation Database (http://archive.uwcm.ac.uk/uwcm/mg/hgmd0.html) and the National Neurofibromatosis Foundation International *NF1* Genetic Mutation Analysis Consortium Web Site (http://www.nf.org/nf1gene/nf1gene.home.html). Although most likely rare, families with different independent *NF1* inactivating mutations in affected individuals have been reported,[14] presumably a reflection of the high mutation rate of the gene (~10^5/gamete/generation). The interpretation of FISH with *NF1* probes can be complicated by mosaicism for an *NF1* microdeletion.[15] Furthermore, until the recent report of an apparent tandem duplication of the *NF1* gene[16] is confirmed or disproven, the interpretation of negative FISH-based test results should be made with caution. The frequency of mosaicism for an *NF1* mutation is not known, however this is likely the underlying mechanism for patients with segmental or localized signs of the disorder.[2]

LABORATORY ISSUES

Optimal detection of mutations that predict a truncated neurofibromin polypeptide occurs when the nonsense-mediated decay pathway is at least partially inhibited, thereby increasing the ratio of mutant transcripts with a premature termination codon to normal transcripts. A protein synthesis inhibitor, such as puromycin, in the culture medium is effective for EBV-transformed lymphoblasts or phytohemaglutinin-stimulated primary lymphocytes.[7, 17] Furthermore, blood handling and shipping protocols must be used to reduce false positives in PTT resulting from environmental effects such as cold shock[18] or delay in mRNA isolation.[7, 17] There is no approved program of interlaboratory comparison for NF1 testing; performance assessment must be conducted by participation in ungraded proficiency survey programs, split sample analysis with other laboratories, or other suitable and documented means. There are no commercially available NF1 testing kits, probes, or controls. Intronic primers for amplification of individual *NF1* exons that apparently do not co-amplify the *NF1* pseudogene fragments located at

multiple chromosomal sites have been published.[19] Some issues related to NF1 testing have been reviewed recently.[20]

NEUROFIBROMATOSIS 2 (NF2)

MOLECULAR BASIS OF DISEASE

The development of bilateral vestibular schwanomas is a hallmark of NF2. Other commonly-associated tumors include schwannomas of other central, spinal, and peripheral nerves and meningiomas (reviewed in Ref [2, 21, 22] and http://www.geneclinics.org/). Although these tumors are not malignant but their location, along with the propensity to develop multiple tumors, make this a life-threatening disorder. Most patients become completely deaf and can have poor balance, vision and weakness. The mean age of onset is 18-24 years and the mean age of death is 36 years. Ependymomas and astrocytomas occur less frequently and are usually indolent CNS tumors. Patients affected with NF2 are at minimal increased risk for malignancy. Juvenile posterior subcapsular cataract is a common nontumor manifestation. The disorder may be under-diagnosed in children who present with ocular and skin manifestations. Early diagnosis improves management, which is primarily surgical and radiological. Modifications to the criteria for a diagnosis of NF2, initially established by the 1987/1991 National Institute of Health Consensus Conference, have been proposed to increase the specificity.[23]

NF2 is caused by haploinsufficiency for the tumor suppressor merlin (or schwannomin), the protein product of the *NF2* gene (Table 20-1). About one-half of patients are the first case of NF2 in the family. These sporadic cases result from *de novo* mutation of the *NF2* gene, a significant fraction of which are postzyogotic mutations that result in mosaicism (see below). The majority of constitutional mutations are private, predict the truncation of merlin, and occur throughout the gene (see below). Vestibular schwannomas develop from a progenitor Schwann cell that does not express merlin due to a somatic mutation that inactivated the single remaining *NF2* gene. Merlin is a protein of the cytoskeleton (reviewed in Ref.[3, 22]). Merline associates with transmembrane proteins important in adhesion, proteins

involved in signaling pathways, and cytoskeletal proteins. Merlin deficiency alters cell adhesion, motility, and spreading. The normal function of merlin remains to be determined but likely involves control of adhesion, proliferation, and the Rho signaling pathway.

CLINICAL UTILITY OF TESTING

DNA-based clinical testing for NF2 is available (http://www.geneclinics.org/) and used primarily for presymptomatic testing of at-risk individuals, typically young children of an affected parent. An early diagnosis of NF2 may improve outcome and at-risk children who did not inherit the *NF2* mutation can be spared costly brain imaging and audiologic screening. Genetic counseling is recommended prior to testing presymptomatic at-risk children. Testing is also useful to confirm a clinical diagnosis, which may be most helpful in sporadic cases of NF2, particularly children who present with ocular or skin manifestations or adults with equivocal findings or mild disease. Some of these cases may be mosaic for an *NF2* mutation, as the frequency of mosaicism is estimated at 16.7 – 24.8% of sporadic cases.[24] Genetic counseling regarding the clinical and reproductive implications of NF2 mosaicism is recommended.[6] Testing is also useful for reproductive counseling and prenatal diagnosis. Prenatal diagnosis of NF2 using amniocytes or chorionic villus tissue is available only in cases where the pathogenic germline mutation has been identified previously in an affected parent. Preimplantation genetic diagnosis of NF2 has been reported.[25]

The primary genetic counseling issues regard predicting the course of the disorder and recurrence risks. There are genotype/phenotype correlations, but they cannot predict the age of onset or the course of disease for an individual patient. Typically, constitutional frameshift and nonsense mutations are associated with severe NF2, defined by earlier age at onset and higher frequency and mean number of tumors.[26, 27] Constitutional missense and small in-frame mutations are thought to be associated with mild disease[27] and mutations in splice donor and acceptor sites result in variable clinical outcomes.[28] Recurrence risks for asymptomatic parents of an affected child are unknown, but are somewhat greater than the population risk due to the possibility of germline mosaicism in a parent.[29] For mosaic patients,

the risk of transmitting NF2 to offspring is ≤50%, depending upon the proportion of gametes that carry the *NF2* mutation.[6] Offspring that do inherit the mutation however, will have a constitutional *NF2* mutation and may have more severe disease than their mosaic parent.

AVAILABLE ASSAYS

NF2 gene mutation is the only known cause of the disorder. About 66% of mutations are nonsense or frameshifts that predict the premature truncation of merlin.[30, 31] About 10% of mutations are missense (although most have yet to be tested in functional assays) and the remaining are at splice donor/acceptor sites or due to submicroscopic rearrangements. A multipronged approach to testing is optimal due to the high frequency of private constitutional mutations, the high frequency of post-zygotic mutations, and the distribution of mutations throughout the gene. Direct sequencing of *NF2* in genomic DNA is clinically available and has a detection rate of about 60% in familial NF2 cases. The exon scanning techniques of SSCP, TGGE, and HA (see Chapter 2), followed by direct sequencing to identify the underlying *NF2* mutation, detected 54-81% of mutations in familial NF2 cases.[26, 27, 32, 33] The detection rate of either sequencing or exon scanning methods is significantly lower (34-51%) in sporadic cases due in part to the high frequency of post-zygotic *NF2* mutations, which can be masked by the presence of normal alleles.[27-29, 32] For mutation scanning tests, the detection rate will be laboratory-specific due to the varying degrees of optimization of the technique; a survey of testing laboratories is recommended.

Because schwannomas are clonal tumors with minimal cellular admixture, *NF2* mutations can be detected at high frequency in tumor tissue. Testing of tumor tissue is available clinically (http://www.geneclinics.org/) and is most useful in cases where a mutation is not detected in primary lymphoblasts, clinical manifestations are suggestive of somatic mosaicism, or constitutional tissue is unavailable. Different exon scanning methods have detected from 60-75% of mutations, primarily in vestibular schwannomas.[24, 34] Mutations are likely to be germline (rather than somatic) if the identical mutation is detected in two or more pathologically or anatomically distinct tumors or if a tumor shows

loss of heterozygosity for *NF2* intragenic/flanking loci, while constitutional tissue is heterozygous at these loci. Mutational analysis of tumors is expected to have the greatest sensitivity for *NF2* somatic mosaic mutations[24] and sporadic cases with negative results from mutation scanning tests.[35] Routine cytogenetic analysis and/or FISH with *NF2* probes will identify chromosomal rearrangements. One study detected submicroscopic rearrangements in 70% of patients in whom mutation scanning test results were negative.[36] Rearrangements (primarily deletions) were intragenic or involved all, or nearly all, of the *NF2* gene. It is not known if submicroscopic whole gene deletions extend into flanking contiguous genes that may contribute to the phenotype as in NF1 microdeletions (see above). Linkage analysis is clinically available for at-risk individuals and fetuses with multiple family members carrying a definitive diagnosis of NF2 who are willing to participate in the testing process. The availability of highly informative *NF2* intragenic markers increases the specificity of this methodology. For certain families, linkage analysis will be the most cost effective, fastest, and definitive test. It can sometimes be an option when mutation scanning test results are negative.

INTERPRETATION OF TEST RESULTS

Interpretation of the results of exon scanning tests requires identifying the underlying *NF2* mutation at the genomic DNA and/or cDNA levels to avoid false positives. Functional assays for merlin have been developed that can provide insight into the interpretation of missense and subtle in-frame alterations as pathogenic mutations versus neutral polymorphisms.[37, 38] No comprehensive *NF2* mutation database is available, however some mutations have been submitted to the Human Gene Mutation Database (http://archive.uwcm.ac.uk/uwcm/mg/hgmd0.html) and to an *NF2* Mutation Information site (http://neuro-trials1.mgh.harvard.edu/nf2/). Somatic mosaicism or *NF2* gene deletions must be considered in patients that have a negative mutation scanning test result, regardless of the severity of their manifestations. It is optimal for NF2 linkage testing not to include the first affected member in a family, since this individual may be mosaic for an NF2 mutation, which can lead to misinterpretation of test results.[39]

LABORATORY ISSUES

There is no approved program of interlaboratory comparison for NF2 testing; performance assessment must be conducted by participation in ungraded proficiency survey programs, split sample analysis with other laboratories, or other suitable and documented means. There are no commercially available NF2 testing kits, probes, or controls. Direct gene sequencing is not the optimal test to detect mosaicism for an NF2 mutation in lymphoblasts, as reliable detection of a low level point mutation will be difficult. Exon scanning techniques that are semi-quantitative, such as TGGE, will detect relative intensity differences between heteroduplexes and homoduplexes that suggest possible mosaicism.[32] Depending upon age, fixation, and storage conditions, some tumors may not yield nucleic acid of sufficient quality for mutational analysis.

SELECTED REFERENCES

1. Friedman JM. Neurofibromatosis 1: clinical manifestations and diagnostic criteria. J Child Neurol 2002; 17:548-554; discussion 571-542, 646-551.
2. Friedman JM, Butmann DH, MacCollin M, et al. Neurofibromatosis. Phenotype, Natural History, and Pathogenesis. Baltimore: The Johns Hopkins University Press, 1999:381.
3. Gutmann DH. The neurofibromatoses: when less is more. Hum Mol Genet 2001; 10:747-755.
4. Dorschner MO, Sybert VP, Weaver M, et al. NF1 microdeletion breakpoints are clustered at flanking repetitive sequences. Hum Mol Genet 2000; 9:35-46.
5. L'Azaro C, Gaona A, Lynch M, et al. Molecular characterization of the breakpoints of a 12-kb deletion in the NF1 gene in a family showing germ-line mosaicism. Am J Hum Genet 1995; 57:1044-1049.
6. Ruggieri M, Huson SM. The clinical and diagnostic implications of mosaicism in the neurofibromatoses. Neurology 2001; 56:1433-1443.
7. Messiaen LM, Callens T, Mortier G, et al. Exhaustive mutation analysis of the NF1 gene allows identification of 95% of mutations and reveals a high frequency of unusual splicing defects. Hum Mutat 2000; 15:541-555.
8. Fahsold R, Hoffmeyer S, Mischung C, et al. Minor lesion mutational spectrum of the entire NF1 gene does not explain its high mutability but points to a functional domain upstream of the GAP-related domain. Am J Hum Genet 2000; 66:790-818.
9. Han SS, Cooper DN, Upadhyaya MN. Evaluation of denaturing high performance liquid chromatography (DHPLC) for the mutational analysis of the neurofibromatosis type 1 (NF1) gene. Hum Genet 2001; 109:487-497.
10. De Luca A, Buccino A, Gianni D, et al. NF1 gene analysis based on DHPLC. Hum Mutat 2003; 21:171-172.
11. Gite S, Lim M, Carlson R, et al. A high-throughput nonisotopic protein truncation test. Nat Biotechnol 2003; 21:194-197.

12. Leppig KA, Viskochil D, Neil S, et al. The detection of contiguous gene deletions at the neurofibromatosis 1 locus with fluorescence in situ hybridization. Cytogenet Cell Genet 1996; 72:95-98.

13. Lopez-Correa C, Dorschner M, Brems H, et al. Recombination hotspot in NF1 microdeletion patients. Hum Mol Genet 2001; 10:1387-1392.

14. Klose A, Peters H, Hoffmeyer S, et al. Two independent mutations in a family with neurofibromatosis type 1 (NF1). Am J Med Genet 1999; 83:6-12.

15. Wu BL, Boles RG, Yaari H, et al. Somatic mosaicism for deletion of the entire NF1 gene identified by FISH. Hum Genet 1997; 99:209-213.

16. Gervasini C, Bentivegna A, Venturin M, et al. Tandem duplication of the NF1 gene detected by high-resolution FISH in the 17q11.2 region. Hum Genet 2002; 110:314-321.

17. Wimmer K, Eckart M, Rehder H, et al. Illegitimate splicing of the NF1 gene in healthy individuals mimics mutation-induced splicing alterations in NF1 patients. Hum Genet 2000; 106:311-313.

18. Ars E, Serra E, de la Luna S, et al. Cold shock induces the insertion of a cryptic exon in the neurofibromatosis type 1 (NF1) mRNA. Nucleic Acids Res 2000; 28:1307-1312.

19. Li Y, P OC, Breidenbach HH, et al. Genomic organization of the neurofibromatosis 1 gene (NF1). Genomics 1995; 25:9-18.

20. Thomson SA, Fishbein L, Wallace MR. NF1 mutations and molecular testing. J Child Neurol 2002; 17:555-561; discussion 571-552, 646-551.

21. Baser ME, DG RE, Gutmann DH. Neurofibromatosis 2. Curr Opin Neurol 2003; 16:27-33.

22. Evans DG, Sainio M, Baser ME. Neurofibromatosis type 2. J Med Genet 2000; 37:897-904.

23. Baser ME, Friedman JM, Wallace AJ, et al. Evaluation of clinical diagnostic criteria for neurofibromatosis 2. Neurology 2002; 59:1759-1765.

24. Kluwe L, Mautner V, Heinrich B, et al. Molecular study of frequency of mosaicism in neurofibromatosis 2 patients with bilateral vestibular schwannomas. J Med Genet 2003; 40:109-114.

25. Abou-Sleiman PM, Apessos A, Harper JC, et al. First application of preimplantation genetic diagnosis to neurofibromatosis type 2 (NF2). Prenat Diagn 2002; 22:519-524.

26. Parry DM, MacCollin MM, Kaiser-Kupfer MI, et al. Germ-line mutations in the neurofibromatosis 2 gene: correlations with disease severity and retinal abnormalities. Am J Hum Genet 1996; 59:529-539.

27. Evans DG, Trueman L, Wallace A, et al. Genotype/phenotype correlations in type 2 neurofibromatosis (NF2): evidence for more severe disease associated with truncating mutations. J Med Genet 1998; 35:450-455.

28. Kluwe L, MacCollin M, Tatagiba M, et al. Phenotypic variability associated with 14 splice-site mutations in the NF2 gene. Am J Med Genet 1998; 77:228-233.

29. Sestini R, Vivarelli R, Balestri P, et al. Neurofibromatosis type 2 attributable to gonosomal mosaicism in a clinically normal mother, and identification of seven novel mutations in the NF2 gene. Hum Genet 2000; 107:366-371.

30. Kluwe L, Bayer S, Baser ME, et al. Identification of NF2 germ-line mutations and comparison with neurofibromatosis 2 phenotypes. Hum Genet 1996; 98:534-538.

31. MacCollin M, Ramesh V, Jacoby LB, et al. Mutational analysis of patients with neurofibromatosis 2. Am J Hum Genet 1994; 55:314-320.

32. Kluwe L, Mautner VF. Mosaicism in sporadic neurofibromatosis 2 patients. Hum Mol Genet 1998; 7:2051-2055.

33. Evans DG, Wallace AJ, Wu CL, et al. Somatic mosaicism: a common cause of classic disease in tumor-prone syndromes? Lessons from type 2 neurofibromatosis. Am J Hum Genet 1998; 63:727-736.

34. Faudoa R, Xue Z, Lee F, et al. Detection of novel NF2 mutations by an RNA mismatch cleavage method. Hum Mutat 2000; 15:474-478.

35. Kluwe L, Friedrich RE, Tatagiba M, et al. Presymptomatic diagnosis for children of sporadic neurofibromatosis 2 patients: a method based on tumor analysis. Genet Med 2002; 4:27-30.

36. Legoix P, Sarkissian HD, Cazes L, et al. Molecular characterization of germline NF2 gene rearrangements. Genomics 2000; 65:62-66.

37. Stokowski RP, Cox DR. Functional analysis of the neurofibromatosis type 2 protein by means of disease-causing point mutations. Am J Hum Genet 2000; 66:873-891.

38. Gutmann DH, Hirbe AC, Haipek CA. Functional analysis of neurofibromatosis 2 (NF2) missense mutations. Hum Mol Genet 2001; 10:1519-1529.

39. Bijlsma EK, Wallace AJ, Evans DG. Misleading linkage results in an NF2 presymptomatic test owing to mosaicism. J Med Genet 1997; 34:934-936.

Table 20-1. Comparison of NF1 and NF2 disorders.

Feature	Neurofibromatosis 1 (NF1)	Neurofibromatosis 2 (NF2)
Alternate name	peripheral neurofibromatosis; von Recklinghausen neurofibromatosis	central neurofibromatosis; bilateral acoustic neuroma
OMIM accession number[1]	162200	101000
Mode of inheritance	autosomal dominant	autosomal dominant
Frequency of disorder	1/3000–1/4000 worldwide	1/33,000–1/40,000 worldwide
Gene symbol	*NF1*	*NF2*
Chromosomal location	17q11.2	22q12.2
Gene size; transcript size	~350 kb; ~11-13 kb[2]	~110 kb; 2 kb[2]
Genbank accession no. (gene;cDNA)[3]	NT_010799; NM_000267	Y18000; NM_000268
Number of exons	60	17
Tissue expression pattern	Widely expressed	Widely expressed
Protein product (size (kD); # residues)	Neurofibromin (>220 kD; 2818)	merlin, also known as schwannomin (65 kD; 595)
Normal functions of protein	tumor suppressor; negative regulator of ras oncogene	tumor suppressor; associates with proteins of the cytoskeleton
Common associated tumors	Neurofibroma, MPNST, optic pathway and brainstem gliomas	Bilateral vestibular schwannomas, schwannomas of other central and peripheral nerves, meningiomas
Animal models	mouse, *Drosophila*	mouse, *Drosophila*

[1]Online Mendelian Inheritance in Man (http://www.ncbi.nlm.nih.gov:80/entrez/query.fcgi?db=OMIM).

[2]Alternative splicing produces transcripts of varying lengths.

[3]See Gene Lynx Human (http://www.genelynx.org/) for a compilation of, and hyperlinks to, gene, protein structure, and genomic resources.

FIGURE LEGENDS

Figure 20-1. Genomic structure and mutations in *NF1* and *NF2* genes. A). At the top is a schematic of the *NF1* gene region at chromosome segment 17q11.2. The 350 kb NF1 gene is flanked by 51 kb paralogs NF1REP-P1 (previously termed NF1REP-P) and NF1REP-M, which are in direct orientation (orange boxes). Homologous recombination between these NF1REP elements results in the recurrent 1.5 Mb *NF1* microdeletion.[4] NF1REP-P2 is a partial element with a limited role in mediating *NF1* microdeletions. The 60 exons of the *NF1* are represented by boxes (not to scale) and exon numbering is sequential except as indicated. The GRD (exons 21-27a) and a cystein/serine-rich domain with 3 cysteine pairs suggestive of ATP binding (exons 11-17) are indicated. Grey boxes indicated alternatively spliced exons that vary in abundance in different tissues. Mutations have been identified in virtually every exon. Exons where mutations are apparently in greater abundance than expected are indicated (green boxes).[7, 8, 10] In one study, exons 7, 10a,b,c, 23-2, 27a, 29, 37 and accounted for 30% of mutations, 15 of which were in exons 10a,b,c, which harbor 3 recurrent mutations, including Y489C, which alone may account for ~2% of mutations.[7] Blue boxes indicate exons that had clusters of missense and/or single codon deletion mutations.[8] Some of the recurrent, although still infrequent, mutations are given below the exons. B) The 17 exons of the *NF2* gene are represented by boxes (not to scale) and exon numbering is sequential. The Protein 4.1-homology domain thought to mediate binding to cell surface glycoproteins (exons 2-8), the α-helical domain (exons 10-15), and the unique C-terminus (exons 16-17) are indicated. Grey boxes indicated alternatively spliced exons; the inclusion of exon 16 creates a alternate termination codon resulting in a slightly truncated protein. Mutations have been identified involving each exon except for 16. Exons containing recurrent mutations indicated (green boxes). In several studies, R57X occurred in 8% of familial constitutional mutations. Other recurrent nonsense codons are shown.

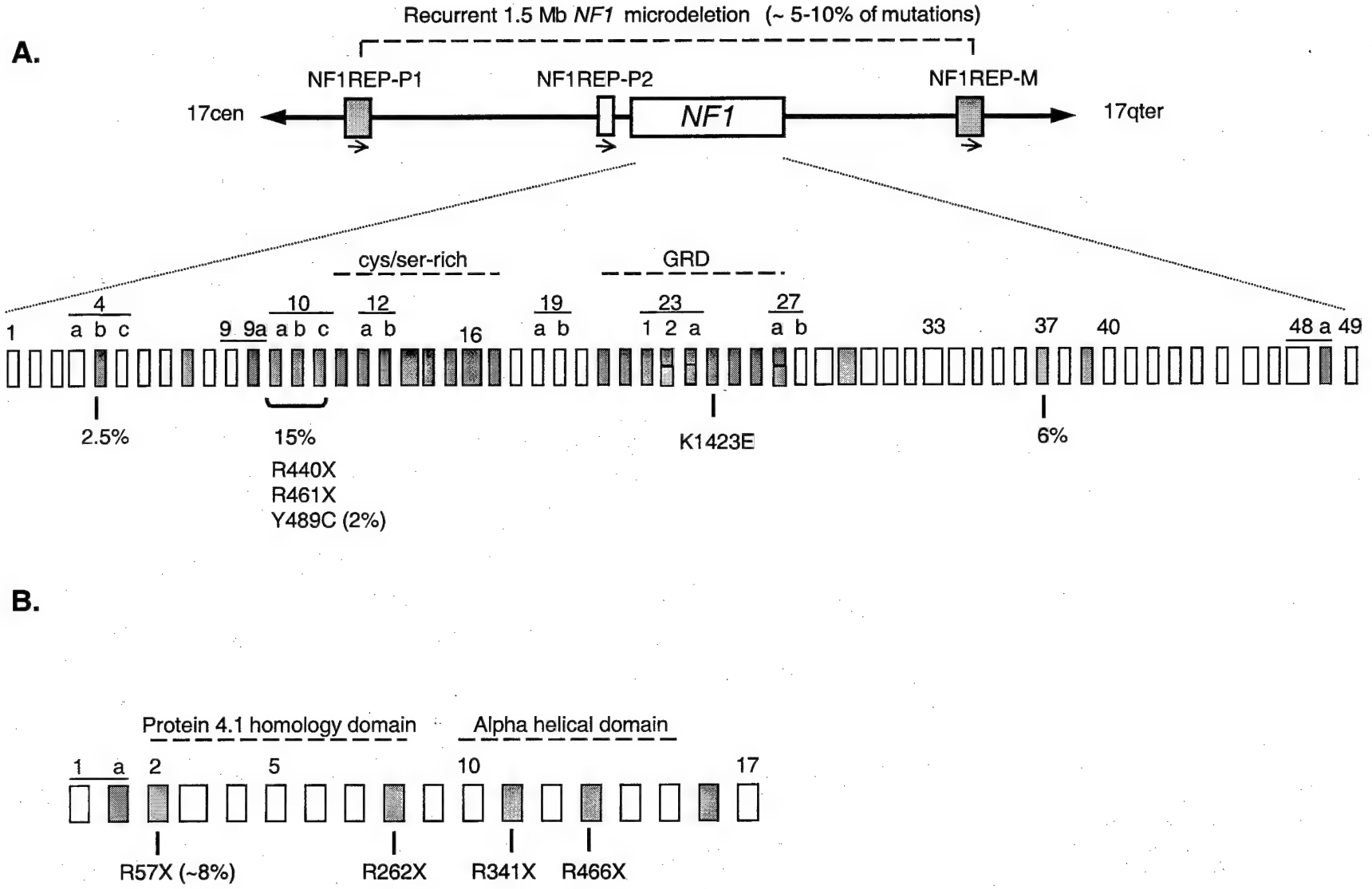
A.
Recurrent 1.5 Mb NF1 microdeletion (~ 5-10% of mutations)
NF1REP-P1
NF1REP-P2
NF1REP-M
17cen
NF1
17qter
cys/ser-rich
GRD
1
4
a b c
9 9a
10
a b c
12
a b
16
19
a b
23
1 2 a
27
a b
33
37
40
48 a 49
2.5%
15%
R440X
R461X
Y489C (2%)
K1423E
6%
B.
Protein 4.1 homology domain
Alpha helical domain
1 a
2
5
10
17
R57X (~8%)
R262X
R341X
R466X

An Association Between the *ERBB2* Codon 655 Polymorphism and NF1

Lauren Fishbein, Nicholas Sanek, and Margaret R. Wallace

University of Florida Departments of Molecular Genetics and Microbiology, and Pediatrics (Genetics), Gainesville, FL 32610

Running Heads: Fishbein, Sanek, and Wallace

ERBB2: Modifier of NF1?

Corresponding author: Margaret Wallace, PhD
Address: University of Florida
Department of Molecular Genetics
PO Box 100266
Gainesville, FL 32610-0266
Phone: 352-392-3055
Fax: 352-846-2042
Email: peggyw@ufl.edu

ABSTRACT

Neurofibromatosis 1 (NF1) is an autosomal dominant disorder characterized by cellular overgrowth of neural crest derived tissues, a key feature being benign Schwann cell tumors called neurofibromas. NF1 is caused by mutations in the *NF1* gene. There is variable expressivity, and it is thought that other genes likely modify the NF1 phenotype. The proto-oncogene *ERBB2* (a.k.a. *HER2/neu*) encodes a tyrosine kinase receptor, which is a member of the epidermal growth factor receptor family. ErbB proteins have been implicated in animal neurofibroma development, via a specific activating *ERBB2* mutation. However, no human tumors have been reported with this mutation, including 29 NF1 tumors and 19 non-NF1 Schwann cell tumors examined in this study. An Ile/Val polymorphism exists at codon 655 in the transmembrane domain near the mutation and is associated with an increased risk for breast cancer. The role that the *ERBB2* gene product plays in cell proliferation, as well as the critical function of the transmembrane domain in receptor activation, make this polymorphism a candidate for a modifier gene for NF1. We examined the genetic association between the *ERBB2* codon 655 alleles and NF1. Among 277 NF1 patients and 290 controls, we found that the risk of having NF1 with the Val/Val genotype was lower than with the Ile/Ile genotype. Furthermore, the number of NF1 patients with a homozygous Val/Val genotype is significantly lower than that found in our control populations. These data, the first report of a genetic association analysis of NF1, suggest that there may be a biological relationship between *ERBB2* genotype and NF1 phenotype.

Key words: Neurofibromatosis 1 (NF1), *ERBB2*, polymorphism, association, modifier gene

INTRODUCTION

Neurofibromatosis 1 (NF1) affects approximately 1 in 3500 individuals, and is characterized by benign overgrowth of neural crest derived tissues, including the formation of café-au-lait spots, Lisch nodules and neurofibromas. Neurofibromas are slow-growing tumors of the peripheral nerve sheath, composed mainly of Schwann cells. Some patients may have only a few small dermal neurofibromas, while other can develop thousands and/or have large neurofibromas from on major nerve branches. Clinical symptoms are highly variable between patients, even within families, but this is not obviously correlated to NF1 mutation type. Consequently, it is thought that along with stochastic factors, other genes may play a role as modifiers in NF1 phenotype (Easton et al., 1993).

The proto-oncogene *ERBB2* (or *HER2/neu*) encodes a transmembrane tyrosine kinase receptor and is a member of the epidermal growth factor receptor family thought to control a number of cellular functions, such as cell proliferation (reviewed in Dougall et al., 1994). The receptor heterodimerizes with other members of the ErbB family, activating the tyrosine kinase domain and transmitting growth factor signals downstream to cytoplasmic targets, including the MAPK pathway (which is also downstream in the *NF1* pathway). These growth factors include ligands known to stimulate Schwann cell proliferation. The *ERBB2* gene is frequently amplified or over-expressed in breast cancer and a number of adenocarcinomas, often signifying a poor prognosis (reviewed in Dougall et al., 1994). Transplacental administration of *N*-nitroso-*N*-ethylurea (ENU) to rats and hamsters induces multiple tumors in offspring at a high incidence (Bargmann and Weinberg, 1988; Nakamura et al., 1994). The rat Schwann cell tumors and hamster neurofibromas contain an activating point mutation in the *ERBB2* transmembrane domain (e.g. rat codon 664; analogous to codon 659 in humans and hamsters), leading to a valine

to glutamic acid amino acid substitution. This mutation is believed to cause an increase in the tyrosine kinase activity, and the mutated gene has been shown to transform NIH 3T3 cells (Bargmann et al., 1986).

To our knowledge, no human tumors have been found with this mutational change, although a coding region polymorphism has been identified in the transmembrane region (Papewalis et al., 1991). The polymorphism is located at codon 655 in humans and encodes either an isoleucine (ATC) or valine (GTC). It is unknown whether the polymorphic proteins differ in their function or tyrosine kinase activity. Interestingly, results from a population-based, case-control study examining the association of the *ERBB2* polymorphism with the risk of breast cancer showed a statistically significant increased risk for early onset breast cancer in women homozygous for the valine allele (Xie et al., 2000). To search for a connection between *ERBB2* and NF1/Schwann cell tumors, we first screened for the codon 659 mutation in a set of tumors, and then searched for a genetic association between the *ERBB2* codon 655 alleles and NF1.

MATERIALS AND METHODS

Patient Populations.

Case samples consisted of unrelated NF1 patient leukocyte DNA previously collected under IRB approval in our laboratory (n= 180) and an anonymous set generously provided by Dr. Karen Stephens (n=97) (University of Washington, Dept. of Pathology). The NF1 diagnosis was made via clinical observations satisfying the NIH diagnostic criteria. These patients were ascertained through genetics or other clinics, or via advertising through the National Neurofibromatosis Foundation. Two control groups were obtained, with the first group (C1) consisting of unrelated non-NF1 individuals whose leukocyte DNA was collected previously in

our laboratory (n=152). The second group (C2) consisted of a panel of anonymous control (non-NF1) DNAs generously given to us by Dr. Lawrence Brody (n=138) (National Human Genome Research Institute, NIH) (Struewing et al., 1995). DNA extractions were performed using the PUREGENE DNA Isolation Kit (Gentra Systems). The NF1 and control samples in our laboratory consist mostly of persons of a Caucasian background from the state of Florida.

The *ERBB2* codon 659 mutation analysis studied DNA extracted from primary tumor samples previously collected in our laboratory. The sporadic neurofibromas are from patients who do not meet the diagnostic criteria for NF1, while the NF1 neurofibromas and MPNSTs (malignant peripheral nerve sheath tumors) are from patients who do meet the diagnostic criteria for NF1. The peripheral, cutaneous schwannomas are from both NF2 and non-NF2 patients.

Mutation Analysis.

A 144bp fragment of the *ERBB2* gene was PCR amplified from tumor DNA using primers from Nakamura et al (1994) (NeuA 5'-AGAGCCAGCCCTCTGACGTC, NeuB 5'-CGTTTCCTGCAGCAGTCTCC) and standard conditions with a 58°C annealing temperature. These products were sequenced using standard cycle-sequencing protocols in our lab (ABI BigDye Terminator Kit) and results analyzed with the SeqEd v1.0.3 program (ABI).

Genetic Polymorphism Analysis.

Genotypes for *ERBB2* were determined with a PCR-RFLP based assay. The primers were designed to amplify the transmembrane domain and were based on the published sequence for the *ERBB2* gene (ErbB2-1F 5'-AGAGTAGGAGAGGGTCCAAGCC-3') or taken from Nakamura et al (1994) as for the mutation analysis (NeuA, NeuB). The PCR amplification was

performed under standard conditions with an annealing temperature of 69°C for the ErbB2-1F/NeuB primer pair and 58°C for the NeuA/NeuB primer pair. The PCR products were then digested with the restriction enzyme BsmBI (NEB). The completely uncut product represents a homozygous isoleucine genotype, while the completely cut product represents the homozygous valine genotype. The digest products were separated with 8% native PAGE and stained with ethidium bromide for visualization. Direct DNA sequencing was performed on some samples to confirm the results for the RFLP analysis.

Due to the lack of detailed information on patient ethnicity, a well-characterized insertion/deletion polymorphism in intron 16 of the human angiotensin converting enzyme (*hACE*) gene was used to provide evidence that ethnic background differences of the NF1 and control populations were not contributing to *ERBB2* differences. Genotypes were determined with a PCR assay using primers from Lindpaintner et al (1995) (hACE3-F 5'-GCCCTGCAGGTGTCTGCAGCATGT-3' and hACE5-R 5'-GGATGGCTCTCCCCGCCTTGTCTC-3'). This product was amplified under standard PCR conditions with an annealing temperature of 58°C. This primer set amplifies both the insertion and deletion alleles, 597 bp and 319 bp respectively. Because the deletion allele can be preferentially amplified in a heterozygous sample, an insertion-specific primer set was used to confirm the absence or presence of this larger allele in samples which were found to be homozygous for the deletion allele (hACE5-F 5'-TGGGACCACAGCGCCCGCCACTAC-3' and hACE5-R 5'-TCGCCAGCCCTCCCATGCCCATAA-3') (Lindpaintner et al., 1995). This product was amplified with a 1 min denaturing step at 94°C and a combined annealing and extension step for 1 min at 72°C, for 35 cycles. PCR products were electrophoretically separated on 1% agarose gels and visualized with ethidium bromide staining.

Statistical Analysis.

Statistical analysis (odds ratios and 95% confidence intervals) was used to determine a possible correlation between *ERBB2* genotype and NF1. Odds ratios (reported as cases/controls) are written as the ratio(95% confidence interval). Hardy-Weinberg analysis and chi-squared analysis for differences in genotype frequencies were completed as well. All statistics are reported based on the comparison of the NF1 group to each control group separately, as well as combined.

RESULTS

Ten sporadic (non-NF1) neurofibromas, 9 Schwannomas, 20 NF1 neurofibromas and 9 NF1 MPNSTs were analyzed for the presence of the *ERBB2* codon 659 missense mutation in the transmembrane domain, and no mutations were found.

Figure 1 shows genotyping from the ErbB2-1F/Neu B PCR product. All three genotypes are represented and the results matched those from the direct sequencing data. A homozygous Ile genotype shows an uncut band at 280 bp (patients 1 and 5). The heterozygous Ile/Val genotype shows one 280 bp band and two lower bands of 165 bp and 115 bp (patients 2, 3, 4). The homozygous Val genotype shows the two lower bands only (patient 6).

Genetic analysis was completed on 277 unrelated NF1 patient samples and 152 C1, 138 C2, and 290 C1 and C2 combined samples (Table 1). The Val allele was less prevalent among NF1 patients (18%) than among either C1 (26%), C2 (26%) or the combined controls (26%). The odds ratios for the allele count are given in Table 1. The risk of having NF1 with the

Val/Val genotype is lower [OR=0.27(0.12-0.65)] than that with the Ile/Ile genotype [OR=0.63(0.44-0.88)].

In addition, the number of samples with a Val/Val genotype is significantly lower in the NF1 population than in the control populations (C1, p=0.001; C2, p=0.002; C1+C2, p=0.002). In contrast, the frequencies for the remaining genotypes are not significantly different among the two populations (Ile/Ile: C1, p=0.120; C2, p=0.086; C1+C2, p=0.111 and Ile/Val: C1, p=0.480; C2, p=0.390; C1+C2, p=0.451). Hardy-Weinberg equilibrium analysis showed that there were small differences between the observed and expected numbers of people in each genotype, but the differences were not statistically significant using chi-squared tests for independence (NF1, p=0.983; C1, p=0.587; C2, p=0.822; C1+C2, p=0.590).

The human angiotensin converting enzyme (*hACE*) gene has a well-characterized insertion/deletion polymorphism in intron 16 for which the genotype frequencies vary based on ethnic background (Mathew et al., 2001). Genotyping of the *hACE* gene in both NF1 and control populations showed no statistically significant difference in genotype frequencies between the populations (Ins/Ins: C1, p=0.870; C2, p=0.729; C1+2, p=0.869 and Ins/Del: C1, p=0.751; C2, p=0.411; C1+2, p=0.671 and Del/Del: C1, p=0.620; C2, p=0.232; C1+2, p=0.533). Allele frequencies also showed no statistically significant difference (data not shown). This implies that the statistically significant differences in genotype frequency seen for the *ERBB2* gene are not a result of ethnic differences between the groups.

DISCUSSION

The *ERBB2* gene product, p185, is a 1255 amino acid glycoprotein that is closely related to the other members of the EGFR family involved in signal transduction. These receptors share

a similar structure consisting of an extracellular ligand-binding domain, a single hydrophobic transmembrane domain, and a cytoplasmic tyrosine kinase domain. Alterations in the transmembrane segment may have profound effects on the receptor activity. The ENU-induced valine to a glutamic acid mutation at rat codon 664 (analogous to human and hamster codon 659) in the transmembrane domain is believed to enhance receptor dimerization, which results in the activation of the receptor tyrosine kinase without ligand binding. NMR studies have shown that this activating mutation can cause significant intramolecular rearrangements which could influence its lateral associations (Sharpe et al., 2000). In addition, *in vitro* studies have shown that activation of *ERBB2* is sufficient to initiate the immortalization and transformation of immature Schwann cells, as well as NIH 3T3 cells (Sherman et al., 1999; Bargmann et al., 1986).

A recent report analyzed a series of spontaneous peripheral nerve sheath tumors from domesticated animals and found the same *ERBB2* mutation in 75% of the malignant tumors (Stoica et al., 2001). Although a homologous mutation has not been found in any human tumors, including our sample set of 48 peripheral nerve sheath tumors, there exists an Ile/Val polymorphism nearby at codon 655 in the transmembrane domain. It is not known if this substitution results in any change in the tyrosine kinase activity. Nevertheless, our study has found that the number of NF1 patients with a homozygous Val genotype is significantly lower than that found in our control populations. This finding suggests that the polymorphism may be an NF1 modifier gene (or linked to a modifier). Interestingly, the heterozygous Ile/Val genotype is not significantly lower in the NF1 population. One possible explanation is a selective embryonic mortality associated with the combination of an NF1 mutation and an *ERBB2* homozygous Val genotype. Heterozygous NF1 cells have decreased NF1-GAP activity and thus have increased signaling through the ras pathway (Kim et al., 1995). This signaling cascade

connects to the MAPK pathway through which ERBB2 signals. Perhaps downstream alterations in MAPK signaling by a combination of *NF1* mutations and homozygosity for *ERBB2* codon 655 valine allele may predispose for a critical effect in development. Alternatively, the Val homozygous genotype at ERBB2 can attenuate NF1 phenotype, such that persons with an *NF1* mutation and Val/Val *ERBB2* genotype might have a greater chance of failing to display sufficient features to be diagnosed and/or brought to medical attention. However, of the 4 (out of 7 total) Val/Val NF1 patients for which phenotype information is known, two each have a serious medical complication; and the other two are only mildly affected, although the serious complications might be due to stochastic factors. Thus, these data support the notion that *ERBB2* genotype may have a biologically-based relationship to NF1 phenotype through mechanisms which bear further investigation.

ACKNOWLEDGEMENTS

We thank Drs. Karen Stephens (University of Washington) and Lawrence Brody (NIH) for providing additional samples; Drs. Lawrence Brody (NIH) and Susan McGorray (University of Florida) for help with initial data analysis strategy; Dr. Wayne McCormack (University of Florida) for critical comments on the manuscript; and Ms. Bonnie Eady for technical assistance. We also thank the many physicians who provided NF1 patient blood samples, and the patients themselves for their participation. This work was supported by an NIH NCI Training Grant in Cancer Biology (LF, T32CA01926), the Hayward Foundation (MRW), and U.S. Army (MRW, DAMD 179818609).

REFERENCES

Bargmann, C.I., M. Hung, and R.A. Weinberg (1986) Multiple independent activations of the *neu* oncogene by a point mutation altering the transmembrane domain of p185. Cell 45: 649-657.

Bargmann, C.I. and R.A. Weinberg (1988a) Increased tyrosine kinase activity associated with the protein encoded by the activated *neu* oncogene. Proc Natl Acad Sci USA 85: 5394-5398.

Dougall, W.C., X. Qian, N.C. Peterson, M.J. Miller, A. Samanta, and M.I. Greene (1994) The *neu*-oncogene: signal transduction pathways, transformation mechanisms and evolving therapies. Oncogene 9(8): 2109-2123.

Easton, D.F., M.A. Ponder, S.M. Huson, and B.A. Ponder (1993) An analysis of variation in expression of neurofibromatosis (NF) type 1: evidence for modifying genes. Am J Med Genet 53: 305-313.

Kim, H.A., T. Rosenbaum, M.A. Marchionni, N. Ratner, and J.E. DeClue (1995) Schwann cells from neurofibromin deficient mice exhibit activation of p21 ras, inhibition of cell proliferation and morphological changes. Oncogene 11: 325-335.

Lindpaintner, K., M.A. Pfeffer, R. Kreutz, M.J. Stampfer, F. Grodstein, F. LaMotte, J. Buring, and C.H. Hennekens (1995) A prospective evaluation of an angiotensin-converting-enzyme gene polymorphism and the risk of ischemic heart disease. N Engl J Med 332(11): 706-711.

Mathew, J., K. Basheeruddin, and S. Prabhakar (2001) Differences in frequency of the deletion polymorphism of the angiotensin-converting enzyme gene in different ethnic groups. Angiology 52(6): 375-379.

Nakamura, T., T. Ushijima, Y. Ishizaka, M. Nagao, T. Nemoto, M. Hara, and T. Ishikawa (1994) *neu* proto-oncogene mutation is specific for the neurofibromas in a N-Nitroso-N-ethylurea-induced hamster neurofibromatosis model but not for hamster melanomas and human schwann cell tumors. Cancer Res 54: 976-980.

Papewalis, J., A.Y. Nikitin, and M.F. Rajewsky (1991) G to A polymorphism at amino acid codon 655 of the human *erbB-2/HER2* gene. Nucleic Acids Res 19: 5452.

Sharpe, S., K.R. Barber, and C.W.M. Grant (2000) Val 659 to Glu mutation within the transmembrane domain of *ErbB-2*: Effects measured by 2H NMR in fluid phospholipid bilayers. Biochemistry 39: 6572-6580.

Sherman, L., J.P. Sleeman, R.F. Hennigan, P. Herrlich and N. Ratner (1999) Overexpression of activated *neu/erb*B2 initiates immortalization and malignant transformation of immature Schwann cells *in vitro*. Oncogene 18: 6692-6699.

Stoica, G., S.I. Tasca and H.-T. Kim (2001) Point mutation of *neu* oncogene in animal peripheral nerve sheath tumors. Vet Pathol 38: 679-688.

Struewing, J.P., D. Abeliovich, T. Peretez, N. Avishai, M.M. Kaback, F.S. Collins, and L.C. Brody (1995) The carrier frequency of the *BRCA1* 185delAG mutation is approximately 1 percent in Ashkenazi jewish individuals. Nat Genet 11: 198-200.

Xie, D., X. Shu, Z. Deng, W. Wen, K.E. Creek, Q. Dai, Y. Gao, F. Jin and W. Zheng (2000) Population-based, case-control study of *HER2* genetic polymorphism and breast cancer risk. J Natl Cancer Inst 92(5): 412-417.

Table 1. *ERBB2* allele frequencies and odds ratios [OR= ratio(95% Confidence Interval)] for the NF1 and control

	NF1 patients	C1	C2
	n=277	n=152	n=138
Allele Frequency, %			
Ile	82	74	74
Val	18	26	26
Genotype Frequency, %			
Ile/Ile	68	57	56
Ile/Val	30	34	36
Val/Val	3	9	8
ORs for Allele Count cases/controls		0.60(0.43-0.85) p=0.003	0.60(0.43-0.85 p=0.004
Homozygous effect, ORs Val/Val		0.26(0.10-0.65) p=0.004	0.30(0.11-.79) p=0.015
Ile/Ile		0.64(0.43-0.97) p=0.035	0.61(0.40-0.92 p=0.020

FIGURE LEGENDS

Fig 1. Ethidium-bromide stained polyacrylamide gel showing genotyping of the *ERBB2* polymorphism. The first lane shows the 1kb ladder marker (Invitrogen). For each sample, the undigested product is shown first (U). The BsmBI digested product is shown second (C), with the top band (280bp) representing the Ile allele and the bottom bands (165bp, 115bp) representing the cut Val allele. Positive control and patient 6 show the Val homozygous genotype.

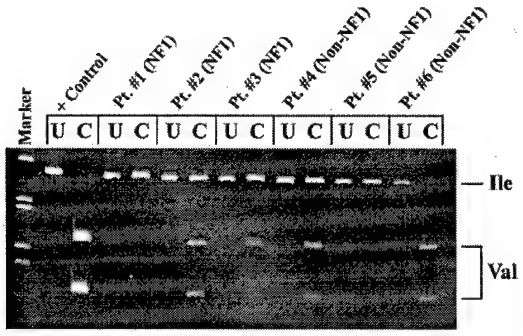
Marker
+ Control
Pt. #1 (NF1)
Pt. #2 (NF1)
Pt. #3 (NF1)
Pt. #4 (Non-NF1)
Pt. #5 (Non-NF1)
Pt. #6 (Non-NF1)
U C U C U C U C U C U C U C
Ile
Val

Paralogous recombination at two distinct hotspots accounts for 69% of *NF1* microdeletions

Michael O. Dorschner[1*], Hilde Brems[2], Rosalynda Le[1], Thomas De Raedt[2], Margaret R. Wallace[3], Cynthia J. Curry[4], Arthur S. Aylsworth[5], Eric A. Haan[6], Elaine H. Zackai[7], Conxi Lazaro[8], Ludwine Messiaen[9], Eric Legius[2], Karen Stephens[1, 10]

Departments of Medicine[1] and of Laboratory Medicine[10], University of Washington, Seattle, WA 98195
[2]Center for Human Genetics, Catholic University Leuven, Herestraat 49, B-3000 Leuven, Belgium
[3]Departments of Molecular Genetics and Microbiology and Pediatrics, and Center for Mammalian Genetics, University of Florida, Gainesville, FL 32610
[4]Children's Hospital Central California, and Department of Pediatrics, University of California San Francisco, Madera, CA 93638
[5]Departments of Pediatrics and Genetics, University of North Carolina, Chapel Hill, NC 27599-7487
[6]South Australian Clinical Genetics Service, Women's & Children's Hospital, North Adelaide SA 5006, Australia and Adelaid University, Adelaide SA 5005, Australia.
[7]Clinical Genetics Center, Children's Hospital Philadelphia, and Department of Pediatrics, University of Pennsylvania School of Medicine, Philadelphia, PA 19104
[8]Medical and Molecular Genetics Center-IRO, Hospital Duran i Reynals, Autovia de Castelldefels Km 2.7 08907 L'Hospitalet de Llobregat, Barcelona, Spain
[9]Center for Medical Genetics, Ghent University Hospital, De pintelaan 185,B-9000 Ghent, Belgium

*Current Address: Rexigen Corporation, 551 N 34th St, Suite 200, Seattle, WA 98193

Corresponding Author:
Karen Stephens, PhD
University of Washington
1959 NE Pacific, Rm I-204
Medical Genetics Box 357720
Seattle, WA 98195
Tel: 206-543-8285
Fax: 206-685-4829
millie@u.washington.edu

ABSTRACT

Microdeletions involving the entire *NF1* gene cause ~10% of neurofibromatosis 1 cases and are associated with an early age of onset of dermal neurofibromas. The majority are recurrent 1.5 Mb deletions mediated by homologous recombination between ~50 kb paralogs, termed NF1REPs, that flank the *NF1* gene. Although over 25 disorders result from rearrangements mediated by paralogous recombination, little is known about the location and nature of the breakpoints at the sequence level. Towards elucidating the mechanism(s) of microdeletion, we sequenced NF1REP-mediated *NF1* microdeletions and identified the breakpoint intervals by use of paralogous specific variants (PSV). We identified 2 paralogous recombination sites, termed PRS1 and PRS2, which are 4,154 and 6,315 bp in length and ~15 kb apart. Within each region, *NF1* microdeletion breakpoints were clustered with 64% (9/14) of sequenced PRS1 breakpoints in a 551 bp hotspot interval, while 86% (25/29) of PRS2 breakpoints occurred in a 2,292 bp hotspot. The breakpoint frequency decreased in a generally symmetrical fashion on both sides of each hotspot, consistent with an initiation site for crossing over in this region. The pattern of PSVs at one breakpoint interval showed evidence of gene conversion, which is consistent with the double-strand break repair model of yeast. We developed PRS1 and PRS2 deletion junction-specific PCR assays, screened a cohort of NF1 deletion patients, and found that 69% (N=78) of breakpoints occurred at these sites; PRS2-mediated deletions were the most prevalent. Our results show that despite ~50 kb of 98% sequence identity between NF1REP paralogs, meiotic recombination preferentially occurs at discrete hotspots.

INTRODUCTION

Neurofibromatosis type 1 (NF1; OMIM 16220) is a common autosomal disorder that predisposes to benign and malignant tumor development (1-3). Virtually all affected individuals develop multiple dermal neurofibromas, which are benign tumors of the peripheral nerve sheath. Dermal neurofibromas typically become apparent around the time of puberty and they increase in number with age (4). Other tumors include non-dermal neurofibromas, optic nerve gliomas, and malignant peripheral nerve sheath tumors. A host of other manifestations can be associated with NF1 including café au lait spots, axillary and inguinal freckling, Lisch nodules, learning disabilities, and distinctive bony abnormalities (1, 5, 6). NF1 patients are constitutionally heterozygous for an inactivating mutation, which results in functional haploinsufficiency of the *NF1* gene product, neurofibromin, as demonstrated in humans by *NF1* microdeletion (7, 8) and in mouse by targeted inactivation (9-11). Neurofibromin is a tumor suppressor that functions, as least in part, as a negative regulator of Ras (reviewed in (12-14).

Submicroscopic microdeletion involving the entire *NF1* tumor suppressor gene at chromosome band 17q11.2 accounts for an estimated 5-20% of NF1 cases (15-19). Although they represent only a fraction of causal mutations, analysis of *NF1* microdeletions is of great interest for clinical, pathological, and molecular genetic reasons. Clinically, microdeletions are the only *NF1* genotype known to be consistently associated with a particular phenotype. Subjects with microdeletions are remarkable for a predisposition to facial anomalies and childhood onset of dermal neurofibromas, or in cases where age of onset is unknown, an excessive number relative to age (7, 8, 15, 18, 20-24). A few deletion cases that do not show an early age of onset of dermal neurofibromas have been reported (15, 18, 24), however, since the extent of the deletions was not delineated, it is unclear whether the same loci are involved. In contrast, about 80% of NF1 cases are caused by subtle intragenic private mutations that predict truncation of neurofibromin (19, 25). Among these subjects, no correlation has been detected between mutation type and/or location and the development of specific manifestations (26-28).

Pathologically, *NF1* microdeletions are important because they hold the promise of identifying a modifying gene that potentiates dermal neurofibromagenesis. The correlation between microdeletion and the early onset tumor phenotype led us to hypothesize that dermal neurofibromas developed earlier due to haploinsufficiency for both neurofibromin and the product of an unknown closely linked gene, designated as *NPL* (neurofibroma-potentiating locus)(8, 23, 29, 30). Two models have been proposed for how *NPL* functions to potentiate dermal neurofibroma development (29). Haploinsufficiency for *NPL* could increase the frequency of somatic second-hit mutations in the *NF1* gene. Homozygous inactivation of the *NF1* gene has been demonstrated in dermal neurofibromas (31-34). A possible mechanism may be genomic instability in microdeletion patients, which is intriguing in view of reports detecting cytogenetic abnormalities and microsatellite instability in some neurofibromas (35, 36). A second model proposes that *NPL* haploinsufficiency increases the probability that a neurofibromin-deficient progenitor Schwann cell will manifest as a dermal neurofibroma. For example, *NPL* could encode (or regulate) a cytokine, cell cycle regulator, tumor suppressor, or oncogene that exerts a positive proliferative advantage on a neurofibromin-deficient cell.

Molecularly, *NF1* microdeletions in humans are important because they typically arise by paralogous recombination at specific sites (30). We recently proposed using the term paralogous recombination (29) to describe homologous recombination between paralogs, which has also been referred to as nonallelic homologous recombination (37) or ectopic homologous recombination (38). Paralogs, also known in the human disease literature as low-copy repeats (LCR) (39, 40), duplicons (41),

or repeats (REPs) (42, 43), are DNA sequences of high identity that derive from duplication of a gene or segment within a genome (44, 45). An estimated 80% of *NF1* microdeletions arise by paralogous recombination between the NF1REP-P and NF1REP-M paralogs that flank the *NF1* gene resulting in deletions about 1.5 Mb in length (30, 46). *NF1* microdeletions can be familial or *de novo* (8, 21, 23, 30, 47). New microdeletions preferentially occur on the maternally-derived allele (17, 48) and detection of crossovers flanking the deleted region is consistent with a mechanism of unequal crossing over between misaligned NF1REPs during maternal meiosis I (48). These NF1REP elements are 51 kb in length (S.H. Forbes et al., unpublished data) and the microdeletion region harbors at least 11 genes in addition to the 350 kb *NF1* gene (30, 49). Which gene may represent the *NPL* locus is unknown, as the functions of these genes remain to be determined.

Previously, we described a 2 kb hotspot where paralogous recombination between NF1REP-P1 and NF1REP-M resulted in a recurrent 1.5 Mb *NF1* microdeletion (20). Forty-six percent of patients (N=54), known to be hemizygous for at least the *NF1* gene, had breakpoints clustered at this hotspot. Towards elucidating the mechanism of NF1REP-mediated *NF1* microdeletions and narrowing the critical region of the *NPL* gene, we mapped and sequenced additional breakpoints. Here we report the identification a second distinct paralogous recombination hotspot, extension and reginement of the initial hotspot region, and the development of deletion junction-specific PCR assays that detected 69% of *NF1* microdeletions.

RESULTS

Identification and amplification of deletion breakpoints

In the course of characterizing the initial 2 kb paralogous recombination hotspot (20), we found that breakpoints in 6 microdeletion cases were not located at the hotspot but had previously been mapped within the NF1REP paralogs (30). This suggested the possibility of additional recombination hotspots within the paralogs. We identified and sequenced the breakpoints of these 6 cases (UWA119-1, UWA123-1, UWA166-2, UWA169-1, UWA172-1, and UWA176-1), which have been described previously (8, 23, 30). Because the NF1REP paralogs share 98% sequence identity (30) it was necessary to identify paralogous sequence variants (PSV) (50), i.e., nucleotide variants specific for NF1REP-P1 and NF1REP-M, to determine the breakpoint interval in the recombinant NF1REP. Because of the recent identification of an additional NF1REP proximal to the *NF1* gene (Dieter Jenne, et al., unpublished data; Stephen Forbes, et al., unpublished data), the previously named NF1REP-P (30) is now referred to as NF1REP-P1 (Figure 1). We employed our previously successful strategy (20) of designing primers from the known sequence of NF1REP-P1 and amplifying that segment from a somatic cell hybrid line carrying only the patient's chromosome 17 with the deletion. Direct sequencing revealed whether the pattern of PSVs was representative of NF1REP-P1 or NF1REP-M, or if it transitioned from NF1REP-P1 to NF1REP-M as expected if the amplicon contained the breakpoint of the recombinant NF1REP. Simultaneously, BAC 271K11 carrying NF1REP-P1 and BACs 640N20 and 951F11 carrying NF1REP-M (30) were also amplified and sequenced. Amplification of BACs 271K11 and 640N20 served as positive controls, while amplification of BAC 951F11 provided sequences not completed by the Human Genome Mapping Project at that time. Analysis of these data identified two clusters of breakpoints. The first cluster was 4,154 bp in length and designated as paralogous recombination site 1 (PRS1)(Figure 1). The second cluster was 6,315 bp in length and extended the cluster harboring the previously defined 2 kb recombination hotspot. This cluster, designated as paralogous recombination site 2 (PRS2), is about 15 kb telomeric to PRS1 (Figure 1).

NF1 microdeletion junction-specific PCR assays were developed by judicious primer design that took advantage of PSVs. Figure 2A shows the results of two different PRS1 assays. The assay with primers mdf4-F and md30-R was robust and gave a 3 kb junction fragment. A longer 7 kb amplicon of the deletion junction generated with primers md4-F and md4-R detected all known breakpoints in the PRS1 region (Figures 2A, 2B, and 3A). Occasionally, the 7 kb PRS1 assay showed a smear of products, which should not be misinterpreted as a positive result (Figure 2B). In this instance, the assay of normal genomic DNA shows a smear of products without the intense 7 kb junction fragment (UWA183-1). Confirmation that this result is a true negative is shown by absence of the 7 kb junction fragment from genomic DNA of a somatic cell hybrid line (UWA183-1-H#15) carrying only the PRS2-mediated deleted chromosome 17 of patient UWA183-1 (Figure 2B). We also verified that this pattern is not due to amplification of NF1REP-like sequences on chromosome 19 (Figure 2B). Although it is unclear why some genomic DNA samples give this diffuse pattern of amplicons, nonspecific products from both PRS1 and PRS2 can be minimized by the use of high purity DNA (see Materials and Methods).

Our previously reported deletion junction-specific assay for breakpoints at the 2 kb recombination hotspot utilized primers DCF and DTR, which gave a 3.4 kb amplicon (20). For this assay, instead of the DCF primer, we now routinely use md21-F, whose one additional base at the 5' end made the assay more reliable and robust (Figure 2C, Table 1). A new assay was needed to amplify the extended length of the breakpoint cluster (now designated as PRS2). The new assay utilized primers md21-F and md7-R and amplified a 7 kb junction fragment (Figure 2C, Table 1). While this assay detects a greater number of deletion breakpoints, we have found that it can be less robust and more sensitive to the purity of the genomic DNA template compared to the smaller amplicon assays (see Materials and Methods).

_NF1_ microdeletion breakpoint sequence analyses

To identify the precise breakpoint intervals within PRS1 and PRS2, deletion junction-specific amplicons (PRS1 7 kb and PRS2 7 kb) were sequenced directly using a series of internal primers. To facilitate differentiating PSVs of NF1REP-P1 and NF1REP-M from allelic polymorphisms (e.g., single nucleotide polymorphisms, SNP), we also amplified, cloned, and sequenced nonrecombinant PRS1 and PRS2 regions from both NF1REP-P1 and NF1REP-M of 8 normal chromosomes and of NF1REP-M carried in BAC 951F11.

Sequenced breakpoints at PRS1. The sequences of 14 breakpoints defined the PRS1 breakpoint cluster as 4,154 bp in length (Figure 3A). Breakpoint distribution was skewed with 64% mapping to a 551 bp hotspot. The remaining breakpoints occurred in unique sequence intervals. The shorter 3 kb PRS1 amplicon assay (primers mdr4-F and md30-R) detected 13/14 of the breakpoints (Figure 3A, breakpoints between 122,140 and 124,221)(Table 2). The sequence of the 170 bp breakpoint interval for patient UWA123-3 was consistent with a gene conversion event (Figure 3B). Since the patient's microdeletion was paternal in origin, we cloned and sequenced both alleles of NF1REP-P1 and NF1REP-M of the father. These data identified the paternal NF1REP-P1 and NF1REP–M alleles that served as the recombination substrates and confirmed the alternating pattern of PSV and SNP between NF1REP-P1 and NF1REP-M across the breakpoint region (Figure 3B).

Sequenced breakpoints at PRS2. The sequences of 29 breakpoints, including 25 previously reported (20) that are summarized in Figure 3C, defined the PRS2 breakpoint cluster as 6,315 bp in length. Breakpoint distribution was skewed with 86% (25/29) mapping to a 2,292 bp hotspot. The previously reported 3.4 kb PRS2 assay (primers DCF and DTR) (20) or the modified md21-F/deljun1-R assay (Figure 2C), detected 25/29 cases (Figure 3B, from 141,992 to 144,299 bp). For the cases whose

breakpoint intervals were published previously (20), it should be noted that some intervals have increased in length. Here we included the sequences of 7 NF1REP-P1 and NF1REP-M alleles from control individuals, along with sequenced BACs, to differentiate between common SNPs and PSV. The identification of base 142,662 as a SNP resulted in extending the intervals of 14 patients to the next PSV at 142,728. Similarly the identification of 143,981 and 143,998 as SNPs extended the interval of 7 patients to the next PSV at 144,299. The originally reported 17 bp recombination interval for patient 99-1(20) was confirmed by sequence analysis of the maternal progenitor alleles that served as recombination substrates, thereby documenting that they carried the SNPs as shown (Figure 3C).

Frequency of PRS1- and PRS2-mediated *NF1* microdeletions

To study a larger cohort of *NF1* deletion patients and determine the frequency of paralogous recombination events at PRS1 and PRS2, we performed deletion junction-specific assays on additional patients known to be hemizygous for all, or nearly all, of the *NF1* gene. A total of 78 patients were studied, including those whose breakpoints were sequenced (Figure 3). These analyses showed that 14/78 (18%) of deletions occurred at PRS1, while 40/78 (51%) occurred at PRS2 (Table 2). The more robust, shorter amplification assays detected the majority of cases. Primers md4-F and md30-R detected 13/14 of the total PRS1 recombination events and primers md21F and deljun1-R (or DCF and DTR (20) detected 33/40 (82%) of the total PRS2 recombination events (Table 2). Neither the 7 kb PRS1 nor the 7 kb PRS2 deletion-junction assays generated products upon amplification of genomic DNA from the peripheral blood of 75 control individuals.

There was no significant difference between PRS1- and PRS2-mediated microdeletions for the parent of origin or for *de novo* versus familial cases (Figure 3)(20). In our series of 59 cases where we have clinical data for the parents, 6 (10%) inherited the *NF1* microdeletion. Among 45 *de novo* cases where parental origin of the microdeletion was determined, 36/45 (80%) were maternally derived, while 9/45 (20%) were paternally derived.

DISCUSSION

By employing sequence analysis of deletion junctions and deletion junction-specific PCR assays, we found that the paralogous recombination events mediating *NF1* microdeletions occurred preferentially at two discrete sites. Sequence analyses of deletion junction fragments of recombinant NF1REPs, along with the comparable region of nonrecombinant NF1REP-P1 and NF1REP-M in control individuals, identified PSVs that were used to delimit the paralogous recombination sites PRS1 and PRS2 to 4,154 bp and 6,315 bp, respectively. Together, recombination at these two distinct sites accounted for 69% of *NF1* microdeletion cases (N=78) and of these 74% occurred at PRS2. Within each PRS region, *NF1* microdeletion breakpoints were clustered (Figure 3). Sixty-four percent (9/14) of sequenced PRS1 breakpoints occurred in a 551 bp interval, while 86% (25/29) of sequenced PRS2 breakpoints occurred in a 2,292 bp interval. The breakpoint frequency decreased in a generally symmetrical fashion on both sides of the PRS1 and PRS2 hotspots, which is consistent with an initiation site for crossing over in this region as predicted by the double-strand break repair model (51) and similar to maps of strand exchange at other recombination hotspots in mammals (52, 53). Both familial and *de novo* microdeletions occurred at both PRSs. Eighty percent (N=45) of *de novo NF1* microdeletions occurred on the maternally-derived chromosome 17 (this manuscript; (20), which is the same frequency reported in a previous smaller study (17, 48). However, both maternally- and paternally-derived microdeletions occurred at both PRS1 and

PRS2. The work of Jenne et al. (54) provides independent confirmation of breakpoint hotspots at both of the PRS intervals. Of 4 reported microdeletion cases, one had a breakpoint in the PRS1 region and 3 had breakpoints in the PRS2 region.

Sequence analysis of the PRS1 deletion junction fragment of patient UWA123-3 revealed a complex pattern of alternating NF1REP sequences from NF1REP-P1/- M/- P1/- M (Figure 3B). This sequence pattern was not due to polymorphism(s) in this individual as demonstrated by sequence analysis of the nonrecombinant NF1REPs of the transmitting parent. These data are consistent with gene conversion during double strand break repair as described in yeast (51, 55). We previously described similar gene conversion events at PRS2 for two *NF1* microdeletion patients (20). The gene conversion tracts in the NF1REPs are relatively short (≤670 bp), which is consistent with the typical <2 kb conversion tracts in yeast (56, 57) and humans (53, 58-62). Sequence analysis of other *NF1* microdeletion patients showed apparent gene conversion tracts, but DNA of the transmitting parent was unavailable for confirmation. Therefore, the frequency of gene conversion events in our series of *NF1* microdeletions is likely underestimated.

While the majority of *NF1* microdeletion breakpoints occurred in intervals of >500 bp in length, we were surprised that several breakpoints occurred in small intervals, in particular, the PRS2 deletion breakpoint of patient 99-1, which mapped to a 17 bp interval (Figure 3)(20). In this case, sequence analysis of the nonrecombinant NF1REP-P1 and NF1REP-M progenitor alleles of the transmitting parent confirmed the interval length by documenting the specific nucleotides at the polymorphic sites 143,981 and 143,998 as shown in Figure 3C. Several other *NF1* microdeletion breakpoints mapped to intervals <300 bp (Figures 3A, C) but the transmitting parent was not available for confirmation. Studies in model organisms support a relationship between the length of perfect uninterrupted stretches of homology and the frequency of homologous recombination (57, 63-66). Previous data suggest that the length of uninterrupted homology for efficient recombination (minimal efficient processing segment, MEPS) in humans may be 337-456 bp (58, 67). Mismatches flanking the 17 bp recombination interval would limit the length of contiguous perfect homology between NF1REP-P1 and NF1REP-M and most likely reduce the recombination frequency in this small interval. Alternatively, the recombination event in the 99-1 case may have originated within either the 950 bp or 310 bp of contiguous homology that flank the 17 bp breakpoint interval (Figure 3C), propagated through the heterology at one border of the interval, and terminated within the 17 bp segment. It has been shown in mouse L cells that recombination events initiated in large intervals of uninterrupted homology, can propagate and terminate in adjacent regions that have significant mismatches (68). Furthermore, in humans homologous unequal crossovers *in vivo* have been reported in small intervals, e.g., 58 bp at the β-globin cluster (69) and 26 bp between Alu repeats (70).

The development of PCR-based deletion junction assays that detect the majority of microdeletions spanning the entire *NF1* gene will facilitate the identification of additional patients for both molecular and clinical studies. Importantly, we will now be able to identify cohorts of microdeletion patients with the same genotype to determine the spectrum of clinical manifestations associated with the recurrent PRS1 and PRS2 microdeletions. For purposes of phenotype/genotype correlations, cases with breakpoints at PRS1 and PRS2 may have virtually the same genotype. These recombination sites are about 15 kb apart and no genes are known to map in this interval (30, 49).

Currently, genetic diagnostic laboratories offer clinical and prenatal testing for *NF1* microdeletion by fluorescence *in situ* hybridization with an *NF1* probe(s) (http://www.genetests.org)(22, 47). This test may

be augmented or replaced by the PRS1 and PRS2 deletion junction-specific assays described here. This would reduce costs, increase specificity, and still be reasonably (but less) sensitive. One potential problem in using PRS1 and PRS2 deletion-specific assays in a clinical setting would involve the possibility of false positives due to a somatic *NF1* microdeletion that results in low-level mosaicism in white blood cells (20). Our negative test results for 150 normal chromosomes indicate that this is not a common phenomenon in white blood cells or their precursors. Furthermore, application of the PRS1 and PRS2 deletion junction assays to the healthy parents of 12 confirmed *de novo* microdeletion cases described here and elsewhere (20) failed to detect a mosaic parent. An affected child with a *de novo* microdeletion and a mosaic parent has been described (24), but it is not known if the breakpoint occurred at either PRS.

Although greater than 25 single gene or chromosomal disorders are caused by rearrangements mediated by recombination between repeats, referred to as genomic disorders (37, 71) or paralogous recombination disorders (29), breakpoints have been sequenced in relatively few. Evidence of apparent gene conversion in the peri-breakpoint regions of *NF1*, *CMT1A*, *AZFa*, and *IDS* rearrangements (20, 58, 59, 72-74) are consistent with a mechanism of double strand break repair (DSB) as described in yeast (72) and recently reviewed in mammals and other eukaryotic cells (75, 76).

Our identification of PRS1 and PRS2 as preferential breakpoint sites within the surrounding 51 kb NF1REP region of 98% identity implies that there is an additional factor(s), such as a sequence motif, functional domain, or higher order chromosomal feature, that influences the site of the DSB and/or the site of strand exchange, which can be distinct from the DSB site due to migration of a Holliday junction. Among known NF1REP-mediated microdeletions, there is a significant preference for recombination at PRSs versus the remaining NF1REP sequence. A previous study provides an estimate of the percent of *NF1* microdeletions with breakpoints in NF1REP-P1 and -M (30). From a series of 17 independent microdeletions, we determined that 14/17 microdeletions had breakpoints in these NF1REPs. In this study, sequence analyses determined that 13 of these occurred in either PRS1 or PRS2 (20), while only 1 occurred in another region of the NF1REP (30). The preference for recombination in either PRS1 or PRS2 together (10.4 kb region) versus the remainder of the NF1REP paralogs (51 kb) is 63:1 as determined by calculation of the relative risk. This is comparable to the preference for paralogous recombination at the hotspot that mediates the 1.4 Mb duplication and 1.4 Mb deletion that cause Charcot-Marie-Tooth type 1A (CMT1A) and hereditary neuropathy with liability to pressure palsies, respectively (reviewed in (77). Despite 98.7% sequence identity between the two 24 kb CMT1AREP paralogs (78), about 75% (N=24) of crossovers occur in a 1.7 kb hotspot, giving a relative risk of about 50:1 (58, 72). Breakpoint hotspots have also been defined for *AZFb* and *AZFc* deletions in men with spermatogenic failure (38). In contrast to *NF1* and *CMT1A*, these recombination events occurred between massive palindromic sequences, which are known to be sites of preferential double strand breaks *in vitro* (79). A mariner insect transposon element (MITE), located about 1 kb from the CMT1A hotspot, has been proposed as a preferred site of double strand breaks that may initiate recombination (80, 81). A search for known recombinogenic motifs and replication-associated sequences near the 2 kb recombination hotspot (short PRS2 deletion junction assay) for the *NF1* microdeletion identified a nearby χ-like element (20), which is known to stimulate recombination in *E. coli* (reviewed in (82). However, no χ-like element was in proximity of PRS1. Additionally, neither palindromes nor MITEs were found in proximity to either PRS1 or PRS2. However, a complete analysis of PRS1 and PRS2 awaits the full sequence and structure analysis of NF1REP-P1 and NF1REP-M.

MATERIALS AND METHODS

Subjects and cell lines

Peripheral blood samples were obtained after informed consent from *NF1* microdeletion patients and their parents, when available. The presence of an *NF1* microdeletion has been reported previously in most of the patients (15-17, 30, 83). In all cases, the *NF1* microdeletion was known to extend beyond the borders of the gene. Rodent/human somatic cell hybrid lines were constructed for a subset of the patients (30) to facilitate breakpoint mapping and sequence analyses of the deleted chromosome 17 homolog.

Identification of *NF1* breakpoints

Breakpoints were mapped in somatic cell hybrids containing the chromosome 17 homolog that carried the *NF1* microdeletion (8, 30) by direct sequencing using the strategy described previously (30).

Nonrecombinant PRS1 and PRS2 regions from normal individuals were sequenced from NF1REP-P1- and NF1REP-M-specific amplicons and from BACs known to map at either NF1REP. The nonrecombinant PRS1 region of NF1REP-P1 was amplified with primers md4-F and 126Kprox1-R and the nonrecombinant PRS1 region of NF1REP-M was amplified with primers md31M-F and md4-R (Table 1). Both reactions were performed in 50 µl reaction volume using the Expand Long Template PCR system (Roche, Indianapolis) containing 200-300 ng genomic DNA, 5 µl of 10X buffer #1, 3.75 U polymerase, 350 µM each dNTP, and 0.3 µM each primer. After heating to 95°C for 5 min, 35cycles of amplification were performed at 95°C for 30 s, 62°C for 30 s for NF1REP-P1 or 62°C for 30 s for NF1REP-M, and 68°C for 5 min, with a final extension of 68°C for 15 min. Amplicons were column purified (Qiagen, Valencia, CA, cat#28706) and cloned into the TOPO XL PCR cloning kit (Invitrogen, Carlsbad, CA). To confirm presence of insert, clones were amplified with md32-F and md32-R in a 50 µl reaction containing 2 µl of overnight culture of *E. coli* in LB, 5 µl 10X Buffer #II (GeneAmp, Applied Biosystems, Foster City, CA), 200 µM each dNTP, 1.5 mM $MgCl_2$, 0.3 µM each primer, and 2.5 U TaqGold polymerase. After an initial incubation at 95°C for 10 min, 35 cycles of amplification were performed at 95°C for 1 min, 60°C for 1min, and 72°C for 1 min, with a final extension at 72°C for 8 min. Plasmid preparations of clones were column purified (Qiagen, Cat#27106) and sequenced directly using internal primers as described below.

The nonrecombinant PRS2 region of NF1REP-P1 was amplified with primers mddj1b-F and P148prx-R using the Expand Long Template PCR system in a 50 µl reaction volume containing 200-300 ng genomic DNA, 5 µl 10X Buffer #3, 500 µM each dNTP, 0.3 µM each primer, and 3.75 U polymerase. After an initial incubation at 95°C for 5 min, 35 cycles of amplification were performed at 95°C for 30 s, 64°C for 30 s, and 68°C for 5 min, with a final extension of 68°C for 15 min. The nonrecombinant PRS2 region of NF1REP-M was amplified with primers 4400S4-F and P148MED-R using the Expand Long Template PCR system in a 50 µl reaction volume containing the same components as the above reaction for NF1REP-P1 amplification. After an initial incubation at 95°C for 5 min, 35 cycles of amplification were performed at 95°C for 30 sec, 62°C for 30 sec, and 68°C for 5 min, with a final extension of 68°C for 15 min. Amplicons were column purified (Qiagen, Cat#28706) and cloned into the TOPO XL PCR cloning kit (Invitrogen). To confirm presence of insert, clones were amplified with RB4-F and RB4-R in a 50 µl reaction containing 2 µl of overnight culture of *E.coli* in LB, 5 µl 10X Buffer #II (GeneAmp, Applied Biosystems), 200 µM each dNTP, 1.5 mM $MgCl_2$, 0.3 µM each primer, and 2.5 U TaqGold polymerase. After an initial incubation at 95°C for 10 min, 35 cycles of amplification were performed at

95°C for 1 min, 60°C for 1min, and 72°C for 1 min, with a final extension at 72°C for 8 min. Plasmid preparations of clones were purified (Qiagen, Cat#27106) and sequenced directly using internal primers as described below.

All amplifications used a mixture of dNTPs (Roche Cat#1581295) and were performed in a MJ Research Cycler (model PTC-200 or PTC-100). Amplicons were sequenced by cycle sequencing using either the Big-Dye Terminator or the SequiTherm EXCELII Long Read (Epicentre, Madison, WI) kits. Extension products were analyzed an either an ABI 377 sequencer (Applied Biosystems) or an A.L.F. sequencer (Pharmacia, Uppsala, Sweden). Raw nucleotide sequences were analyzed with Sequencher (GeneCodes, Ann Arbor, MI).

PRS1 and PRS2 deletion junction fragment assays

The 3 kb PRS1 deletion junction fragment assay utilized primers md4-F and md30-R and the 7 kb PRS1 assay utilized primers md4-F and md4-R (Table 1). Assay conditions for both were a 50 µl reaction volume using the Expand Long Template PCR System (Roche Molecular Systems, Indianapolis, IN) with 200-300 ng genomic DNA, 0.3 µM each primer, 350 µM each dNTP, 5 µl 10X PCR buffer #1, and 3.75 U polymerase. After heating to 95°C for 5 min, 35 cycles of amplification were performed at 95°C for 30 s, 64°C for 30 s, and 68°C for 5 min, with a final extension of 68°C for 15 min.

The 3.4 kb PRS2 assay utilized primers md21-F and deljun1-R (Table 1) (previously reported as DCF and DTR (20). Here we report an alternate ~3.4 kb PRS2 assay with forward primer mddj1c, which is identical to md21-F except for an additional T at the 5' end. The 7 kb PRS2 assay was performed with primers md21-F and md7-R. The conditions for all three assays were a 50 µl reaction volume using the Expand Long Template PCR System (Roche Molecular Systems, Indianapolis, IN) with 200-300 ng DNA, 0.15 µM each primer, 350 µM each dNTP, 5 µl 10X PCR buffer #1, and 3.75 U polymerase. After heating to 95°C for 5 min, 35 cycles of amplification were performed at 95°C for 30 s, 68°C for 5 s, and 68°C for 5 min, with a final extension of 68°C for 15. In addition, the PRS2 7 kb assay had 250 mM betaine (Sigma, BO300).

All primers designed for amplification of NF1REP sequences were based on homology or heterology, between NF1REP-P1, NF1REP-M, and another NF1REP-E19 at chromosome 19p on BACs 548K16 and 2189E23. All amplifications used a mixture of dNTPs (Roche, Cat#1581295) and were performed in a MJ Research Cycler (South San Francisco, CA, model PTC-200 or PTC-100). DNA must be of high quality to avoid non-specific products in the PRS1 and PRS2 assays. We routinely used the Puregene DNA Isolation Kit (Gentra Systems, Minneapolis, MN, Cat. D-5000) to purify DNA from peripheral blood and immortalized cell lines. DNA that had been extracted previously using phenol/chloroform protocols, purified by other investigators, or stored for an extended period of time was "repurified" using the DNeasy Tissue Kit (Qiagen). PCR products were visualized by ethidium bromide staining after electrophoresis through a 0.8% agarose gel with TAE buffer. Because the longer PRS1 and PRS2 involve amplifying a 7 kb fragment, all samples were pretested to determine if the DNA was of sufficient quality for robust amplification of large fragments. For this purpose, we typically used primers md31m-F and md4-R (Table 1), which amplify a 7 kb segment of NF1REP-M. None of assays described in this manuscript amplified the NF1REP-like sequences on chromosome 19 as determined by lack of amplification of cell line 10449, which is a monochromosomal human chromosome 19 cell line (NIGMS Human Genetic Cell Repository; Coriell Institute, Camden, NJ)(Figure 2B and data not shown).

ACKNOWLEDGEMENTS

This work was supported by grant DAMD17-00-1-0542 awarded to K.S. T.D. was supported by Het Vlaams instituut voor de bevordering van Wetenschappelijk-Technologisch onderzoek in de industrie (IWT). E.L. is part-time clinical researcher of the Fonds voor Wetenschappelijk Onderzoek Vlaanderen (FWO). HB is supported by the Fonds voor Wetenschappelijk Onderzoek Vlaanderen (G.0096.02 to E.L.). M.R.W. contributions were supported by grant DAMD17-98-8609 and the Hayward Foundation. C.L. was supported by grants of the Fondo de Investigaciones Sanitarias de la Seguridad Social (01/1475), the Ministerio de Ciencia y Tecnologia (SAF2002-00573), and the Institut Catala de la Salut.

REFERENCES

1. Friedman, J.M., Butmann, D.H., MacCollin, M. and Riccardi, V.M. (eds.) (1999) *Neurofibromatosis. Phenotype, Natural History, and Pathogenesis.* Third ed. The Johns Hopkins University Press, Baltimore.
2. Korf, B.R. (2001) Diagnosis and management of neurofibromatosis type 1. *Curr Neurol Neurosci Rep,* **1,** 162-7.
3. Lakkis, M.M. and Tennekoon, G.I. (2000) Neurofibromatosis type 1. I. General overview. *J Neurosci Res,* **62,** 755-63.
4. Huson, S.M. and Highes, R.A.C. (eds.) (1994) *The Neurofibromatoses: A pathogenetic and clinical overview.* first ed. Chapman and Hall Medical, London.
5. Huson, S.M. (1994) Neurofibromatosis 1: a clinical and genetic overview. In Huson, S.M. and Hughes, R.A.C. (eds.), *The Neurofibromatoses: a Pathogenetic and Clinical Overview.* First ed. Chapman and Hall Medical, London, pp. 160-203.
6. North, K. (2000) Neurofibromatosis type 1. *Am J Med Genet,* **97,** 119-27.
7. Kayes, L.M., Riccardi, V.M., Burke, W., Bennett, R.L. and Stephens, K. (1992) Large de novo DNA deletion in a patient with sporadic neurofibromatosis 1, mental retardation, and dysmorphism. *J Med Genet,* **29,** 686-90.
8. Kayes, L.M., Burke, W., Riccardi, V.M., Bennett, R., Ehrlich, P., Rubenstein, A. and Stephens, K. (1994) Deletions spanning the neurofibromatosis 1 gene: identification and phenotype of five patients. *Am J Hum Genet,* **54,** 424-36.
9. Brannan, C.I., Perkins, A.S., Vogel, K.S., Ratner, N., Nordlund, M.L., Reid, S.W., Buchberg, A.M., Jenkins, N.A., Parada, L.F. and Copeland, N.G. (1994) Targeted disruption of the neurofibromatosis type-1 gene leads to developmental abnormalities in heart and various neural crest-derived tissues. *Genes Dev,* **8,** 1019-29.
10. Jacks, T., Shih, T.S., Schmitt, E.M., Bronson, R.T., Bernards, A. and Weinberg, R.A. (1994) Tumour predisposition in mice heterozygous for a targeted mutation in Nf1. *Nature Genet,* **7,** 353-61.
11. Zhu, Y., Ghosh, P., Charnay, P., Burns, D.K. and Parada, L.F. (2002) Neurofibromas in NF1: Schwann cell origin and role of tumor environment. *Science,* **296,** 920-2.
12. Cichowski, K. and Jacks, T. (2001) NF1 tumor suppressor gene function: narrowing the GAP. *Cell,* **104,** 593-604.
13. Zhu, Y. and Parada, L.F. (2001) Neurofibromin, a tumor suppressor in the nervous system. *Exp Cell Res,* **264,** 19-28.
14. Gutmann, D.H. (2001) The neurofibromatoses: when less is more. *Hum Mol Genet,* **10,** 747-55.
15. Cnossen, M.H., van der Est, M.N., Breuning, H., van Asperen, C.J., Breslau-Siderius, E.J., van der Ploeg, A.T., de Goede-Bolder, A., van den Ouweland, A.M.W., Halley, D.J.J. and Niermeijer, M.F. (1997) Deletions spanning the neurofibromatosis type 1 gene: implications for genotype-phenotype correlations in neurofibromatosis type 1? *Hum Mutation,* **9,** 458-464.
16. Rasmussen, S.A., Colman, S.D., Ho, V.T., Abernathy, C.R., Arn, P.H., Weiss, L., Schwartz, C., Saul, R.A. and Wallace, M.R. (1998) Constitutional and mosaic large NF1 gene deletions in neurofibromatosis type 1. *J Med Genet,* **35,** 468-71.
17. Upadhyaya, M., Ruggieri, M., Maynard, J., Osborn, M., Hartog, C., Mudd, S., Penttinen, M., Cordeiro, I., Ponder, M., Ponder, B.A. *et al.* (1998) Gross deletions of the neurofibromatosis type 1 (NF1) gene are predominantly of maternal origin and commonly associated with a learning disability, dysmorphic features and developmental delay. *Hum Genet,* **102,** 591-7.

18. Valero, M.C., Pascual Castroviejo, I., Velasco, E., Moreno, F. and Hernandez Chico, C. (1997) Identification of de novo deletions at the NF1 gene: no preferential paternal origin and phenotypic analysis of patients. *Hum Genet,* **99,** 720-6.
19. Messiaen, L.M., Callens, T., Mortier, G., Beysen, D., Vandenbroucke, I., Van Roy, N., Speleman, F. and Paepe, A.D. (2000) Exhaustive mutation analysis of the NF1 gene allows identification of 95% of mutations and reveals a high frequency of unusual splicing defects. *Hum Mutat,* **15,** 541-555.
20. Lopez-Correa, C., Dorschner, M., Brems, H., Lazaro, C., Clementi, M., Upadhyaya, M., Dooijes, D., Moog, U., Kehrer-Sawatzki, H., Rutkowski, J.L. *et al.* (2001) Recombination hotspot in NF1 microdeletion patients. *Hum Mol Genet,* **10,** 1387-1392.
21. Wu, B.L., Schneider, G.H. and Korf, B.R. (1997) Deletion of the entire NF1 gene causing distinct manifestations in a family. *Am J Med Genet,* **69,** 98-101.
22. Leppig, K.A., Viskochil, D., Neil, S., Rubenstein, A., Johnson, V.P., Zhu, X.L., Brothman, A.R. and Stephens, K. (1996) The detection of contiguous gene deletions at the neurofibromatosis 1 locus with fluorescence in situ hybridization. *Cytogenet Cell Genet,* **72,** 95-8.
23. Leppig, K., Kaplan, P., Viskochil, D., Weaver, M., Orterberg, J. and Stephens, K. (1997) Familial neurofibromatosis 1 gene deletions: cosegregation with distinctive facial features and early onset of cutaneous neurofibromas. *Am J Med Genet,* **73,** 197-204.
24. Tonsgard, J.H., Yelavarthi, K.K., Cushner, S., Short, M.P. and Lindgren, V. (1997) Do NF1 gene deletions result in a characteristic phenotype? *Am J Med Genet,* **73,** 80-6.
25. Ars, E., Serra, E., Garcia, J., Kruyer, H., Gaona, A., Lazaro, C. and Estivill, X. (2000) Mutations affecting mRNA splicing are the most common molecular defects in patients with neurofibromatosis type 1. *Hum Mol Genet,* **9,** 237-47.
26. Kluwe, L., Friedrich, R.E. and Mautner, V.F. (1999) Allelic loss of the NF1 gene in NF1-associated plexiform neurofibromas. *Cancer Genet Cytogenet,* **113,** 65-9.
27. Kaufmann, D., Muller, R., Bartelt, B., Wolf, M., Kunzi-Rapp, K., Hanemann, C.O., Fahsold, R., Hein, C., Vogel, W. and Assum, G. (2001) Spinal neurofibromatosis without cafe-au-lait macules in two families with null mutations of the NF1 gene. *Am J Hum Genet,* **69,** 1395-400.
28. Side, L., Taylor, B., Cayouette, M., Conner, E., Thomspon, P., Luce, M. and Shannon, K. (1997) Homozygous inactivation of the NF1 gene in bone marrow cells from children with neurofibromatosis type 1 and malignant myeloid disorders. *N Engl J Med,* **336,** 1713-1720.
29. Stephens, K. (in press) Genetics of neurofibromatosis 1-associated peripheral nerve sheath tumors. *Cancer Invest,* in press.
30. Dorschner, M.O., Sybert, V.P., Weaver, M., Pletcher, B.A. and Stephens, K. (2000) NF1 microdeletion breakpoints are clustered at flanking repetitive sequences. *Hum Mol Genet,* **9,** 35-46.
31. Sawada, S., Florell, S., Purandare, S.M., Ota, M., Stephens, K. and Viskochil, D. (1996) Identification of NF1 mutations in both alleles of a dermal neurofibroma. *Nature Genet,* **14,** 110-2.
32. Serra, E., Puig, S., Otero, D., Gaona, A., Kruyer, H., Ars, E., Estivill, X. and Lazaro, C. (1997) Confirmation of a double-hit model for the NF1 gene in benign neurofibromas. *Am J Hum Genet,* **61,** 512-519.
33. Serra, E., Rosenbaum, T., Winner, U., Aledo, R., Ars, E., Estivill, X., Lenard, H.G. and Lazaro, C. (2000) Schwann cells harbor the somatic NF1 mutation in neurofibromas: evidence of two different Schwann cell subpopulations. *Hum Mol Genet,* **9,** 3055-64.
34. Serra, E., Ars, E., Ravella, A., Sanchez, A., Puig, S., Rosenbaum, T., Estivill, X. and Lazaro, C. (2001) Somatic NF1 mutational spectrum in benign neurofibromas: mRNA splice defects are common among point mutations. *Hum Genet,* **108,** 416-29.

35. Birindelli, S., Perrone, F., Oggionni, M., Lavarino, C., Pasini, B., Vergani, B., Ranzani, G.N., Pierotti, M.A. and Pilotti, S. (2001) Rb and TP53 pathway alterations in sporadic and NF1-related malignant peripheral nerve sheath tumors. *Lab Invest,* **81,** 833-44.
36. Ottini, L., Esposito, D.L., Richetta, A., Carlesimo, M., Palmirotta, R., Ver'i, M.C., Battista, P., Frati, L., Caramia, F.G., Calvieri, S. *et al.* (1995) Alterations of microsatellites in neurofibromas of von Recklinghausen's disease. *Cancer Res,* **55,** 5677-80.
37. Stankiewicz, P. and Lupski, J.R. (2002) Genome architecture, rearrangements and genomic disorders. *Trends Genet,* **18,** 74-82.
38. Repping, S., Skaletsky, H., Lange, J., Silber, S., Van Der Veen, F., Oates, R.D., Page, D.C. and Rozen, S. (2002) Recombination between palindromes P5 and P1 on the human Y chromosome causes massive deletions and spermatogenic failure. *Am J Hum Genet,* **71,** 906-22.
39. Bentivegna, A., Venturin, M., Gervasini, C., Corrado, L., Larizza, L. and Riva, P. (2001) Identification of duplicated genes in 17q11.2 using FISH on stretched chromosomes and DNA fibers. *Hum Genet,* **109,** 48-54.
40. Edelmann, L., Pandita, R.K., Spiteri, E., Funke, B., Goldberg, R., Palanisamy, N., Chaganti, R.S., Magenis, E., Shprintzen, R.J. and Morrow, B.E. (1999) A common molecular basis for rearrangement disorders on chromosome 22q11. *Hum Mol Genet,* **8,** 1157-67.
41. Eichler, E.E. (1998) Masquerading repeats: paralogous pitfalls of the human genome. *Genome Res,* **8,** 758-62.
42. Amos-Landgraf, J.M., Ji, Y., Gottlieb, W., Depinet, T., Wandstrat, A.E., Cassidy, S.B., Driscoll, D.J., Rogan, P.K., Schwartz, S. and Nicholls, R.D. (1999) Chromosome breakage in the Prader-Willi and Angelman syndromes involves recombination between large, transcribed repeats at proximal and distal breakpoints. *Am J Hum Genet,* **65,** 370-86.
43. Pentao, L., Wise, C.A., Chinault, A.C., Patel, P.I. and Lupski, J.R. (1992) Charcot-Marie-Tooth type 1A duplication appears to arise from recombination at repeat sequences flanking the 1.5 Mb monomer unit. *Nat Genet,* **2,** 292-300.
44. Fitch, W.M. (2000) Homology a personal view on some of the problems. *Trends Genet,* **16,** 227-31.
45. Sonnhammer, E.L. and Koonin, E.V. (2002) Orthology, paralogy and proposed classification for paralog subtypes. *Trends Genet,* **18,** 619-20.
46. Korf, B.R. (1999) Plexiform neurofibromas. *Am J Med Genet,* **89,** 31-7.
47. Wu, B.-L., Austin, M., Schneider, G., Boles, R. and Korf, B. (1995) Deletion of the entire NF1 gene detected by FISH: four deletion patients associated with severe manifestations. *Am J Med Genet,* **59,** 528-535.
48. Lopez-Correa, C., Brems, H., Lazaro, C., Marynen, P. and Legius, E. (2000) Unequal Meiotic Crossover: A Frequent Cause of NF1 Microdeletions. *Am J Hum Genet,* **66,** 1969-1974.
49. Jenne, D.E., Tinschert, S., Stegmann, E., Reimann, H., Nurnberg, P., Horn, D., Naumann, I., Buske, A. and Thiel, G. (2000) A common set of at least 11 functional genes is lost in the majority of NF1 patients with gross deletions. *Genomics,* **66,** 93-7.
50. Estivill, X., Cheung, J., Angel Pujana, M., Nakabayashi, K., Scherer, S.W. and Tsui, L.C. (2002) Chromosomal regions containing high-density and ambiguously mapped putative single nucleotide polymorphisms (SNPs) correlate with segmental duplications in the human genome. *Hum Mol Genet,* **11,** 1987-1995.
51. Szostak, J.W., Orr-Weaver, T.L., Rothstein, R.J. and Stahl, F.W. (1983) The double-strand-break repair model for recombination. *Cell,* **33,** 25-35.
52. Guillon, H. and de Massy, B. (2002) An initiation site for meiotic crossing-over and gene conversion in the mouse. *Nat Genet,* **32,** 296-9.

53. Lopes, J., Tardieu, S., Silander, K., Blair, I., Vandenberghe, A., Palau, F., Ruberg, M., Brice, A. and LeGuern, E. (1999) Homologous DNA exchanges in humans can be explained by the yeast double-strand break repair model: a study of 17p11.2 rearrangements associated with CMT1A and HNPP. *Hum Mol Genet,* **8,** 2285-92.
54. Jenne, D.E., Tinschert, S., Reimann, H., Lasinger, W., Thiel, G., Hameister, H. and Kehrer-Sawatzki, H. (2001) Molecular Characterization and Gene Content of Breakpoint Boundaries in Patients with Neurofibromatosis Type 1 with 17q11.2 Microdeletions. *Am J Hum Genet,* **69,** 3.
55. Haber, J.E. (2000) Partners and pathways repairing a double-strand break. *Trends Genet,* **16,** 259-64.
56. Borts, R.H. and Haber, J.E. (1989) Length and distribution of meiotic gene conversion tracts and crossovers in Saccharomyces cerevisiae. *Genetics,* **123,** 69-80.
57. Haber, J.E., Leung, W.Y., Borts, R.H. and Lichten, M. (1991) The frequency of meiotic recombination in yeast is independent of the number and position of homologous donor sequences: implications for chromosome pairing. *Proc Natl Acad Sci U S A,* **88,** 1120-4.
58. Reiter, L.T., Hastings, P.J., Nelis, E., De Jonghe, P., Van Broeckhoven, C. and Lupski, J.R. (1998) Human meiotic recombination products revealed by sequencing a hotspot for homologous strand exchange in multiple HNPP deletion patients. *Am J Hum Genet,* **62,** 1023-1033.
59. Lagerstedt, K., Karsten, S.L., Carlberg, B.M., Kleijer, W.J., Tonnesen, T., Pettersson, U. and Bondeson, M.L. (1997) Double-strand breaks may initiate the inversion mutation causing the Hunter syndrome. *Hum Mol Genet,* **6,** 627-33.
60. Campbell, L., Potter, A., Ignatius, J., Dubowitz, V. and Davies, K. (1997) Genomic variation and gene conversion in spinal muscular atrophy: implications for disease process and clinical phenotype. *Am J Hum Genet,* **61,** 40-50.
61. Collier, S., Tassabehji, M., Sinnott, P. and Strachan, T. (1993) A de novo pathological point mutation at the 21-hydroxylase locus: implications for gene conversion in the human genome [published erratum appears in Nat Genet 1993 May;4(1):101]. *Nat Genet,* **3,** 260-5.
62. Zangenberg, G., Huang, M.-M., Arnheim, N. and Erlich, H. (1995) New HLA-DPB1 alleles generated by interallelic gene conversion detected by analysis of sperm. *Nat Genet,* **10,** 407-414.
63. Shen, P. and Huang, H.V. (1986) Homologous recombination in Escherichia coli: dependence on substrate length and homology. *Genetics,* **112,** 441-57.
64. Singer, B.S., Gold, L., Gauss, P. and Doherty, D.H. (1982) Determination of the amount of homology required for recombination in bacteriophage T4. *Cell,* **31,** 25-33.
65. Liskay, R.M., Letsou, A. and Stachelek, J.L. (1987) Homology requirement for efficient gene conversion between duplicated chromosomal sequences in mammalian cells. *Genetics,* **115,** 161-7.
66. Jinks-Robertson, S., Michelitch, M. and Ramcharan, S. (1993) Substrate length requirements for efficient mitotic recombination in Saccharomyces cerevisiae. *Mol Cell Biol,* **13,** 3937-50.
67. Smith, R.A., Ho, P.J., Clegg, J.B., Kidd, J.R. and Thein, S.L. (1998) Recombination breakpoints in the human beta-globin gene cluster. *Blood,* **92,** 4415-21.
68. Waldman, A.S. and Liskay, R.M. (1988) Dependence of intrachromosomal recombination in mammalian cells on uninterrupted homology. *Mol Cell Biol,* **8,** 5350-7.
69. Metzenberg, A.B., Wurzer, G., Huisman, T.H. and Smithies, O. (1991) Homology requirements for unequal crossing over in humans. *Genetics,* **128,** 143-61.
70. Markert, M.L., Hutton, J.J., Wiginton, D.A., States, J.C. and Kaufman, R.E. (1988) Adenosine deaminase (ADA) deficiency due to deletion of the ADA gene promoter and first exon by homologous recombination between two Alu elements. *J Clin Invest,* **81,** 1323-7.
71. Lupski, J.R. (1998) Genomic disorders: structural features of the genome can lead to DNA rearrangements and human disease traits. *Trends Genet,* **14,** 417-22.

72. Lopes, J., Ravise, N., Vandenberghe, A., Palau, F., Ionasescu, V., Mayer, M., Levy, N., Wood, N., Tachi, N., Bouche, P. *et al.* (1998) Fine mapping of de novo CMT1A and HNPP rearrangements within CMT1A-REPs evidences two distinct sex-dependent mechanisms and candidate sequences involved in recombination. *Hum Mol Genet,* **7,** 141-8.
73. Aradhya, S., Bardaro, T., Galgoczy, P., Yamagata, T., Esposito, T., Patlan, H., Ciccodicola, A., Munnich, A., Kenwrick, S., Platzer, M. *et al.* (2001) Multiple pathogenic and benign genomic rearrangements occur at a 35 kb duplication involving the NEMO and LAGE2 genes. *Hum Mol Genet,* **10,** 2557-67.
74. Sun, C., Skaletsky, H., Rozen, S., Gromoll, J., Nieschlag, E., Oates, R. and Page, D.C. (2000) Deletion of azoospermia factor a (AZFa) region of human Y chromosome caused by recombination between HERV15 proviruses. *Hum Mol Genet,* **9,** 2291-6.
75. Johnson, R.D. and Jasin, M. (2001) Double-strand-break-induced homologous recombination in mammalian cells. *Biochem Soc Trans,* **29,** 196-201.
76. Haber, J.E. (2000) Partners and pathwaysrepairing a double-strand break. *Trends Genet,* **16,** 259-64.
77. Boerkoel, C.F., Inoue, K., Reiter, L.T., Warner, L.E. and Lupski, J.R. (1999) Molecular mechanisms for CMT1A duplication and HNPP deletion. *Ann N Y Acad Sci,* **883,** 22-35.
78. Reiter, L.T., Murakami, T., Koeuth, T., Gibbs, R.A. and Lupski, J.R. (1997) The human COX10 gene is disrupted during homologous recombination between the 24 kb proximal and distal CMT1A-REPs. *Hum Mol Genet,* **6,** 1595-603.
79. Zhou, Z.H., Akgun, E. and Jasin, M. (2001) Repeat expansion by homologous recombination in the mouse germ line at palindromic sequences. *Proc Natl Acad Sci U S A,* **98,** 8326-33.
80. Kiyosawa, H. and Chance, P.F. (1996) Primate origin of the CMT1A-REP repeat and analysis of a putative transposon-associated recombinational hotspot. *Hum Mol Genet,* **5,** 745-53.
81. Reiter, L.T., Murakami, T., Koeuth, T., Pentao, L., Muzny, D.M., Gibbs, R.A. and Lupski, J.R. (1996) A recombination hotspot responsible for two inherited peripheral neuropathies is located near a *mariner* transposon-like element. *Nature Genet,* **12,** 288-297.
82. Kowalczykowski, S.C. (2000) Initiation of genetic recombination and recombination-dependent replication. *Trends Biochem Sci,* **25,** 156-65.
83. Lopez Correa, C., Brems, H., Lazaro, C., Estivill, X., Clementi, M., Mason, S., Rutkowski, J.L., Marynen, P. and Legius, E. (1999) Molecular studies in 20 submicroscopic neurofibromatosis type 1 gene deletions. *Hum Mutat,* **14,** 387-93.

Table 1. Primers for analysis of NF1REP paralogous recombination sites.

Segment location	NF1REP-specificity	Amplicon (kb)	Primer Name	Sequence (5' →3')
PRS1	NF1REP-P1	4.5	md4-F 126Kprox1-R	ATCCTGTAGCCCAGTTCTCCTC AACACAAGTTGGGAGCCTTCTG
PRS1	NF1REP-M	7	md31m-F md4-R	CCCAGTTCCCTAAACCTCCAG ACAGTCTCGCTCTGATGCCCGT
internal PRS1	NF1REP-P1 and NF1REP-M	0.2	md32-F md32-R	AGGCTAGAGCAGAAGCTAACATCA GGTTTCAGTGAGCTGAGATCGTG
PRS2	NF1REP-P1	7.5	Mddj1b-F P148prx-R	AACCTCCCAGGCTCCCGAATA TGAACAGGCCCATTTCTTGTC
PRS2	NF1REP-M	6	4400s4-F P148med-R	ACTGTGCCCAGCATCTTGGT TTCTGATACTGAACTGGCTTAGG
internal PRS2	NF1REP-P1 and NF1REP-M	0.15	RB4-F RB4-R	CGGAGCGATGACTCCATCAC TCCTTGCCTGGAAACCTTGC
PRS1 deletion junction	Recombinant NF1REP-P1 and –M	3	md4-F md30-R	See above CAGTGAACCGAGATTGTACTACCA
		7	md4-F md4-R	See above. See above
PRS2 deletion junction	Recombinant NF1REP-P1 and –M	3.4	md21-F deljun1-R[1]	CAACCTCCCAGGCTCCCGAA AGCCCCGAGGGAATGAAAAGC
		3.4	mddjlc-F deljun1-R[1]	TCAACCTCCCAGGCTCCCGAA See above.
		7	md21-F md7-R	See above GGCAGGGTTAGGAGCTCTGGA A

[1]Reported previously as primer DTR (Lopez-Correa, 2001 #939).

Table 2. NF1 microdeletion cases detected by PRS deletion junction assays.

Deletion Junction	Assay		
	Shorter amplicon (3-3.4 kb)	Extended amplicon (7 kb)	Junction fragment sequenced (# cases)
PRS1	13	14	14
PRS2	33	40	29
Total	46/78	54/78	

FIGURE LEGENDS

Figure 1. Schematic of the *NF1* gene region at chromosome segment 17q11.2. The 350 kb *NF1* gene is shown along with the 51 kb flanking paralogs denoted as NF1REP-P1 (previously known as NF1REP-P; (30) and NF1REP-M, which are in direct orientation. Paralogous recombination between these NF1REP elements results in a recurrent 1.5 Mb deletion of the entire *NF1* locus (30). The locations of the paralogous recombination sites, PRS1 and PRS2, are shown. The stippled portion of PRS2 designates the previously reported 2 kb recombination hotspot (20), while the hatchmarks designate the extended portion of the site reported here. The basepair coordinates are relative to BAC 271K11, which contains NF1REP-P1 (30).

Figure 2. *NF1* deletion junction-specific assays for PRS1 and PRS2. A. A schematic of the recombinant NF1REP after paralogous recombination in PRS1 has deleted the intervening 1.5 Mb and the *NF1* gene. The relative positions of primers in NF1REP-P1 and –M are shown. The left side of the gel shows the 3 kb amplicon generated by the primers md4-F and md30-R for patients UWA119-1, UWA123-3 and UWA240-1. The right side of the gel shows the 7 kb amplicon generated by primers md4-F and md4-R. This amplifies a larger segment that can detect deletion breakpoints of additional patients such as UWA241-1. No amplicons are generated in either assay for cases UWA128-3 and UWA156-1, which have breakpoints at PRS2. B. The gel documents a PRS1 assay result that can be mistakenly interpreted as positive. True positives for PRS1 junction assays of genomic DNA are shown for patients UWA119-1 and the somatic cell hybrid carrying the deleted chromosome 17 of patient UWA119-1 and UWA123-3-H#97. Genomic DNA sample UWA183-1, which should be negative in this assay since it has a breakpoint at PRS2, gives a smear of products and lacks the intense 7 kb junction fragment. Confirmation that this result is a true negative is given by lack of 7 kb junction fragment from genomic DNA of somatic cell hybrid line (UWA183-1-H#15) carrying the deleted chromosome 17 of patient UWA183-1. CH19 is genomic DNA from monochromosomal 19 somatic cell hybrid line, which confirms the NF1REP-E19 does not interfere with the assay. C. A schematic of the recombinant NF1REP after paralogous recombination at PRS2 deleted the intervening 1.5 Mb with the relative positions of primers in NF1REP-P1 and –M shown. The left side of the gel shows the 3.4 kb amplicon generated by primers DCF and deljun1-R (also known as DTR in reference (20) for patients UWA128-3 and UWA156-1. Since our earlier report (20), we have replaced primer DCF with md21-F, which has one additional base at the 5' end, which makes the reaction more reliable and robust (data not shown). The right side of the gel shows the 7.5 kb amplicon generated by primers md21-F and md7-R. This assay detects deletion breakpoints of additional patients, such as UWA172-1 and UWA176. No amplicons are generated in either assay for UWA119-1 and UWA123-3, who have breakpoints at PRS1. In all gels, NEG indicates the negative control without DNA template and MW denotes the 1 kb ladder of molecular weight standards (Promega).

Figure 3. *NF1* microdeletion breakpoints at PRS1 and PRS2. The top of each figure shows selected PSV of NF1REP-P1 and NF1REP-M, with the nucleotide coordinates according to the BAC 271K11. All PSV between 121,991 and 123,963 are shown based on the sequences of the BACs and 7 NF1REP-P1 and NF1REP-M alleles of control individuals. PSVs for the region 123,963 to 126,402 are based on BAC sequences only. Coordinates designated with the "p" suffix indicate SNPs, however, not all SNPs are not shown. The black bars denote the interval where paralogous recombination occurred between NF1REP-P1 and NF1REP-M to generate the microdeletion breakpoint. Parental origin is M, maternal; P, paternal; F, familial; U, unknown. A. *NF1* microdeletion breakpoints are shown for 14 patients at PRS1. The dashed line indicates the 551 bp hotspot where 64% (9/14) of breakpoints in PRS1 map. The recombination interval for case UWA123-3 is detailed below. B. Details of PSVs in the breakpoint

region of patient UWA123-3 showing a pattern consistent with gene conversion. The breakpoint interval of this patient was defined by sequencing the paternal nonrecombinant NF1REP-P1 and NF1REP-M that served as recombination substrates during generation of the patient's *de novo* deletion. Three SNPs (coordinates with "p" suffix) were informative in defining the interval and demonstrating gene conversion. C. *NF1* microdeletion breakpoints are shown for 29 patients at PRS2. *Indicates previously reported breakpoint data for 25 patients (20), which were modified in this study by identification of polymorphisms from normal alleles (see Materials and Methods). The precise breakpoint intervals and apparent gene conversion events in cases 984412 and 973287 (among the 14 patient group) have been detailed previously (20). All PSV between 140,852 and 144,507 are shown; however, there are an additional 36 PSV between 144,507 and 147,167 that are not indicated. The dashed line indicates the 2,292 bp hotspot interval where 86% of breakpoints in PRS1 map.

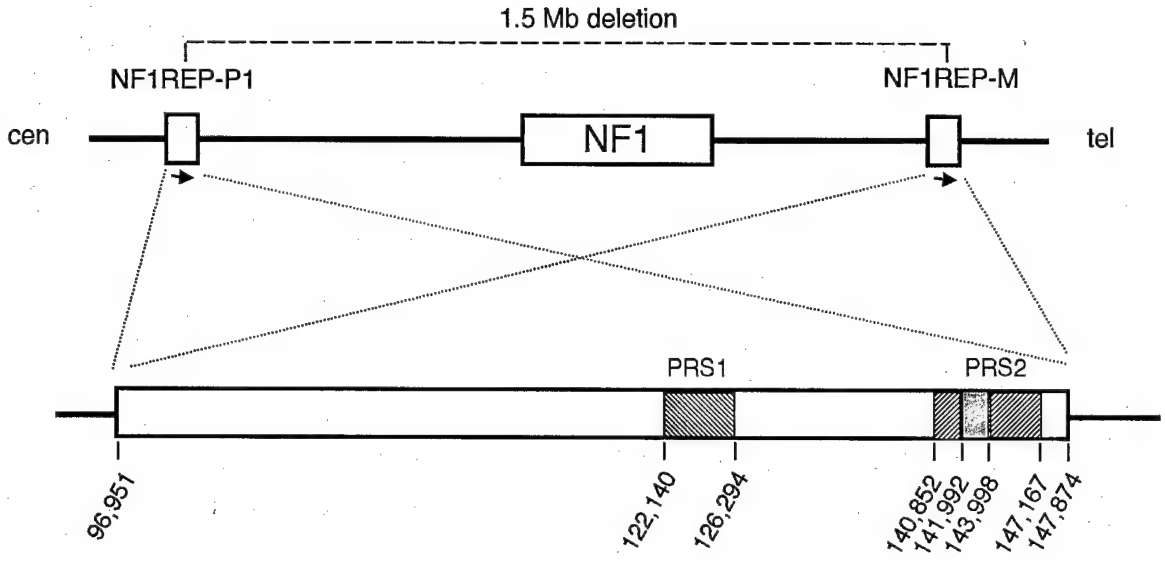
1.5 Mb deletion
NF1REP-P1
NF1REP-M
cen
NF1
tel
PRS1
PRS2
96,951
122,140
126,294
140,852
141,992
143,998
147,167
147,874

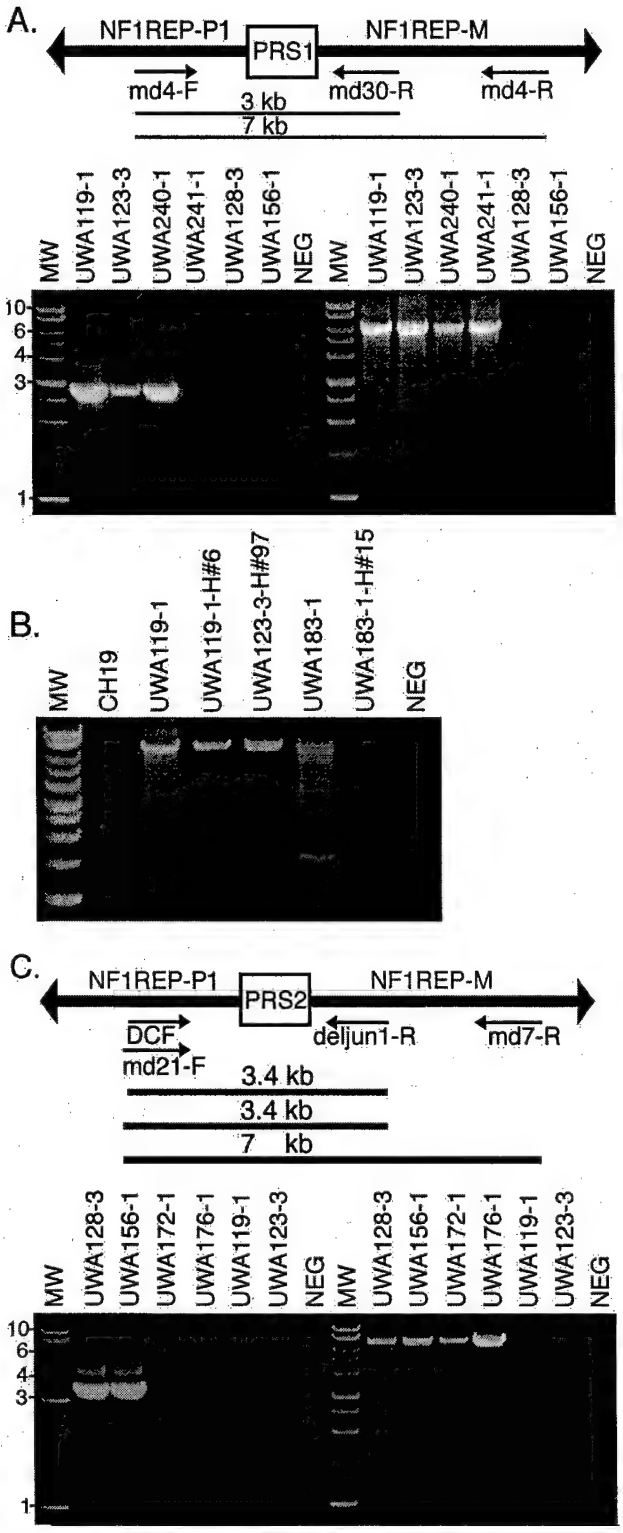
A.
NF1REP-P1
PRS1
NF1REP-M
md4-F
md30-R
md4-R
3 kb
7 kb
MW
UWA119-1
UWA123-3
UWA240-1
UWA241-1
UWA128-3
UWA156-1
NEG
MW
UWA119-1
UWA123-3
UWA240-1
UWA241-1
UWA128-3
UWA156-1
NEG
10
6
4
3
1
B.
MW
CH19
UWA119-1
UWA119-1-H#6
UWA123-3-H#97
UWA183-1
UWA183-1-H#15
NEG
C.
NF1REP-P1
PRS2
NF1REP-M
DCF
md21-F
deljun1-R
md7-R
3.4 kb
3.4 kb
7 kb
MW
UWA128-3
UWA156-1
UWA172-1
UWA176-1
UWA119-1
UWA123-3
NEG
MW
UWA128-3
UWA156-1
UWA172-1
UWA176-1
UWA119-1
UWA123-3
NEG
10
6
4
3
1

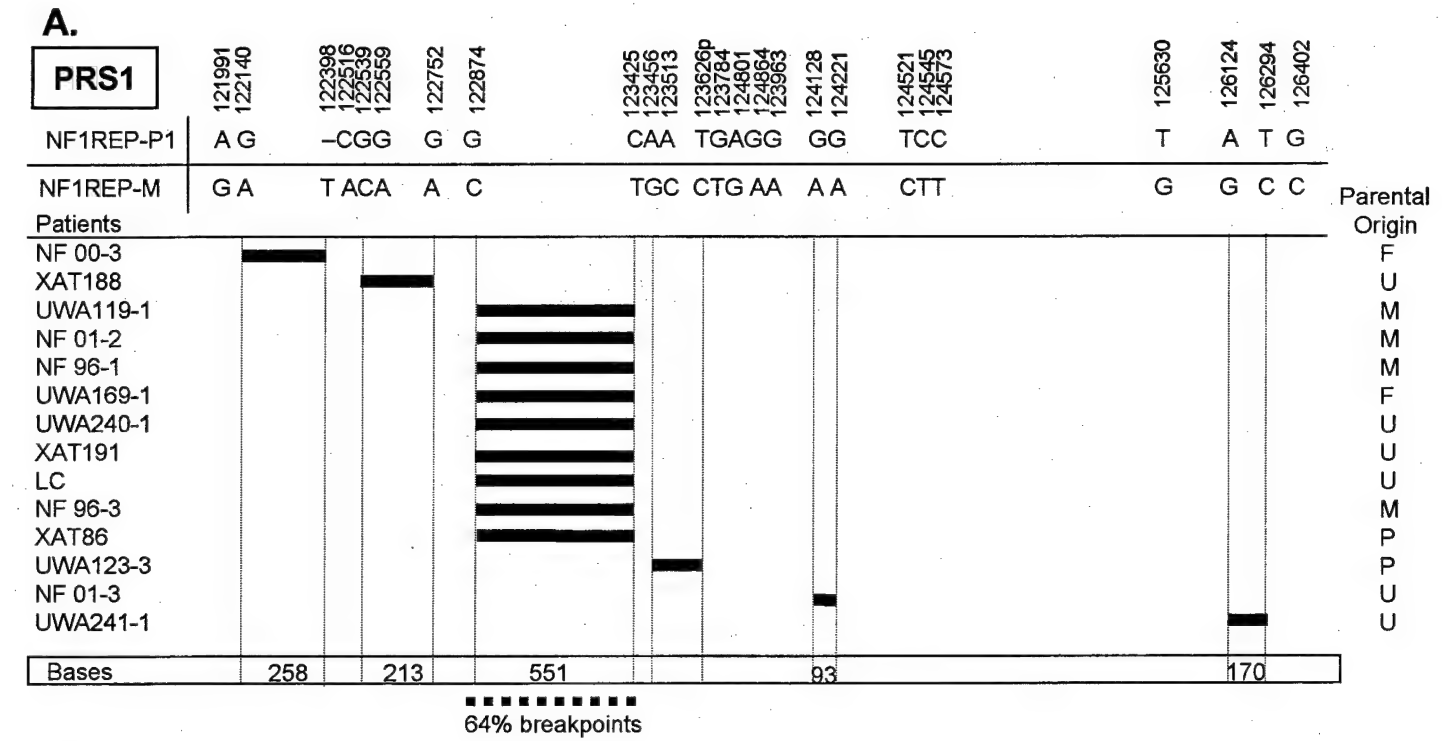
A.
PRS1
121991
122140
122398
122516
122539
122559
122752
122874
123425
123456
123513
123626p
123784
124801
124864
123963
124128
124221
124521
124545
124573
125630
126124
126294
126402
NF1REP-P1
A G
–CGG
G G
CAA
TGAGG
GG
TCC
T
A T G
NF1REP-M
G A
T ACA
A C
TGC
CTG AA
A A
CTT
G
G C C
Parental Origin
Patients
NF 00-3
XAT188
UWA119-1
NF 01-2
NF 96-1
UWA169-1
UWA240-1
XAT191
LC
NF 96-3
XAT86
UWA123-3
NF 01-3
UWA241-1
F
U
M
M
M
F
U
U
U
M
P
P
U
U
Bases
258
213
551
93
170
64% breakpoints

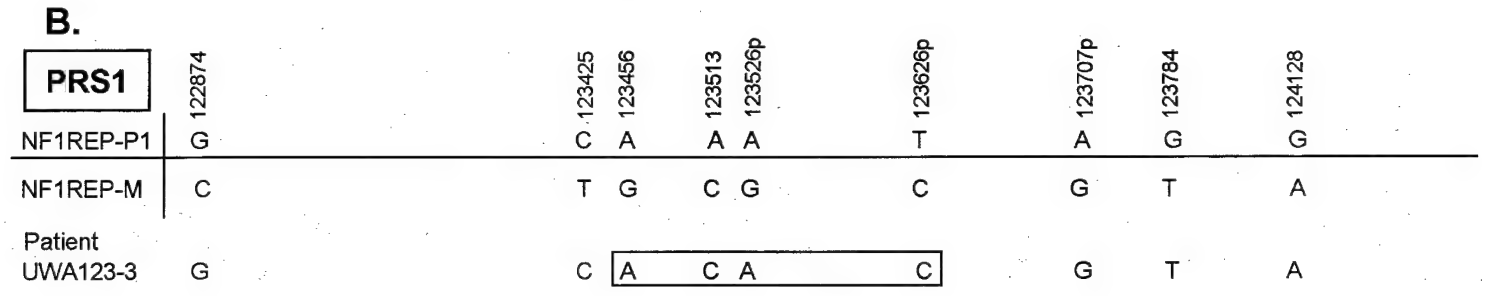
B.
PRS1
122874
123425
123456
123513
123526p
123626p
123707p
123784
124128
NF1REP-P1
G
C
A
A
A
T
A
G
G
NF1REP-M
C
T
G
C
G
C
G
T
A
Patient
UWA123-3
G
C
A
C
A
C
G
T
A

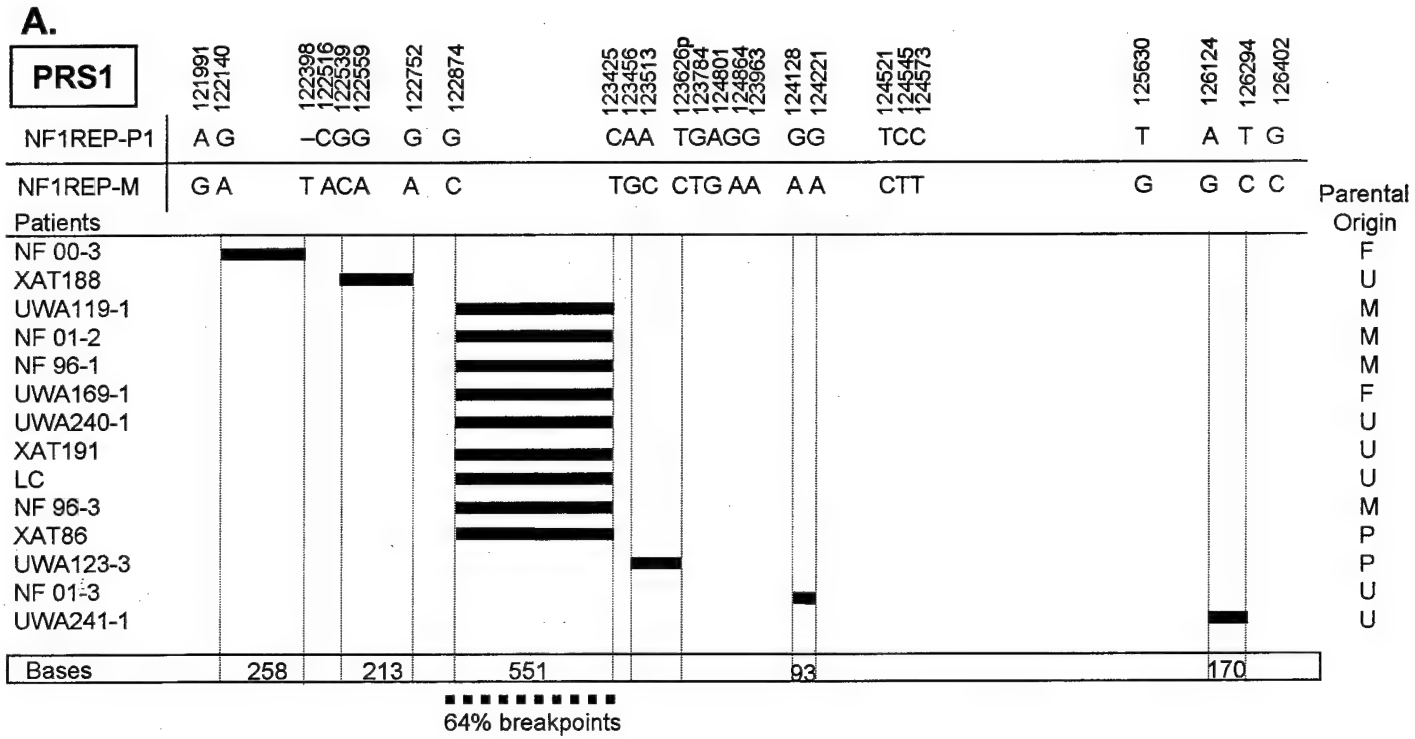
A.
PRS1
121991 122140
122398 122516 122539 122559
122752
122874
123425 123456 123513
123626p 123784 124801 124864 123963
124128 124221
124521 124545 124573
125630
126124
126294
126402
NF1REP-P1 A G –CGG G G CAA TGAGG GG TCC T A T G
NF1REP-M G A T ACA A C TGC CTG AA A A CTT G G C C
Parental Origin
Patients
NF 00-3 F
XAT188 U
UWA119-1 M
NF 01-2 M
NF 96-1 M
UWA169-1 F
UWA240-1 U
XAT191 U
LC U
NF 96-3 M
XAT86 P
UWA123-3 P
NF 01-3 U
UWA241-1 U
Bases 258 213 551 93 170
64% breakpoints
B.
PRS1
122874
123425
123456
123513
123526p
123626p
123707p
123784
124128
NF1REP-P1 .G C A A A T A G G
NF1REP-M C T G C G C G T A
Patient
UWA123-3 G C A C A C G T A

C.

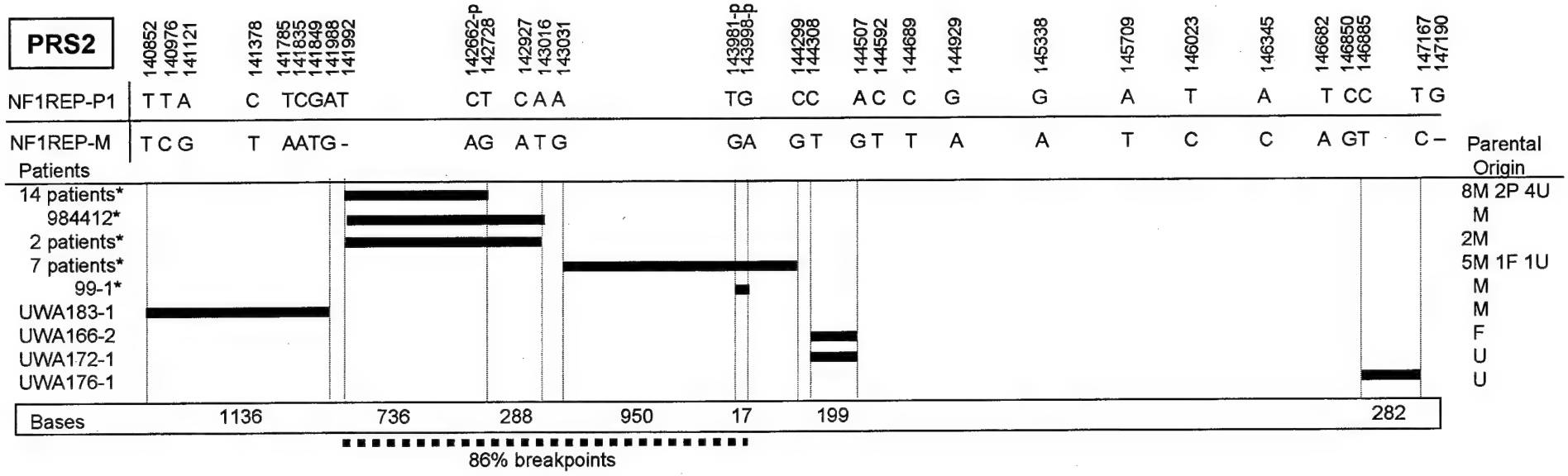
PRS2
140852 140976 141121
141378
141785 141835 141849 141988 141992
142662-p 142728
142927 143016 143031
143981-p 143998-p
144299 144308
144507 144592
144689
144929
145338
145709
146023
146345
146682 146850 146885
147167 147190
NF1REP-P1 T T A C TCGAT CT C A A TG CC A C C G G A T A T CC T G
NF1REP-M T C G T AATG - AG A T G GA G T G T T A A T C C A GT C –
Parental Origin
Patients
14 patients* 8M 2P 4U
984412* M
2 patients* 2M
7 patients* 5M 1F 1U
99-1* M
UWA183-1 M
UWA166-2 F
UWA172-1 U
UWA176-1 U
Bases 1136 736 288 950 17 199 282
86% breakpoints

Genomic context of paralogous recombination substrates mediating the recurrent *NF1* region microdeletion

Stephen H. Forbes[1], Michael O. Dorschner[1,†], Rosalynda Le[1], Karen Stephens[1,2]

Departments of Medicine[1] and Laboratory Medicine[2], University of Washington, Seattle, WA 98195

[†]Present address: Rexagen Corporation, Seattle, WA 98103

Corresponding author:
Karen Stephens, PhD
University of Washington
1959 NE Pacific St., Room I-204
Seattle, WA 98195-7720
millie@u.washington.edu; FAX: (206) 685-4829; Phone 206-543-8285.

Running title: Genomic context of paralogous recombination sites

Key words: paralogs, paralogous recombination, neurofibromatosis 1, *NF1*, microdeletion

ABSTRACT

Recombination between paralogs that flank the *NF1* gene at 17q11.2 typically results in a 1.5 Mb microdeletion that includes *NF1* and at least 14 contiguous genes. The principal sequences responsible are two 51-kb blocks with 97.5% sequence identity (NF1REP-P1-51 and NF1REP-M-51). Here we show that these paralogs belong to a complex group of paralogs from different sequence families with three components on 17q and another at 19p13. Multiple breakpoint sequencing reveals two paralogous recombination hotspots within the 51-kb blocks. We seek to explain the location of the hotspots based on sequence motifs, quality of alignment match, and nucleotide sequence identity. Hotspot locations with respect to relatively large paralogous alignment gaps suggest that the gaps may a primary factor localizing pairing and exchange. Gene conversion tests reveal a 700 bp gene conversion tract at the predominant paralogous recombination hotspot. Thus, high sequence identity at a hotspot may be a result, as well as a potential cause, of propensity to pair at a particular site. Whether alignment gaps are a key breakpoint localization factor may be eventually assessed by discovery and comparison of more systems that—like the NF1REPs—show relatively high levels of alignment mismatch between paralogs.

INTRODUCTION

In the past five years, it has become apparent that recombination between pairs of non-allelic, high-identity, low-copy number DNA repeat sequences is an important mechanism for chromosomal rearrangements that cause human genetic disease (reviewed by Emanuel and Shaikh 2001; Stankiewicz and Lupski 2002a). These repeated DNA elements have been referred to as REP (repeats; Lupski et al. 1991), LCR (low copy repeats; Shaikh et al. 2000), duplicons, or paralogs. Recombination between misaligned paralogs (unequal crossing over) on sister or non-sister chromatids, between paralogs on the same chromatid (loop out-excision), or between paralogs on different chromosomes can result in deletion, duplication, inversion, or translocation (reviewed by Inoue and Lupski 2002). Recombination between paralogs has been referred to as "nonallelic homologous recombination" (Stankiewicz and Lupski 2002b), "ectopic recombination," (Kuroda-Kawaguchi et al. 2001) or "paralogous recombination" (Stephens 2003) to distinguish it from classical, allelic homologous recombination. Investigation into the molecular basis of paralogous recombination diseases is in its infancy, as few breakpoints have been mapped at the sequence level and few REPs have undergone sequence and structural analyses.

Paralogous recombination is the dominant mechanism for submicroscopic contiguous gene deletions that encompass the *NF1* gene at chromosome 17q11.2. The consequent haploinsufficiency for the *NF1* protein product causes neurofibromatosis 1 (NF1), an autosomal dominant multi-systemic disorder that affects ~1/3500 individuals worldwide. NF1 is primarily characterized by multiple benign nerve sheath tumors or neurofibromas (reviewed by Korf 2002). An estimated 5-10% of cases are due to submicroscopic *NF1* microdeletion (Cnossen et al. 1997; Rasmussen et al. 1998), while most remaining cases result from premature translation

termination or splicing defects (Messiaen et al. 2000). *NF1* microdeletion carriers are of great interest because they are predisposed to developing early-onset and excessive numbers of neurofibromas (Kayes et al. 1994; Leppig et al. 1997; Dorschner et al. 2000) and are at increased risk of developing malignant peripheral nerve sheath tumors (De Raedt et al. 2003; Kluwe et al. 2003). Whether they are at increased risk for other manifestations, related or unrelated to NF1, awaits a comprehensive clinical evaluation of a cohort of *NF1* microdeletion subjects.

STS mapping of 17 independent *NF1* microdeletions revealed that 82% had proximal and distal breakpoints clustered in two low copy repeat elements, designated NF1REPs, that flanked the *NF1* gene (Dorschner et al. 2000) (Figure 1). The direct orientation of the NF1REPs suggests a mechanism whereby NF1REP-P1 and NF1REP-M misalign during meiosis with subsequent unequal crossing over between chromatids, or loop-out excision between the repeats on a single chromatid, resulting in a recurrent 1.5 Mb *NF1* microdeletion (Dorschner et al. 2000) (Figure 1). About 80% of *de novo NF1* microdeletions occur on maternally-derived chromosomes (Upadhyaya et al. 1998; Lopez-Correa et al. 2001; Dorschner et al. submitted). This is consistent with haplotype analyses of healthy ancestors of *de novo NF1* microdeletion subjects that suggested paralogous recombination occurred during maternal meiosis II (Lopez-Correa et al. 2000).

The *NF1* microdeletion breakpoints were mapped to intervals defined by paralogous sequence variants (PSV; Estivill et al. 2002) that were specific to an individual NF1REP paralog. The pattern of PSVs from amplicons of the deleted chromosomes 17 were expected to match that of either NF1REP-P1 or NF1REP-M, or transition from NF1REP-P1 to NF1REP-M if the amplicon contained the breakpoint of the recombinant NF1REP. This procedure identified a 2 kb recombination hotspot that accounted for 46% (N=54) of cases with *NF1* contiguous gene

deletions (Lopez-Correa et al. 1999). Recent breakpoint mapping of additional cases has extended this breakpoint cluster region, herein designated PRS2 (paralogous recombination site 2) to a 4,155 bp interval and identified an additional, independent breakpoint cluster region (designated PRS1) of 6,323 bp.

Together, breakpoints at PRS1 and PRS2 accounted for 69% of *NF1* whole gene deletions (Lopez-Correa et al. 2001; Dorschner et al. submitted). In all cases, the sequence of the breakpoint intervals was consistent with a perfect homologous exchange; there was no evidence of small deletions commonly associated with non-homologous end joining (Valerie and Povirk 2003). Three of these cases (one at PRS1 and two at PRS2) showed evidence of gene conversion, with alternate NF1REP-P1 and NF1REP-M PSVs in the exchange region (Lopez-Correa et al. 2001; Dorschner et al. submitted). Apparent gene conversion tracts are consistent with a mechanism similar to the double strand break (DSB) repair model in yeast (Haber 2000; Johnson and Jasin 2001). Under this model, the breakpoint hotspots at PRS1 and PRS2 imply the presence of a sequence motif, functional domain, or higher order chromosomal feature that predisposes to DSB. The primary sequences of the short PRS1 and PRS2 recombination substrates revealed no apparent basis for regional DSBs (Dorschner et al. 2000; Lopez-Correa et al. 2001). However, knowledge about number, orientation, and structure of NF1REPs in the genome in which PRS1 and PRS2 were embedded was lacking. Here we detail the primary structure of four NF1REPs, including the larger sequence context of the PRS1 and PRS2. We search for sequence features at breakpoint clusters that may explain their location and discuss evidence for gene conversion between the NF1REP paralogs.

RESULTS

NF1REPs Are Complex Assemblies of Paralogs from Different Sequence Families

The paralogs NF1REP-P1, NF1REP-P2, and NF1REP-M flanking the NF1 gene at 17q11.2 (Figure 1A) are represented by finished BACs in the April 2003 assembly of the public Human Genome Project (National Center for Biotechnology Information (NCBI) build 32). This is the first NCBI assembly in which NF1REP ordering and orientation are consistent with all evidence previously reported, including public Human Genome Project BAC sequences, STS mapping, sequencing of breakpoint regions in *NF1 de novo* microdeletion patients and normal controls, and *NF1* microdeletion-specific assays (Dorschner et al. 2000; Jenne et al. 2001; Lopez-Correa et al. 2001; Dorschner et al. submitted). This public assembly and the BAC contig of Jenne et al. (Jenne et al. 2003) are based largely on different BACs, but both nevertheless show a finished tiling path across 1.5 Mb from NF1REP-P1 through NFREP-M.

Sequence and structural analysis showed that the NF1REP-P1, NF1REP-P2, and NF1REP-M paralogs vary in length and composition, but are generally comprised of gene and gene-derived fragments and larger sequence blocks apparently lacking genes (Fig. 1B). NF1REP-P1 is 131 kb in length, is contained largely on BAC RP11-271K11 (nt 75,477-199,182), and extends 6,944 bp into the overlapping BAC CTD-2349P21. NF1REP-M is 75 kb in length and is fully contained in BAC RP11-640N20 (nt 102147-177525). NF1REP-P2 is 43 kb and fully contained in BAC RP11-229K15 (nt 43619-86245).

The apparently functional copy of the gene *KIAA0563rel* is contained in NF1REP-M (Jenne et al. 2003). It is supported by a full-length mRNA (*KIAA0563-related gene*; Genbank NM_052888) and a substantial Unigene cluster (Hs.367593). This gene is also known by an STS marker (WI-12393) contained within it (Jenne et al. 2000; Jenne et al. 2001). Fragments

derived from this gene are present in NF1REP-P1, the distal region of NF1REP-M, and in NF1REP-P2 (green blocks, Figure 1B). NF1REP-M carries the 12 exons and introns of the functional *KIAA0563rel*, while NF1REP-P1 has an inverted segment containing intron 7, exon 8, and part of intron 8 followed by exons and introns 9-12. Additional *KIAA0563rel* fragments are scattered throughout distal 17q and on several other chromosomes. A 33,692 bp paralogous sequence block (BAC RP11-271K11; nt 112,506-146,198) is shared by NF1REP-P1 and NF1REP-M and apparently lacks genes or pseudogene sequences (Figure 1B, dark blue)

The largest sequence blocks shared by NF1REP-P1 and NF1REP-M are 51 kb in length and show 97.5 percent sequence identity (analysis of manually aligned sequences using the DnaSP program; Rozas and Rozas 1999). Here we refer to these blocks (represented by BAC RP11-271K11; nt 96,901-147,876) as NF1REP-P1-51 and NF1REP-M-51, or collectively as NF1REP-51. These repeats are of particular interest because they contain PRS1 and PRS2, the sites where an estimated 69% *NF1* microdeletion breakpoints occur (Figure 1B, red blocks)(Lopez-Correa et al. 2001; Dorschner et al. submitted).

Two additional pseudogenes comprise the flanking regions of NF1REP-P1. *SMURF2* pseudogene fragments (Figure 1B, yellow blocks) are present on NF1REP-P1 (RP11-271K11; nt 75,477-91,072) and on NF1REP-P2 (RP11-229K15; nt 43,619-64,829). The functional copy of the *SMURF2* gene encodes E3 ubiquitin ligase (NM_022739), located at 17q24 and not associated with any other NF1REP-related elements. Distal to the NF1REP-P1-51 is a segment with no apparent genes (RP11-271K11, nt 147,872-184,526), and a *LEC2* pseudogene fragment beginning at RP11-271K11 nt 184,527 and extending into CTD-2349P21 (Figure 1C, light blue and purple, respectively). Parts of NF1REP-P1-51 and these distal blocks have paralogs at chromosome 19p13, which we designated NF1REP-E19 (Figure 1C). This REP contains the

functional *LEC2* gene and resides on the three BACs indicated. It spans 151 kb, including 33 kb of dispersed blocks matching NF1REP-P1and -M and containing the PRS1 and PRS2 breakpoint clusters (Fig. 1B; dark blue blocks). NF1REP-E19 matches both NF1REP-P1and -M at only 94-95% sequence identity. It contains no sequences matching *KIAA0563rel*, and *KIAA0563rel* copies are not associated with any *SMURF2* or *LEC2* copies elsewhere.

Sequence Composition Of Breakpoint Clusters and Hotspots

The positions of breakpoint intervals with respect to sequence features of the NF1REPs are detailed in Figure 2. The breakpoint intervals that defined PRS1 and PRS2 were reported previously (Lopez-Correa et al. 2001; Dorschner et al. submitted). Within each PRS a majority of breakpoints is concentrated in a smaller hotspot. Within PRS1 an interval of 551 bp accounts for 60% of the breakpoints (9/15), and within PRS2 an interval of 2292 bp accounts for 93% of the breakpoints (27/29)(Fig. 2).

Here we report an additional, unique *NF1* microdeletion case with breakpoints mapping within the NF1REP-51 repeats, but outside of either PRS. The breakpoint interval of patient UWA160-1 mapped to the interval located about 20 kb proximal to PRS1 (nt 102,102-102,186 in BAC RP11-271K11; Figure 2). Sequencing the breakpoint region of the deleted chromosome 17, which had been segregated into a human-rodent somatic cell hybrid line, showed a single transition from an NF1REP-P1-specific PSV to an NF1REP-M-specific PSV. This case demonstrates that paralogous recombination can occur between the NF1REP-51 repeats at sites other than PRS1 and PRS2, albeit at a significantly reduced frequency.

If recombination hotspots are due to obligate local sequence features, we might expect the PRS clusters to show some similarity of sequence composition, but sequence and structural

analysis of PRS1 and PRS2 revealed no commonalities. BLAST comparison of PRS1 and PRS2 showed no significant sequence identity, with the exception of Alu elements, LINES, SINES, and other high copy repeats, which typically shared <80% identity and lengths of <500 bp. Furthermore, PRS1 and PRS2 showed entirely different patterns of high-copy repeats and G+C content (Fig. 2). PRS1 has high-copy repeats spread throughout and contains 67% repeats overall, while PRS2 is only 44% repeats and the PRS2 hotspot is devoid of high-copy repeats. The entire NF1REP-51 repeat is composed of 55% high-copy repeats, and the entire BAC 271K11 is 51% high-copy repeats. Thus, one PRS region has more repeats than average for the region, and the other has fewer. The PRS1 and PRS2 clusters both have higher-than-average G+C for their contexts (53.0% and 55.7% respectively, versus 48.4% for the entire 51 kb high-identity repeat). However, the PRS2 hotspot is especially G+C-rich (63.7%), while the PRS1 hotspot is not (52.7%). These sequence composition values are calculated for the NF1REP-P1-51, but due to the 97.5% identity, these values did not differ markedly from those for the paralogous NF1REP-M-51 repeat.

NF1REP Sequence Alignment, Sequence Identity, and Breakpoint Localizations

The NF1REP-51 paralogs that harbor the breakpoints in 69% of the *NF1* whole gene deletions differ more than do typical, allelic recombination substrates. Mean sequence similarity is 97.5% considering both indels and PSVs. Of the 2.5% overall divergence, 1.4% is represented by PSVs and 1.1% by indels (analysis of manually aligned sequences using the DnaSP program; Rozas and Rozas 1999).

Segments of the aligned NF1REP-51 differ in alignment quality. The top panel of Figure 3 shows the size of all alignment gaps between the NF1REP-P1-51 and NF1REP-M-51 repeats.

PRS1 and PRS2 contain sparse misalignments of 1 to 4 bp. Both PRS are devoid of large gaps, although both are flanked proximally by markedly larger gaps. The 36-bp alignment gap at the front of PRS1 is due to a $(GA)_n$ microsatellite that is fixed at nine repeat units in NF1REP-P1 and ranges from 15 to 31 units in NF1REP-M. PRS2 is bordered by a unique 24 bp indel that is a fixed difference among the three NF1REP-P1 and two NF1REP-M sequences currently available in Genbank (accession numbers in Methods; our own PRS2 sequences in patients and normals did not extend proximally to this site). These relatively large alignment gaps flanking the PRS apparently do not prevent pairing for recombination, as exchange can occur within distances of less than 1 kb from the gaps. However, the principle hotspots are located 1 to 2 kb distal to these alignment gaps (Figure 2), where paralogous misalignments are limited to 1 to 4 bp both in available Genbank entries and in our hotspot sequences from patients and normals (see Methods).

On a kilobase scale, the PRS are not regions of greater or lesser paralogous sequence identity, as shown by the spatial distribution of PSVs in the middle panel of Figure 3. The overall percent divergence for NF1REP-P1-51 and NF1REP-M-51 is 1.36% (indels excluded), and the corresponding values for PRS1 (1.17%) and PRS2 (1.45%) are not significantly different from the overall mean (2x2 contingency *Chi*-square tests; $p>0.1$). Nucleotide site differences (PSVs) appear uniformly distributed across the entire NF1REP-51, with two notable exceptions. The high divergence tract at 98.4 kb contains a matrix attachment region (MAR; see below). The other high divergence tract at 118 kb is a short (95 bp) segment with 15 variable sites (13 PSVs and 2 indels of 1 bp each) where NF1REP-P1-51 matches a segment of NF1REP-E19. These variable sites are fixed in the three sequenced alleles of NF1REP-P1-51 available in Genbank (accession numbers in Methods), and they likely represent an early gene conversion

event that followed duplication of the NF1REP-51 paralogs. The NF1REP-E19 blocks matching the NF1REP-P1-51 (Figure 1C) show only 94-95% identity between these inter-chromosomal paralogs. Gene conversion tests and searches for other NF1REP-specific variants shared between NF1REP-E19 and its paralogs on chromosome 17 show no other evidence of historical gene conversion or recombination (data not shown).

Recombinogenic Structures and Domains

We searched the NF1REP breakpoint clusters for structures reported to be associated with recombination in other settings. In addition, we looked for commonalities between the breakpoint clusters of NF1 and those reported in Charcot-Marie-Tooth disease type 1A (CMT1A), another paralogous recombination disorder in which breakpoints have been mapped in similar detail.

Several genomic rearrangements have been associated with palindromes including the large, recurrent deletions in the Y-chromosome AZFc region that lead to male infertility (Repping et al. 2002) and translocations by AT-rich palindromic sequences involving t(11;22) (Kurahashi and Emanuel 2001) and t(17;22) (Kurahashi et al. 2003), the latter of which occurs in *NF1* intron 31. Furthermore, studies in yeast demonstrate that palindromes longer than 50 bp can be recombination hotspots (Nag and Kurst 1997; Nasar et al. 2000). The NF1REP-51 repeats contain no palindromes larger than 18 bp and separated by 63 bp when the arms are allowed to be 100 bp and separated by up to 100 bp. Yet, these default settings of the *Palindrome* program readily detected the AT-rich palindrome in NF1 intron 31. More permissive pattern searches for large inverted repeats performed on the entire NF1REP-P1 and NF1REP-M revealed a single significant pair of sequences that straddles the proximal boundary

of the NF1REP-P1-51 repeat (Fig. 1B; light green blocks). These non-tandem inverted repeats are 5,778 bp long, are separated by 3,708 bp of unrelated sequence, show 98.6% sequence identity, and contain copies of *KIAA0563rel* exon 8. The "inverted" segment of the pair is present only on NF1REP-P1 (Figure 1B). Pairing between these repeats of NF1REP-P1 is unlikely to account for preferential DSB that initiate paralogous recombination at PRS1 and PRS2, which are 15 kb and 36 kb telomeric to the distal copy of the repeat.

A role for specific sequence signals in mammalian recombination is not established, but tests for the presence of motifs with demonstrated or suspected roles in recombination, transcription, or replication are still warranted. In *E. coli*, recombination is stimulated by the 8-bp *Chi* sequence [5'-GCTGGTGG-3']. BAC 271K11 contains 20 *Chi*-like sites in a span of 200 kb. Within this span, the NF1REP-P1-51 kb block contains 5 *Chi*-like sites, one of which falls within the PRS2 hotspot (Lopez-Correa et al. 2001), but the other four are evenly distributed without apparent association with breakpoints. NF1REP-M-51 has *Chi*-like sequences at the same five sites. Due to their association with recombination in yeast (Gale et al. 1992; Badge et al. 2000), we also searched for autonomously replicating sequences (ARS). BAC 271K11 contains 13 *S. cerevisiae* ARS sites. The NF1REP-51 both contain the same five *S. cerevisiae* ARS sites, one of which is within PRS1 but 2 kb distal to the PRS1 hotspot. This does not indicate a marked excess of ARS sites in the 51 kb repeat or in the PRS, and the proximity of one ARS site to the PRS1 hotspot could be happenstance. Neither were the other putative recombinogenic motifs (see Methods) found to be preferentially associated with PRS1 or PRS2 (Dorschner et al. 2000; Lopez-Correa et al. 2001; Dorschner et al. submitted).

In yeast, recombination is locally stimulated by transcription (Freedman and Jinks-Robertson 2002; Gonzalez-Barrera et al. 2002). There is one known, expressed gene

(*KIAA0563rel)* in NF1REP-M (Fig. 1B) and 5 of its exons are in the NF1REP-M-51 repeat, indicating that this is at least at times functionally accessible chromatin. NF1REP-P1 is missing the promoter region of this gene. However, a Unigene cluster (Hs.306516) does map to proximal NF1REP-P1. This transcription unit is distinct from that matching *KIAA0563rel* (Hs.367593), suggesting that both regions are transcribed, although an examination for ORFs did not indicate a functional protein product from the proximal site. A search for functional chromatin based on promoter sequences (First Exon Finder; see Methods) found two overlapping promoter/first exons on opposite strands within the PRS2 hotspot and one proximal to PRS1 (Figures 4 and 5). PRS1 and PRS2 are not associated with any known genes, but the possibility that promoter-like sequences render chromatin accessible even when not associated with functional genes must be considered.

Singh et al. (Singh et al. 1997) established six decision rules for identifying DNA sites associated with chromatin function: origin of replication (ORI) signals, TG-richness, curved DNA, kinked DNA, topoisomerase II binding, and AT richness. Together these rules define the MAR, or matrix attachment region. An 800 bp long, high-scoring MAR is centered 1500 bp into the NF1REP-51 repeats (Fig. 3), and the NF1REP-P1 and NF1REP-M paralogs of this tract are each the highest-scoring MAR in their respective BAC context. Both score most strongly for the ORI rule, the topoisomerase II binding rule, and the AT-richness rule, and they are very low-GC (37.6%). The paralogs differ in this region by the insertion of several AT-rich tracts in NF1REP-M-51, and by numerous apparent PSVs in regions of complex AT-rich sequence that are difficult to align. Together, these findings suggest a site involved in chromatin function located within *KIAA0563rel*, the only known expressed, apparently functional gene in the NF1REP-51 repeats, and the openness of this chromatin may enhance the likelihood of paralogous pairing. Promoter-

like sequences near the PRS1 and PRS2 hotspots (Figs. 3 and 4) may likewise enhance accessibility for pairing in these regions.

Gene Conversion Tests in the NF1REPs

In the absence of gene conversion or recombination, paralogous sequences should have evolved independently and sequence differences should be distributed at random. Larger stretches of perfect match than expected at random are evidence in support of gene conversion. The longest fragment of perfect match between the finished BAC sequences for NF1REP-P1 and NF1REP-M is a 700-bp tract located in the PRS2 hotspot (nt 143,268-143,967; Figs. 2, 3 and 4). A statistical test (GeneConv; Sawyer 1999) on the NF1REP-51 repeats from the reference BACs 271K11 and 640N20 revealed this to be the single significant fragment ($p = 0.008$; indels included as polymorphisms). Among the five Genbank NF1REP sequences (three proximal and two medial; accession numbers in Methods) a perfect tract at this location was the largest in each of the six paralogous comparisons, ranging in size from 627 to 700 bp due to polymorphisms. In each case when the tract was shorter (e.g. 627 bp using proximal BAC 271K11and medial BAC 2646J6), the *p*-value of the test was higher but still significant ($p = 0.019$; indels included as polymorphisms).

We also searched the alignment of the five copies of NF1REPs for shared polymorphisms. Two sites, both on the proximal border of the 700-bp putative gene conversion tract, showed the same two variants in both paralogs (a 3-bp, +/-[AGC] indel, and a G/A SNP; nt 142,308 and 143,314 respectively; Fig. 4). Such polymorphisms in both paralogs—especially the identical 3-bp indel—suggest a gene conversion event subsequent to duplication of the region.

DISCUSSION

Disease-causing genome rearrangements due to recombination between paralogs range in size from less than 10 kb to as large as four megabases, and the size of the REPs involved ranges from a few kb to more than 500 kb (reviewed by Inoue and Lupski 2002; Stankiewicz and Lupski 2002a). The NF1REPs that mediate *NF1* microdeletion have a modular sequence structure, scattered pseudogene fragments, a single expressed, functional gene and a related set of paralogs on a different chromosome. The NF1REPs are more complex than CMT1A REPs (Reiter et al. 1996; Lopes et al. 1999), which are simple related sequence blocks in direct orientation. However, they are not so complex as several other examples such as the REPs that mediate deletion in Smith-Magenis and Williams-Beuren Syndromes (Park et al. 2002) (Bayes et al. 2003), which contain multiple clusters of larger blocks in different combinations and different orientations. In all of these examples the REPs contain, or are contained within, transcription units, and often the derived paralog contains a pseudogene or pseudogene fragment(s) of the original gene.

Hotspots and Sequence Motifs

The predominant mechanism of *NF1* microdeletion is pairing and recombination between NF1REP-P1-51 and NF1REP-M-51, with all but one of the exchange events occurring in one of two clusters (PRS1 and PRS2). These clusters represent only 19% of the alignable 51 kb sequence apparently available for pairing and exchange. Breakpoint mapping in the CMT1A/HNPP duplication/deletion disorders also identified two recombination hotpots (Lopes et al. 1998; Reiter et al. 1998) and additional comparisons to the NF1REPs are instructive. In

neither *NF1* nor CMT1A were there common, sequence-level features that would suggest why the breakpoint clusters occur where they do. We found no actual sequence identity between paralogous recombination hotspots either within or between these two disorders, and no similarity in sequence features or composition. NF1REP PRS2 contains a *Chi*-like site and promoter-like elements, but PRS1 contains neither. Likewise, the two CMT1A paralogous recombination hotspots are entirely different. The major hotspot (75% of cases) is flanked by a Mariner-like transposon element, a *Chi*-like site, and a minisatellite, but the secondary hotspot (20% of cases) is associated with no such motifs (Reiter et al. 1998). At only 24 kb (Reiter et al. 1996), the CMT1A REPs are smaller than the NF1REP-51 and the modular structure of the CMT1A REPs is simpler (Inoue et al. 2001). The CMT1A REPs also have lower percent G+C (41% vs. 48% for NF1REP-51), fewer high-copy repeats (31% vs. 55% for NF1REP-51), no strong MAR sites, and tighter breakpoint clustering. From the evidence of these two paralogous recombination disorders, there is no support for the existence of obligate, consensus recombinogenic motifs or features.

There are to date many more examples of breakpoints mapped at the sequence-level for allelic recombination events (reviewed by de Massy 2003) than for paralogous recombination events. In both homologous and paralogous recombination, however, multiple examples suggest that putative recombinogenic motifs may be influential but they are not obligatory. Several examples in yeast (Nag and Kurst 1997; Nasar et al. 2000) suggest that large palindromes enhance recombination by inducing DSBs, and a variety of local sequence features ranging from simple repeats to promoters and transposons can enhance recombination at a specific sites. For example, a hotspot 1.0-1.6 kb in the mouse MHC was found to be centered on an MT element (Yauk et al. 2003), and in humans specific sequences such as microsatellites (Benet et al. 2000)

and minisatellites (Wahls et al. 1990; Boan et al. 1998; Jeffreys et al. 1998) are strongly associated with recombination hotspots. It is unclear what features serve to localize breakpoints when such recombinogenic motifs are apparently lacking, as in the case of the *NF1* microdeletion.

Breakpoint Clustering and Alignment Mismatch

The NF1REPs and the CMT1A REPs differ markedly in the degree and nature of sequence differences between paralogs, and this may relate to different causes of breakpoint localization in the two systems. The NF1REP-51 repeats show 97.5% sequence identity, lower than for the CMT1A REPs at 98.3%. The proportions of PSVs are approximately the same (1.4% and 1.2%, respectively). However, the NF1REP-51 repeats have nearly three times the proportion of bases in alignment gaps in the CMT1A REPs (1.1% and 0.4%, respectively). Despite the greater proportion of gaps in the NF1REPs, within them the PRS are regions of relatively good alignment, with indels of only 1-4 bp (Figs. 3 and 4). Larger gaps of approximately 10 to 40 bp are contiguous to but not contained within the two PRS. The lack of such large alignment gaps in the CMT1A REPs means that study of these REPs doesn't so directly address the effect of gaps on breakpoint clustering. The simplest explanation for the location of the NF1 PRS clusters is that gaps of 1-4 bp do not prevent effective pairing and subsequent genetic exchange, but that larger gaps (here approximately 10 to 40 bp) do not allow effective pairing and exchange in their immediate vicinity.

Chromatin Accessibility

If local motifs are not obligatory, another reasonable explanation of breakpoint clustering is accessibility of DNA to proteins of the recombination machinery. In yeast there is abundant evidence that crossovers occur at sites of accessible chromatin (promoters, transcription factor binding sites) (Baudat and Nicolas 1997; de Massy 2003). This may be true in mammals but the evidence to date is less strong. For *NF1* microdeletion, the PRS1 and PRS2 hotspots appear to be in non-transcribed DNA in both participating paralogs, NF1REP-P1 and NF1REP-M. The only NF1REP-51 breakpoint in a coding region is that of case UWA160-1 (Figure 2), which occurs in intron 7 of *KIAA0563rel.* However, chromatin accessibility due to promoters even substantially upstream of an exchange region may play a role enhancing recombination, and the mere presence of promoter-like sequences even unattached to a gene (apparently the case for NF1REP PRS2) may make the site more accessible to recombination proteins. About half of reported paralogous recombination disorders involve recombination between either related expressed genes, or between an expressed gene and its pseudogene (Stankiewicz and Lupski 2002a), and the relative accessibility of the chromatin may persist even as the transcription unit becomes non-functional.

Another chromatin feature thought to bear on recombination is the matrix attachment region (MAR). Strong topoisomerase II sites have been shown in translocation studies to co-localize with experimentally detected DNase I sensitive sites, and several have been mapped at inter-chromosomal translocation breakpoints (Zhang et al. 2002). None of the *NF1* microdeletion breakpoints occurred at the MAR site in the NF1REP-51 repeat (Figure 3), arguing against matrix/scaffold attachment as a primary breakpoint-localizing feature in this disorder.

Gene Conversion Between Paralogs

The finding of significantly long identical sequences and shared polymorphisms suggest that gene conversion has occurred in the NF1 PRS2 hotspot. In addition, above we cited three cases where sufficient sequence detail from the parental chromosomes demonstrated gene conversion in the process of strand exchange (Lopez-Correa et al. 2001; Dorschner et al. submitted). The same evidence for gene conversion accompanying crossover was detailed for the primary CMT1A/HNPP recombination hotspot (Reiter et al. 1998; Lopes et al. 1999). If gene conversion accompanies crossover events ascertained by pathology, it is also possible—even likely—that gene conversion between the same paralogs may occur in the absence of crossover. Such events would not be pathological but should be detectable by sequencing large numbers of normal alleles. The two diseases cited here are promising early evidence that recombination hotspots coincide with and are mechanistically related to gene conversion hotspots.

It is suggested that gene conversion acts to homogenize paralogous sequences, and that this in turn makes them more likely to pair (Hurles 2001; Stankiewicz and Lupski 2002b) but we cannot say with certainty which is cause and which is effect. That is, either: 1) a hotspot region is prone to effective pairing for reasons external to the tract, and gene conversion events within the tract serve to homogenize the paralogs at this site; or 2) a hotspot region preferentially pairs because it happens to be a larger perfect tract than the neighboring sequence, and the resulting gene conversion helps to maintain this high sequence identity.

Some care is warranted in using single copies of paralogous sequences to test for paralogous gene conversion, because the size of perfect fragments depends strongly on population variation for the defining PSVs. Among the five copies of the NF1REPs available in

Genbank (two of NF1REP-P1 and two of NF1REP-M; see Methods), a fragment at the site of the 700 bp matching fragment reported above varies in size but is always the largest (and a statistically significant; all $p<0.05$) matching fragment. We also applied the same test we used on the NF1REPs (Sawyer's GeneConv; see Methods) to the original Genbank copies of the CMT1A REPs (Reiter et al. 1996); accession numbers in Methods) and found a 950-bp significant fragment ($p = 0.0004$; indels included as variants). This tract coincides with the secondary (20%) CMT1A recombination hotspot (nt 24879-25830 in Genbank #U71218). Using alternate CMT1A REP sequences (accession numbers in Methods) shortens the significant 950 bp fragment to 658 bp but even at this length it is still significant ($p=0.020$). Hurles et al. (2001) reported statistical evidence of gene conversion in these sequences, but they did not identify particular significant fragments.

Analysis of normal sequences for conversion tracts detects where paralogous pairing apparently has occurred but crossover did not. Deeper allele sampling of these sites in normal genomes would greatly help characterize these events. If born out by subsequent studies, the coincidence of the hotspots for both crossover and gene conversion would strongly support a dual pathway recombination model in humans similar to that proposed for yeast, where the initial steps include a DSB and pairing, but the outcome may be either gene conversion without crossover, or recombination (with or without gene conversion; reviewed by de Massy 2003).

Pairings between paralogs are "mistakes," where the paired sequences may differ considerably more than typical alleles (homologs), but they still match sufficiently that subsequent recombination steps apparently proceed normally. The main contribution of paralogous pairing to our knowledge of recombination in general may be in those examples where the paralogs are especially small or (as in the NF1REPs) the paralogous alignment match

displays substantial gaps. Accumulation of such examples will serve to illustrate the minimal length and quality of sequence pairing needed to effect recombination in humans.

METHODS

Patients

NF1 patients carrying microdeletions have been described previously (Dorschner et al. 2000; Lopez-Correa et al. 2001); (Dorschner et al. submitted) and references therein. Patient NF160-1 is described in Leppig et al. (1997).

Identification of a Novel Breakpoint

The breakpoints of UWA160-1 were mapped previously to NF1REP-P1 and NF1REP-M by STS analyses of somatic cell hybrid lines carrying only the deleted chromosome 17 (Lopez-Correa et al. 2001; Dorschner et al. submitted). Here we mapped the breakpoint to a region about 10 kb centromeric of PRS1 by comparing sequences of the deleted chromosome 17 to paralogous sequences from BAC clones and normal chromosome 17s, as described previously (Dorschner et al. 2000; Dorschner et al. submitted). An approximately 5 kb amplicon containing the breakpoint was amplified from genomic DNA of the hybrid line carrying the deleted chromosome with primers 160P1-F (5'-GGCTCATGTGTAATGATCTTTAACGCG-3') and MD1-R(v2) (5'-CAAAGATTATCACTGATGGAGTTGG-3'). This amplicon was sequenced with several internal primers to identify the breakpoint interval. Note that the above primers are not necessarily NF1REP-specific and may amplify non-recombinant NF1REP from normal individuals.

Defining REP-Specific Nucleotide Site Variants

Paralogous sequence variants, or "PSVs" were initially defined by differences between the reference BACS (see below) for each paralog. The pattern of PSVs from amplicons of the deleted chromosomes 17 were expected to match that of either NF1REP-P1 or NF1REP-M, or transition from NF1REP-P1 to NF1REP-M if the amplicon contained the breakpoint of the recombinant NF1REP. This strategy narrowed the recombination interval, which was subsequently identified by repeating the process with closely spaced primers from the interval of interest.

To help differentiate PSVs from common polymorphisms at allelic sites (SNPs), we also amplified, cloned, and partially sequenced nonrecombinant PRS1 and PRS2 regions from both NF1REP-P1 and NF1REP-M of six normal chromosomes and of the NF1REP-M carried in BAC 951F11, using the Expand LT PCR system (Roche Molecular Biochemicals, Mannheim, Germany). Amplicons were column purified and cloned into the TOPO XL PCR cloning kit (Invitrogen Corporation, Carlsbad, CA). Plasmid preparations of clones were purified and sequenced directly using internal primers as described previously (Dorschner et al. 2000; Lopez-Correa et al. 2001; Dorschner et al. submitted).

Genomic Contigs and Reference Sequences

The region spanning between and including NF1REP-P1 and NF1REP-M is finished, assembled sequence in NCBI build 32 (April 2003). Finished BACs for the two regions (RP11-271K11 and CTD-2349P21 for NF1REP-P1 and RP11-640N20 for NF1REP-M) were used as primary reference sequences. Two additional BACs closely matching NF1REP-P1 are in draft state (RP13-715K7; RP11-1403G4) and one additional BAC matching NF1REP-M is finished (CTD-

2646J6). Finished chromosome 19 BACs representing NF1REP-E19 are indicated in Fig. 1C. For the proximal and distal CMT1A REPs our primary references were Genbank U71217 and U71218, respectively. Additional, finished copies of the CMT1A REPs were taken from AC005838 (proximal) and assembled using AC005389 and AC005838 (distal).

Sequence Composition and Motif Searches

We searched for short sequence motifs using the EMBOSS program "Fuzznuc." Putative recombination motifs were chosen from lists in Lopes et al. (1998), Badge et al. (2000) and Lopez-Correa et al. (2001): E. coli *Chi* sequence (5'-GCTGGTGG-3'), yeast Ade6-M26 heptamer (5'-ATGACGT-3'), XY32 homopurine/homopyrimidine (5'-AAGGGAGAARGGGTAAAGGGRAAGAGGGAA-3'), retroposon LTR (5'-TCATACACCACGCAGGGGTAGAGGACT-3'), the long terminal repeat element LTR-IS (5'-TGGAAATCCCC-3'), protein binding site *pur* (5'-GGNNGAGGGAGARRRR-3'), translin consensus 1 (5'-GCNCWSSWN$_{(0-2)}$GCCCWSSW-3'), translin consensus 2 (5'-MTGCAGN$_{(0-4)}$GCCCWSSW-3'), *Saccharomyces cerevisiae* ARS (5'-WTTTATRTTTW-3'), *Schizosaccharomyces pombe* ARS (5'-WRTTTATTTAW-3'), human replication origin consensus (5'-WAWTTDDWWWDHWGWHMA-WTT-3'), and human minisatellite core sequences (5'-GGGCAGGAG-3'; 5'-GGAGGTG-GGCAGGARG-3'; 5'-AGAGGTGGGCAGGTGG-3'). Minisatellite core sequences were searched using the 9 bp core sequence allowing one mismatch, and the 16 bp core sequences allowing up to 4 mismatches.

Known genes and annotated features were assessed with the NCBI (Genbank) and UCSC Human Genome Working Draft databases and browsers. We searched the NF1REP for internal repeats by pairwise BLAST (NCBI), Tandem Repeats Finder (Benson 1999), PatternHunter - (Ma et al. 2002), and the EMBOSS program "Palindrome." We tested for matrix attachment regions (MARs) using MarWiz (Singh et al. 1997). High-copy repeats, simple repeats and other simple DNA were detected with RepeatMasker (see Web Site References), and graphical results for repeats and GC percent were obtained with Gestalt Workbench (Glusman and Lancet 2000). Candidate promoters and first exons were detected with First Exon Finder ("FirstEF"; Davuluri et al. 2001).

Polymorphic Sites and Gene Conversion Tests

Sliding window sequence polymorphism and divergence plots were created with DnaSP (Rozas and Rozas 1999), which tabulates differences within and between populations, reports shared variants, and outputs alignments listing polymorphic sites only (with alignment gaps included or excluded). The gene conversion test of Sawyer (GeneConv; Sawyer 1989) tabulates all differences between sequences, tests the distribution of perfect fragment sizes against random simulations of the dataset, and reports *p*-values for the probability of obtaining a particular perfect match by chance. This can be done with or without inclusion of indels as polymorphic sites. When included, contiguous indel sites are treated as single variants. Significance values are Bonferroni corrected for the number of tests, and results are listed by decreasing fragment size and p-value. A program that performs these tests is available (see Web Site References).

ACKNOWLEDGEMENTS

This work was supported by grant DAMD17-00-1-0542 awarded to K.S. S.H.F. was supported in part by DAMD17-00-1-0542 and T32 GM07454-27. M.O.D was supported by DAMD17-00-1-0542.

REFERENCES

Badge, R.M., Yardley, J., Jeffreys, A.J., and Armour, J.A. 2000. Crossover breakpoint mapping identifies a subtelomeric hotspot for male meiotic recombination. *Hum Mol Genet* **9:** 1239-1244.

Baudat, F. and Nicolas, A. 1997. Clustering of meiotic double-strand breaks on yeast chromosome III. *Proc Natl Acad Sci U S A* **94:** 5213-5218.

Bayes, M., Magano, L.F., Rivera, N., Flores, R., and Perez Jurado, L.A. 2003. Mutational mechanisms of Williams-Beuren syndrome deletions. *Am J Hum Genet* **73:** 131-151.

Benet, A., Molla, G., and Azorin, F. 2000. d(GA x TC)(n) microsatellite DNA sequences enhance homologous DNA recombination in SV40 minichromosomes. *Nucleic Acids Res* **28:** 4617-4622.

Benson, G. 1999. Tandem repeats finder: a program to analyze DNA sequences. *Nucleic Acids Res* **27:** 573-580.

Boan, F., Rodriguez, J.M., and Gomez-Marquez, J. 1998. A non-hypervariable human minisatellite strongly stimulates in vitro intramolecular homologous recombination. *J Mol Biol* **278:** 499-505.

Cnossen, M.H., van der Est, M.N., Breuning, H., van Asperen, C.J., Breslau-Siderius, E.J., van der Ploeg, A.T., de Goede-Bolder, A., van den Ouweland, A.M.W., Halley, D.J.J., and Niermeijer, M.F. 1997. Deletions spanning the neurofibromatosis type 1 gene: implications for genotype-phenotype correlations in neurofibromatosis type 1? *Hum Mutat* **9:** 458-464.

Davuluri, R.V., Grosse, I., and Zhang, M.Q. 2001. Computational identification of promoters and first exons in the human genome. *Nat Genet* **29:** 412-417.

de Massy, B. 2003. Distribution of meiotic recombination sites. *Trends Genet* **19:** 514-522.

De Raedt, T., Brems, H., Wolkenstein, P., Vidaud, D., Pilotti, S., Perrone, F., Mautner, V., Frahm, S., Sciot, R., and Legius, E. 2003. Elevated risk for MPNST in NF1 microdeletion patients. *Am J Hum Genet* **72:** 1288-1292.

Dorschner, M.O., Brems, H., Le, R., De Raedt, T., Wallace, M.R., Curry, C.J., Aylsworth, A.S., Haan, E.A., Zackai, E.H., Lazaro, C., Messiaen, L., Legius, E., and Stephens, K. submitted. Two paralogous recombination hotspots mediate 69% of *NF1* microdeletions.

Dorschner, M.O., Sybert, V.P., Weaver, M., Pletcher, B.A., and Stephens, K. 2000. NF1 microdeletion breakpoints are clustered at flanking repetitive sequences. *Hum Mol Genet* **9:** 35-46.

Emanuel, B.S. and Shaikh, T.H. 2001. Segmental duplications: an 'expanding' role in genomic instability and disease. *Nat Rev Genet* **2:** 791-800.

Estivill, X., Cheung, J., Angel Pujana, M., Nakabayashi, K., Scherer, S.W., and Tsui, L.C. 2002. Chromosomal regions containing high-density and ambiguously mapped putative single nucleotide polymorphisms (SNPs) correlate with segmental duplications in the human genome. *Hum Mol Genet* **11:** 1987-1995.

Freedman, J.A. and Jinks-Robertson, S. 2002. Genetic requirements for spontaneous and transcription-stimulated mitotic recombination in Saccharomyces cerevisiae. *Genetics* **162:** 15-27.

Gale, J.M., Tobey, R.A., and D'Anna, J.A. 1992. Localization and DNA sequence of a replication origin in the rhodopsin gene locus of Chinese hamster cells. *J Mol Biol* **224:** 343-358.

Glusman, G. and Lancet, D.O. 2000. GESTALT: a workbench for automatic integration and visualization of large-scale genomic sequence analyses. *Bioinformatics* **16:** 482-483.

Gonzalez-Barrera, S., Garcia-Rubio, M., and Aguilera, A. 2002. Transcription and double-strand breaks induce similar mitotic recombination events in Saccharomyces cerevisiae. *Genetics* **162:** 603-614.

Haber, J.E. 2000. Partners and pathways - repairing a double-strand break. *Trends Genet* **16:** 259-264.

Hurles, M.E. 2001. Gene conversion homogenizes the CMT1A paralogous repeats. *BMC Genomics* **2:** 11.

Inoue, K., Dewar, K., Katsanis, N., Reiter, L.T., Lander, E.S., Devon, K.L., Wyman, D.W., Lupski, J.R., and Birren, B. 2001. The 1.4-Mb CMT1A duplication/HNPP deletion genomic region reveals unique genome architectural features and provides insights into the recent evolution of new genes. *Genome Res* **11:** 1018-1033.

Inoue, K. and Lupski, J.R. 2002. Molecular mechanisms for genomic disorders. *Annu Rev Genomics Hum Genet* **3:** 199-242.

Jeffreys, A.J., Murray, J., and Neumann, R. 1998. High-resolution mapping of crossovers in human sperm defines a minisatellite-associated recombination hotspot. *Mol Cell* **2:** 267-273.

Jenne, D.E., Tinschert, S., Dorschner, M.O., Hameister, H., Stephens, K., and Kehrer-Sawatzki, H. 2003. Complete physical map and gene content of the human NF1 tumor suppressor region in human and mouse. *Genes Chromosomes & Cancer* **37:** 111-120.

Jenne, D.E., Tinschert, S., Reimann, H., Lasinger, W., Thiel, G., Hameister, H., and Kehrer-Sawatzki, H. 2001. Molecular characterization and gene content of breakpoint boundaries in patients with neurofibromatosis type 1 with 17q11.2 microdeletions. *Am J Hum Genet* **69:** 3.

Jenne, D.E., Tinschert, S., Stegmann, E., Reimann, H., Nurnberg, P., Horn, D., Naumann, I., Buske, A., and Thiel, G. 2000. A common set of at least 11 functional genes is lost in the majority of NF1 patients with gross deletions. *Genomics* **66:** 93-97.

Johnson, R.D. and Jasin, M. 2001. Double-strand-break-induced homologous recombination in mammalian cells. *Biochem Soc Trans* **29:** 196-201.

Kayes, L.M., Burke, W., Riccardi, V.M., Bennett, R., Ehrlich, P., Rubenstein, A., and Stephens, K. 1994. Deletions spanning the neurofibromatosis 1 gene: identification and phenotype of five patients. *Am J Hum Genet* **54:** 424-436.

Kluwe, L., Friedrich, R.E., Peiper, M., Friedman, J., and Mautner, V.F. 2003. Constitutional NF1 mutations in neurofibromatosis 1 patients with malignant peripheral nerve sheath tumors. *Hum Mutat* **22:** 420.

Korf, B.R. 2002. Clinical features and pathobiology of neurofibromatosis 1. *J Child Neurol* **17:** 573-577; discussion 602-574, 646-551.

Kurahashi, H. and Emanuel, B.S. 2001. Long AT-rich palindromes and the constitutional t(11;22) breakpoint. *Hum Mol Genet* **10:** 2605-2617.

Kurahashi, H., Shaikh, T., Takata, M., Toda, T., and Emanuel, B.S. 2003. The constitutional t(17;22): another translocation mediated by palindromic AT-rich repeats. *Am J Hum Genet* **72:** 733-738.

Kuroda-Kawaguchi, T., Skaletsky, H., Brown, L.G., Minx, P.J., Cordum, H.S., Waterston, R.H., Wilson, R.K., Silber, S., Oates, R., Rozen, S., and Page, D.C. 2001. The AZFc region of the Y chromosome features massive palindromes and uniform recurrent deletions in infertile men. *Nat Genet* **29:** 279-286.

Leppig, K.A., Kaplan, P., Viskochil, D., Weaver, M., Ortenberg, J., and Stephens, K. 1997. Familial neurofibromatosis 1 microdeletions: cosegregation with distinct facial phenotype and early onset of cutaneous neurofibromata. *Am J Med Genet* **73:** 197-204.

Lopes, J., Ravise, N., Vandenberghe, A., Palau, F., Ionasescu, V., Mayer, M., Levy, N., Wood, N., Tachi, N., Bouche, P., Latour, P., Ruberg, M., Brice, A., and LeGuern, E. 1998. Fine mapping of de novo CMT1A and HNPP rearrangements within CMT1A-REPs evidences two distinct sex-dependent mechanisms and candidate sequences involved in recombination. *Hum Mol Genet* **7:** 141-148.

Lopes, J., Tardieu, S., Silander, K., Blair, I., Vandenberghe, A., Palau, F., Ruberg, M., Brice, A., and LeGuern, E. 1999. Homologous DNA exchanges in humans can be explained by the yeast double-strand break repair model: a study of 17p11.2 rearrangements associated with CMT1A and HNPP. *Hum Mol Genet* **8:** 2285-2292.

Lopez-Correa, C., Brems, H., Lazaro, C., Estivill, X., Clementi, M., Mason, S., Rutkowski, J.L., Marynen, P., and Legius, E. 1999. Molecular studies in 20 submicroscopic neurofibromatosis type 1 gene deletions. *Hum Mutat* **14:** 387-393.

Lopez-Correa, C., Brems, H., Lazaro, C., Marynen, P., and Legius, E. 2000. Unequal meiotic crossover: a frequent cause of NF1 microdeletions. *Am J Hum Genet* **66:** 1969-1974.

Lopez-Correa, C., Dorschner, M., Brems, H., Lazaro, C., Clementi, M., Upadhyaya, M., Dooijes, D., Moog, U., Kehrer-Sawatzki, H., Rutkowski, J.L., Fryns, J.P., Marynen, P., Stephens, K., and Legius, E. 2001. Recombination hotspot in NF1 microdeletion patients. *Hum Mol Genet* **10:** 1387-1392.

Lupski, J.R., Deocaluna, R.M., Slaugenhaupt, S., Pentao, L., Guzzetta, V., Trask, B.J., Saucedocardenas, O., Barker, D.F., Killian, J.M., Garcia, C.A., Chakravarti, A., and Patel, P.I. 1991. DNA duplication associated with Charcot-Marie-Tooth disease type 1A. *Cell* **66:** 219-232.

Ma, B., Tromp, J., and Li, M. 2002. PatternHunter: faster and more sensitive homology search. *Bioinformatics* **18:** 440-445.

Messiaen, L.M., Callens, T., Mortier, G., Beysen, D., Vandenbroucke, I., Van Roy, N., Speleman, F., and Paepe, A.D. 2000. Exhaustive mutation analysis of the NF1 gene allows identification of 95% of mutations and reveals a high frequency of unusual splicing defects. *Hum Mutat* **15:** 541-555.

Nag, D.K. and Kurst, A. 1997. A 140-bp-long palindromic sequence induces double-strand breaks during meiosis in the yeast Saccharomyces cerevisiae. *Genetics* **146:** 835-847.

Nasar, F., Jankowski, C., and Nag, D.K. 2000. Long palindromic sequences induce double-strand breaks during meiosis in yeast. *Mol Cell Biol* **20:** 3449-3458.

Park, S.S., Stankiewicz, P., Bi, W., Shaw, C., Lehoczky, J., Dewar, K., Birren, B., and Lupski, J.R. 2002. Structure and evolution of the Smith-Magenis syndrome repeat gene clusters, SMS-REPs. *Genome Res* **12:** 729-738.

Rasmussen, S.A., Colman, S.D., Ho, V.T., Abernathy, C.R., Arn, P.H., Weiss, L., Schwartz, C., Saul, R.A., and Wallace, M.R. 1998. Constitutional and mosaic large NF1 gene deletions in neurofibromatosis type 1. *J Med Genet* **35:** 468-471.

Reiter, L.T., Hastings, P.J., Nelis, E., De Jonghe, P., Van Broeckhoven, C., and Lupski, J.R. 1998. Human meiotic recombination products revealed by sequencing a hotspot for homologous strand exchange in multiple HNPP deletion patients. *Am J Hum Genet* **62:** 1023-1033.

Reiter, L.T., Murakami, T., Koeuth, T., Pentao, L., Muzny, D.M., Gibbs, R.A., and Lupski, J.R. 1996. A recombination hotspot responsible for two inherited peripheral neuropathies is located near a *mariner* transposon-like element. *Nat Genet* **12:** 288-297.

Repping, S., Skaletsky, H., Lange, J., Silber, S., Van Der Veen, F., Oates, R.D., Page, D.C., and Rozen, S. 2002. Recombination between palindromes P5 and P1 on the human Y chromosome causes massive deletions and spermatogenic failure. *Am J Hum Genet* **71:** 906-922.

Rozas, J. and Rozas, R. 1999. DnaSP version 3: an integrated program for molecular population genetics and molecular evolution analysis. *Bioinformatics* **15:** 174-175.

Sawyer, S. 1989. Statistical tests for detecting gene conversion. *Mol Biol Evol* **6:** 526-538.

---. 1999. GENECONV: A computer package for the statistical detection of gene conversion. *Distributed by the author, Department of Mathematics, Washington University in St. Louis, available at http://www.math.wustl.edu/~sawyer.*

Shaikh, T.H., Kurahashi, H., Saitta, S.C., O'Hare, A.M., Hu, P., Roe, B.A., Driscoll, D.A., McDonald-McGinn, D.M., Zackai, E.H., Budarf, M.L., and Emanuel, B.S. 2000. Chromosome 22-specific low copy repeats and the 22q11.2 deletion syndrome: genomic organization and deletion endpoint analysis. *Hum Mol Genet* **9:** 489-501.

Singh, G.B., Kramer, J.A., and Krawetz, S.A. 1997. Mathematical model to predict regions of chromatin attachment to the nuclear matrix. *Nucleic Acids Res* **25:** 1419-1425.

Stankiewicz, P. and Lupski, J.R. 2002a. Genome architecture, rearrangements and genomic disorders. *Trends Genet* **18:** 74-82.

---. 2002b. Molecular-evolutionary mechanisms for genomic disorders. *Curr Opin Genet Dev* **12:** 312-319.

Stephens, K. 2003. Genetics of neurofibromatosis 1- associated peripheral nerve sheath tumors. *Cancer Invest* **in press**.

Upadhyaya, M., Ruggieri, M., Maynard, J., Osborn, M., Hartog, C., Mudd, S., Penttinen, M., Cordeiro, I., Ponder, M., Ponder, B.A., Krawczak, M., and Cooper, D.N. 1998. Gross deletions of the neurofibromatosis type 1 (NF1) gene are predominantly of maternal origin and commonly associated with a learning disability, dysmorphic features and developmental delay. *Hum Genet* **102:** 591-597.

Valerie, K. and Povirk, L.F. 2003. Regulation and mechanisms of mammalian double-strand break repair. *Oncogene* **22:** 5792-5812.

Wahls, W.P., Wallace, L.J., and Moore, P.D. 1990. Hypervariable minisatellite DNA is a hotspot for homologous recombination in human cells. *Cell* **60:** 95-103.

Yauk, C.L., Bois, P.R., and Jeffreys, A.J. 2003. High-resolution sperm typing of meiotic recombination in the mouse MHC Ebeta gene. *Embo J* **22:** 1389-1397.

Zhang, Y., Strissel, P., Strick, R., Chen, J., Nucifora, G., Le Beau, M.M., Larson, R.A., and Rowley, J.D. 2002. Genomic DNA breakpoints in AML1/RUNX1 and ETO cluster with topoisomerase II DNA cleavage and DNase I hypersensitive sites in t(8;21) leukemia. *Proc Natl Acad Sci U S A* **99:** 3070-3075.

WEB SITE REFERENCES

http://www.ncbi.nlm.nih.gov/genome/guide/human, NCBI genome resources.

http://genome.ucsc.edu/index.html, UCSC Human Genome Working Draft.

http://bioinformatics.weizmann.ac.il/GESTALT/, Gestalt Workbench.

http://bioweb.pasteur.fr/seqanal/EMBOSS/, EMBOSS package

http://www.futuresoft.org/modules/MarFinder/index.html, MarWiz.

http://www.cshl.org/mzhanglab/, First Exon Finder.

http://c3.biomath.mssm.edu/trf.html, Tandem Repeats Finder.

http://www.bioinformaticssolutions.com/products/ph.php, PatternHunter.

http://ftp.genome.washington.edu/cgi-bin/RepeatMasker, RepeatMasker.

http://www.ub.es/dnasp/, DnaSP, DNA Sequence Polymorphism.

http://www.math.wustl.edu/~sawyer/mbprogs/index.html, GeneConv: Statistical Tests for Detecting Gene Conversion - Version 1.81

FIGURE LEGENDS

Figure 1. Arrangement and structure of the NF1REP paralogs flanking the *NF1* gene. (A) The 350 kb *NF1* gene (transcribed left to right) is flanked by the paralogs NF1REP-P1, -P2, and –M (boxes). NF1REP-P1 and NF1REP-M are in direct orientation (arrows). The extent of the recurrent 1.5 Mb, germline microdeletion is shown above the map (Dorschner et al. 2000). Genes labeled with vertical bars are presumed, functional genes from the RefSeq database, with the exception of *JJAZ1-Ψ*, a pseudogene of *JJAZ1* (Jenne et al. 2003). The BAC identifiers and accession numbers refer to the first finished Genbank sequences for that feature. Drawing is to scale. (B) The three paralogs in the NF1 region are shown oriented from centromere to telomere. BAC identities and accession numbers are shown. Green color indicates sequences of the *KIAA0563rel* functional gene and related pseudogene fragments (*Ψ*), with numbered black vertical bars designating exons or related, exon-derived sequences. Light green boxes within *KIAA0563rel* copies indicate the orientation of a 5.8 kb inverted repeat with two copies on NF1REP-P1, and a third copy in NF1REP-M. Landmark STSs in the *KIAA0563rel* gene and pseudogenes cited previously (Dorschner et al. 2000) are indicated above NF1REP-P1. Yellow boxes depict *SMURF2*-derived pseudogene fragments, and red boxes denote the PRS. (C) Comparison of NF1REP-P1 to NF1REP-E19 located at chromosome 19p13.13. Colored boxes match those described for panel B. PRS1 and PRS2 sites in NF1REP-E19 are not known to serve as recombination substrates. NF1REP-E19 contains the *LEC2* functional gene and NF1REP-P1 contains pseudogene fragments of *LEC2* (purple).

Figure 2. Paralogous recombination sites and sequence composition of the NF1REP-51 paralogs. Nucleotide coordinates and sequence features refer to the NF1REP-P1 reference BAC RP11-271K11. Breakpoint intervals are shown as red bars, with the number of *NF1* microdeletion cases mapped to each interval indicated (Dorschner et al. 2000; Lopez-Correa et al. 2001; Dorschner et al. submitted). Dotted arrows indicate the PRS1 and PRS2 recombination hotspots. The black bar below PRS2 indicates the 700 bp putative gene conversion tract between NF1REP-51 repeats (see text and Fig. 4). Patient UWA160-1 is a new microdeletion case that maps within NF1REP-51 but outside the PRS clusters (see text). High-copy repeats in NF1REP-P-51 (forward strand on top, reverse strand on bottom) and percent G+C are displayed using graphical output from the Gestalt Workbench (Glusman and Lancet 2000). Bar size indicates the relative repeat age, and colors indicate repeat class (LINE elements in green, Alus in red, MIRs in purple, tRNAs in blue (none found here) and all others in brown). Overall GC content is 48.4%, and the blue-to-red transition indicates an isochore transition from H1-2 (43-50 percent GC) to H3 (>50 percent GC).

Figure 3. Alignment, sequence identity, and sequence features of the 51 kb high-identity paralogs NF1REP-P1-51 and NF1REP-M-51. Nucleotide coordinates refer to the NF1REP-P1 reference BAC RP11-271K11. The top panel shows the size of alignment gaps using reference BACs 271K11 (NF1REP-P1) and 640N20 (NF1REP-M). The middle panel shows nucleotide site differences between REPs (paralogous sequence variants, or PSVs), indels excluded, tabulated with a sliding 100 bp window stepped by 25 bp. Noted are two sites of greater sequence difference, including a single, high-scoring Matrix Attachment Region (MAR) and an apparent gene conversion tract with variants matching NF1REP-E19 (see Results). The location

of the 700-bp fragment of perfect match with statistical evidence of gene conversion is indicated. Breakpoint intervals (red blocks) repeat those shown in Fig. 2. Blue arrows in bottom panel are promoter-like sequences detected by FirstEF (see Methods) but these are not associated with known genes.

Figure 4. Detailed structure of the PRS2 region. Top panel with alignment gaps match those for this region shown in Fig. 3. Ninety-three percent of all PRS2 exchanges occurred in the indicated 2.3 kb hotspot interval. The chart shows indels based on the two finished reference BACS (271K11 and 640N20), but variants used for interval mapping (PSVs and indels) were based on fixed polymorphisms in seven NF1REP-P1 and seven NF1REP-M clones for PRS1 and PRS2 from normal individuals (Dorschner et al. 2000; Dorschner et al. submitted). Hence, the intervals here contain indels and site variants that were not used for breakpoint mapping. The shared variants are sites found polymorphic in both paralogs, based on the 3 proximal and 2 medial Genbank sequences (see Methods). Simple sequence sites were found by RepeatMasker, and high-scoring promoter sequences were found with FirstEF.

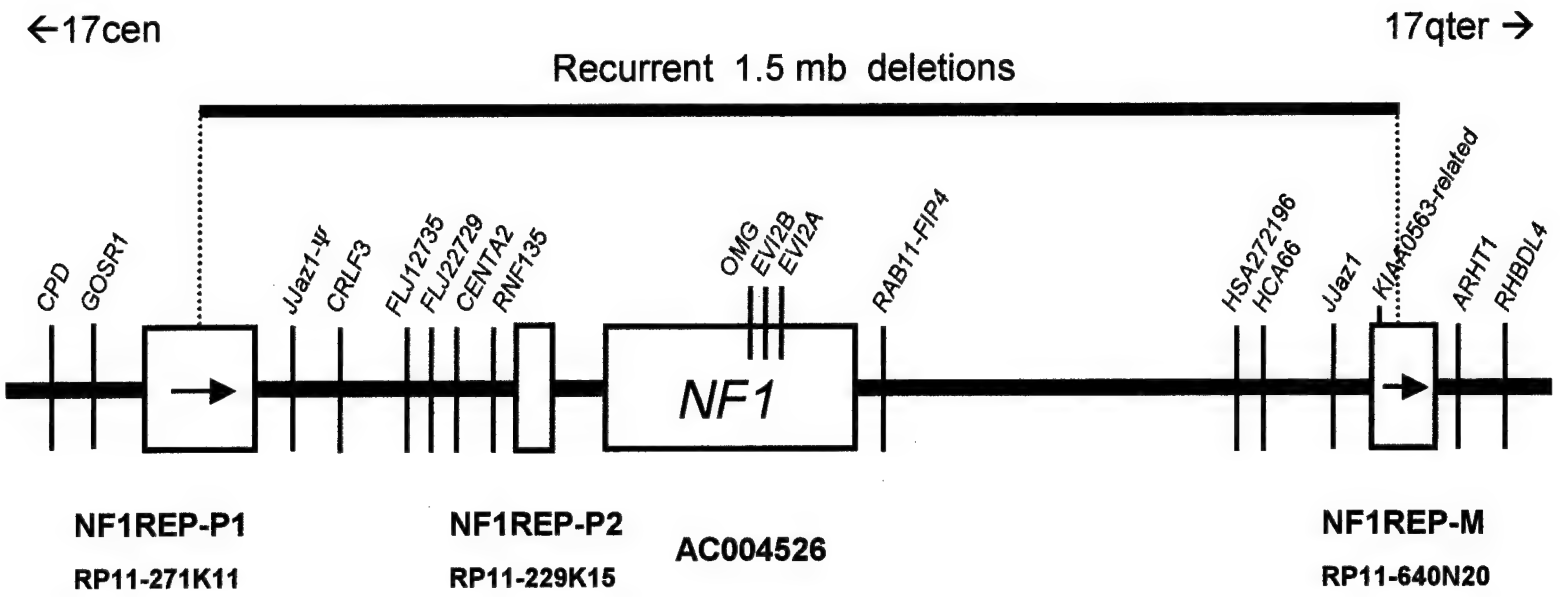
←17cen
17qter →
Recurrent 1.5 mb deletions
CPD
GOSR1
JJaz1-ψ
CRLF3
FLJ12735
FLJ22729
CENTA2
RNF135
OMG
EVI2B
EVI2A
RAB11-FIP4
NF1
HSA272196
HCA66
JJaz1
KIAA0563-related
ARHT1
RHBDL4
NF1REP-P1
RP11-271K11
NF1REP-P2
RP11-229K15
AC004526
NF1REP-M
RP11-640N20

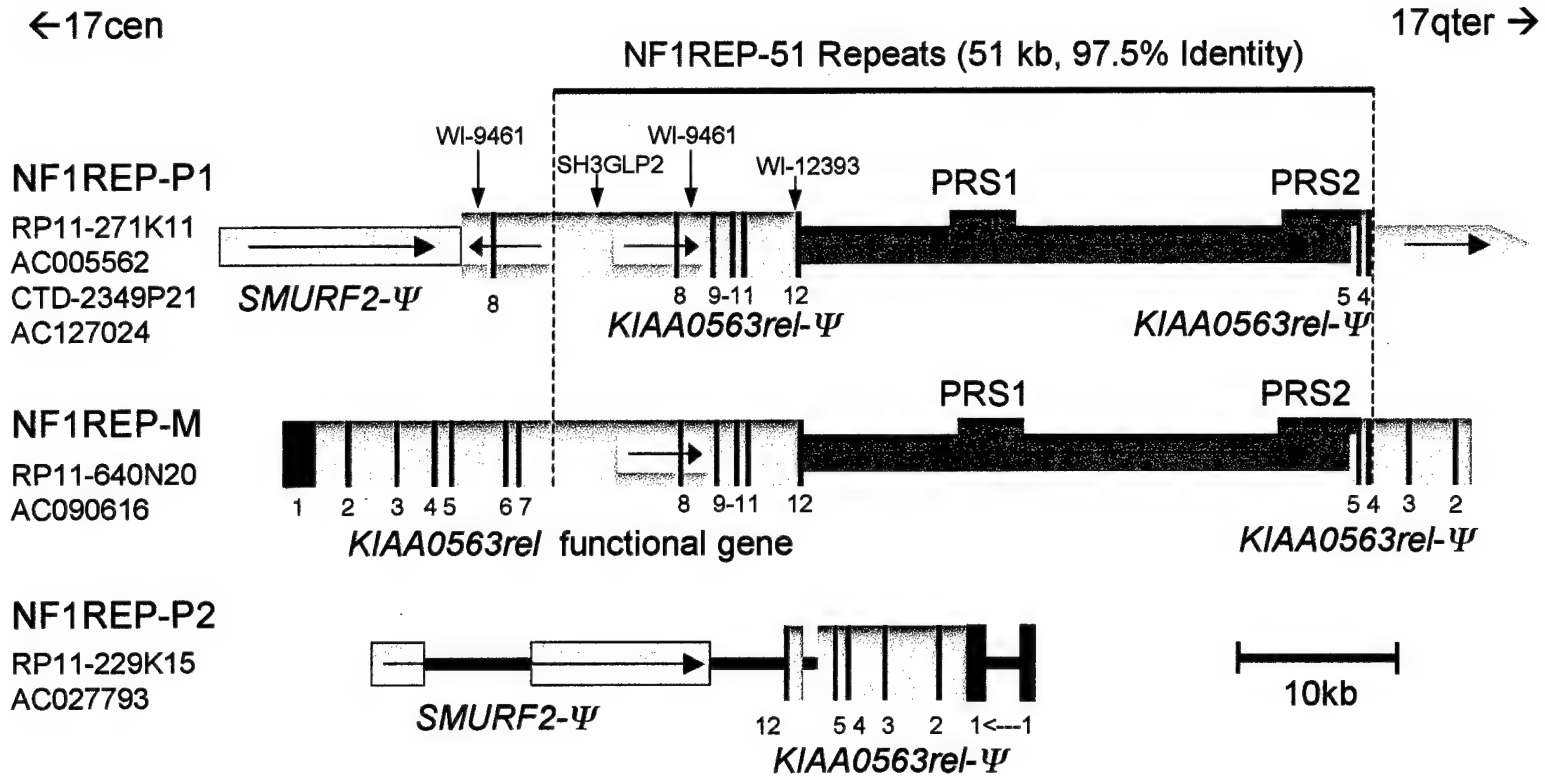
←17cen
17qter →
NF1REP-51 Repeats (51 kb, 97.5% Identity)
WI-9461
WI-9461
SH3GLP2
WI-12393
PRS1
PRS2
NF1REP-P1
RP11-271K11
AC005562
CTD-2349P21
AC127024
SMURF2-Ψ
8
8 9-11 12
KIAA0563rel-Ψ
5 4
KIAA0563rel-Ψ
PRS1
PRS2
NF1REP-M
RP11-640N20
AC090616
1 2 3 4 5 6 7
8 9-11 12
5 4 3 2
KIAA0563rel functional gene
KIAA0563rel-Ψ
NF1REP-P2
RP11-229K15
AC027793
SMURF2-Ψ
12 5 4 3 2 1<---1
KIAA0563rel-Ψ
10kb

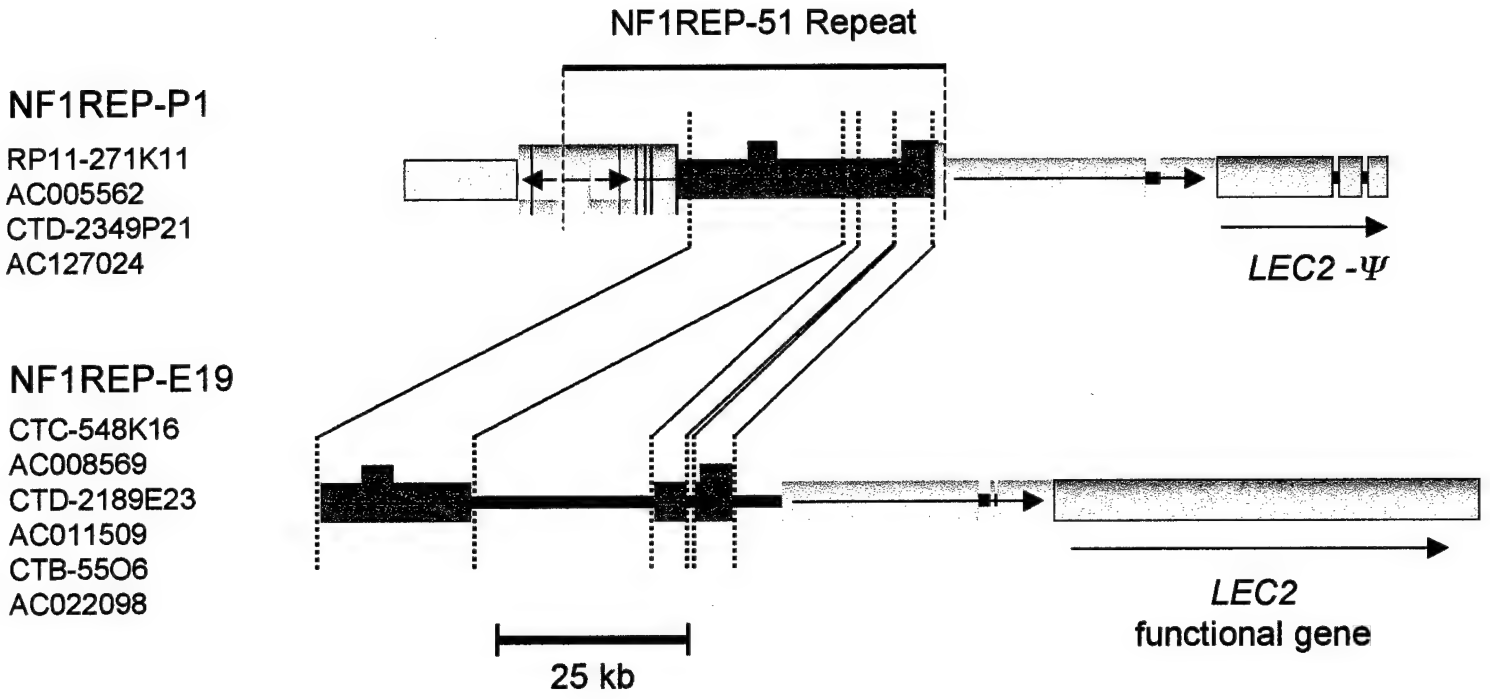
NF1REP-51 Repeat
NF1REP-P1
RP11-271K11
AC005562
CTD-2349P21
AC127024
LEC2 -Ψ
NF1REP-E19
CTC-548K16
AC008569
CTD-2189E23
AC011509
CTB-55O6
AC022098
LEC2
functional gene
25 kb

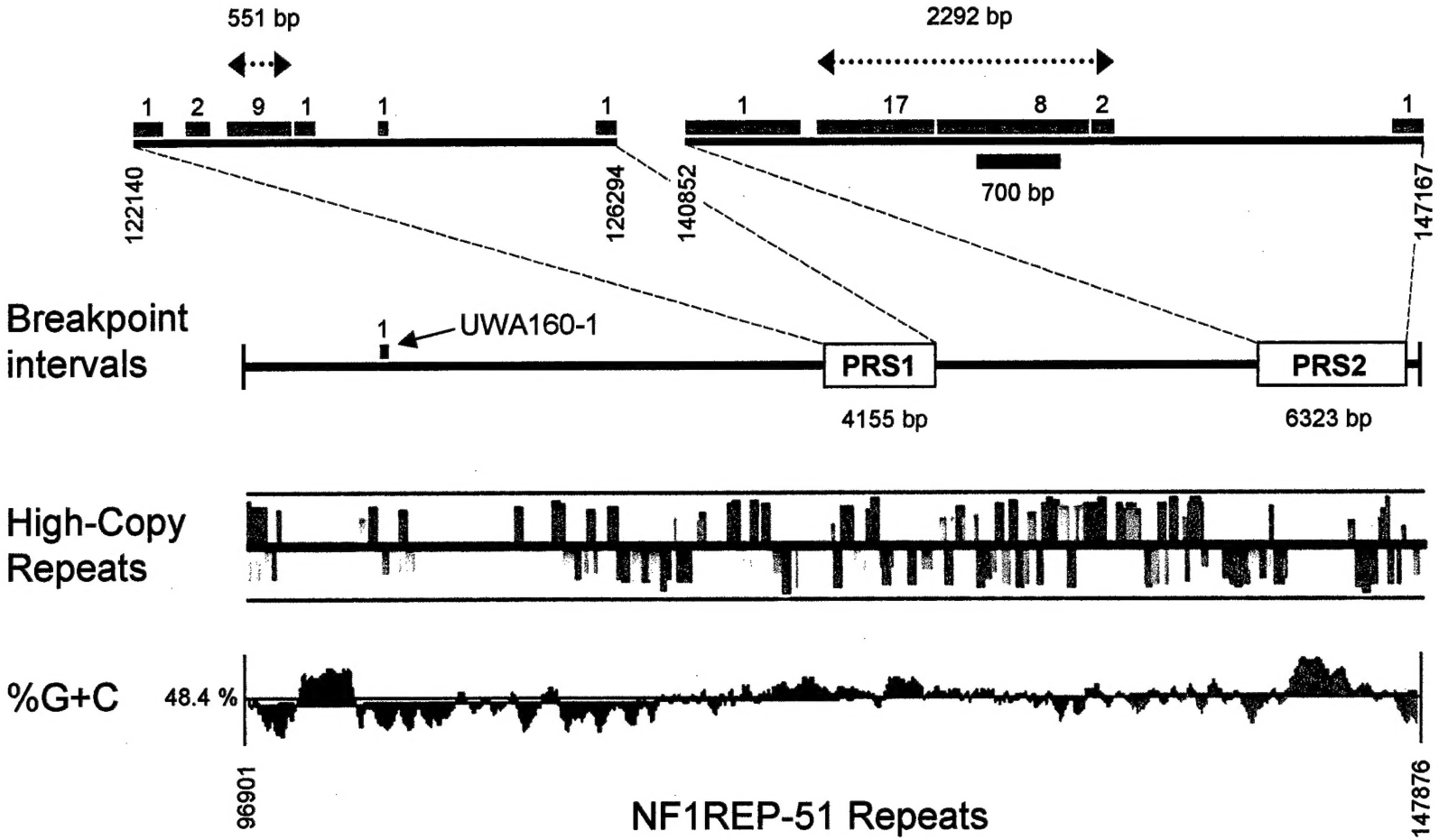
551 bp
2292 bp
1 2 9 1 1 1
1 17 8 2 1
700 bp
122140
126294
140852
147167
Breakpoint intervals
1
UWA160-1
PRS1
PRS2
4155 bp
6323 bp
High-Copy Repeats
%G+C
48.4 %
96901
147876
NF1REP-51 Repeats

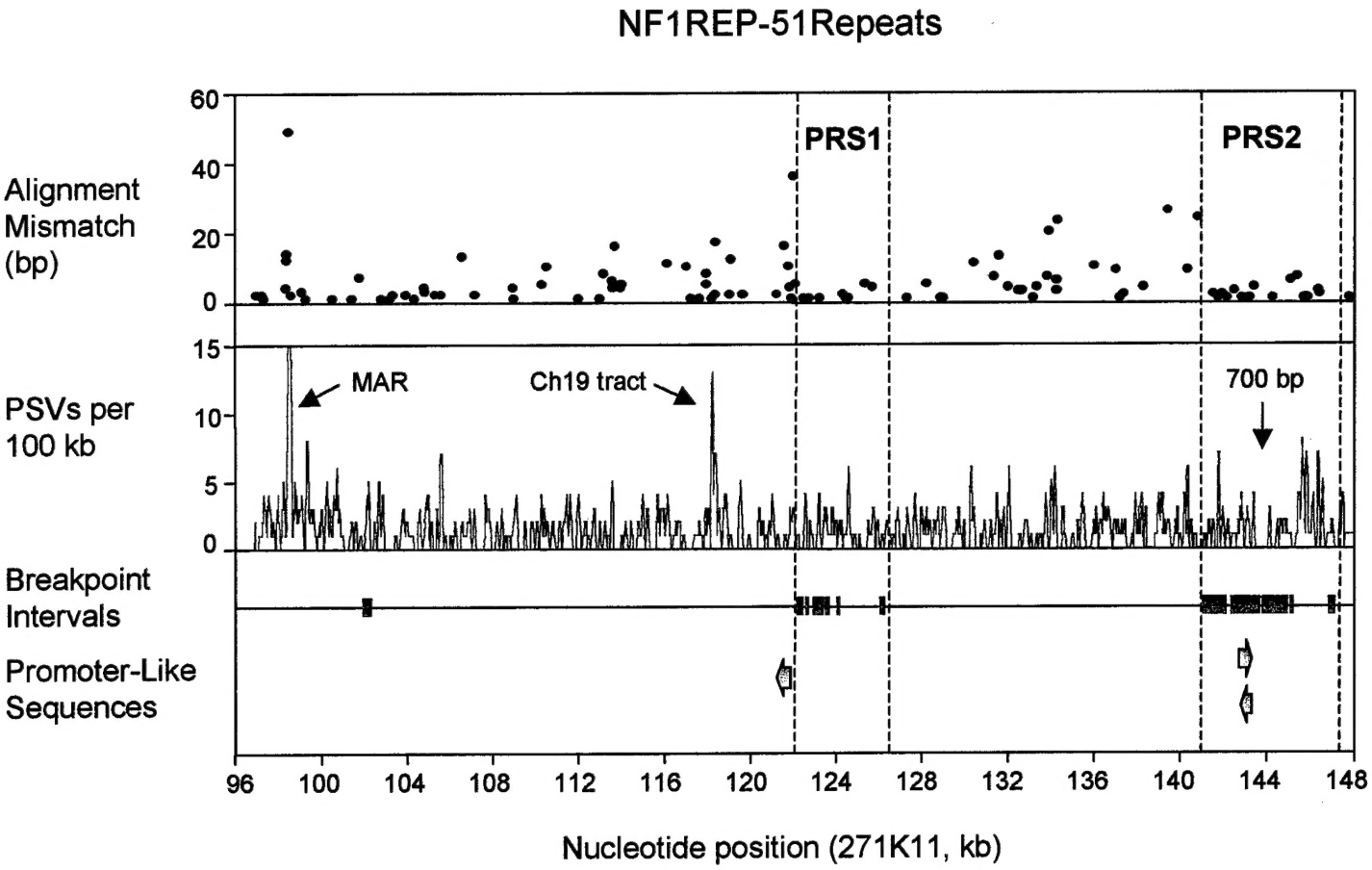
NF1REP-51Repeats
Alignment Mismatch (bp)
PSVs per 100 kb
Breakpoint Intervals
Promoter-Like Sequences
PRS1
PRS2
MAR
Ch19 tract
700 bp
60
40
20
0
15
10
5
0
96
100
104
108
112
116
120
124
128
132
136
140
144
148
Nucleotide position (271K11, kb)

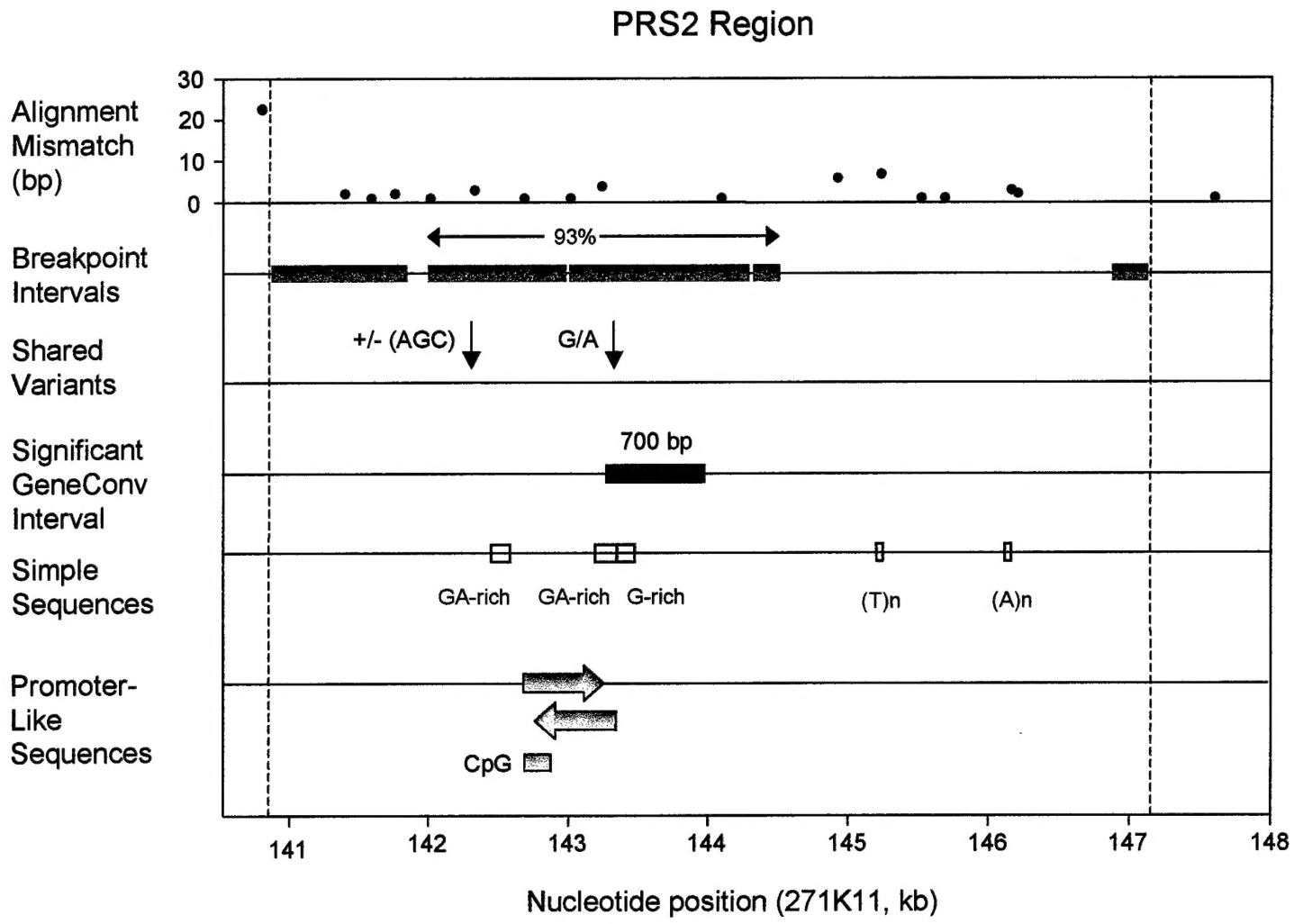
PRS2 Region
Alignment Mismatch (bp)
30
20
10
0
Breakpoint Intervals
93%
Shared Variants
+/- (AGC)
G/A
Significant GeneConv Interval
700 bp
Simple Sequences
GA-rich
GA-rich
G-rich
(T)n
(A)n
Promoter-Like Sequences
CpG
141
142
143
144
145
146
147
148
Nucleotide position (271K11, kb)

Appendix 8

Check one box only
_X__ ***The following abstract is submitted for oral presentation or poster presentation.***
___ ***The following abstract is submitted for poster presentation only***

ABSTRACT FORM (Abstract not to exceed this frame)

TITLE : About 70% of *NF1* microdeletions are recurrent and occur at discrete recombination sites within the flanking NF1REP paralogs, which are complex modular assemblies of low-copy repeats of different sequence families.

Author(s) : Karen Stephens, PhD

Position of
Presenting author : Research Professor of Medicine and of Laboratory Medicine
Affiliation : University of Washington

Address : 1959 NE Pacific St., Rm I-204, Box 357720
Seattle, WA 98195

Tel.# : 206-543-8285 Fax #: 206-685-4829 e-mail:millie@u.washington.edu

Check box if presenting author is student or postdoctoral fellow.

Microdeletions involving the entire *NF1* gene cause ~5% of neurofibromatosis 1 (NF1) cases and predispose to an early age of onset and large numbers of dermal neurofibromas. The majority are recurrent 1.5 Mb deletions mediated by homologous recombination between paralogs, termed NF1REPs, that flank the *NF1* gene. Towards elucidating the mechanism(s) of *NF1* microdeletion, we sequenced NF1REP-mediated *NF1* microdeletions and identified the breakpoint intervals by use of paralogous specific variants (PSV). We found that breakpoints clustered to two paralogous recombination sites, termed PRS1 and PRS2, which are 4,154 and 6,315 bp in length and ~15 kb apart. Each PRS had a recombination hotspot. At PRS1 64% (9/14) of sequenced PRS1 breakpoints occurred in a 551 bp hotspot, while 86% (25/29) of PRS2 breakpoints occurred in a 2,292 bp hotspot. The breakpoint frequency decreased in a generally symmetrical fashion on both sides of each hotspot, consistent with an initiation site for crossing over in this region. We developed PRS1 and PRS2 deletion junction-specific PCR assays, screened a cohort of NF1 deletion patients, and found that 69% (N=78) of breakpoints occurred at the PRS, and of these 74% occurred at PRS2. The PRS assays are highly specific reactions that can be used to define a cohort of patients with the same deletion genotype for phenotypic studies and/or to provide clinical diagnostic testing.

Experimental and *in silico* genomic analyses revealed that there are four NF1REPs in the genome that are complex modular assemblies of paralogs from different sequence families. NF1REP-P1 and NF1REP-M, which serve as recombination substrates for the recurrent 1.5 Mb *NF1* microdeletion, are 133 and 75 kb in length and share a 51 kb region of 98% sequence identity in which PRS1 and PRS2 are located. Therefore, despite 51 kb of high sequence identity meiotic recombination preferentially occurs at discrete hotspots of <2.2 kb. NF1REP-P1 is 44 kb and located just centromeric to the *NF1* gene. It can recombine with NF1REP-M and result in smaller 1 Mb deletions involving *NF1*. The fourth paralog, NF1REP-E19 is 155 kb and located at 19p13. NF1REP-E19 harbors both PRS1 and PRS2 but only fragments of the 51 kb high identity segment compared to NF1REP-P1 and –M. It is unknown whether the NF1REP E19 participates in interchromosomal rearrangements with NF1REPs in the *NF1* region. Together these 4 NF1REP elements are primarily comprised of low-copy repeats, pseudogene fragments, and two genes, KIAA0563-related gene and *Lec2*. Possible recombinogenic features distinctive for each PRS separately include several closely spaced microsatellites proximal to the PRS1 hotspot, and a generally high G+C content punctuated by GA-rich and G-rich islands for the PRS2 hotspot. Our identification of PRS1 and PRS2 as preferential breakpoint sites within the surrounding 51 kb NF1REP region of 98% identity implies that there is an additional factor(s), such as a functional domain or higher order chromosomal feature, that influences the site of paralogous recombination in the *NF1* region.